



This work is protected by copyright and other intellectual property rights and duplication or sale of all or part is not permitted, except that material may be duplicated by you for research, private study, criticism/review or educational purposes. Electronic or print copies are for your own personal, non-commercial use and shall not be passed to any other individual. No quotation may be published without proper acknowledgement. For any other use, or to quote extensively from the work, permission must be obtained from the copyright holder/s.



Chemoenzymatic synthesis of sugar-nucleotide
analogues: tools to probe a strategic
dehydrogenase from *Pseudomonas aeruginosa*

Laura Elizabeth Mary Beswick

*A thesis submitted to Keele University for the degree of Doctor of
Philosophy*

Supervisor: Dr. Gavin Miller

June 2020

Table of Contents

Abstract.....	iv
Abbreviations.....	v
Acknowledgements	x
Publications	xi
Chapter 1: Introduction	1
1.1 Cystic Fibrosis.....	1
1.1.1 Pathogenesis	2
1.1.2 Treatments and prognosis	5
1.2 <i>Pseudomonas aeruginosa</i>	8
1.2.1 Pathogenesis	8
1.2.2 Biofilm formation	17
1.2.3 Antibiotic resistance	21
1.3 Strategic Bacterial Biosynthesis Enzymes.....	23
1.3.1 NAD ⁺ -dependent dehydrogenases	24
1.3.2 GDP-mannose dehydrogenase (GMD).....	27
1.4 Synthetic Carbohydrate Chemistry	33
1.4.1 Background to carbohydrate glycosylation.....	33
1.4.2 Sugar-nucleotides.....	39
1.5 Carbohydrate Chemical Biology.....	53
1.5.1 Sugar-nucleotides as chemical biology tools	54
1.6 Summary	57
1.7 Work described within this thesis.....	58
Chapter 2: Synthesis of GDP-ManA	59
2.0 Introduction and aims.....	59
2.1 Synthesis of glycosyl 1-phosphates.....	63
2.1.1 Synthesis of α -D-mannopyranuronic acid derivatives: acetyl protected methyl uronate series.....	63
2.1.2 Synthesis of α -D-mannopyranuronic acid derivatives: acetyl protected benzyl uronate series.....	69

2.1.3 Synthesis of α -D-mannopyranuronic acid derivatives: benzoyl protected uronate series	71
2.2 Synthesis of GDP-ManA.....	76
2.2.1 Chemical synthesis	77
2.2.2 Enzymatic synthesis.....	80
2.3 Conclusions and Future Directions.....	82
Chapter 3: Sugar-nucleotide tools for GMD	84
3.0 Introduction and aims.....	84
3.1 C6-modified GDP-Man analogues	87
3.1.1 Biological rationale	87
3.1.2 Optimisation of MacDonald Phosphorylation	89
3.1.3 Studies towards the synthesis of 6-chloro-6-deoxy- α -D-mannopyranosyl phosphate.....	92
3.1.4 Studies towards the synthesis of α -D-mannopyranosyluronitrile phosphate.....	97
3.1.5 Synthesis of 6-azido-6-deoxy- α -D-mannopyranosyl phosphate	107
3.1.6 Synthesis of 6-deoxy-6-thio- α -D-mannopyranosyl phosphate	111
3.2 C4-modified GDP-Man analogues.....	116
3.2.1 Biological rationale	116
3.2.2 Synthesis of 4-deoxy-4-fluoro- α -D-mannopyranosyl phosphate.....	116
3.2.3 Studies towards the synthesis of 4-deoxy- α -D-manno-hex-4-eno-1,5-pyranosyl phosphate.....	126
3.3 Active site intermediate analogues	143
3.3.1 Biological rationale	143
3.3.2 Synthesis of 6-amino-6-deoxy- α -D-mannopyranosyl phosphate.....	146
3.3.3 Studies towards the synthesis of 6-deoxy-6-methoxyamino- α -D-mannopyranosyl phosphate.....	148
3.4 Evaluating the substrate specificity of GDP-ManPP: chemoenzymatic synthesis of modified GDP-Man analogues.....	154
3.4.1 Discussion	158
3.5 Conclusions and Future Directions.....	160

Chapter 4: Biochemical evaluation of GDP-Man analogues	163
4.0 Introduction and aims.....	163
4.1 GDP-6-azido-6-deoxy-mannose	164
4.1.1 Evaluation as a substrate of GMD	164
4.2 GDP-4-deoxy-4-fluoro-mannose	165
4.2.1 Evaluation as a substrate of GMD	165
4.2.2 Discussion	166
4.3 GDP-6-amido-6-deoxy-mannose	168
4.3.1 Evaluation as an inhibitor of GMD	168
4.3.2 Evaluating potential hydrolysis of GDP-6-amido-6-deoxy-mannose by GMD	170
4.3.3 Discussion	172
4.4 Conclusions and Future Directions.....	173
Chapter 5: Overall Conclusions and Future Directions.....	176
Chapter 6: Experimental	177
6.0 General experimental details	177
6.1 General experimental procedures.....	180
6.2 Enzyme production	184
6.2.1 GDP-mannose pyrophosphorylase (GDP-ManPP).....	184
6.2.2 GDP-mannose dehydrogenase (GMD).....	185
6.3 Determination of GMD activity and assay.....	186
6.4 Experimental details for Chapter 2.....	188
6.5 Experimental details for Chapter 3.....	211
7. References	274

Abstract

Pseudomonas aeruginosa (*P. aeruginosa*) is an opportunistic bacterium, responsible for causing life threatening infections amongst fibrosis (CF) patients. Mucoïd phenotypes of *P. aeruginosa* are characterised by overproduction of alginate, an extra-cellular polysaccharide (EPS) composed of β -D-mannuronic acid and α -L-guluronic acid, which is involved in bacterial biofilm formation and results in a multi-drug antibiotic resistance profile.

Guanosine diphosphate-mannose dehydrogenase (GMD), a NAD^+ -dependent dehydrogenase responsible for production of the feedstock sugar-nucleotide building block guanosine diphosphate-mannuronic acid (GDP-ManA), has been identified as a strategic biosynthetic enzyme to investigate potential inhibition of alginate production. This oxidation is mediated by a catalytic Cys²⁶⁸ residue, providing a template for rational structure-based design of sugar-nucleotide tools.

This thesis describes the synthesis of GDP-ManA, the native tool for studies into alginate biosynthesis. A chemical strategy employing a P(V)-P(V) pyrophosphorylation approach towards the target was complemented by an enzymatic synthesis using the native enzyme, GMD.

To permit further mechanistic study of GMD, the synthesis of a series of structurally defined GDP-Man analogues was presented *via* a chemoenzymatic approach, to investigate substrate specificity and identify functionalities capable of interacting with Cys²⁶⁸. Modified GDP-Man analogues were accessed chemically from differentially protected C6-OH and C4-OH mannose building blocks. Following a series of functional group interconversions, transformation to the respective sugar-nucleotides was evaluated using guanosine diphosphate-mannose pyrophosphorylase (GDP-ManPP). The synthesised GDP-Man analogues were then evaluated as substrates of GMD, providing a foundation for the future design and synthesis of probes to target and inhibit GMD.

Abbreviations

A	Adenine
Ac ₂ O	Acetic anhydride
AcOH	Acetic acid
AgCO ₃	Silver carbonate
AgOTf	Silver trifluoromethanesulfonate
ASL	Airway surface liquid
BAIB	Bis(acetoxy) iodobenzene
BDMA	Benzaldehyde dimethyl acetal
BF ₃ •OEt ₂	Boron trifluoride diethyl etherate
BnBr	Benzyl bromide
BnNH ₂	Benzylamine
BzCl	Benzoyl chloride
C	Cytosine
c-AMP	Cyclic adenosine monophosphate
CAN	Ceric ammonium nitrate
CBr ₄	Carbon tetrabromide
CCl ₄	Carbon tetrachloride
c-di-GMP	Bis(3'-5')-cyclic dimeric guanosine monophosphate
CeCl ₃ •7H ₂ O	Cerium trichloride heptahydrate
CF	Cystic fibrosis
CFTR	Cystic fibrosis transmembrane conductance regulator
CHCl ₃	Chloroform
CO ₂	Carbon dioxide
COSY	Correlation spectroscopy
CV	Column volume
<i>cyclo</i> -Sal	<i>Cyclo</i> -saligenyl
D ₂ O	Deuterium oxide
DAST	Diethylaminosulfur trifluoride
DBP	Dibenzyl phosphate
DCC	Dicyclohexylcarbodiimide
DCE	1,2-dichloroethane
DCI	4,5-dicyanoimidazole
DCM	Dichloromethane
DFT	Density functional theory
DMAP	4-dimethylaminopyridine
DMAPA	3-(dimethylamino)-1-propylamine
DMC	2-chloro-1,3-dimethylimidazolium chloride
DMF	<i>N,N</i> -dimethylformamide

DMP	Dess-Martin periodinane
DMSO	Dimethyl sulfoxide
DTT	Dithiothreitol
EDA	Ethylene diamine
eDNA	Extracellular DNA
ENaC	Epithelial sodium channels
EPS	Extra-cellular polysaccharide
equiv.	Equivalent
Et ₂ O	Diethyl ether
Et ₃ N	Triethylamine
EtOAc	Ethyl acetate
EtOH	Ethanol
EtSH	Ethanethiol
FDA	Food and Drug Administration
Fmoc	Fluorenylmethoxycarbonyl
Fuc	L-fucose
G	Guanine
Gal	D-galactose
GalA	D-galacturonic acid
GDP	Guanosine 5'-diphosphate
GDP-Man	Guanosine 5'-diphosphate-mannose
GDP-ManA	Guanosine 5'-diphosphate-mannuronic acid
GDP-ManPP	Guanosine 5'-diphosphate-mannose pyrophosphorylase
Glc	D-glucose
GlcA	D-glucuronic acid
GlcN	D-glucosamine
GMD	Guanosine 5'-diphosphate-mannose dehydrogenase
GMP	Guanosine 5'-monophosphate
GMP-morpholidate	Guanosine 5'-phosphoromorpholidate
GOase-M ₁	Galactose oxidase
GT	Glycosyltransferase
GTP	Guanosine 5'-triphosphate
GulA	L-guluronic acid
H ₂ O	Water
H ₂ SO ₄	Sulphuric acid
H ₃ PO ₄	Phosphoric acid
HBF ₄ •OEt ₂	Tetrafluoroboric acid diethyl ether complex
HBr	Hydrobromic acid
Hex	Hexane
HisD	Histidinol dehydrogenase

HMBC	Heteronuclear multiple bond correlation spectroscopy
HMG-CoA reductase	3-hydroxy-3-methylglutaryl coenzyme A reductase
HPLC	High-performance liquid chromatography
HRMS	High resolution mass spectrometry
HSAB theory	Hard soft acid base theory
HSQC	Heteronuclear single quantum coherence spectroscopy
HSQC-DEPT	Heteronuclear single quantum coherence-distortionless enhancement by polarisation transfer spectroscopy
I ₂	Iodine
IdoA	L-iduronic acid
IPA	Isopropyl alcohol
iPPase	Inorganic pyrophosphatase
IR	Infrared
K ₂ CO ₃	Potassium carbonate
ED pathway	Entner-Doudoroff pathway
KDPG	2-keto-deoxy-6-phosphogluconate
KOH	Potassium hydroxide
KSAc	Potassium thioacetate
LDA	Lithium diisopropyl amide
LPS	Lipopolysaccharide
Man	D-mannose
ManA	D-mannuronic acid
ManT	Mannosyltransferase
MCC	Mucociliary clearance
mCPBA	3-chloroperbenzoic acid
Me ₂ EtSiH	Dimethylethylsilane
MeCN	Acetonitrile
MeI	Methyl iodide
MeOH	Methanol
MeONH ₂ •HCl	Methoxyamine hydrochloride
MFP	Periplasmic membrane fusion protein
MgCl ₂	Magnesium chloride
MgSO ₄	Magnesium sulphate
MRSA	Methicillin-resistant <i>Staphylococcus aureus</i>
MS	Molecular sieves
Na ₂ S ₂ O ₃	Sodium thiosulphate
NaBH ₃ CN	Sodium cyanoborohydride
NaBH ₄	Sodium borohydride
NaCl	Sodium chloride
NAD(H)	Nicotinamide adenine dinucleotide (reduced form)

NAD ⁺	Nicotinamide adenine dinucleotide (oxidised form)
NaH	Sodium hydride
NaHCO ₃	Sodium hydrogen carbonate
NaI	Sodium iodide
NaN ₃	Sodium azide
NaOCl	Sodium hypochlorite
NaOH	Sodium hydroxide
NaOMe	Sodium methoxide
Nd(OTf) ₃	Neodymium trifluoromethanesulfonate
NDP-sugar	Nucleoside diphosphate-sugar
NH ₂ OH•HCl	Hydroxylamine hydrochloride
NH ₄ Cl	Ammonium chloride
NH ₄ HCO ₃	Ammonium bicarbonate
NH ₄ OH	Ammonium hydroxide
NHS	National Health Service
NICE	National Institute for Health and Care Excellence
NIS	<i>N</i> -iodosuccinimide
<i>N</i> -MIC	<i>N</i> -methylimidazolium chloride
NMP	Nucleoside monophosphate
NMR	Nuclear magnetic resonance
OMF	Outer membrane factor
OPME	One pot multi-enzyme
<i>P. aeruginosa</i>	<i>Pseudomonas aeruginosa</i>
P ₂ O ₅	Phosphorus pentoxide
PBr ₃	Phosphorus tribromide
Pd(OH) ₂ /C	Palladium hydroxide on carbon
Pd/C	Palladium on carbon
Pet. ether	Petroleum ether
Ph ₂ SO	Diphenyl sulphoxide
Ph ₃ P	Triphenyl phosphine
PhIO	Iodosobenzene
PhSH	Thiophenol
PMI	Phosphomannose isomerase
POCl ₃	Phosphoryl chloride
ppm	Parts per million
PTFE	Polytetrafluoroethylene
<i>p</i> TsCl	<i>p</i> -Toluenesulfonyl chloride
<i>p</i> TsOH	<i>p</i> -Toluenesulfonic acid
RPM	Revolutions per minute
RT	Room temperature

<i>S. enterica</i>	<i>Salmonella enterica</i>
SAX	Strong anion exchange
SO ₃ •pyridine	Sulfur trioxide pyridine complex
T	Thymine
TBAF	tetra- <i>N</i> -butylammonium fluoride
TBDMS	<i>tert</i> -Butyldimethylsilyl
TBDMSCl	<i>tert</i> -Butyldimethylsilyl chloride
TBPP	Tetrabenzyl pyrophosphate
<i>t</i> BuOH	<i>Tert</i> -butyl alcohol
<i>t</i> BuOOH	<i>tert</i> -butyl hydroperoxide
TCA	Tricarboxylic acid cycle
TCEP	Tris(2-carboxyethyl)phosphine
TEAB	Triethylammonium bicarbonate
TEMPO	2,2,6,6-tetramethylpiperidin-1-yl)oxyl
Tf ₂ O	Trifluoromethanesulfonic anhydride
TfOH	Trifluoromethanesulfonic acid
THF	Tetrahydrofuran
TLC	Thin layer chromatography
TMS	Trimethylsilyl
TMSOTf	Trimethylsilyl trifluoromethanesulfonate
TrCl	Trityl chloride
TTBP	2,4,6-Tri- <i>tert</i> -butylpyrimidine
U	Uridine
UGD	Uridine diphosphate-glucose dehydrogenase
UGM	UDP-galactopyranose mutase
UNAcMD	Uridine diphosphate- <i>N</i> -acetyl-mannosamine dehydrogenase
Zn(OAc) ₂	Zinc acetate

Acknowledgements

I would firstly like to thank my supervisor Dr. Gavin Miller for his invaluable support and guidance over the past three years. Thank you for always being patient, positive and fighting our corner – I could not have wished for a better mentor over the past three years. I am also grateful for the many travel and networking opportunities you helped to provide over the course of this project.

I would also like to thank Keele University for financial support, alongside staff within the department, particularly David Evans, for his ongoing technical support over the course of this research, and Dr. Graeme Jones for providing HRMS analyses.

I am grateful to Prof. Rob Field, who allowed me to undertake research and training within his laboratory that were crucial for progression of this project. Special thanks are given to Dr. Martin Rejzek and Dr. Sanaz Ahmadipour for their assistance in performing chemoenzymatic syntheses and biochemical assays. Thank you for always making me feel so welcome during my visits to the John Innes Centre. I would also like to thank Dr. Ayesha Zafar and Dr. Jóhannes Reynisson for providing DFT and molecular docking data to supplement this work.

This experience would not have been the same without the members of the Miller group and our office, past and present. Thanks for providing endless laughter and enjoyment on our many outings over the years. Special thanks go to Dr. Aisling Ní Cheallaigh for advice and lending a supportive ear when times were tough, and Eleni Dimitriou for being an amazing support throughout my PhD. We have been through every step of this journey together and I couldn't have done this without you or your motivational Spotify playlists in the lab!

Finally, I would like to thank my family and friends for their ongoing support throughout this research, particularly my fiancé Joe and Mum and Dad. Thank you for always believing in me and giving me a confidence boost when things weren't going to plan! I owe you all so much and I hope you know how much I have appreciated your love and encouragement over these past few years.

Publications

1. **L. Beswick**, S. Ahmadipour, G. J. Hofman, H. Wootton, E. Dimitriou, J. Reynisson, R. A. Field, B. Linclau, G. J. Miller, Exploring anomeric glycosylation of phosphoric acid: Optimisation and scope for non-native substrates, *Carbohydr. Res.*, 2020, **488**, 107896.
2. **L. Beswick**, S. Ahmadipour, J. P. Dolan, M. Rejzek, R. A. Field, G. J. Miller, Chemical and enzymatic synthesis of the alginate sugar nucleotide building block: GDP-D-mannuronic acid, *Carbohydr. Res.*, 2019, **485**, 107819.
3. S. Ahmadipour, **L. Beswick**, G. J. Miller, Recent advances in the enzymatic synthesis of sugar-nucleotides using nucleotidyltransferases and glycosyltransferases, *Carbohydr. Res.*, 2018, **469**, 38-47.
4. **L. Beswick**, G. J. Miller, 1,2,3,4-Tetra-O-Acetyl- β -D-Mannuronic Acid, *Molbank*, 2017, M947.

Chapter 1: Introduction

1.1 Cystic Fibrosis

Cystic fibrosis (CF) is an autosomal recessive genetic disorder that was reported to affect over 10500 people in the UK alone in 2017¹, with 200-300 new diagnoses occurring annually.² The disease affects exocrine organs, primarily the respiratory and gastrointestinal tracts and the pancreas, whilst also having secondary effects on the reproductive organs.³ In approximately 75% of cases, CF is diagnosed before the age of two, with the major physiological marker being an increased concentration of electrolytes in sweat due to the reduced permeability of epithelial apical membranes to chloride ions.⁴ The 'sweat test' measures the amount of chloride in sweat, and remains one of the most commonly performed initial tests in suspected cases of CF.⁵

The condition is characterised by a build-up of abnormally thick, sticky mucus that is hard to clear mechanically, *i.e.* by coughing (Figure 1.1). Consequently, non-inflammatory response mechanisms against foreign substances, such as inhaled allergens and pathogens, become redundant. This leads to inflammatory response mechanisms, such as those of antibodies and macrophages, prevailing which leads to a vicious cycle of recurrent/chronic bacterial infections and excessive inflammation, primarily within the lungs.⁶ Other symptoms of the disease include malnutrition, resulting from the suppression of pancreatic function, and infertility, almost exclusively observed in men.⁷

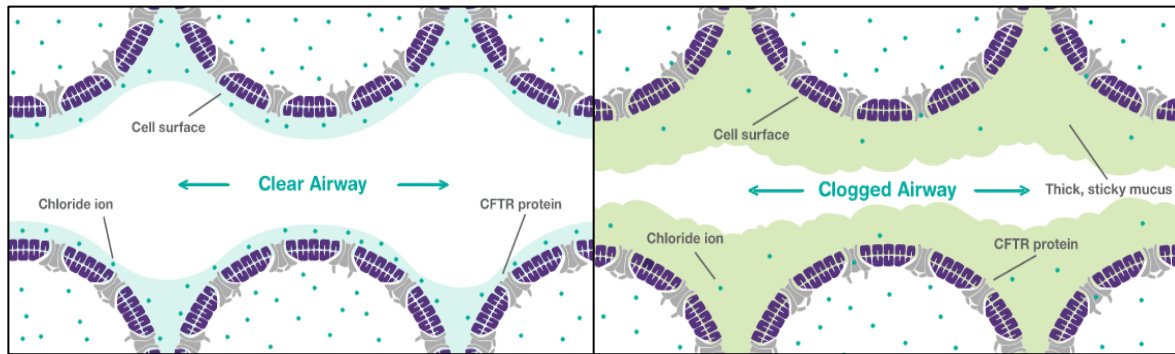


Figure 1.1: Comparison between normal (left) and CF (right) airways.⁸

1.1.1 Pathogenesis

CF is caused by a mutation in the cystic fibrosis transmembrane conductance regulator (CFTR) gene (Figure 1.2). Discovered in 1989 by Riordan *et al.*⁹, the CFTR locus was found to be located on chromosome 7 and deletion of a phenylalanine residue was identified within CF patients. Since discovery of the gene over 1600 alternative mutations of the CFTR have been described, however deletion of phenylalanine, denoted the $\Delta F508\text{del}$ mutation, remains the most common, being found in 70% of CF chromosomes.¹⁰ Found in a variety of epithelial tissues, the main function of the CFTR exists as a cyclic adenosine monophosphate (c-AMP) regulated chloride ion channel, however it has also been identified to regulate other ion channels such as epithelial sodium channels (ENaC). The CFTR maintains the liquid volume on epithelial surfaces, which is essential for effective clearance of mucus and foreign particles contained within it, providing the body with a crucial non-inflammatory response mechanism against infection.

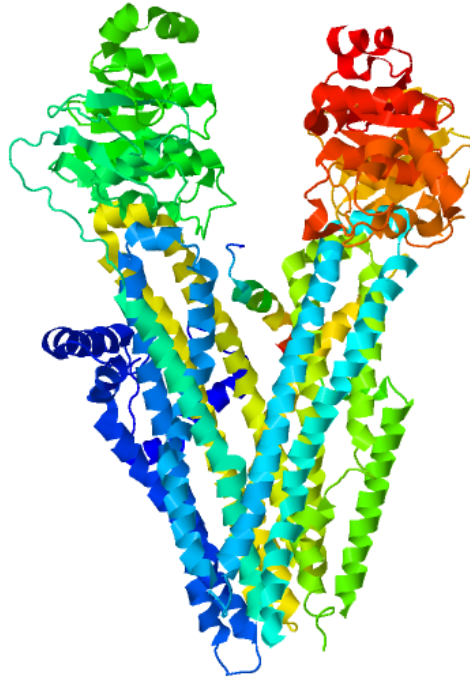


Figure 1.2: Crystal structure of human CFTR gene determined by electron microscopy.¹¹

The human airway is comprised of two aqueous layers. The first is a mucus layer that traps any inhaled allergens and pathogens, whilst the second is a thin layer known as the airway surface liquid (ASL). The ASL spans the surface of the epithelium, creating a microenvironment that allows cilia to clear mucus from the airways, known as mucociliary clearance (MCC).¹² The ASL is maintained by both secretory (+ve) and absorptive (-ve) processes of the CFTR and ENaC, respectively. In CF patients, absence of the CFTR protein leads to the defective secretion of chloride ions, in turn disrupting osmotic gradients that control fluid release which causes dehydration of the ASL. This process leads to thickening of the mucus and causes the cilia to collapse, impairing MCC, as shown in Figure 1.3.^{10,13}

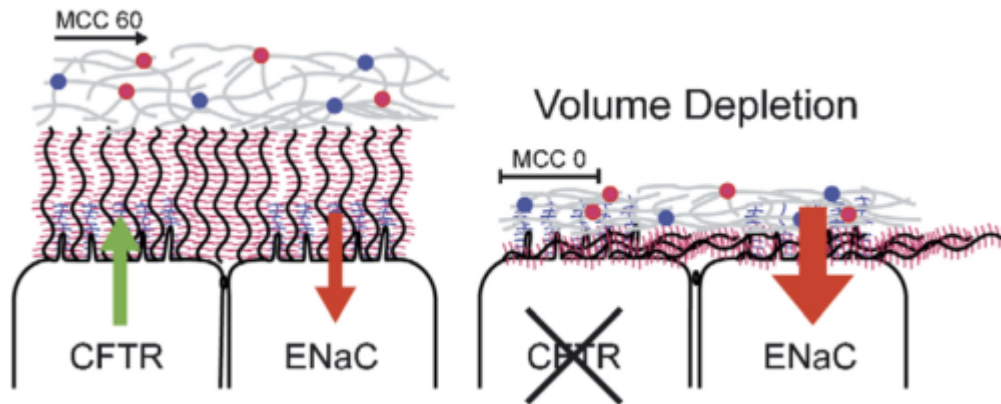


Figure 1.3: Comparison of ion transport mechanisms and ASL volume in normal (left) and CF (right) airways.

The mutation present in the CFTR gene results in a variety of protein defects, from total absence of the protein, failure to produce mature CFTR protein or the absence of the protein in its usual location at the apical plasma membranes of epithelial cells.¹⁴ Given this wide variation between individuals, precisely how the defective CFTR gene leads to airway disease has been highly disputed, with several opposing theories presented in the literature.

The 'low volume' hypothesis is the most commonly accepted explanation, whereby the depleted volume of ASL drastically reduces MCC so the patient is unable to clear opportunistic bacteria. The bacteria then colonise, inducing chronic lung infections and extensive lung damage over a prolonged period of time.¹² This is supported by *in vitro* findings that showed that ASL volume/depth in CF epithelia was reduced from a normal level of approximately 7 μm to 3-4 μm .¹⁵

Alternatively, a 'high salt' hypothesis suggested that elevated salt concentrations in CF epithelia inactivated a natural bactericidal factor present in the ASL, hence CF

epithelia are readily colonised by *P. aeruginosa* and other bacteria as it is unable to eradicate them.¹⁶ Although studies have suggested that a difference in osmolality between normal and CF ASL does exist, the CF ASL was found to be either hypotonic or isotonic, not hypertonic as would be expected from this hypothesis.¹⁰

1.1.2 Treatments and prognosis

In recent years, improved management of CF has considerably increased patient survival rates, with epidemiological studies indicating that the median life expectancy of babies born in the 21st century now exceeds fifty years of age.¹⁷ Nevertheless, the quality of life for patients is still impaired due to the need for regular treatment, either at home or in hospital, reliance on medication and the possibility of surgical intervention due to irreparable lung damage caused by fibrosis.

A variety of airway clearance techniques, known as chest physiotherapy, help to keep the airways as clear as possible, involving a series of breathing and postural exercises which dislodge and remove mucus *via* coughing.¹³ Although these techniques are initially performed by trained physiotherapists/nurses, they can be performed by parents and friends at home, minimising disruption to daily life.

Several medications are also available to treat the symptoms of CF, including bronchodilators to widen airways, and agents such as mannitol dry powder to reduce the thickness of the mucus. The latter treatments work by inducing an osmotic gradient, to permit the flow of water into the lumen of the airways, leading to mucus hydration and increased MCC.¹⁸

At present, few drugs are available that target the CFTR gene mutation directly. Ivacaftor **1** (Figure 1.4) marketed as Kalydeco[®] by Vertex Pharmaceuticals, was the first drug licensed for use by the Food and Drug Administration (FDA). Unfortunately, this treatment is only effective for 4% of the UK population, as very few CF sufferers have the gene mutation for which this treatment is suitable (at least one G551D mutation or a R117H mutation in the CFTR gene). Described as a CFTR potentiator, the drug binds to the channel directly, stimulating ion function of activated cell-surface CFTR by increasing the probability of the gates being open which increases ASL volume and promotes MCC.¹⁹

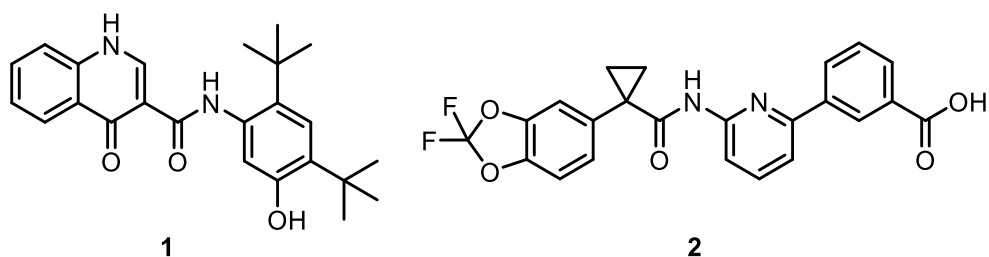


Figure 1.4: Chemical structures of Ivacaftor **1** and Lumacaftor **2**.

On the other hand, the combination medicine Orkambi[®] can treat around 50% of the UK population, being suitable for patients who have two copies of the most common $\Delta F508\text{del}$ mutation. In addition to **1** it contains Lumacaftor **2** (Figure 1.4), a CFTR corrector, which acts to increase the amount of CFTR protein at the cell surface. Though the drug is licensed for use in people with CF over the age of two, it was rejected for use on the National Health Service (NHS) by the National Institute for Health and Care Excellence (NICE), who stated that the benefits did not justify the significant cost of £105,000 per patient per year. As data suggested that the drug slowed the decline in lung function by as much as 42%, the NHS faced increasing

pressure from CF sufferers and their families and offered Vertex a deal worth £500 million over a five-year period, which was initially rejected. In October 2019, a deal with Vertex Pharmaceuticals was agreed to enable access to these medicines on the NHS.²⁰

Arguably of most importance for CF patients is antibiotic therapy to combat acute and chronic bacterial infections caused by *Haemophilus influenzae*, *Burkholderia cepacia* and the life-threatening *Pseudomonas aeruginosa* (*P. aeruginosa*). The type of bacteria and extent of colonisation within the airways determines the best course of antibiotics to effectively treat the infection. In mild infections, oral antibiotics are usually sufficient, however in more serious infections patients are often hospitalised to receive intravenous treatment.¹³ Unfortunately, antibiotic resistance is leading to many antibiotics becoming ineffective against bacterial infections, proving extremely damaging for CF patients and contributing to the high mortality rates observed amongst this population.

1.2 *Pseudomonas aeruginosa*

P. aeruginosa is an opportunistic, Gram-negative bacterium that grows readily between 25-42 °C in both aerobic and anaerobic conditions, allowing it to survive in a range of environments. Its genome is relatively large (5.5-7.0 Mb) and consists of a single circular chromosome, of which 8% encodes for regulatory genes that enable its adaptation to difficult growth environments. *P. aeruginosa* also encodes many virulence factors which lead to serious infections in immunocompromised patients, such as those with CF and hospitalised patients, such as those with burn wounds.^{21,22}

1.2.1 Pathogenesis

1.2.1.1 Adhesins and secretion of toxins/exoenzymes

P. aeruginosa exhibits its pathogenesis *via* several mechanisms. A minimum of three adhesins are associated with *P. aeruginosa*, allowing it to colonize, obtain nutrients and proliferate in host tissues. Type IV pili are flexible filaments comprised of pilin protein that mediate bacterial adhesion to epithelial cells. The single flagellum of *P. aeruginosa* also plays an important role in adhesion and motility, targeting mucins that exist to lubricate and protect tissues from pathogens. *P. aeruginosa* with defective flagella has been shown to have reduced pathogenicity.²³

Lipopolysaccharide (LPS) is a major outer-membrane component of Gram-negative bacteria including *P. aeruginosa*. Structurally, LPS consists of a hydrophobic lipid section (Lipid A), a hydrophobic core polysaccharide chain and a hydrophilic O-antigen oligosaccharide side chain specific to the bacterial serotype (see Figure 1.5).

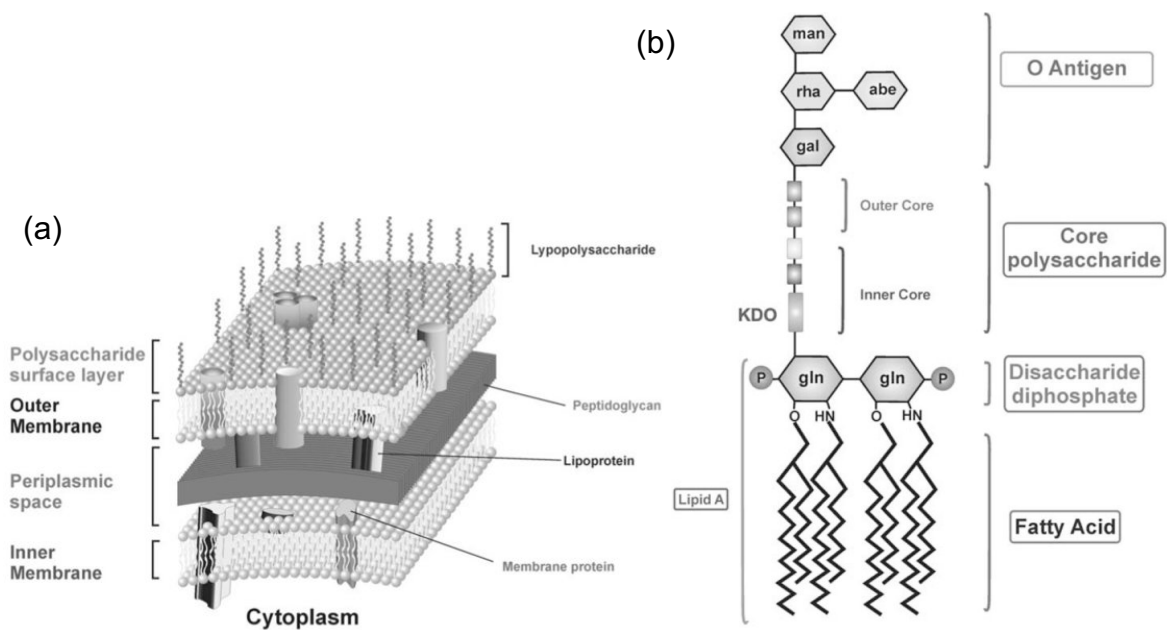


Figure 1.5: a) Structure of Gram-negative bacterial cell wall.
 b) Outer-membrane components of Gram-negative bacteria.²⁵

The carbohydrate component of LPS is recognised for its role in inducing strong immune responses in human cells, whilst also providing protection against bile salts and lipophilic antibiotics. Lipid A is an important endotoxin capable of causing septic shock.²⁴ The *P. aeruginosa* LPS outer core recognises CFTR amino acid sequence 108-117, and this interaction leads to internalization of the bacteria. Overproduction of mucus due to defective CFTR protein provides a favourable environment for its survival.

P. aeruginosa also delivers virulence factors through a series of five complex secretion systems, either to the extracellular environment or directly into the cytosol of host cells. The mechanism by which each system delivers virulence factors vary, with type I secretion systems composed of an outer-membrane protein and ATP-

binding cassette transporter. Type II and V secretion systems take place *via* a two-step process, whereas type III and VI utilise needle-like structures to inject toxic proteins directly into the cytosol.²⁶ Examples of toxins and exoenzymes secreted by *P. aeruginosa* include Endotoxin A, elastase, alkaline protease, phospholipase C and rhamnolipid, each of which contribute to bacterial virulence through disruption of receptor and cell signalling pathways.

1.2.1.2 Mucoïd conversion

Infections caused by *P. aeruginosa* are one of the leading causes of morbidity and mortality amongst CF patients. Strains of bacteria colonising the lungs and respiratory tract undergo conversion to a mucoïd phenotype that is characterised by overproduction of the extracellular polysaccharide (EPS) alginate.²⁷

1.2.1.3 Alginate: structure and function

Alginate belongs to a family of unbranched linear, non-repeating copolymers, comprising variable amounts of β -D-mannuronic acid (ManA) and its C5-epimer, α -L-guluronic acid (GulA), joined by β -1,4 glycosidic linkages (Figure 1.6). The ratio of monosaccharides within the polymer diversifies its chemical and physical properties, with the alginate source determining both the ratio and specific sequence of monomers.^{21,28}

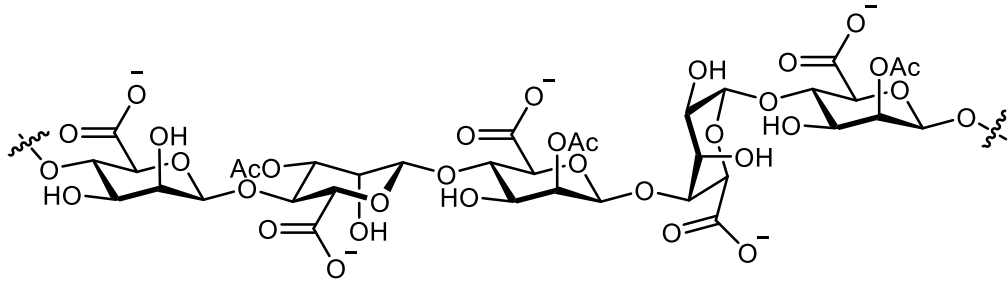


Figure 1.6: Chemical structure of alginate.

Alginate is commercially available through harvesting of brown seaweed (*Phaeophyceae*), but aside from being produced by *P. aeruginosa*, only one other genera of bacteria, *Azotobacter*, has been discovered to produce alginate. In *P. aeruginosa*, alginate is a key virulence factor, providing protection from host immune response by decreasing the amount of phagocytosis by neutrophils and macrophages. It has also been shown to influence expression of other virulence factors, such as the flagellum and type III secretion system. In combination, this leads to the persistence of *P. aeruginosa* in the airways and reduces susceptibility of the bacteria to antibiotic treatment. Opposed to *P. aeruginosa*, in *Azotobacter vinelandii* alginate plays a structural role in the formation of desiccation resistant cysts.²⁸ Alginate is also important in both the food and beverage and pharmaceutical industries, whereby the varying properties of alginate, ranging from viscous solutions to gel-like structures when in the presence of divalent cations such as Ca^{2+} , can be exploited in numerous applications (Figure 1.7).²⁹

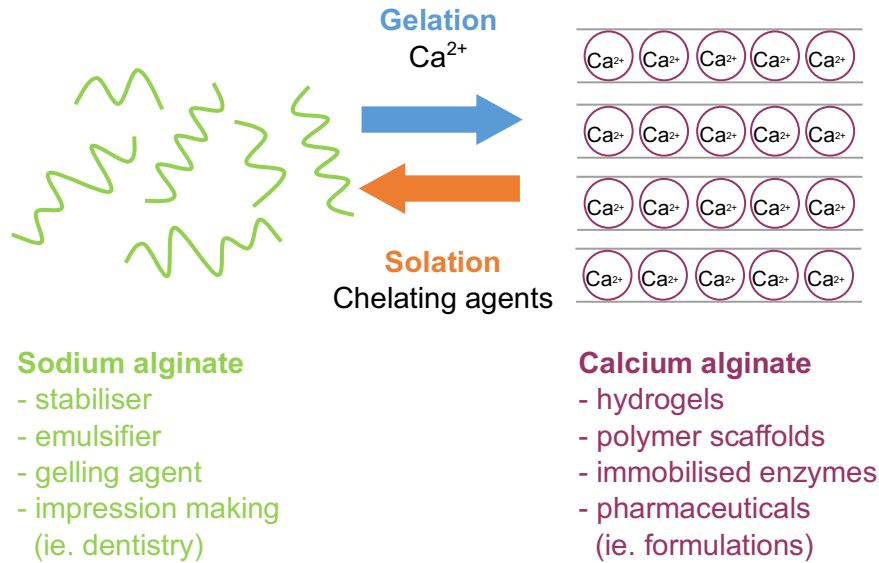


Figure 1.7: An overview of the properties and uses of alginate in the presence of sodium and calcium cations.

1.2.1.4 Alginate Biosynthesis

The biosynthesis of alginate occurs *via* a protein complex that is encoded within the *alg* operon (Figure 1.8), which was reported by Chitnis and Ohman in 1993.³⁰ At the transcriptional level, alginate production is regulated by a sigma factor known as AlgT/U, where upon binding to the *alg* promoter, transcription is initiated.³¹

Conversion to the mucoid phenotype during chronic infection in CF is associated with mutations in the *algT/U mucABCD* gene cluster, which encodes for an extreme stress response system that is highly conserved amongst Gram-negative bacteria. This system comprises the AlgT/U sigma factor and four other regulatory proteins including MucA, an inner membrane protein that inhibits AlgT/U and the periplasmic protein MucB that negatively controls AlgT/U.³²

In non-mucoid strains of *P. aeruginosa*, transcription of AlgT/U is usually inactive. This is due to the actions of anti-sigma factors MucA and MucB which sequester AlgT/U to prevent transcriptional activation. During CF infections, loss of function mutations in MucA or reduction in MucA/MucB interactions have been observed, leading to reduced levels of MucA available for direct complexation with AlgT/U. This leads to upregulation and continual transcription of the *alg* operon, ultimately resulting in mucoid conversion and oversecretion of alginate.

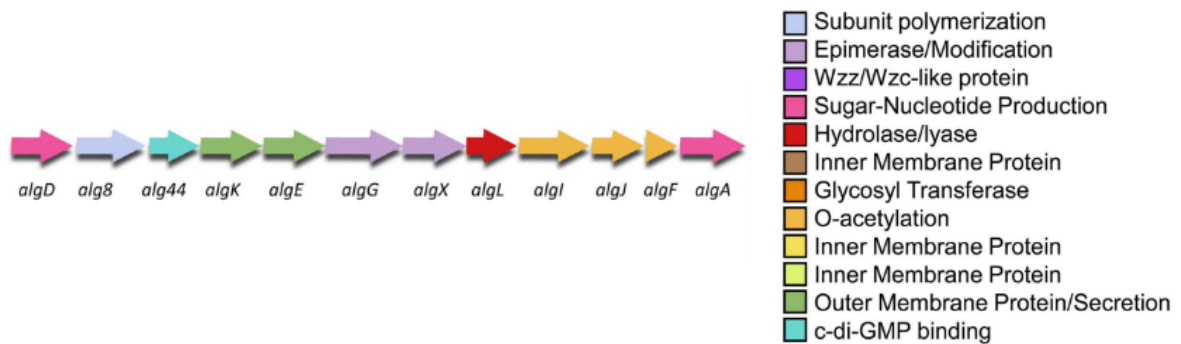


Figure 1.8: Genetic structure of the *alg* operon, where genes are colour coded by their proposed function.²¹

Following transcription, alginate biosynthesis can be divided into four stages: precursor synthesis, polymerisation and cytoplasmic membrane transfer, periplasmic transfer and modification and export through the outer membrane (Figure 1.9).²⁸

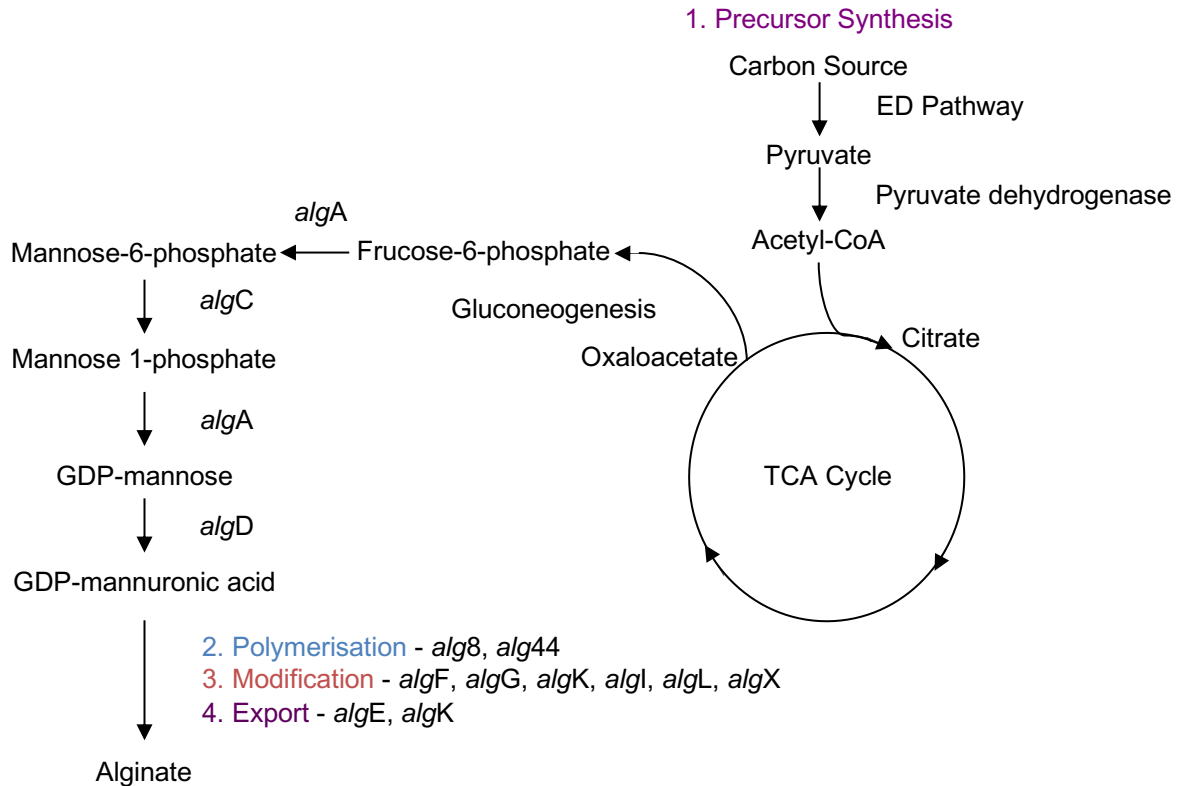


Figure 1.9: An overview of the alginate biosynthetic pathway.²⁹

1. Precursor Synthesis

The first stage, conversion of sugar metabolites into guanosine diphosphate mannuronic acid (GDP-ManA), is well characterised and occurs in the cytosol of the bacterial cell. First, a carbon source is converted into a pyruvate intermediate *via* the Entner-Douderoff (ED) pathway. This pathway uses two unique enzymes, 6-phosphogluconate and 2-keto-deoxy-6-phosphogluconate (KDPG) aldolase to catabolise glucose. Next, pyruvate is converted into acetyl CoA which enters the tricarboxylic acid cycle (TCA cycle). The oxaloacetate formed in this cycle undergoes gluconeogenesis to form fructose 6-phosphate, which is then transformed into mannose 6-phosphate. This reaction is catalysed by

phosphomannose isomerase (PMI), encoded for by *algA* – a bifunctional protein that also has GDP-mannose pyrophosphorylase (GDP-ManPP) activity. Directed towards the alginate biosynthetic pathway, mannose 6-phosphate is directly converted into mannose 1-phosphate *via* phosphomannomutase, a gene product of *algC*. Next, the GDP-ManPP activity of *algA* is utilised, catalysing the conversion of mannose 1-phosphate into GDP-mannose (GDP-Man). The final stage is the oxidation of GDP-Man into GDP-ManA *via* GDP-mannose dehydrogenase (GMD), *algD*.^{28,29}

2. Polymerisation and Cytoplasmic Membrane Transfer

Prior to polymerisation, the GDP-ManA precursor must be transferred across the cytoplasmic membrane into the cytosol. Polymerisation is one of the most poorly understood aspects in this biosynthetic pathway, as a suitable polymerase has not been purified and fully characterised to date.²⁸ The most plausible alginate polymerase enzyme was suggested as *alg8* in 2006 from ¹⁴C-labelling studies.³³ This gene is thought to be related to class II glycosyltransferases (GTs), enzymes that catalyse reactions between glycosyl acceptors and donors to form oligosaccharides. Additionally, it has also been found to have structural similarities with other functionally-related enzymes such as cellulose synthase.²⁹ The inner membrane protein *Alg44* is also known to be required for polymerisation, with no secretion of alginate fragments shown in *alg44*-deletion mutants.³⁴ Binding of *Alg44* to the signalling molecule bis(3'-5')-cyclic dimeric guanosine monophosphate (c-di-GMP) is imperative for alginate biosynthesis and provides further control of the biosynthetic pathway at post-translational level.³¹ The relationship between these

two gene products is still under scrutiny, with the two likely interacting as part of wider signalling pathways, amongst other proteins involved in later stages of alginate biosynthesis.

3 & 4. Periplasmic Transfer, Modification and Export

Once polymerised, the polymannuronate chain is translocated across the periplasm *via* a multiprotein scaffold, known to contain the periplasmic proteins *algG*, *algK* and *algX*. These proteins direct the polymer and protect it from the action of periplasmic lyase enzymes such as *algL*, responsible for the degradation of alginate.³⁵ Modification, the penultimate stage of alginate biosynthesis, takes place exclusively in the periplasm, implying that all modification appears to take place at polymer level opposed to monomer level.²⁸ The first step in modification is acetylation of the polymannuronate chain, utilising a series of acetyltransferase enzymes, encoded for by *algI*, *algJ*, *algF* and *algX*. Occurring solely on ManA residues, O-acetylation takes place at C2 and C3 positions, preventing the epimerisation of ManA into GulA – a process catalysed by C5-mannuronan-epimerase, *algG*. Additionally, as O-acetylation also prevents the action of *algL* degrading the alginate chain this process is key to controlling both ManA/GulA ratio and chain length. *AlgG* is the only enzyme that has been discovered with epimerase activity in *P. aeruginosa* to date³⁶, with the isolated alginate found to contain a majority of ManA residues which are interspersed randomly with GulA residues. The final stage in alginate biosynthesis is export, involving the genes *algE* and *algK*. Considerable information is known about *algE*, with the crystal structure being deduced by Whitney *et al.* in 2011.³⁷ *AlgE* is an outer membrane protein that is incorporated into lipid bilayers, and has

been found to have an electropositive pore structure which has high selectivity for negatively charged alginate, proving essential for its intact secretion. Deletion mutants of *algK* suggest that it is involved in the localisation of *algE*, therefore it is thought that the two proteins may interact to form a unique secretin structure that is different from other bacterial polysaccharide secretory complexes.²¹

1.2.2 Biofilm formation

Defined as “*surface-attached communities of bacteria embedded in an extracellular matrix of biopolymeric substances*”, biofilms present many difficulties in the areas of sanitation and healthcare as they are capable of growing on a variety of mediums, including water pipes and primary care medical devices such as catheters.³⁸ A variety of components, including microbial EPS, proteins and extracellular DNA (eDNA) are present within the matrix. Biofilm formation is also commonly observed during chronic infections caused by *P. aeruginosa* (Figure 1.10), where they play an important role to provide the bacteria with structural stability and protection from host-defence mechanisms and antibiotic treatment.

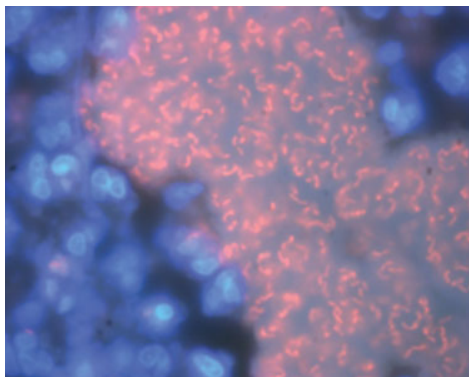


Figure 1.10: *P. aeruginosa* biofilm from an infected CF lung obtained using confocal laser scanning microscopy.^{40,41}

In a biofilm, the bacteria exist in architecturally and biochemically distinct forms compared to their free-swimming counterparts, and it is reported that when contained within a mature biofilm, they can develop an antibiotic resistance profile that is up to one thousand times greater than that of its planktonic equivalent.^{27,39}

Given the abundance of alginate produced by mucoid strains of *P. aeruginosa*, this EPS serves as the main matrix component of such biofilms and contributes to the formation of large finger-like microcolonies. A mature biofilm can be formed in as little as 5-7 days *in vitro*, with the final composition consisting of several layers of cells encompassed within the matrix, of which pieces can detach and colonise new areas of the airway.^{42,43}

1.2.2.1 Psl and Pel

In contrast, the biofilm composition of wild-type, non-mucoid strains of *P. aeruginosa* is not dependent on the presence of alginate, instead being rich in two alternative EPS: Psl and Pel.

Encoded by the *Psl* operon, the chemical structure of Psl is proposed as a neutral pentasaccharide containing D-mannose, L-rhamnose and D-glucose in a 3:1:1 ratio.²¹ This structure is widely disputed, as anti-Psl monoclonal antibodies targeting one epitope were unable to bind synthetic Psl oligosaccharides synthesised by Li *et al.* in 2013 (Figure 1.11), suggesting additional modifications to the structure of Psl are yet to be discovered.⁴⁴ Psl plays an important role in the initiation of biofilm formation, promoting both cell-cell and cell-surface interactions. In mature biofilms, Psl is associated with caps of mushroom-like microcolony formation to form a complex meshwork that regulates the adhesion of biofilms to the surface, whilst also

providing cells with protection against oxidative stress and a broad spectrum of antibiotics.^{45–47}

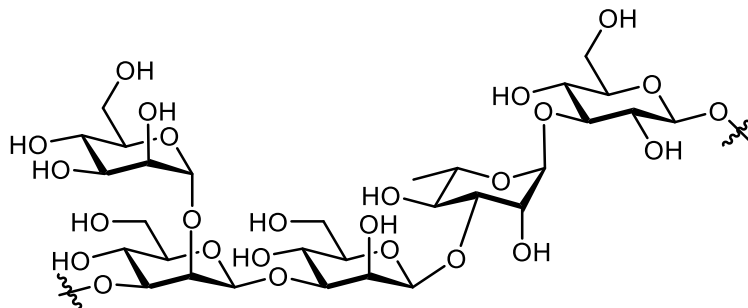


Figure 1.11: Proposed chemical structure of Psl.

The chemical structure of Pel has been recently described as a partially acetylated *N*-acetylgalactosamine and *N*-acetylglucosamine containing polysaccharide, joined by 1,4-glycosidic linkages. Under acidic conditions, Pel is positively charged, permitting crosslinking to eDNA within biofilms.^{48,49} In addition to its involvement in cell-cell interactions, its most important role is in the formation of a pellicle at the air-liquid interface, which comprises a layer of proteins embedded within the extracellular matrix.⁵⁰

The biosynthetic pathways of Psl and Pel have not yet been fully elucidated, however they are believed to be synthesised by two opposing biosynthetic mechanisms. Evidence suggests that the Psl pathway resembles an isoprenoid lipid carrier dependent mechanism, similar to that of *Escherichia coli* group 1 capsular and extracellular polysaccharides. The *psl* operon is predicted to code for at least 12 proteins involved in Psl biosynthesis (see Figure 1.12).^{21,51}

On the other hand, Pel biosynthesis is likely to proceed *via* a mechanism more closely related to that of alginate and bacterial cellulose biosynthesis, that is lipid carrier independent. As information regarding Pel is limited, with only a handful of the seven *Pel* gene products (Figure 1.12) having been experimentally examined, the biosynthetic model cannot yet be confirmed. Research does however suggest that notable differences that distinguish Pel from other secretion systems exist.²¹

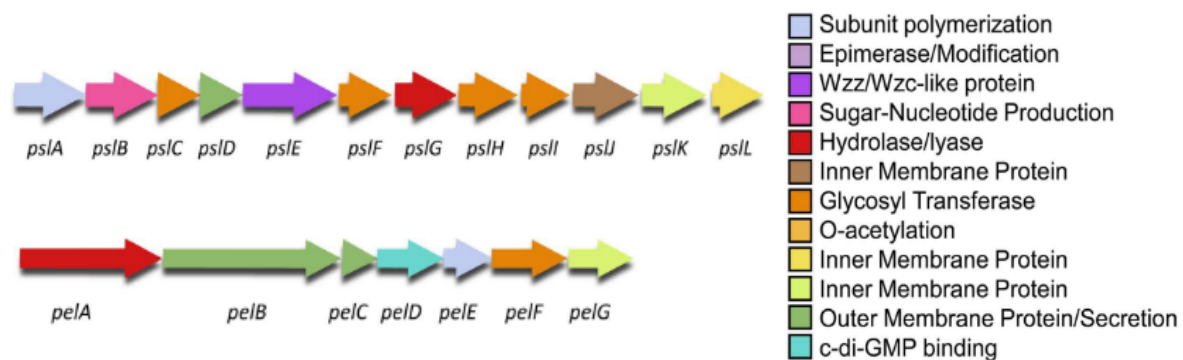


Figure 1.12: Genetic structure of the *Psl* and *Pel* operons, where genes are colour coded by their proposed function.²¹

1.2.3 Antibiotic resistance

P. aeruginosa is ranked amongst 'superbugs' such as Methicillin-resistant *Staphylococcus aureus* (MRSA) and *Clostridium difficile* because of its multi-drug resistant profile.⁵² The difficulty faced in treatment of infections caused by *P. aeruginosa* can be associated to two categories of resistance. Intrinsic resistance refers to chromosomally encoded resistance mechanisms, whereas acquired resistance is achieved *via* chromosomal DNA mutations that modify existing proteins. This can often be the result of genetic material transfer from alternative species or genera.⁵³

The *P. aeruginosa* genome naturally encodes for several resistance genes, including at least two classes of β -lactamases. The class C β -lactamase, cephalosporinase, is encoded by *ampC* and the class D variant oxacillinase is encoded by *poxB*. When exposed to benzylpenicillin or narrow-spectrum cephalosporins, *ampC* expression is induced by two mechanisms: induction and derepression. When significantly high levels of *ampC* are reached, *P. aeruginosa* becomes resistant to almost all classes of β -lactams except carbapenems, which are reserved for serious infections involving multi-drug resistant bacteria.^{54,55} Resistance to aminoglycoside antibiotics by *P. aeruginosa* is caused by chromosomally encoded or acquired aminoglycoside-modifying enzymes, of which some strains have more than one of these enzymes, resulting in broad-spectrum resistance.⁵⁶

Reducing the amount of antibiotic that can accumulate in the cytoplasm is also an important resistance mechanism for *P. aeruginosa*, of which two mechanisms exist: membrane impermeability and efflux-mediated resistance.

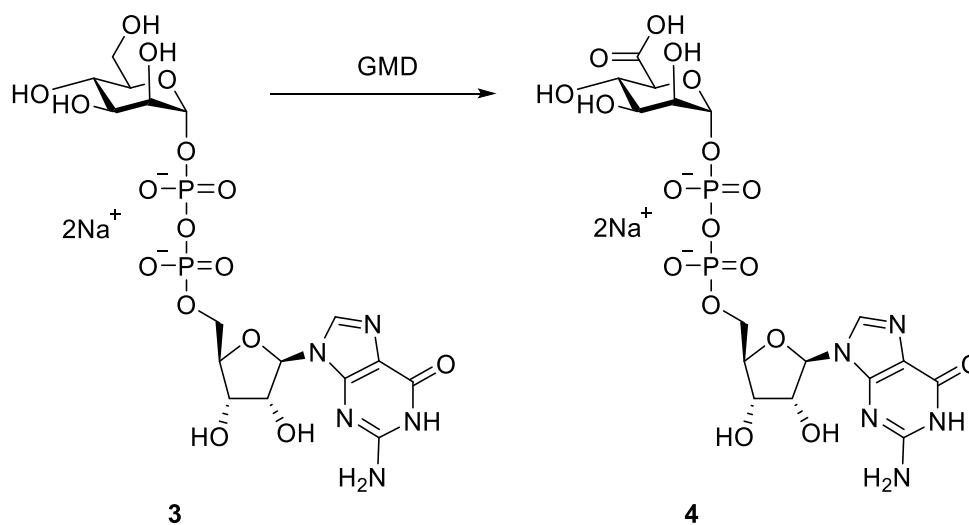
The outer membrane of Gram-negative bacteria naturally prevents the passage of large hydrophilic molecules into the cell, therefore in order to enter they must pass through a porin, most likely OprF. Several classes of antibiotic including β -lactams, aminoglycosides, tetracyclines and quinolones can diffuse into the cell *via* this protein channel; however, dysfunction of such porins decreases the susceptibility of *P. aeruginosa* to antibiotic treatment. Whilst alterations to OprF does not correlate significantly to antibiotic resistance, mutations that result in decreased transcription and translational production of the OprD porin is linked to resistance against carbapenems.⁵⁷

Efflux pumps belonging to the resistance-nodulation-division family are the most significant contributors to antibiotic resistance in *P. aeruginosa*, with a total of twelve systems encoded by the genome. Involved in intrinsic resistance, such pumps comprise a periplasmic membrane fusion protein (MFP), outer membrane factor (OMF) and cytoplasmic membrane transporter. The MexAB-OprM efflux pump was the first multi-drug efflux pump identified in *P. aeruginosa*, responsible for the export of numerous classes of antibiotic out of the cell, including β -lactams, tetracyclines, macrolides and fluoroquinolones.^{58,59}

1.3 Strategic Bacterial Biosynthesis Enzymes

The opportunistic nature of *P. aeruginosa* presents a major threat to immunocompromised patients, given its high level of intrinsic resistance mechanisms that leads to a multi-drug resistance profile. As this bacterium becomes more resistant to antibiotics, alternative approaches are vital to ensure such infections can be treated, with research currently ongoing into immunotherapy and vaccination. Conversion of *P. aeruginosa* to its mucoid phenotype is a major virulence factor, contributing to high morbidity and mortality rates amongst infected patients. Given the breadth of information available regarding the biosynthesis of alginate, many enzyme targets could be investigated as potential alternative treatments for such infections.

One of the most promising targets is guanosine diphosphate-mannose dehydrogenase (GMD), which catalyses the conversion of GDP-Man **3** into GDP-ManA **4** (Scheme 1.1), the constituent building block of alginate.



Scheme 1.1: Oxidation of GDP-Man **3** to GDP-ManA **4** by GMD.

Evidence for its role as a key regulatory enzyme in alginate biosynthesis was discovered following metabolic studies in 1993, which revealed that **3** accumulated in all strains of *P. aeruginosa*, whilst the product **4** was only detected in mucoid strains at considerably lower concentrations than those of **3**.⁶⁰ GMD is a logical target to block alginate biosynthesis as there is no equivalent enzyme found in humans, hence the possibility of detrimental side effects from its inhibition is considerably reduced.

1.3.1 NAD⁺-dependent dehydrogenases

GMD belongs to the family of nicotinamide adenine dinucleotide (NAD⁺) dependent four-electron-transfer dehydrogenases, that catalyse the oxidation of a pyranose to a uronic acid using NAD⁺ as co-factor. This reaction occurs within a single active site without the release of an aldehyde intermediate.

Examples of related dehydrogenases include uridine diphosphate-glucose dehydrogenase (UGD) and uridine diphosphate-*N*-acetyl-mannosamine dehydrogenase (UNAcMD). These enzymes share a common catalytic cysteine residue and employ similar reaction mechanisms but show some variation in sequence homology and domain organisation.

Two other enzymes, 3-hydroxy-3-methylglutaryl coenzyme A reductase (HMG-CoA reductase) and histidinol dehydrogenase (HisD) also belong to this family. However, they vary in terms of catalytic residue and, in the case of HisD, mechanism of action.

1.3.1.1 UDP-glucose dehydrogenase and UDP-*N*-acetyl-mannosamine dehydrogenase

The enzymatic activity of UDP-glucose dehydrogenase (UGD) was first reported in 1954 following its isolation from bovine liver. Catalysing the oxidation of UDP-glucose to UDP-glucuronic acid, this sugar-nucleotide is an important building block in biosynthesis of glycosaminoglycans such as heparan sulfate and capsular polysaccharides. It is also essential for Phase II glucuronidation, an important biotransformation in preparation for excretion in mammals and bacteria.

Exhaustive studies of UGD suggested the enzyme followed a '*bi-uni-uni-bi ping-pong*' mechanism which was catalysed by a Cys²⁶⁰ residue. Following oxidation of UDP-glucose to the aldehyde, the reaction proceeds *via* thiohemiacetal and thioester intermediates before hydrolysis and release of UDP-glucuronic acid.⁶¹ Cys²⁶⁰ was proven to be the catalytic residue in both mammalian and bacterial UGD, with studies showing Cys²⁶⁰Ser mutants form covalently bound ester intermediates that were hydrolysed slowly and accumulated.⁶²

Uridine diphosphate-*N*-acetyl-mannosamine dehydrogenase (UNAcMD) catalyses the conversion of UDP-*N*-acetyl-mannosamine to UDP-*N*-acetyl-mannosaminuronic acid. *N*-acetyl-mannosaminuronic acid is a key component of many bacterial capsular polysaccharides including those of *Staphylococcus aureus*. This dehydrogenase adopts the same dimeric conformation as UGD and utilises a catalytic Cys²⁵⁸, with the residues responsible for acid/base catalysis, tetrahedral intermediate formation and hydride transfer also conserved. Whilst this suggests the same mechanism of action is employed, unlike UGD UNAcMD is also regulated by

a redox-switch mechanism and tyrosine phosphorylation, a conserved mechanism for bacteria to control EPS production.⁶³

1.3.1.2 HMG-CoA reductase and histidinol dehydrogenase (HisD)

HMG-CoA reductase catalyses the interconversion of HMG-CoA to mevalonate, the first step in isoprenoid biosynthesis. Unlike other reductases in the family, the involvement of catalytic cysteine residues was disproved following site-directed mutagenesis. Instead, glutamate and histidine residues that are essential for catalysis have been identified.⁶⁴

HisD is a homodimeric zinc metalloenzyme that catalyses the conversion of L-histidinol to L-histidine. It was initially thought that Zn^{2+} had a direct role in catalysis, however this was disproved in 2002 by Barbosa *et al.* who concluded that the Zn^{2+} was only required for positioning of the reaction intermediates and the catalytic residue was in fact His³²⁷.⁶⁵

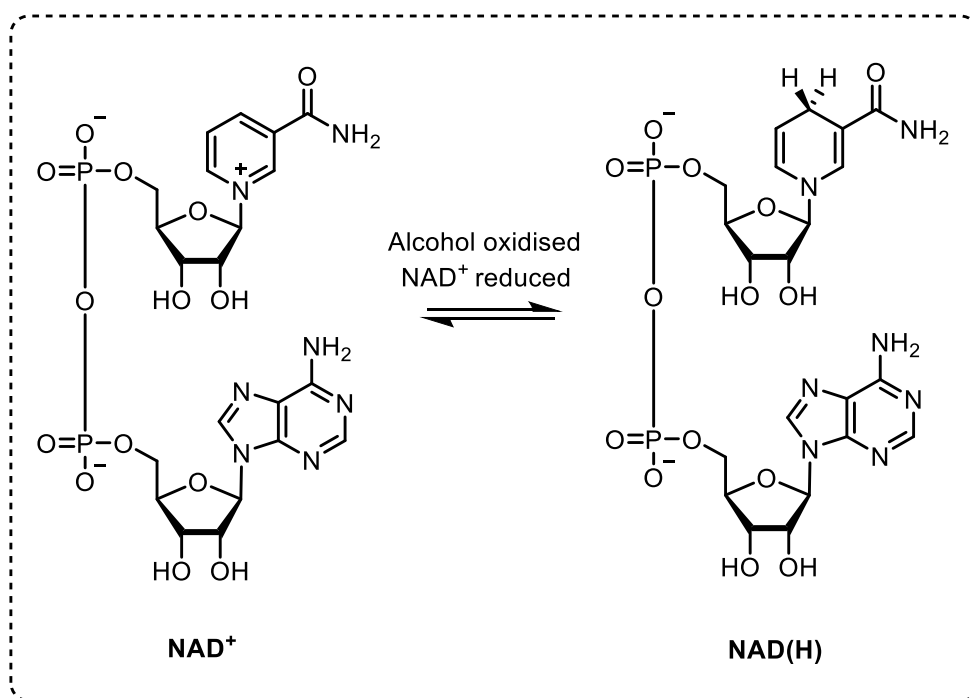
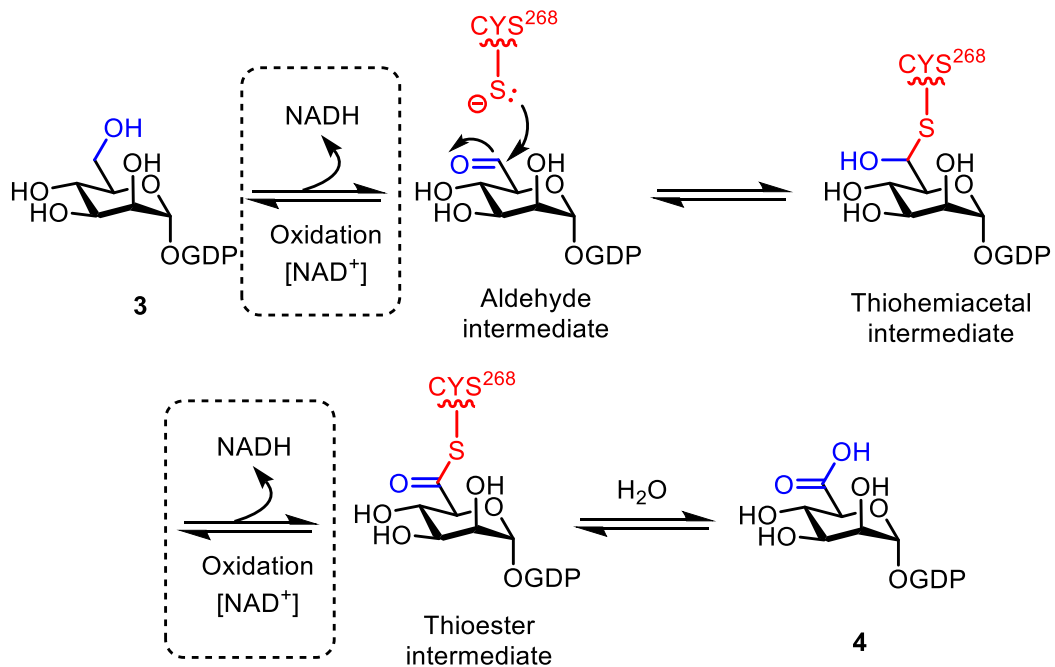
1.3.2 GDP-mannose dehydrogenase (GMD)

1.3.2.1 Crystal structure and catalytic mechanism

The crystal structure of GMD was solved by Snook *et al.* in 2003⁶⁶, and revealed two distinct domains of similar size, connected by a long α -helix consisting of 33 residues. The monomer exists in an unusual open conformation with N- and C-terminal domains located on opposite sides of the connecting α -helix. Two monomers associate to form an intertwined dimer that places the N-terminal domain of monomer A in close contact with the C-terminal domain of monomer B. Therefore, GMD can be described as a domain-swapped dimer, unlike in UGD where chains from the same monomer pack against one another.

Similarly to UGD, the active site of GMD is made up of 80 residues, approximately half from each monomer, forming a large binding pocket for NAD^+ and GDP-ManA **4** that lies within a cleft between the two domains. The N-terminus is responsible for NAD^+ cofactor binding and the C-terminus makes contacts with the substrate/product. The total surface area of the active site spans 1900 \AA^2 and the ligands were found to be deeply buried, with only the edges of their purine bases exposed to solvent.

Based on information known about UGD, GMD catalysis has been proposed to take place *via* a 'bi-uni-uni-bi ping-pong' reaction mechanism in 4 discreet steps, outlined in Scheme 1.2.⁶⁷



Scheme 1.2: Proposed mechanism of GMD catalysed oxidation of GDP-Man 3 to GDP-ManA 4 and structures of NAD⁺ and NAD(H). ⁶⁶

The C6-OH of GDP-Man **3** is first oxidised to an aldehyde, utilising one equivalent of NAD⁺. Following the addition of the Cys²⁶⁸ side chain into the carbonyl to form a thiohemiacetal intermediate, further oxidation using a second equivalent of NAD⁺ affords a thioester intermediate which is hydrolysed to deliver GDP-ManA **4**.

The nucleophilic thiol residue was proposed to be Cys²⁶⁸, with the crystal structure showing distances of 3.3-3.5 Å between Cys²⁶⁸ and the carboxylate oxygen atoms in GDP-ManA **4** (Figure 1.13). Upon rotation this distance is further reduced to 2.4 Å and given the potency of the nucleophile it was proposed that the thiolate anion acts as the active species. Cysteine side chains have a typical pK_a value of 9.0, therefore factors stabilising the thiolate anion would be expected within the active site. The residue proposed to facilitate this is Lys²⁷¹, which upon rotation of the side chain is within 3.0 Å of the thiolate. Alternatively, a helix dipole effect may stabilise Cys²⁶⁸, as it is located immediately prior to an α-helix in the C-terminal domain therefore the partial positive charge of the dipole could result in stabilisation.

The residue proposed as the general acid/base catalyst is Lys²¹⁰ from monomer A, located 2.9 Å from the carboxylate oxygen or a tetrahedrally coordinated water molecule. Hydrolysis of the thioester intermediate is achieved by the activation of a water molecule by Glu¹⁵⁷, located less than 3.0 Å from the carboxylate oxygen.

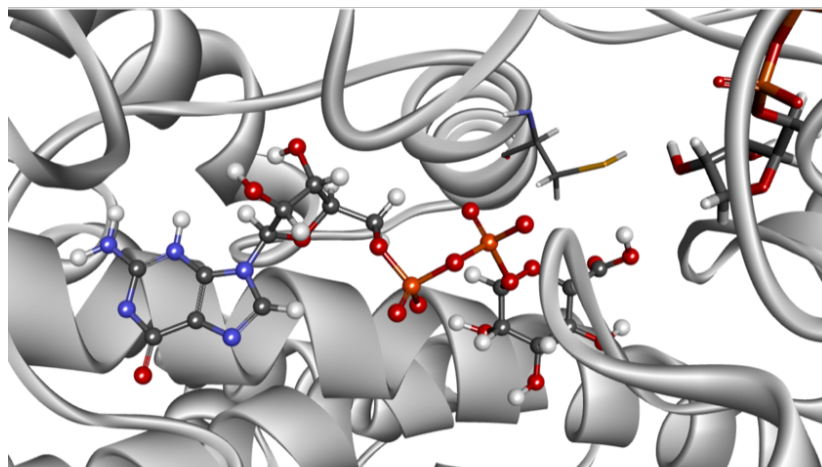


Figure 1.13: Molecular docking image showing GDP-ManA **4** in the active site of GMD in close proximity to Cys^{268.66}.

1.3.2.2 Structure-based inhibitor design

Even before the identification of the key Cys²⁶⁸ residue, microbial metabolite screening results indicated that the macrolide antibiotic erythromycin A **5** and penicillic acid **6** (Figure 1.14), a mycotoxin produced by many species of *Penicillium* and *Aspergillus* fungi, inhibited alginate production.

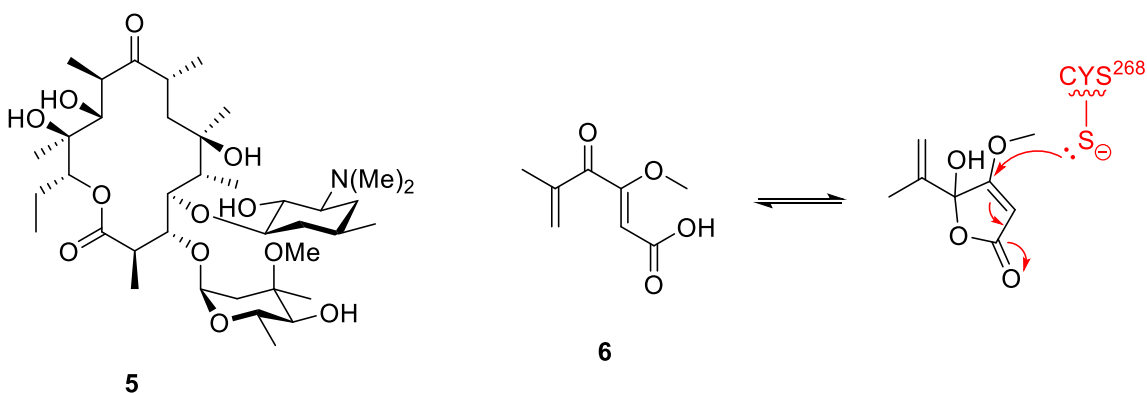


Figure 1.14: Chemical structures of erythromycin A **5** (left) and penicillic acid **6** (right), showing the conjugate addition of Cys²⁶⁸.

Morphological changes of a mucoid strain of *P. aeruginosa* to a non-mucoid colony in the presence of these compounds was observed on agar plates, and were successfully correlated to the inhibition of GMD through use of HPLC to estimate the total amount of alginate production per bacterial cell.⁶⁸

Previous reports also indicated that **6** was an inhibitor of alcohol and lactic dehydrogenases, however the mechanism by which GMD was inhibited was not yet understood.⁶⁹ Penicillic acid **6** contains a conjugated π -system, suggesting it irreversibly inhibits GMD by acting as a Michael acceptor to form a series of covalent adducts. Though **6** is too cytotoxic to be of relevance *in vivo*, the results revealed that it was not exclusively directed at the GMD active site and had low potency, with mass spectrometry data showing that several cysteine residues, including Cys²¹³, Cys²⁴⁶ and the catalytic Cys²⁶⁸ residue were alkylated by penicillic acid.⁷⁰

Based on this knowledge, a necessity for rational structure-based inhibitor design is apparent, however the synthesis of such biological probes has not been reported, with the exception of a publication in 1992 describing the synthesis of a GDP-6-ethynyl-mannose analogue **7** (Figure 1.15).⁷¹ Although this analogue was reported to show 75% inhibition of GMD at a concentration of 0.1 mM, the associated experimental procedures and characterisation data and inhibition studies were insufficiently detailed to provide convincing evidence of GMD inhibition.

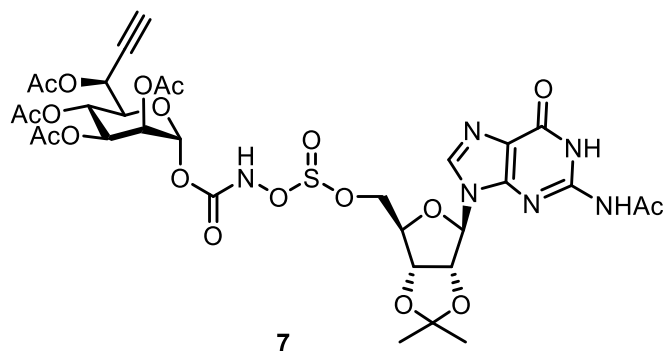


Figure 1.15: Chemical structure of GDP-6-ethynyl-Man analogue **7**.

Nevertheless, the work provided an important foundation for the rationale behind the synthesis of such derivatives, with potential for an array of functional groups capable of acting as inhibitors of GMD. Electrophilic GDP-Man probes incorporating alkyne, α,β -unsaturated carbonyl, epoxide or nitrile functionalities (compounds **8** to **11** respectively) are all plausible species that could intercept a nucleophilic cysteine residue with the potential to reduce or inhibit the production of GDP-ManA. The proposed mechanism of each analogue is outlined in Figure 1.16.

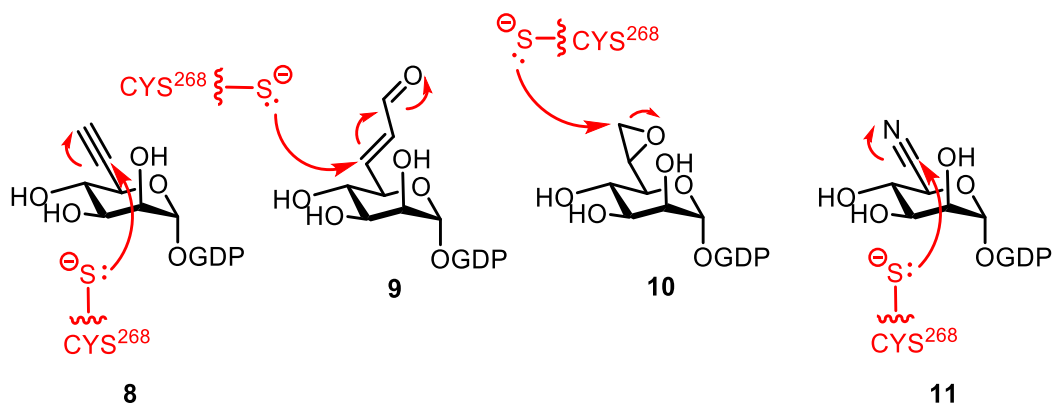


Figure 1.16: Functional groups that could be incorporated into GDP-Man analogues to explore the mechanism of GMD: alkyne, α,β -unsaturated carbonyl, epoxide, nitrile and potential interactions with Cys²⁶⁸.

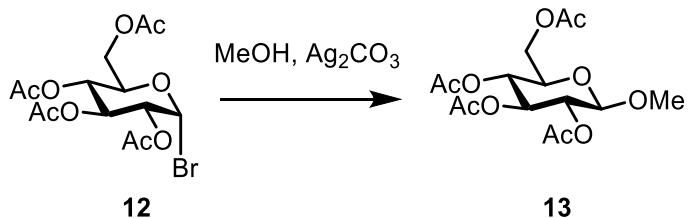
1.4 Synthetic Carbohydrate Chemistry

The importance of oligosaccharides and sugar-nucleotides in medicinal chemistry and in biochemical applications cannot be understated. Despite this, progress in synthetic carbohydrate chemistry lags in comparison to other areas, complicated by a lack of general methods for their routine preparation. Hindering the development of robust synthetic methods are their high polarity, poor solubility in organic solvents and the susceptibility of glycosidic and diphosphate linkages to hydrolysis.⁷²

1.4.1 Background to carbohydrate glycosylation

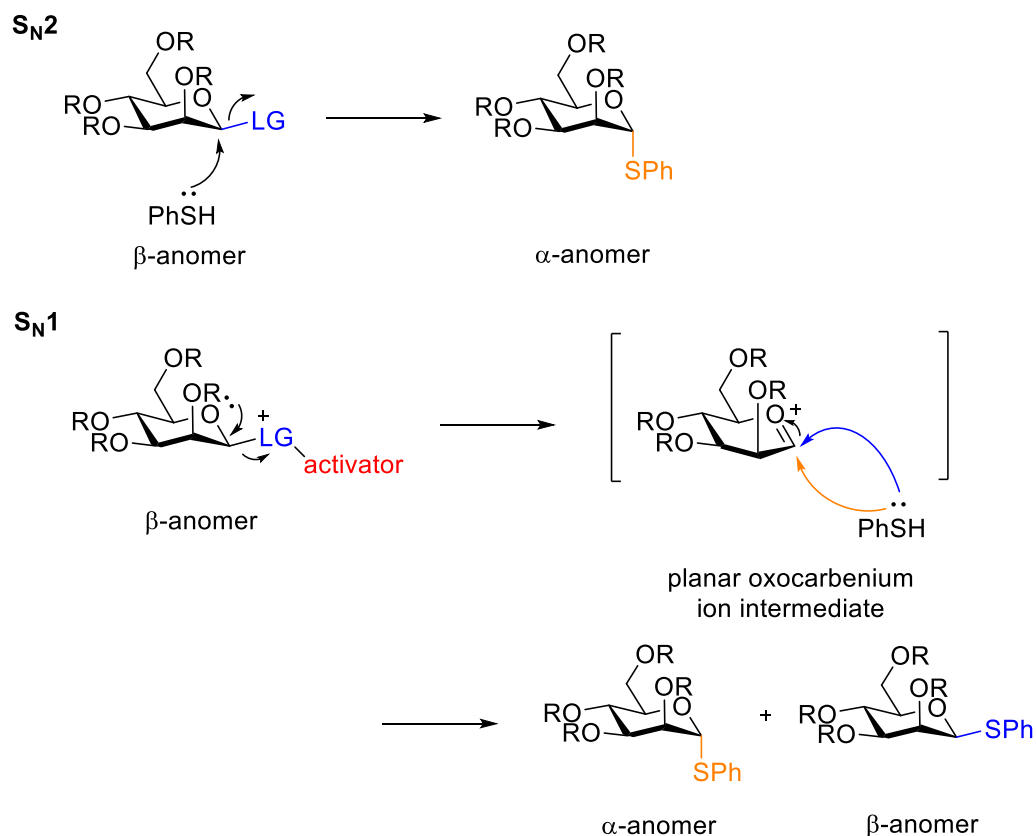
Given the inherent reactivity of hydroxyl groups present in free sugars, carbohydrate syntheses are reliant on protecting group strategy. This methodology relies on the orthogonal nature of protecting groups, essential to exploit the varying reactivity of hydroxyl groups, i.e. 1° versus 2° alcohol reactivity to allow selective protection in the synthesis of increasingly complicated structures. Coupled with the difficult production of oligosaccharides with the desired glycosidic stereochemistry, this unfortunately leads to long, multi-step reaction sequences that often require purification between each step, diminishing yields of the target structures.

Central to carbohydrate chemistry is the formation of the glycosidic bond, with the earliest method reported by Koenigs and Knorr at the beginning of the 20th century.⁷³ The original reaction involved the coupling of acetobromoglucose **12** (glycosyl donor) with methanol (glycosyl acceptor) using silver carbonate (Ag₂CO₃) as the promoter to form **13** (Scheme 1.3).



Scheme 1.3: Original Koenigs-Knorr glycosylation conditions.

Anomeric substitution is considered to take place by both S_N2 and S_N1 mechanisms, with some substrates capable of reacting through both pathways. The mechanism by which substitution takes place determines the anomeric stereochemistry of the product, outlined in Scheme 1.4. An S_N2 reaction proceeds *via* a concerted mechanism, with the nucleophile attacking from the opposite face at 180° to the leaving group (backside attack). Upon departure of the leaving group, the resultant product has an inversion of stereochemistry. In an S_N1 reaction, the leaving group must be suitably activated prior to its removal, which then results in the formation of a planar oxocarbenium ion intermediate. The nucleophile can attack either face of the oxocarbenium ion, leading to the formation of an anomeric mixture.

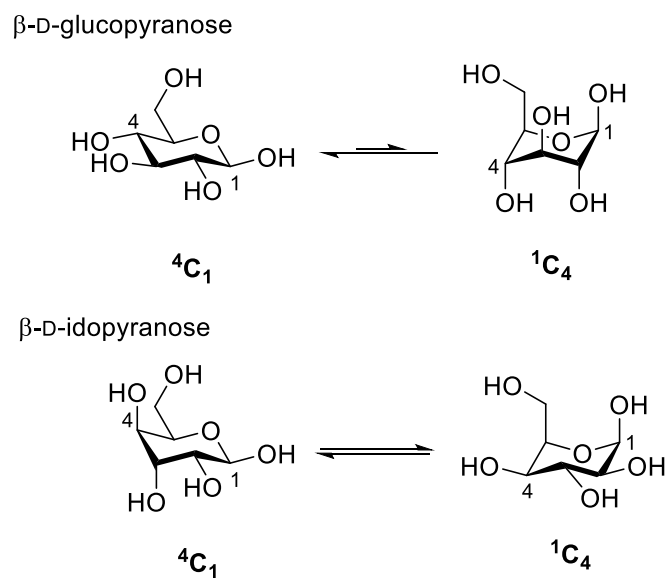


Scheme 1.4: S_N2 and S_N1 mechanisms of anomeric substitution.

The 6-membered ring of a monosaccharide primarily exists in two isomeric chair conformations, denoted ⁴C₁ and ¹C₄. The letter C stands for chair and the numbers correspond to the carbon atoms situated above or below the plane of the chair, which is made up of C2, C3, C5 and the ring oxygen. Pyranoses can also adopt several other conformations, including half-chair, boat and skew however the chair conformation predominates.⁷⁴

The conformation in which a pyranose exists is governed by the relative stability of its two possible chair conformations, with one of which often being energetically unfavourable due to undesired repulsion between 1,3-diaxial ring substituents (Scheme 1.5).

This is observed in β -D-glucopyranose, where the 4C_1 conformation is favoured over 1C_4 and results in a free energy difference of 25 kJ/mol between the two chair forms. Conversely, the energy difference between the two chair conformations of β -D-idopyranose is small therefore both conformations can be observed in its 1H NMR spectra.



Scheme 1.5: Comparison of 4C_1 and 1C_4 chair conformations in pyranoses.

The identity of the group at the C2 position on the donor must be considered carefully in glycosylation reactions, as the anomeric stereochemistry is controlled by two different effects. When the group at C2 is a non-participating group, such as *O*-benzyl, the anomeric effect dominates. Two explanations for the origin of the anomeric effect are described in the literature: *endo* and *exo*. In both instances a non-bonding electron pair on the endocyclic $2sp^3$ hybridised oxygen atom plays an important role, forming a dipole pointing in the exocyclic direction. The polarised bond between the anomeric carbon and exocyclic heteroatom form another dipole.

In 4C_1 conformations, electron density from the non-bonding $2sp^3$ lone pair of oxygen is donated into the empty anti-bonding (σ^*) orbital of the C-X bond, where X is an electronegative substituent such as fluorine, oxygen, or sulphur. As the orbitals are aligned in a syn-periplanar configuration when the C-X bond adopts an axial position, they can mix and a hyperconjugative $\eta\text{-}\sigma^*$ interaction is established. This is *the endo-anomeric effect*, made energetically possible due to the reduction in energy of the σ^* orbital by the electronegative substituent, resulting in a longer, weakened C1-X bond and a shorter, stronger O-C1 bond. The thermodynamically stable α -anomer is formed preferentially over the β -anomer, which cannot be stabilised as the orbitals are incorrectly aligned for overlap (Figure 1.17).

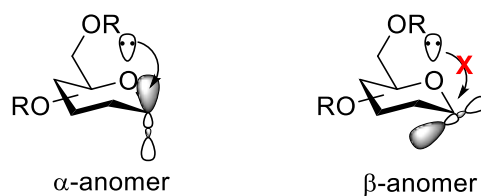


Figure 1.17: The *endo*-anomeric effect.

Alternatively, the *exo*-anomeric effect arises from rotation around the exocyclic C1-X bond, where the non-bonding electrons from the anomeric heteroatom occupy different three different positions. The most favourable is rotamer (b) as an overlap between a non-bonding orbital and σ^* orbital of the endocyclic O-C1 bond is possible. Whilst this is also possible in (c), it is less favourable because the bulky R-substituent is placed directly under the plane of the pyranose (Figure 1.18).

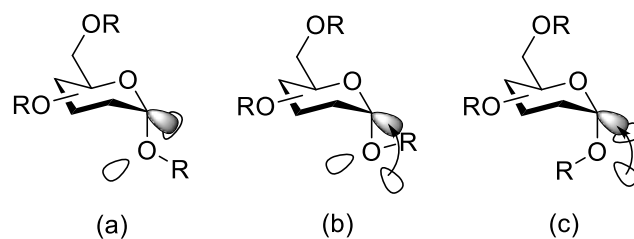
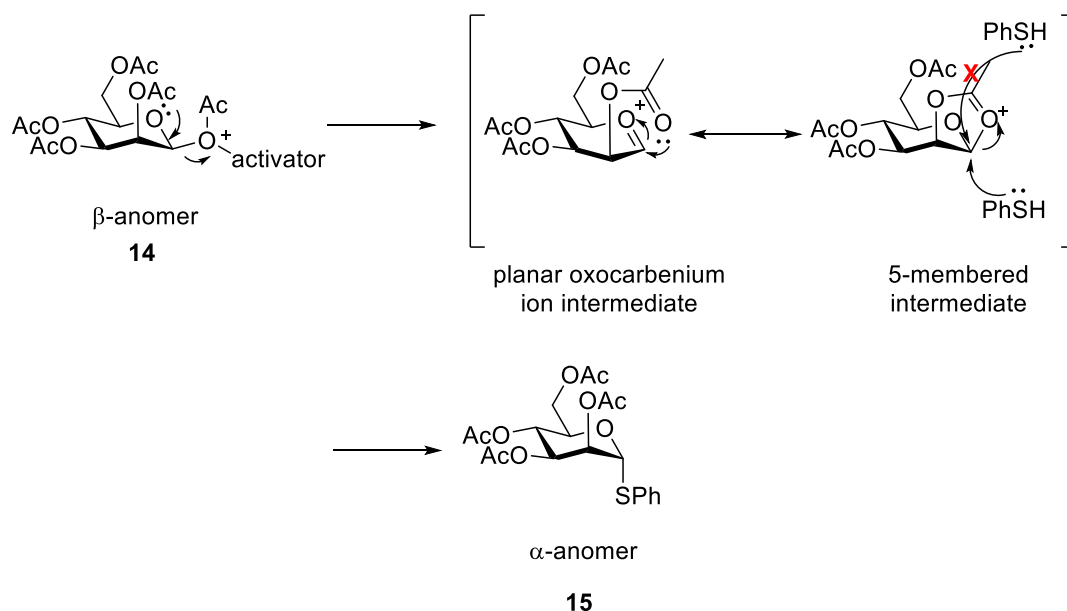


Figure 1.18: The *exo*-anomeric effect.

Alternatively, if the group at C2 is an ester, such as an *O*-acetyl or *N*-phthalimido group, the stereochemistry can be controlled *via* neighbouring group participation (NGP). Such groups can form 5-membered intermediates which lower the energy of the transition state, directing the mechanism by which the product forms by blocking either the top (β) or bottom (α) face of the ring (depending on the C2 stereochemistry). As illustrated in Scheme 1.6, following initial formation of the planar oxocarbenium ion intermediate in *per-O*-acetylated mannose **14**, the C2 ester attacks to form a 5-membered intermediate on the β -face. As this face is effectively blocked, the acceptor can only open the ring through attack from the α -face to yield the corresponding α -thioglycoside **15**.



Scheme 1.6: Mechanism for formation of **15** from per-O-acetylated mannose **14** using NGP.

1.4.2 Sugar-nucleotides

Sugar-nucleotides (nucleoside diphosphate sugars) are composed of a sugar linked to a nucleoside diphosphate and have important functions in carbohydrate metabolism and biosynthesis of glycoconjugates. These important species are of particular interest as carbohydrate-based tools to study biosynthetic pathways and as potential enzyme inhibitors. In mammalian cells, sugar-nucleotides most commonly contain a uridine or guanosine nucleoside diphosphate however thymidine nucleoside diphosphate sugars are also present in bacterial systems, with some examples shown below in Figure 1.19.

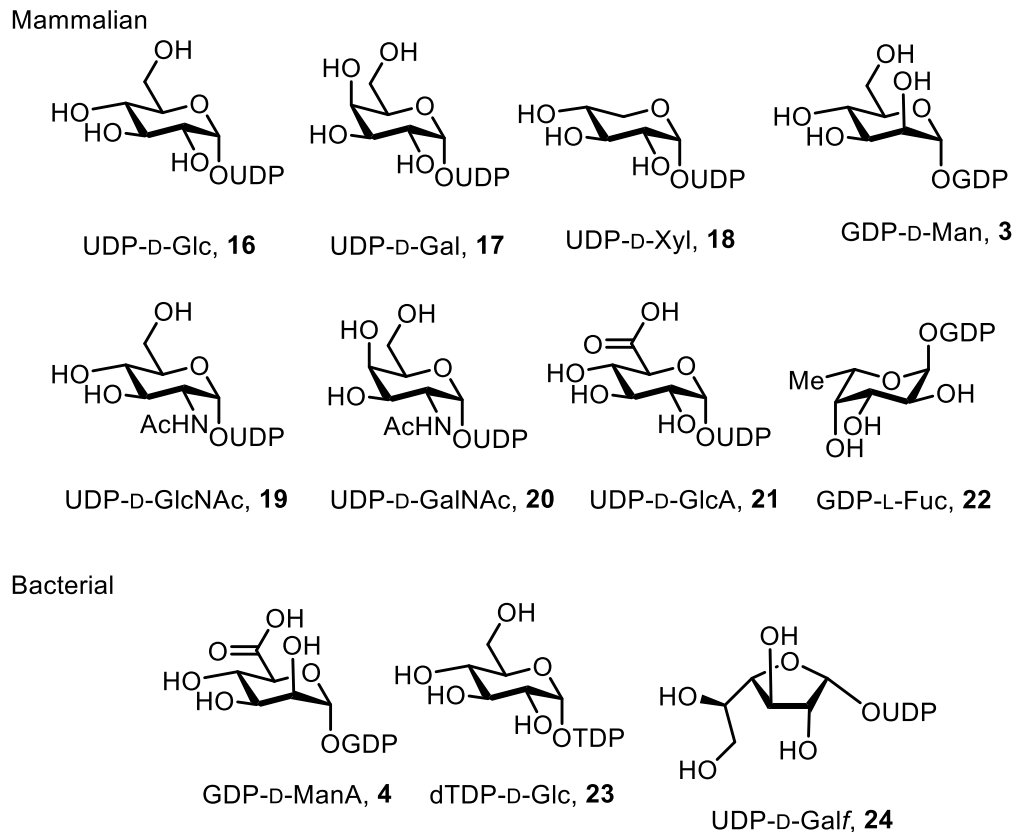
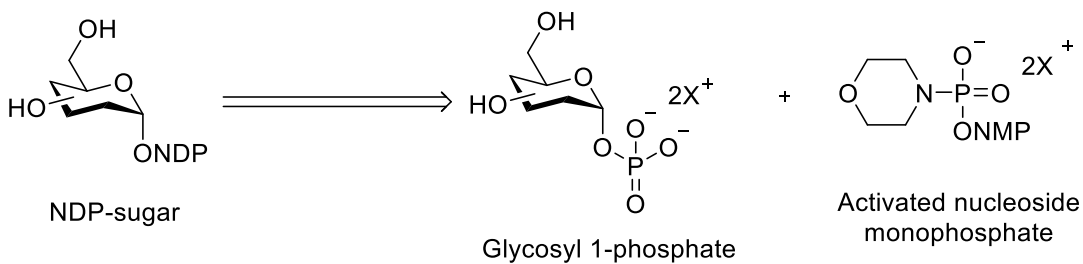


Figure 1.19: Chemical structures of mammalian and bacterial NDP-sugars.

The chemical synthesis of sugar-nucleotides most commonly involves the coupling of two monophosphate precursors, as shown in Scheme 1.7. The first is a glycosyl 1-phosphate, the source of the sugar moiety and the second is an activated nucleoside diphosphate species, which is attacked by the glycosyl 1-phosphate to form a diphosphate bond.

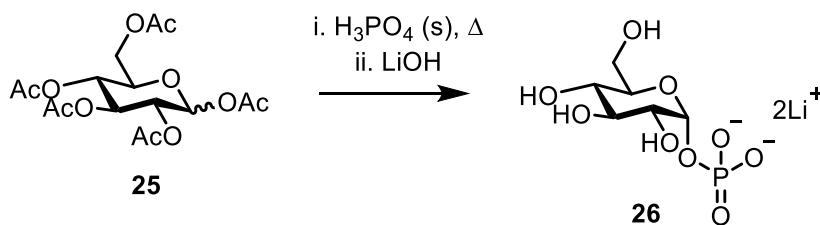


Scheme 1.7: Retrosynthetic analysis of NDP-sugar synthesis.

1.4.2.1 Synthesis of glycosyl 1-phosphates

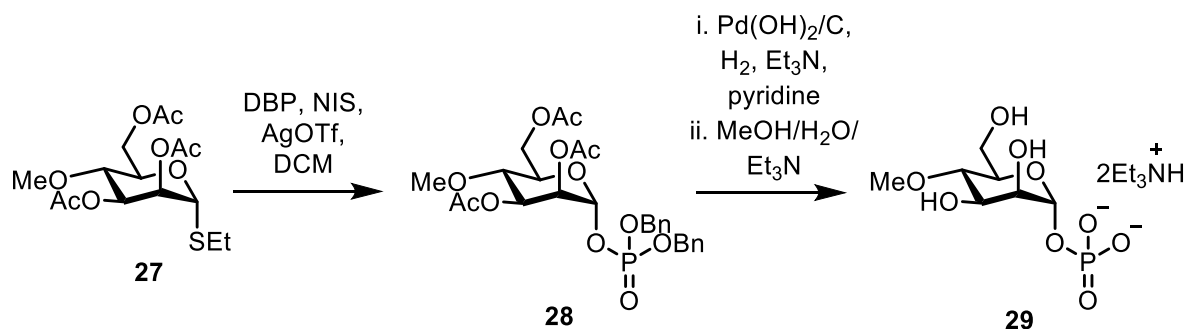
The synthesis of glycosyl 1-phosphates can be achieved through both chemical and enzymatic methodologies, with many literature procedures available for their preparation. The most well-established methods are discussed herein.

In 1962, MacDonald reported the synthesis of glycosyl 1-phosphates of glucose and galactose through reaction of their respective per-*O*-acetylated counterparts with H_3PO_4 (s) at elevated temperatures under high vacuum (Scheme 1.8).⁷⁵ Though its use has since been applied widely, the reaction scope is limited by the requirement for strictly anhydrous conditions and poor yields, typically $\leq 45\%$.



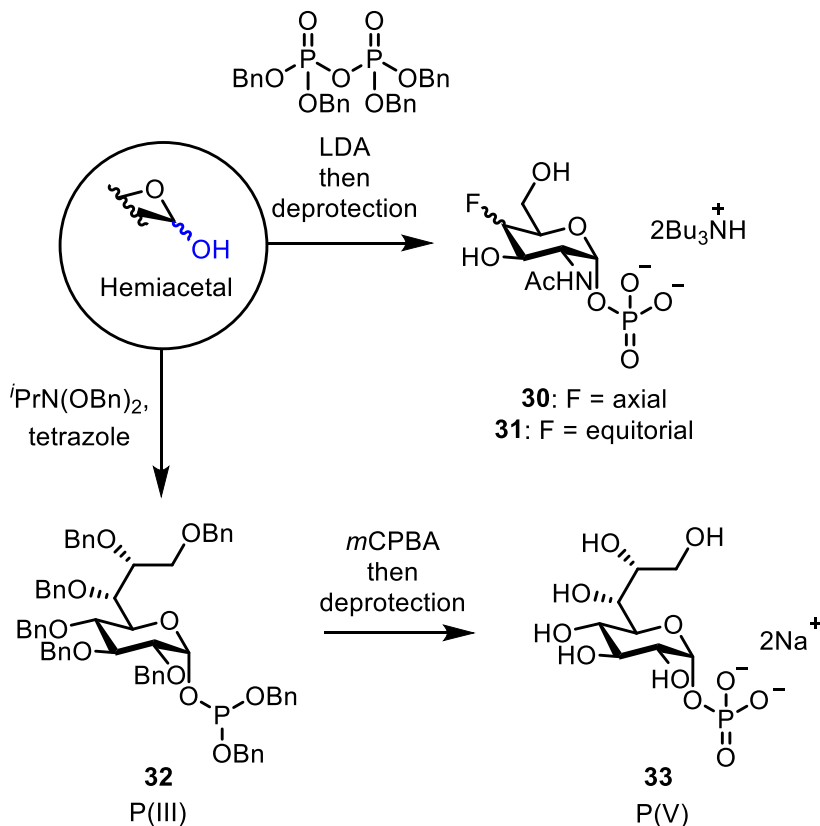
Scheme 1.8: MacDonal phosphorylation of per-*O*-acetyl-glucopyranose **25** to afford α -D-glucopyranosyl phosphate **26**.

Methodologies developed since this procedure usually involve the synthesis of an appropriate glycosyl donor, such as a thioglycoside or trichloroacetimidate which can be reacted with dibenzyl phosphate (DBP) in the presence of a promoter. Deprotection of the resultant glycosyl 1-phosphate is achieved by hydrogenolysis using palladium catalysts, shown in Scheme 1.9. This method was employed by Zou *et al.* in the synthesis of a series of mannose 1-phosphate analogues for use as substrates for GDP-ManPP.⁷⁶



Scheme 1.9: Synthesis of a 3-methoxy-mannopyranosyl phosphate **29** from thioglycoside donor **27**.

An alternative approach derives from the hemiacetal, where the corresponding glycosyl 1-phosphate can be synthesised from a variety of phosphorus sources either directly at the P(V) oxidation level or *via* a P(III) species, followed by oxidation. Schultz *et al.* utilised the electrophilic P(V) reagent tetrabenzyl pyrophosphate (TBPP) with lithium diisopropyl amide (LDA) as the base in their synthesis of 4-fluoro derivatives of GalNAc and GlcNAc. Modified glycosyl 1-phosphates **30** and **31** were afforded in high yields (>70%) with high α -selectivity reported.⁷⁷ The opposing strategy employs a phosphoramidite reagent, $i\text{Pr}_2\text{N}(\text{OBn})_2$ with tetrazole activation then subsequent oxidation to the desired P(V) species using *m*CPBA. This method has been used successfully towards the synthesis of octose 1-phosphate **33** and 6-deoxy-gulose 1-phosphate.^{78,79} A summary of the described methods is shown in Scheme 1.10.

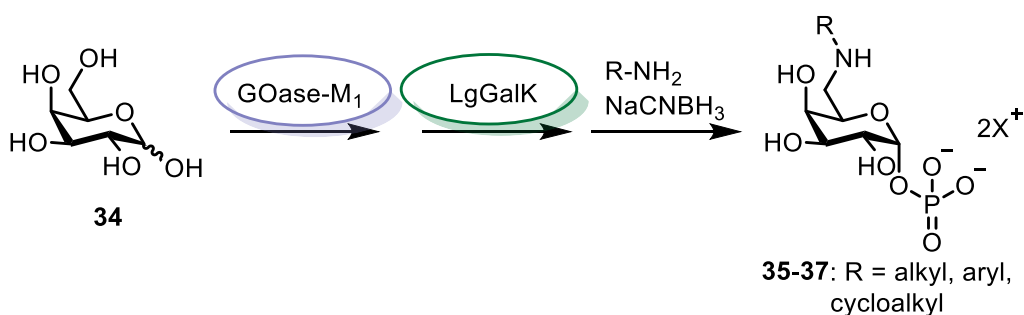


Scheme 1.10: Summary of strategies to access glycosyl 1-phosphates *via* a hemiacetal.

The enzymatic synthesis of glycosyl 1-phosphates from their corresponding hemiacetal using kinases is also frequently reported in the literature. This transformation can be complicated by unwanted phosphorylation at the C6-position and the limited substrate scope of many kinases with non-native sugars. In general, bacterial enzymes display greater promiscuity, hence greater promise to access modified target glycosyl 1-phosphates for use as chemical tools.

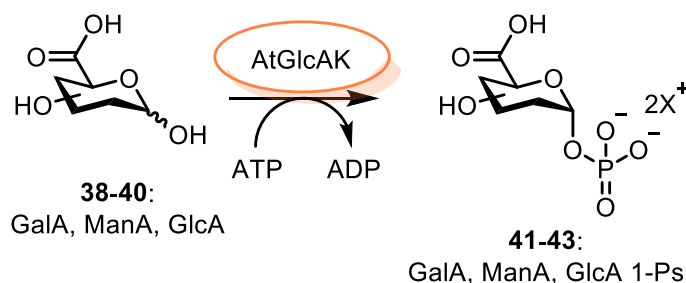
Kinases are regularly employed in one pot multi-enzyme (OPME) approaches towards the synthesis of sugar-nucleotides. Examples include SpGalK, a bifunctional kinase capable of synthesising a range of galactose and glucose 1-

phosphate derivatives, and a new bacterial galactokinase LgGalK.⁸⁰ This enzyme demonstrates high tolerance towards a broad range of substrates including deoxy and deoxy-fluoro galactose analogues. Recently, it has been utilised for the synthesis of C6-position modified galactose 1-phosphates using galactose oxidase (GOase-M₁). Following oxidation to the corresponding aldehyde and *in-situ* reductive amination, an array of 6-amino-6-deoxy-galactose 1-phosphate derivatives were afforded (Scheme 1.11).⁸¹



Scheme 1.11: One pot access to C6-position modified galactose 1-phosphates **35-37** using GOase-M₁ and LgGalK.

In 2015, Muthana *et al.* reported the use of the bacterial glucuronokinase AtGlcAK for a OPME approach to access UDP-uronic acids. The enzyme accepted galacturonic acid (GalA) and ManA in addition to glucuronic acid (GlcA) (**38-40**), producing the desired uronic acid 1-phosphates **41**, **42** and **43** in 31%, 95% and quantitative yields respectively for substrate evaluation against two GDP-sugar pyrophosphorylases (Scheme 1.12). The synthesis of uronic acid 1-phosphates using kinases is less well documented in the literature and any advances in this area is welcomed, given the importance of uronic acid containing sugar-nucleotides in bacterial systems.⁸²

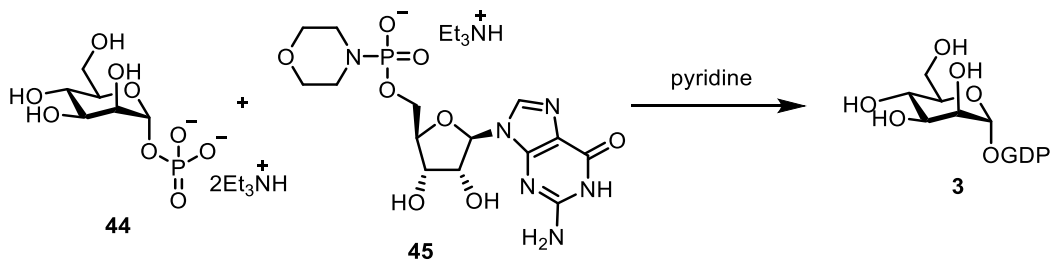


Scheme 1.12: Synthesis of uronic acid glycosyl 1-phosphates **41-43** using AtGlcAK.

1.4.2.2 Chemical synthesis of sugar-nucleotides

The chemical synthesis of sugar-nucleotides remains non-trivial, with commonly encountered problems including poor solubility of reaction components in organic solvents, elongated reaction times and susceptibility to hydrolysis. Furthermore, purification of the species is often complex due to the presence of multiple charged species in the crude reaction mixture that often co-elute during strong anion-exchange (SAX) chromatographic purification. Several comprehensive reviews cover this field, including an initial survey by Wagner *et al.* presented in 2008 and a more recent overview by Ahmadipour *et al.* in 2017.^{83,84}

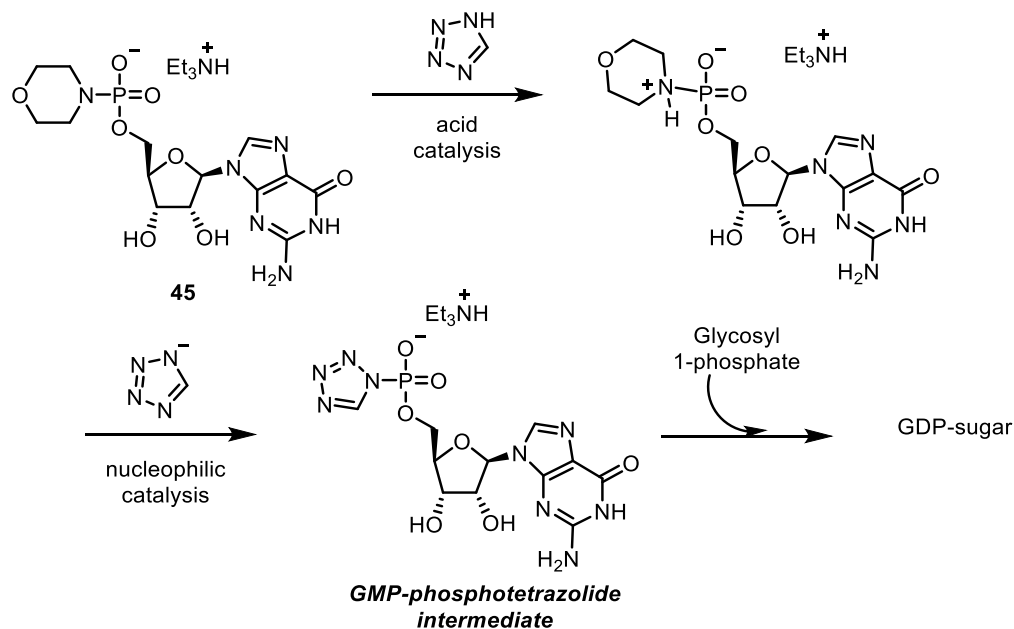
As introduced earlier, the dominant method to synthesise sugar-nucleotides is *via* formation of a pyrophosphate bond between two monophosphate precursors, of which one is activated (Scheme 1.13). The original procedure was first established by Roseman *et al.*⁸⁵, and despite being reported over 50 years ago it remains amongst one of the most commonly used methods to date. It involves the coupling an activated nucleoside phosphoromorpholidate species to a glycosyl 1-phosphate. Several nucleoside phosphoromorpholidates are commercially available, however they are expensive.



Scheme 1.13: Synthesis of GDP-mannose **3** using phosphoromorpholidate methodology.

The popularity of this method can be attributed to the fact that the anomeric configuration of the glycosyl 1-phosphate precursor is retained in the product. However, the reaction does present problems, particularly the in requirement for strictly anhydrous conditions and the poor solubility of some NMP-morpholidates in pyridine. Thus, reaction times are very long, in some cases up to 9 days, and the yields are variable. This is due to the increased likelihood of hydrolytic degradation as the reaction time is lengthened.⁷²

As sugar-nucleotides have limited stability, use of elevated temperatures or strongly acidic/basic conditions cannot be employed in attempts to improve their yield using synthesis. In 1997, Wittman *et al.*⁸⁶ reported the use of tetrazole as a catalyst in the synthesis of sugar-nucleotides (Scheme 1.14). As morpholine must be protonated before acting as a suitable leaving group in the condensation reaction, addition of an acid catalyst was a logical step to improve reaction outcome. Acting as both a Brønsted acid ($pK_a = 4.9$) and a nucleophile, experimental results showed that both properties were essential for effective catalysis, with reactions using a variety of other acids and nucleophiles not delivering the same rate accelerating effects.



Scheme 1.14: Tetrazole catalysed NDP-sugar synthesis.

Use of tetrazole resulted in a significantly shorter reaction time in comparison to the original procedure, with the most notable improvement being the synthesis of GDP- β -L-fucose where the reaction time was reduced from 9 to 2 days and the yield improved by 35%.⁷² This method is arguably the most significant breakthrough in the chemical synthesis of sugar-nucleotides, being reliable and high yielding across a range of natural and modified sugar-nucleotides. Unfortunately, rising concerns about the safety of tetrazole, due to its explosive nature, has led to a gradual decline in its use and alternative catalysts have been investigated. Reported by Tsukamoto *et al.* in 2011, *N*-methylimidazolium chloride (*N*-MIC) **46** (Figure 1.20) was shown to be more active and affordable than tetrazole. It is proposed that *N*-MIC not only acts as an acid but also as a nucleophile to form cationic intermediates that are more susceptible to nucleophilic displacement by a glycosyl 1-phosphate.⁸⁷ This activator was successfully used in the synthesis of

nucleobase modified sugar-nucleotides, 5-iodo-UDP-Gal and 5-iodo-UDP-GlcNAc for evaluation as glycosyltransferase inhibitors. The optimised conditions used 3.3 equivalents of freshly lyophilised *N*-MIC and DMF as the solvent to afford the desired sugar-nucleotides in consistent yields between 40 and 43%.⁸⁸ In 2014, 4,5-dicyanoimidazole (DCI) **47** (Figure 1.20) was also employed as an activator in the synthesis of sugar-nucleotides.⁸⁹ Whilst its catalytic activity was comparable to that of *N*-MIC, it had improved solubility in DMF and was less hygroscopic, making handling easier.

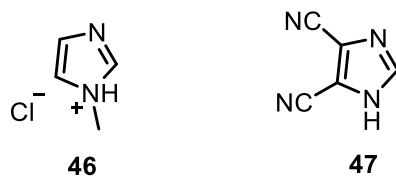


Figure 1.20: Chemical structures of *N*-MIC **46** and DCI **47**.

The strategy employing DCI featured a phosphoropiperidate approach, a less commonly used activated nucleoside monophosphate in the literature, shown in Figure 1.21. It is suggested to be a more reactive species than the respective phosphoromorpholidate due to its increased pKa value of 11.2 compared to 8.26.

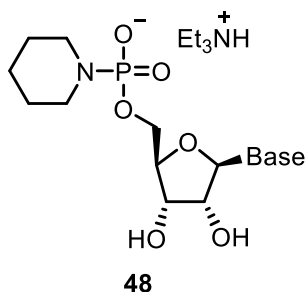
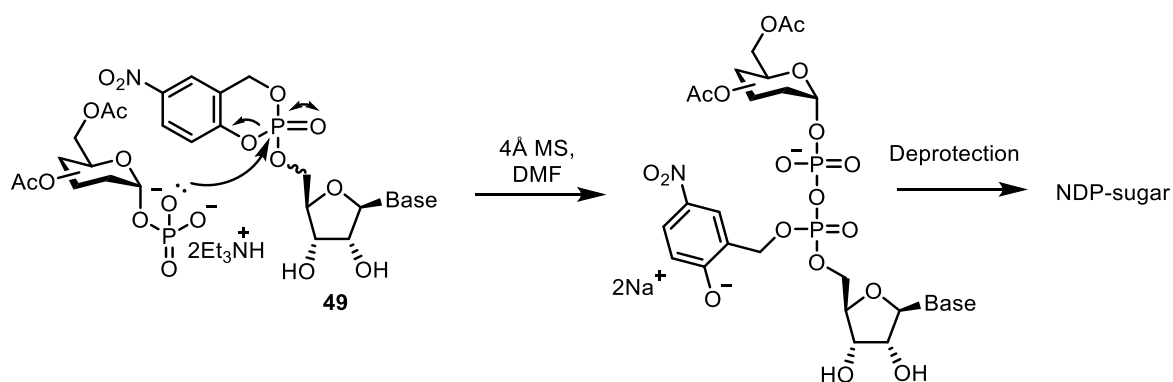


Figure 1.21: Chemical structure of nucleoside 5'-phosphoropiperidate **48**.

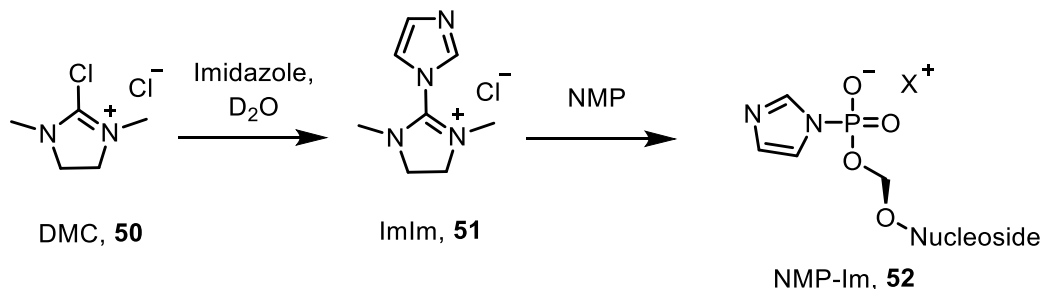
Work in the last decade has identified several other strategies for NDP-sugar synthesis. A notable advance was made by Wolf *et al.*⁹⁰, who presented the synthesis of an impressive library of 25 sugar-nucleotides containing varying sugar moieties and nucleobases using new *cyclo*-saligenyl (*cyclo*-Sal) nucleotides **49** as active ester building blocks. Their reaction with glycosyl 1-phosphates proceeds *via* nucleophilic displacement and subsequent hydrolysis, illustrated in Scheme 1.15, to afford purine and pyrimidine sugar-nucleotides in yields ranging from 60-87%. To ensure sufficient electrophilicity at phosphorus, the *cyclo*-Sal moiety featured electron-withdrawing 5-nitro or 5-methylsulfonyl groups.



Scheme 1.15: Formation of NDP-sugars using *cyclo*-Sal nucleotides *via* nucleophilic displacement by a glycosyl 1-phosphate.

One of the most interesting advances was made in 2012 by Tanaka *et al.*, describing the one-pot synthesis of NDP-sugars from commercially available materials in deuterium oxide (D₂O).⁹¹ The resultant NDP-sugars were used as donors in glycosyltransferase-mediated synthesis. Employing a phosphoroimidazolide approach to NMP activation, 2-chloro-1,3-dimethylimidazolinium chloride (DMC) **50**

was reacted with imidazole to form the active ImIm species **51**, which produces the NMP-Im **52** component *in-situ* (Scheme 1.16).

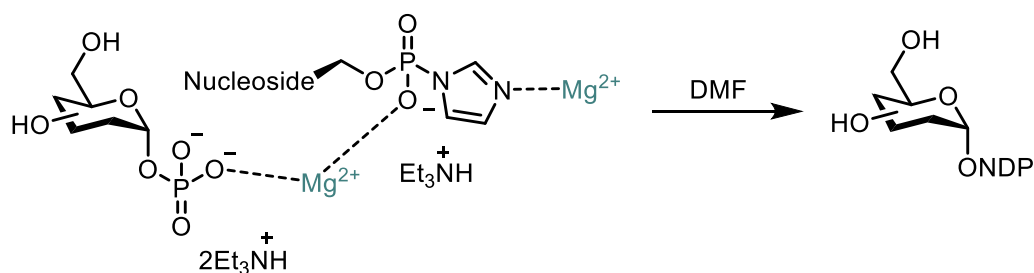


Scheme 1.16: Formation of NMP-Im from DMC and imidazole.

Not only did use of D₂O permit facile monitoring of the reaction by NMR, it also ensured a respectively high concentration of the active NMP-imidazole component, which was significantly decreased when the experiment was repeated in H₂O. Unfortunately, these coupling reactions are generally limited to small scale syntheses as only 10% of the NMP introduced into the reaction is converted to product. However, recent literature has described the synthesis of several nucleoside 5'-polyphosphates in H₂O/acetonitrile, using the same ImIm activation procedure in improved yields of 31-70%.⁹² Nevertheless, this procedure permits access to sugar-nucleotides for those without experience in performing protecting group manipulations and moisture-sensitive reactions.

In 2017, Dabrowski-Tumanski *et al.* reported a protecting group free, MgCl₂-promoted strategy to access NDP-sugars using the same nucleoside 5'-phosphoroimidazolide species. Use of a metal chloride provided several improvements to the procedure; these included increased solubility of reagents in DMF, activation of imidazole as a leaving group and coordination of the

monophosphate precursors to form a diphosphate (Scheme 1.17). The optimised conditions used 2.0-4.0 equivalents of MgCl_2 and was applied to a range of nucleosides (A, G and U) and glycosyl 1-phosphates (Glc, Gal, Fuc), with yields ranging from 63-92%.⁹³



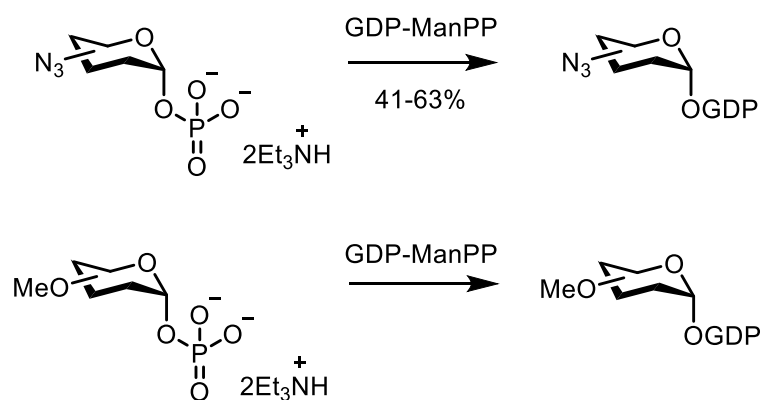
Scheme 1.17: MgCl_2 -promoted NDP-sugar synthesis.

1.4.2.3 Enzymatic synthesis of sugar-nucleotides

In comparison to the chemical synthesis of sugar-nucleotides, enzymatic methods proceed with much greater efficiency, with reaction times dramatically reduced and problems associated with poor solubility removed. Several nucleotidyltransferases and glycosyltransferases have been investigated in the synthesis of native and modified sugar-nucleotide analogues by many research groups, offering facile approaches towards the synthesis of these important structural probes to investigate a variety of biochemical processes. A review detailing recent advances in this field was published in 2018⁹⁴, with only the most common methods to synthesise GDP-Man analogues, which are of key significance for this project, discussed in this section.

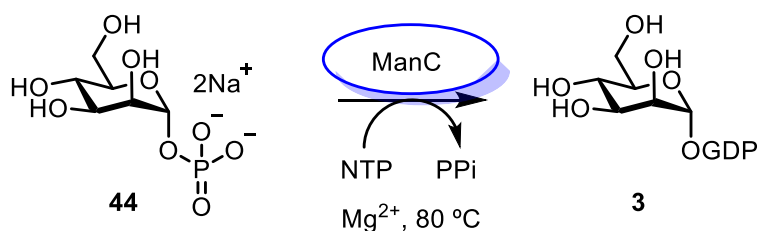
In the literature, the most frequently used enzyme to access GDP-Man and its analogues is GDP-ManPP from *Salmonella enterica* (*S. enterica*), of which multiple

studies into its substrate specificity have been undertaken. With previous work having already established that the C6-OH group does not take part in enzyme-substrate recognition, Watt *et al.* reported the synthesis of a number of deoxy mannopyranosyl phosphate derivatives to investigate the role of the other hydroxyl groups in substrate recognition.⁹⁵ V_{\max} values were least affected by removal of C3-OH and similarly affected by removal of C2- and C4-OH groups but the effect on K_m value was more significant, with 2-deoxy-glucose 1-phosphate being the worst substrate, suggesting that all four hydroxyl groups contribute to binding in GDP-ManPP. Nevertheless, GDP-2-deoxy-glucose and GDP-lyxose could both be synthesised on preparative scale, yielding useful probes to investigate mannosyltransferase (ManT) activity and *N*-glycan biosynthetic pathways. Alternative modified mannopyranosyl phosphates including C2,3,4 and 6-azido and methoxy derivatives, shown in Scheme 1.18, have also been used to probe the substrate specificity of GDP-ManPP.^{76,96} All analogues were transformed to their corresponding GDP-Man analogue with varying conversion rates.



Scheme 1.18: Synthesis of azido and methoxy GDP-Man analogues using GDP-ManPP.

Though limited examples are reported in the literature, Mizanur *et al.* characterised archaeal enzymes capable of synthesising GDP-Man, one of which is the bifunctional PMI/GDP-ManPP, ManC.^{97,98} Isolated from hyperthermophile *Pyrococcus furiosus*, GDP-Man **3** was accessed in yields exceeding 85% (Scheme 1.19). Furthermore, this enzyme was shown to be highly permissive, providing potential for the synthesis of both natural and non-natural sugar-nucleotides containing a range of nucleosides and glycosyl 1-phosphates that can be otherwise difficult to access chemically.



Scheme 1.19: Synthesis of GDP-Man **3** from **44** by ManC.

1.5 Carbohydrate Chemical Biology

The interdisciplinary field of chemical biology encompasses all branches of chemistry that are used to improve understanding of biological systems on a molecular level. Biological macromolecules of interest to the chemical biologist include peptides, oligodeoxynucleotides, oligosaccharides and sugar-nucleotides.⁹⁹ As discussed previously, sugar-nucleotides are interesting small molecules that play vital roles in bacterial systems with relevance in the area of health and disease.

Therefore, it is essential to synthesise such structures for use in elucidation of complicated biochemical pathways, with the potential to identify new therapeutic targets. From a synthetic chemistry perspective, this primarily entails the synthesis

of small molecule probes that have been designed for a specific purpose based on biochemical analyses, for example the crystal structure of an enzyme.

1.5.1 Sugar-nucleotides as chemical biology tools

The use of sugar-nucleotide probes for elucidation of biochemical mechanisms is well documented in the literature. Such probes have been designed to act in varying capacities, such as participating as key intermediates of reaction pathways or acting as chain terminators, with several key examples reported in recent years discussed herein.

In 1997, Campbell *et al.* described the chemoenzymatic synthesis of UDP- α -D-gluco-hexodialdose **53** (Figure 1.21), the putative intermediate in UGD catalysed oxidation of UDP-Glc to UDP-GlcA, discussed earlier in Section 1.3. This probe was designed to investigate the kinetic parameters surrounding this key oxidation step, as UDP-GlcA is used by pathogenic bacteria such as *Streptococcus pneumoniae* to construct antiphagocytic capsules. This work proved that the aldehyde was kinetically viable as a reaction intermediate, disproving earlier suggestions that UDP-Glc was converted directly to an enzyme-linked imine to provide new insights into the oxidation mechanism.¹⁰⁰

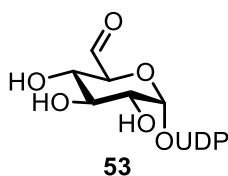


Figure 1.21: Chemical structure of UDP- α -D-gluco-hexodialdose **53**.

In nature, the biosynthesis of heparin, the most widely studied glycosaminoglycan, involves glycosyltransferases and epimerases to afford a series of alternating 1,4-linked α -L-IdoA, β -D-GlcA and β -D-GlcN residues. Access to structurally defined heparin oligosaccharides is key to further understanding its interactions with proteins, therefore Wiewer *et al.* synthesised UDP-IdoA **54** and UDP-HexUA **55** analogues to evaluate a chemoenzymatic synthesis of heparin (Figure 1.22). The substrate specificity of glycosyltransferases was explored, and whilst **54** was accepted only GlcA was incorporated into the products suggesting further enzymatic processes, such as isomerisation were yet to be understood. On the other hand, **55** was not accepted and could not be used as a chain terminator to create defined molecular weight range heparin oligosaccharides.¹⁰¹

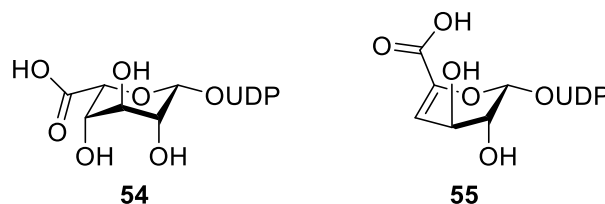


Figure 1.22: Chemical structures of UDP-IdoA **54** and UDP-HexUA **55**.

In 2009, the synthesis of GDP-Glc-2,3-diNAcA **56** (Figure 1.23), a key intermediate in cell surface polysaccharide biosynthesis amongst respiratory pathogens such as *P. aeruginosa*, was reported by Rejzek *et al.*¹⁰² Access to this sugar-nucleotide was vital for biochemical investigation of enzymes associated with its biosynthetic pathway, notably epimerases, and aided identification of a revised mechanism for this process.

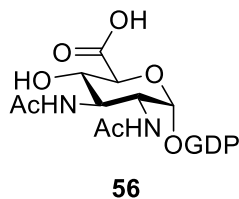


Figure 1.23: Chemical structure of GDP-Glc-2,3-diNacA **56**.

Recent literature has frequently described the synthesis of fluorinated sugar-nucleotides for use as chemical biology tools. In 2016, Lin *et al.* reported the chemical synthesis of UDP-5-fluoro-Gal **57** to study the mechanism of action of UDP-galactopyranose mutase (UGM). Catalysing the interconversion of UDP-Galp **17** to UDP-Galf **59**, shown in Figure 1.24, this enzyme is important in pathogenic bacteria such as *Mycobacterium tuberculosis*, where *Galf* residues are found on the cell surface.¹⁰³

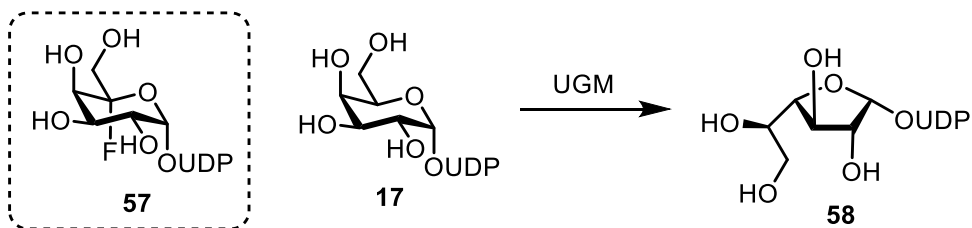


Figure 1.24: Chemical structure of UDP-5-deoxy-fluoro-Gal **57** used to probe the interconversion of UDP-Galp **17** to UDP-Galf **58** catalysed by UGM.

1.6 Summary

Though the field of sugar-nucleotide synthesis has undoubtedly progressed over the past two decades, improved chemical synthesis methods to access these important molecules and their precursors are still required. Due to their high moisture-sensitivity, access to sugar-nucleotides is still limited to those with prior training in performing reactions under inert conditions, however recent examples show promise of overcoming this in the near future.

Arguably the most important advance in this field has been the widespread use of chemoenzymatic strategies, which has permitted access to native and crucially, non-native sugar-nucleotides to study biological pathways implemented in various diseases. Accessibility of these strategies, however, is limited to those with relevant biological/biochemical training and access to appropriate facilities to undertake syntheses of this nature.

As more enzymes capable of producing sugar-nucleotides are discovered, more probes are required to explore structure-activity relationships of these enzymes, to assess their promiscuity, particularly in the synthesis of non-native sugar-nucleotides. Furthermore, many sugar-nucleotide utilising enzymes that play crucial roles in pathogenesis are yet to be explored, requiring the synthesis of new sugar-nucleotide tools to investigate their biosynthetic mechanisms.

1.7 Work described within this thesis

As outlined in this chapter, sugar-nucleotides are useful synthetic targets to probe biosynthetic mechanisms implemented in bacterial pathogenesis. *P. aeruginosa* causes chronic bacterial infection amongst cystic fibrosis patients, with its pathogenesis characterised by biosynthesis of alginate. The strategic biosynthesis enzyme GMD has been identified as a potential target to reduce alginate production, with minimal research into this enzyme reported in the literature. This thesis aimed to synthesise and evaluate a series of modified sugar-nucleotide tools to provide new insights into substrate specificity of this important regulatory enzyme, with the view to creating analogues capable of interacting with a key active site Cys²⁶⁸ residue to reduce or inhibit production of GDP-ManA.

First, Chapter 2 details two complimentary approaches to synthesise the feedstock sugar-nucleotide, GDP-ManA, the key building block for alginate biosynthesis in *P. aeruginosa*. Access to this material is essential for studies into alginate biosynthesis. Chapter 3 describes efforts towards the synthesis of eight modified GDP-Man analogues using a chemoenzymatic strategy. These tools were designed to bear a range of functionalities at the C6 and C4 positions of mannose, with the view to probe substrate specificity of GMD and the mechanism of oxidation of GDP-Man to GDP-ManA *via* an active site Cys²⁶⁸ residue. Finally, Chapter 4 investigates the activity of the synthesised GDP-Man analogues against GMD using a colorimetric assay, which was performed in collaboration with the group of Prof. Rob Field at the John Innes Centre, Norwich.

Chapter 2: Synthesis of GDP-ManA

2.0 Introduction and aims

The bacterial nucleoside diphosphate sugar GDP-ManA **4** (Figure 2.1) is the native tool for studies into alginate biosynthesis. The chemical synthesis of uronic acid-containing sugar-nucleotides is less well documented in the literature, and an opportunity to expand knowledge within this important area was presented. Several approaches towards the synthesis of uronic acid containing NDP-sugars are described herein.

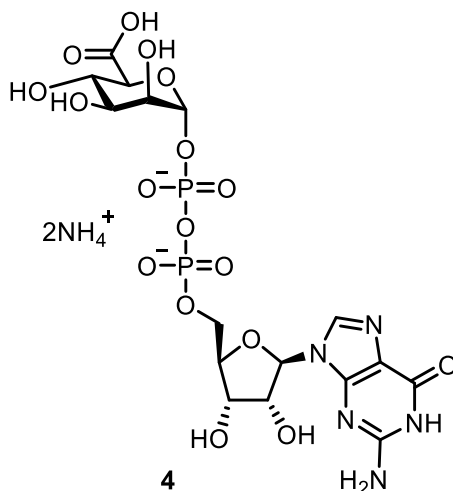
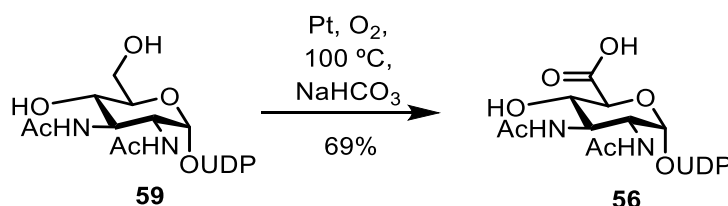


Figure 2.1: Chemical structure of GDP-ManA **4**.

As discussed in Chapter 1.5.1, Schultz *et al.* reported the chemical synthesis of UDP-IdoA **54** for use in studies towards the chemoenzymatic synthesis of heparin. Three approaches were attempted towards the synthesis of the IdoA 1-phosphate required for UDP-sugar synthesis, with the formation of a glycosyl bromide followed by displacement with the tetrabutylammonium salt of phosphoric acid found to be the optimum route towards the monophosphate precursor. The deprotected

monophosphate was then reacted with UMP-morpholidate to afford UDP-IdoA in a modest yield of 26%.¹⁰¹

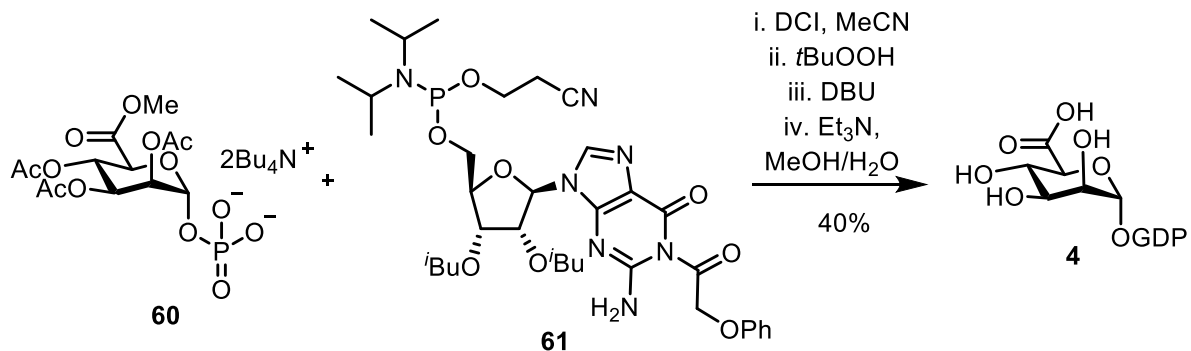
A contrasting method to synthesise uronic acid NDP-sugars involves the oxidation of the C6-OH *post* sugar-nucleotide synthesis (Scheme 2.1). Developed by Rejzek *et al.*, this work describes the use of a platinum-catalysed oxidation using molecular oxygen at elevated temperature (100 °C). Attempted use of 2,2,6,6-tetramethylpiperidin-1-yl)oxyl (TEMPO) as a catalyst resulted in over-oxidation of the ribose ring, *via* competing secondary oxidation to an unstable diketone.¹⁰⁴



Scheme 2.1: Platinum based oxidation of NDP-sugars.

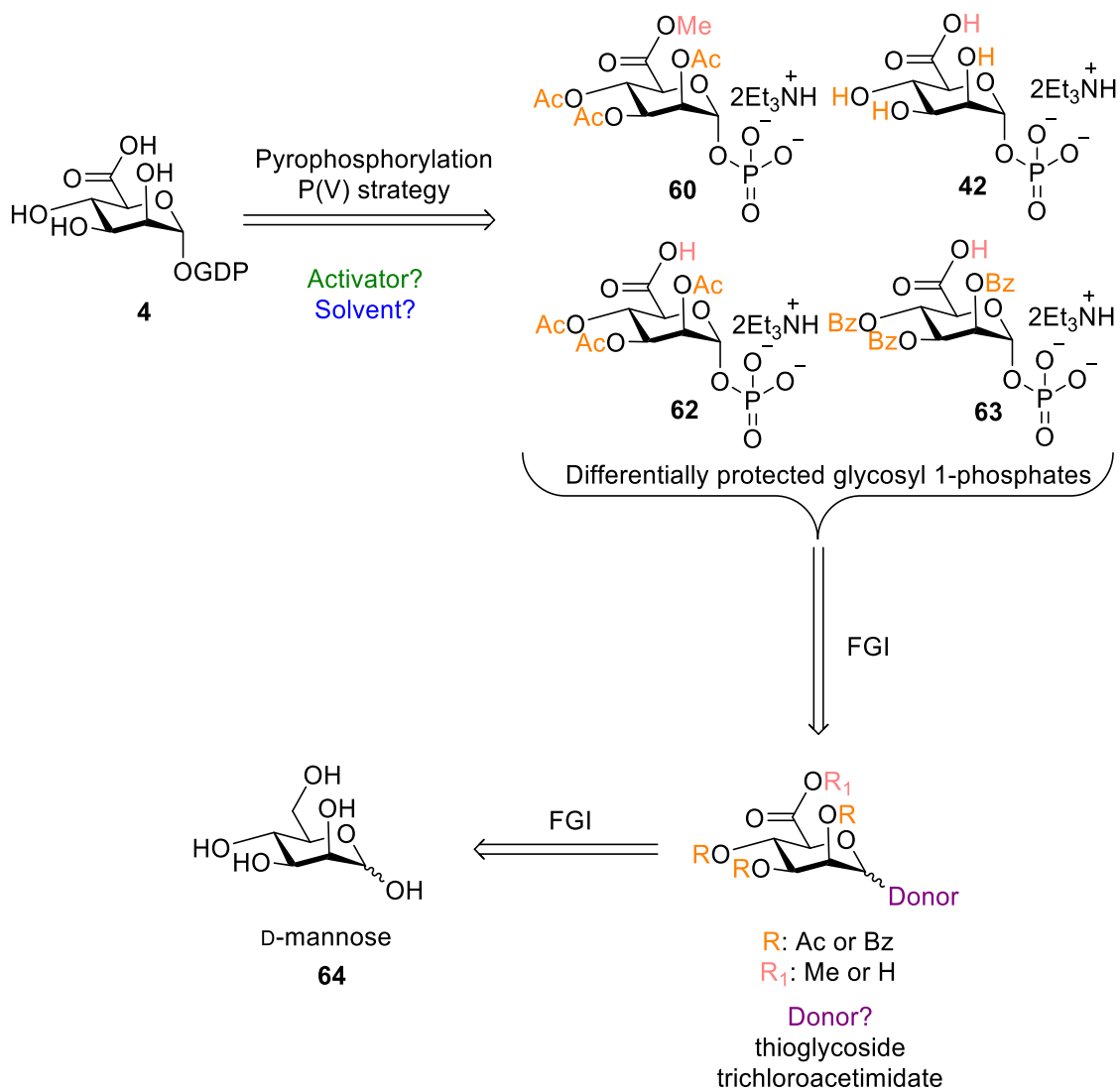
This method was successfully employed in the chemical synthesis of GDP-Glc-2,3-diNAcA **56**. Following reaction of the respective monophosphate with UMP-morpholidate, UDP-Glc-2,3-diNAc was afforded in 49% yield after 14 days. The platinum-catalysed oxidation procedure was then used to afford the corresponding uronic acid **56** in an impressive 69% yield.¹⁰²

In 2017, Codée *et al.* published the first chemical synthesis of GDP-ManA **4** using a protected phosphoramidite P(III) approach. Generation of the P(V)-P(III) intermediate was catalysed by DCI, which was then oxidised to with *tert*-butyl hydroperoxide (*t*BuOOH) and deprotected. **4** was isolated in a reasonable yield of 40% in multi-milligram quantities (Scheme 2.2).¹⁰⁵



Scheme 2.2: Synthesis of GDP-ManA **4** using a phosphoramidite approach.

Access to GDP-ManA **4** was sought *via* a simpler route that would require fewer protecting group manipulations and use the more robust P(V)-P(V) strategy to access this key building block. A series of four differentially protected glycosyl 1-phosphates, **60**, **42**, **62** and **63**, were designed to permit assessment of any solubility differences on pyrophosphorylation. Exploration of additional reaction parameters such as activator and solvent choice were also proposed. To facilitate this investigation, scalable access to mannopyranuronic acid derivatives was required, derived from D-mannose **64** (Scheme 2.3).

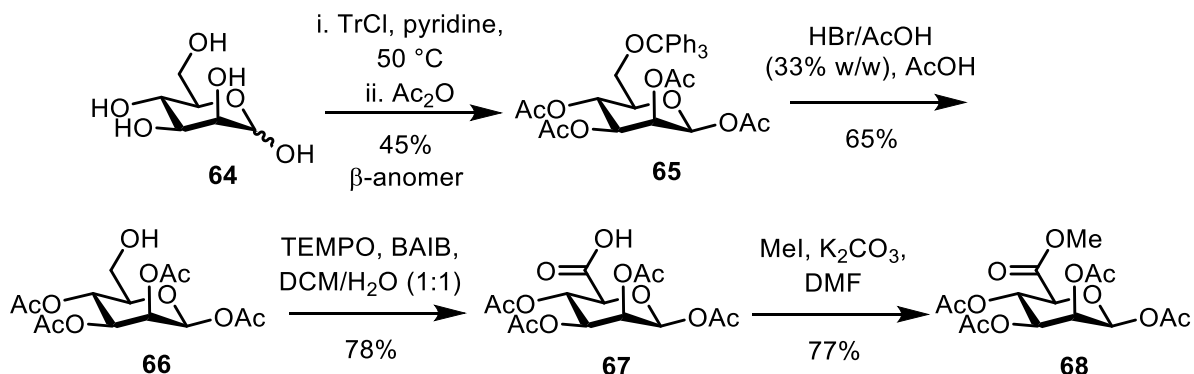


Scheme 2.3: Retrosynthetic analysis for GDP-ManA 4.

2.1 Synthesis of glycosyl 1-phosphates

2.1.1 Synthesis of α -D-mannopyranuronic acid derivatives: acetyl protected methyl uronate series

The synthetic strategy towards differentially protected α -D-mannopyranuronic acid derivatives **60** and **42** was derived from D-mannose **64**, outlined in Scheme 2.4. Following selective tritylation of the C6-OH and per-O-acetylation, compound **65** was obtained *via* recrystallisation from absolute EtOH as the β -anomer. Removal of the trityl moiety was achieved using HBr/AcOH (33% w/w) to afford C6-alcohol **66**.



Scheme 2.4: Synthesis of methyl uronate **68**.

Problems were encountered when scaling up the TEMPO/BAIB oxidation of **66** to **67** above 500 mg, with a significant decrease in yield observed. To address this, alterations to the solvent ratio and equivalents of TEMPO/BAIB were explored, as illustrated in Table 2.1. The optimised conditions used 0.5 and 5.0 equiv, of TEMPO and bis(acetoxy) iodobenzene (BAIB) respectively (Table 2.1, Entry 3). The work-up was also modified to deliver the product without a need for column chromatography, through acidification of the aqueous layer and subsequent extraction of the product with EtOAc. The optimised conditions produced uronic acid **67** in a consistent yield

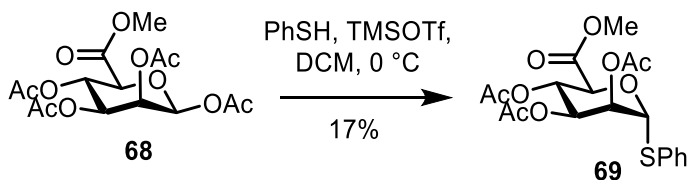
of 78% on scales exceeding 2 g ¹⁰⁶, which was subsequently esterified using methyl iodide (MeI) and K₂CO₃ to afford **68**.

Entry	66 (g)	DCM:H ₂ O	TEMPO (equiv.)	BAIB (equiv.)	Yield (%)
1	1.0	2:1	0.2	2.5	36
2	0.5	2:1	0.5	10.0	30
3	2.0	2:1	0.5	5.0	78

Table 2.1: Optimisation of TEMPO/BAIB mediated oxidation of **66**.

Attempted synthesis of a thioglycoside donor

The synthesis of α-D-mannopyranuronic acid derivatives was first attempted *via* synthesis of thioglycoside **69**, shown in Scheme 2.5. Two different Lewis acids, boron trifluoride diethyl etherate (BF₃•OEt₂) and trimethylsilyl trifluoromethanesulfonate (TMSOTf), were evaluated.



Scheme 2.5: Optimisation of TMSOTf mediated thioglycoside formation.

Methyl uronate **68** is considered a poor glycosyl donor due to the inactivation of its anomeric centre by the electron-withdrawing C6 uronate.¹⁰⁷ Furthermore, the use of acetate protecting groups further disarms the donor. Reaction times with BF₃•OEt₂ as Lewis acid were long, despite use of 5.0 equivalents, and desired thioglycoside **69** was not isolated. Alternatively, use of TMSOTf showed complete conversion of starting material in 18 h (Table 2.2, Entry 1). The desired product was

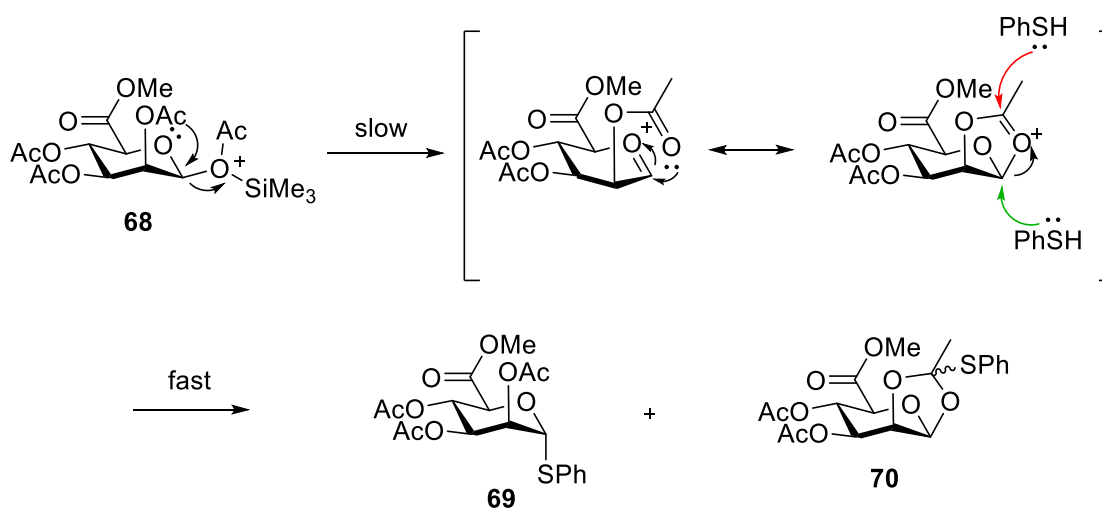
isolated as an anomeric mixture in addition to an orthoester by-product **70**, common to glycosylation reactions with participating 2-O-acetyl substituents.

Entry	Temperature (°C)	Time (h)	Yield (%)	α/β 69	69 α / 70
1	-15→RT	18	63 ^c	5:1	4:1
2	0→RT	6	42 ^c	5:1	8:1
3	0	6	15 ^p	5:1	25:1
4	0	32	17 ^p	6:1	33:1

Table 2.2: Optimisation of TMSOTf mediated formation of thioglycoside **69**.

^c = crude yield and ^p = yield after purification.

The products could be distinguished by chemical shift of the anomeric proton resonances (**69** α = δ_{H} 5.60 ppm and **70** = δ_{H} 6.21 ppm). The proposed mechanism for formation of by-product **70** is illustrated in Scheme 2.6.



Scheme 2.6: Proposed mechanism for the formation of α -thioglycoside **69** and orthoester **70** from methyl uronate **68**.

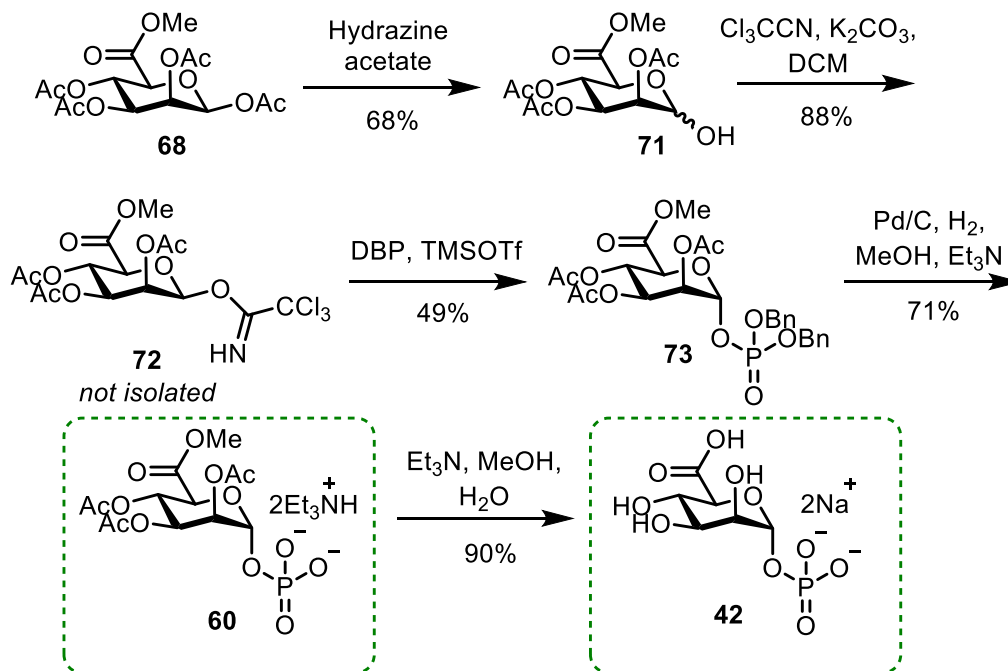
To investigate suppressing the formation of **70**, the reaction temperature was increased from $-15\text{ }^{\circ}\text{C}$ to $0\text{ }^{\circ}\text{C}$ (Table 2.2, Entry 2). In comparison to previous attempts, which afforded an average product/orthoester ratio of 4:1, the ratio was improved to 8:1 but the side reaction was not completely stopped.

Isolation of pure **69** was difficult given the similarity in R_f values between the α/β -anomers and orthoester **70**. Although separation from **70** could be achieved on larger scale ($\geq 500\text{ mg}$) attempts to further minimise its formation were made and the reaction repeated with the temperature maintained at $0\text{ }^{\circ}\text{C}$ for 6 h (Table 2.2, Entry 3). This reaction did not reach completion and **69** was isolated in only 15% yield (44% returned **68**). These results suggested that product/orthoester ratio worsened upon increasing temperature, however when maintained at $0\text{ }^{\circ}\text{C}$ the product formed, but slowly.

Finally, the reaction was maintained at $0\text{ }^{\circ}\text{C}$ for a longer time period (Table 2.2, Entry 4), with the hope of completely suppressing orthoester formation and improving conversion to **69**. Though the product/orthoester ratio was dramatically improved (33:1), the conversion of starting material was again very slow and gave a poor isolated yield of 17% (20% returned **68**).

Synthesis of a trichloroacetimidate donor

Due to the problems encountered with orthoester formation the route was changed to explore a trichloroacetimidate donor (Scheme 2.7).



Scheme 2.7: Synthesis of α -D-mannopyranuronic acid derivatives **60** and **42**.

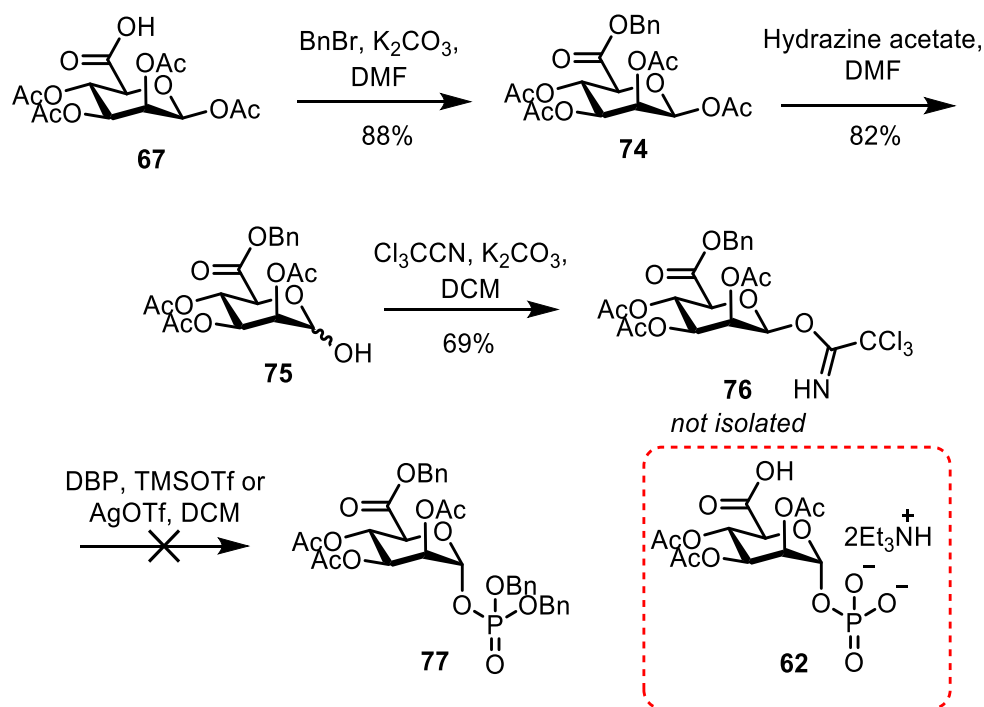
Selective removal of the anomeric acetate in methyl uronate **68** was attempted using established literature procedures for related substrates. Cleavage using ethylene diamine (EDA) and AcOH ¹⁰⁸ was not reproducible, and afforded highly variable yields of hemiacetal **71** between 20-64%. The use of 3(dimethylamino)-1-propylamine (DMAPA) had recently been reported to remove pyranose anomeric acetate groups in high yield.¹⁰⁹ Unfortunately, adoption of this procedure did not yield **71**. Finally, hydrazine acetate anomeric deacetylation¹¹⁰ was attempted and delivered **71** in 68% yield.

Reaction of **71** with trichloroacetonitrile in the presence of K_2CO_3 afforded trichloroacetimidate donor **72** which was used crude in the synthesis of protected ManA 1-phosphate **73**. Reaction of **72** with dibenzyl phosphate (DBP) in the presence of TMSOTf successfully afforded **73**, although the average yield was only 49%. Attempts to improve this yield, through more rigorous drying procedures and use of various batches of DBP from a range of suppliers were unsuccessful. Following purification, the expected ^{31}P NMR resonance for the anomeric phosphate ($\delta_P -3.2$ ppm) and characteristic doublet of doublets for the anomeric proton ($J_{H1-P} = 6.4$ Hz, $J_{H1-H2} = 2.0$ Hz) were observed.⁷⁶

Deprotection of **73** via hydrogenolysis using Pd/C catalysis successfully yielded the desired ManA 1-phosphate **60**, which was isolated as the *bis*-triethylammonium salt following concentration *in vacuo* with Et_3N . A resonance at $\delta_P -0.9$ ppm with a J_{H1-P} of 7.0 Hz was identified in the ^{31}P spectrum. This material was then fully deprotected through treatment with Et_3N in MeOH/ H_2O , to afford **42** in 90% yield, which was confirmed by ^{31}P NMR ($\delta_P 1.4$ ppm, $J_{H1-P} = 8.6$ Hz) and HRMS, where the *m/z* peak corresponding to $[42-H]^-$ was calculated as 273.0013. The desired α -D-mannopyranuronic acid derivatives **60** and **42** were accessed over 8 or 9 steps in respective overall yields of 5 and 4%, from **64** for use in the chemical synthesis of GDP-ManA **4**, discussed later in this chapter.

2.1.2 Synthesis of α -D-mannopyranuronic acid derivatives: acetyl protected benzyl uronate series

As hydrogenolysis of protected glycosyl 1-phosphate **73** is necessary to deprotect α -D-mannopyranuronic acid derivatives, the precursor synthesis was modified to form a benzyl protected uronate, illustrated in Scheme 2.8. This would permit simultaneous hydrogenolysis of the benzyl ester and benzyl phosphate ester protecting groups, proposed to furnish an additional α -D-mannopyranuronic acid derivative **62** with a different solubility prospect to evaluate towards synthesis of GDP-ManA **4**.



Scheme 2.8: Attempted synthesis of **62**.

Compound **75** was synthesised in two steps, following successive benzylation and anomeric acetate cleavage using the previously established conditions for **71**. Following synthesis of trichloroacetimidate donor **76**, the crude compound was

reacted with DBP in the presence of TMSOTf and monitored for 24 h. During this time, TLC analysis did not indicate any formation of protected glycosyl 1-phosphate **77** and only **75** was recovered by column chromatography.

Attempted purification of donor **76** to improve purity of the starting material was unsuccessful, only resulting in decomposition despite the addition of 2% v/v Et₃N to the column eluent. When the experiment was repeated using increased equivalents of promoter, ³¹P NMR analysis revealed two resonances at δ_P -3.0 and -3.2 ppm. Given that both values were in the expected chemical shift range for protected dibenzyl phosphate derivatives, it appeared that a mixture of anomers may have formed.

Changing the promoter from TMSOTf to silver trifluoromethanesulfonate (AgOTf) also delivered the same result, with crude ³¹P NMR analysis revealing two resonances in a similar region, δ_P -3.1 and -3.3 ppm, to previous compound **73** with a resonance at δ_P -3.2 ppm. Batches of DBP from various suppliers were also screened, however no improvement to the yield was observed, which ranged from 11-14%. The synthesis of derivative **62** was unsuccessful using these conditions and no further optimisation was undertaken.

2.1.3 Synthesis of α -D-mannopyranuronic acid derivatives: benzoyl protected uronate series

To enrich the substrate scope for evaluation of chemical sugar-nucleotide synthesis of GDP-ManA **4**, a route towards benzoyl protected α -D-mannopyranuronic acid derivative **63** (Figure 2.) was also designed to evaluate any difference in solubility compared acetyl protected compound **62**. The route is outlined in Scheme 2.9.

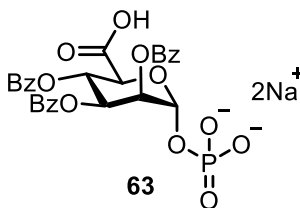
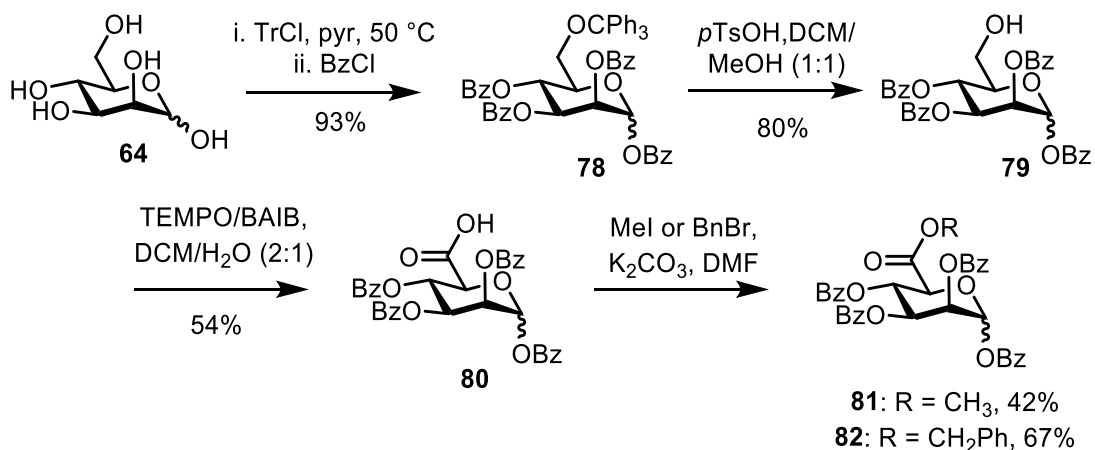


Figure 2.2: Chemical structure of target glycosyl 1-phosphate **63**.

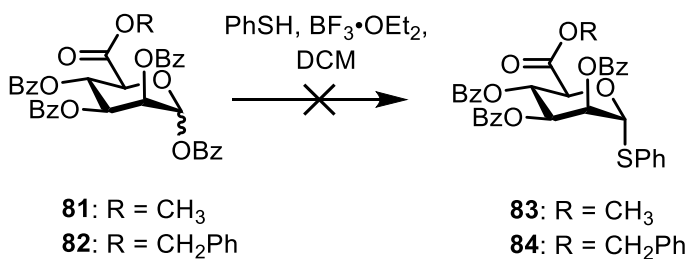
Following one-pot tritylation and benzoylation of **64**, purification by column chromatography afforded **78** as a mixture of inseparable anomers (5.8:1 α/β). Cleavage of the trityl group to reveal the C6-OH for oxidation was initially performed using HBr/AcOH (33% w/w) in AcOH. The starting material was less soluble in AcOH in comparison to the acetyl counterpart **65** therefore **79** was only afforded in 27% yield and alternative conditions were sought. Use of catalytic *p*-Toluenesulfonic acid (*p*TsOH) (0.22 equivalents) in DCM/MeOH had been used previously for trityl removal on a similar substrate¹¹¹, however these conditions did not lead to complete deprotection. The procedure was repeated using varying equivalents of *p*TsOH, with the optimised procedure requiring 1.2 equivalents to afford **79** in a yield of 80% (4:1 α/β mixture).



Scheme 2.9: Synthesis of protected uronates **81** and **82**.

Oxidation to the uronic acid was performed using TEMPO/BAIB conditions, producing **80** in an average yield of 54%. The optimised purification procedure discussed earlier in this chapter could not be applied to these derivatives due to their different solubility profile, and column chromatography was required to afford pure **80**. Successful oxidation was confirmed by identification of a new resonance at δ_c 171.8 ppm corresponding to CO₂H. Esterification of **80** with MeI or benzyl bromide (BnBr) under basic conditions afforded desired compounds **81** and **82** respectively for use in thioglycoside formation.

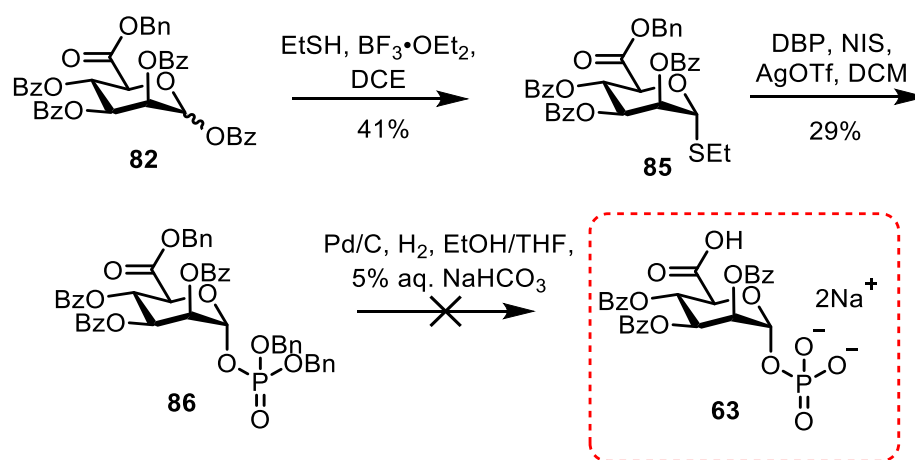
With protected uronates **81** and **82** in hand, installation of a thioglycoside donor was attempted using BF₃•OEt₂, outlined in Scheme 2.10.



Scheme 2.10: Attempted synthesis of thioglycoside donors **83** and **84**.

Attempted glycosylation of thiophenol (PhSH) with **81** in the presence of $\text{BF}_3 \cdot \text{OEt}_2$ was sluggish, and a further 2.0 equivalents of promoter was added in an attempt to induce conversion. After 48 h, the reaction was quenched as no conversion to **83** was observed by TLC and only starting material could be recovered. The reaction of **82** with PhSH under the same conditions also showed no conversion of **82** even after 32 h. Further attempts using increased quantities of $\text{BF}_3 \cdot \text{OEt}_2$ (3.0-4.0 equivalents) and a different promoter, TMSOTf (2.0-3.0 equivalents) also failed to afford **84**. All attempts to synthesise a phenyl thioglycoside donor failed under the conditions attempted.

Next, attention was focused on preparation of a thioglycoside using ethanethiol (EtSH), which is more reactive than PhSH, illustrated in Scheme 2.11.



Scheme 2.11: Attempted synthesis of **63** via ethyl thioglycoside **85**.

First, benzyl uronate **82** was dissolved in DCM with EtSH and activated with $\text{BF}_3 \cdot \text{OEt}_2$. The reaction was very sluggish, with little conversion of **82** observed even with 4.0 equivalents of promoter. Following purification, desired product **85** was isolated in a poor yield of 6%, although 50% of **82** could be recovered.

An alternative procedure reported by Sail *et al.*¹¹² used dichloroethane (DCE) as solvent. Following this procedure, 1.8 equivalents of promoter was used, however the isolated yield was only 19%. Increasing the quantity of promoter to 2.0-3.0 equivalents had little effect on yield on scales up to 250 mg, and it was observed that hydrolysis began to occur before conversion of starting material was complete. Therefore, the reaction mixture was quenched before completion to prevent loss of the product. Following purification by column chromatography desired thioglycoside **85** was isolated, with the optimised procedure giving **85** in a yield of 41%, (66% based on returned starting material) which could be scaled up to ≥ 1 g. A clear upfield shift of the anomeric proton from δ_{H} 6.79 ppm to δ_{H} 5.71 ppm was observed in NMR of **85**, with resonances corresponding to the $-\text{CH}_2$ and $-\text{CH}_3$ protons of the ethyl thioglycoside functionality identified as a quartet at δ_{H} 2.87 ppm ($J = 8.0$ Hz) and a triplet at δ_{H} 1.35 ppm ($J = 8.0$ Hz).

Activation of thioglycoside **85** with *N*-iodosuccinimide (NIS)/AgOTf in the presence of DBP afforded glycosyl 1-phosphate **86** in a modest yield of 29%. The anomeric phosphate resonance was identified at δ_{P} -3.1 ppm with $J_{\text{H1-P}}$ 7.3 Hz and further confirmed by HRMS, with a m/z peak of 874.2625 corresponding to the $[\mathbf{86}+\text{NH}_4]^+$ species.

Finally, **86** was subjected to hydrogenolysis to cleave the benzyl protecting groups. The starting material was dissolved in EtOH/THF (1:1) and stirred vigorously under an atmosphere of H_2 with Pd/C for 36 h, where TLC analysis appeared to show conversion of **86** to a baseline R_f value spot. Following work-up, a white powder was afforded and analysed by NMR. Unfortunately, HSQC-DEPT analysis showed

presence of a CH₂ resonance suggesting incomplete deprotection. The residue was reconstituted in MeOH/H₂O and hydrogenolysis continued however no further change by TLC, using a more polar eluent system, was observed even after 24 h. Analysis of the crude residue by NMR still suggested incomplete benzyl removal.

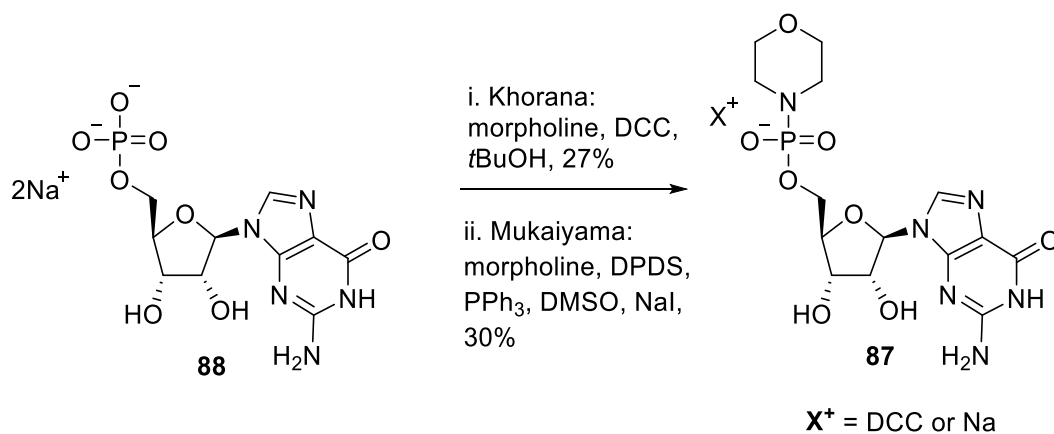
Deprotection of **86** was repeated using the previous conditions and within 24 h, conversion of **86** to two lower R_f value spots was observed by TLC. At this time, the catalyst was replaced, and the residue suspended in MeOH for a further 8 h where only one baseline R_f value spot was observed by TLC. Following work-up and concentration *in vacuo*, the resultant residue was poorly soluble in MeOD-d₄ and CDCl₃ leading to poorly resolved NMR spectra that could not be fully characterised. Again, the HSQC-DEPT spectrum indicated presence of at least one -OCH₂Ph group and the ³¹P was now a very broad, poorly resolved singlet at δ_P -2.2 ppm. HRMS analysis did not find the correct molecular ion for the proposed structure.

Compared to the acetyl protected uronate series, benzoyl protected uronate donors were, as expected, less reactive. Whilst the reaction of **68** with PhSH did proceed but slowly, no equivalent reaction was observed with benzoyl counterpart **81**. Thioglycoside synthesis was possible when using EtSH to produce **85**. Advantageously, no competing formation of an orthoester by-product was observed during this transformation, unlike in the synthesis of acetylated thioglycoside **69**. This eased purification and reduced the overall number of steps in the synthetic route but unfortunately, hydrogenolysis failed and target glycosyl 1-phosphate **63** could not be isolated. This may be attributed to the limited solubility profile of **63** and in future work more solvent combinations should be screened to optimise hydrogenolysis.

2.2 Synthesis of GDP-ManA

With two protected glycosyl 1-phosphates **60** and **42** in hand, the final stage of this route was formation of the pyrophosphate linkage to afford GDP-ManA **4**. The phosphoromorpholidate methodology was selected to complete this transformation, therefore access to the activated monophosphate precursor guanosine 5'-phosphoromorpholidate (GMP-morpholidate) **87** was required. This reagent is commercially available, but it is expensive (~ £100 per 100 mg), therefore it was important to be able to access this species in larger quantities to enable optimisation of the pyrophosphorylation step.

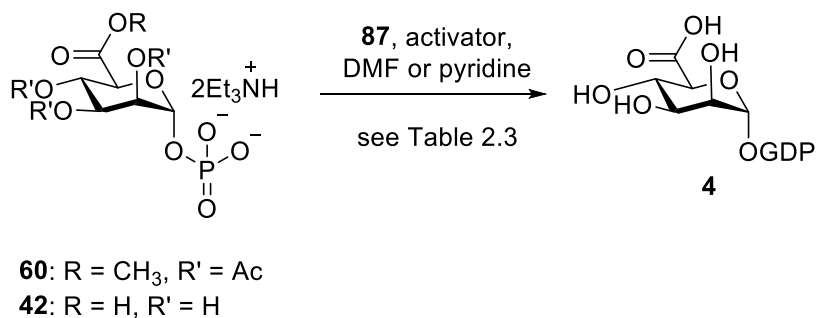
The predominant methods used in the literature to synthesise **87** are those of Khorana¹¹³ and Mukaiyama¹¹⁴ from guanosine 5'-monophosphate (GMP) **88**, of which both were attempted (Scheme 2.12) to afford **87** in 27 and 30% yields respectively.



Scheme 2.12: Synthesis of GMP-morpholidate **87**.

2.2.1 Chemical synthesis

The chemical synthesis of GDP-ManA **4** was first attempted using per-*O*-acetylated methyl uronate **60** and *N*-MIC as the activator (Scheme 2.13 and Table 2.3, Entry 1).⁸⁷ The monophosphate components were exchanged to their triethylammonium salt forms prior to phosphorylation to improve solubility and co-evaporated with anhydrous pyridine or toluene.



Scheme 2.13: Chemical synthesis of GDP-ManA **4**.

The optimum TLC system to monitor sugar-nucleotide synthesis was IPA/NH₄OH/H₂O (6:3:1) and analysis was performed on large 7 × 7 cm plates in two sections that were stained with H₂SO₄/MeOH and orcinol (Figure 2.3).

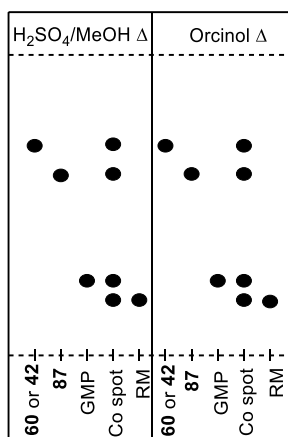


Figure 2.3: TLC plate used to monitor chemical synthesis of GDP-ManA **4**.

Entry	Glycosyl 1-phosphate	Activator (equiv.)	Time (h)	Solvent (conc.)	Yield (%)	Comments
1	60	<i>N</i> -MIC (2.9)	60	DMF (0.06)	0	No reaction
2	60	DCI (4.0)	56	DMF (0.05)	<5	DCI contamination
3	60	DCI (1.0)	108	DMF (0.05)	<5	Reduced DCI, long reaction time
4	60	None then DCI (1.0)	144	Pyr. (0.06)	22	Reduced DCI
5	60	DCI (1.0)	120	Pyr. (0.06)	46	Reduced DCI
6	42	DCI (1.0)	40	DMF (0.07)	0	No reaction
7	42	None	144	Pyr. (0.04)	0	No reaction

Table 2.3: Evaluation of glycosyl 1-phosphates **60** and **42** for chemical synthesis of GDP-ManA **4**.

After 60 h, a lower R_f value spot was observed, however crude ^{31}P NMR (CDCl_3) analysis revealed only one resonance at δ_{P} 0.4 ppm, inconsistent with the two expected resonances for a sugar-nucleotide, reported between δ_{P} -11.0 and -14.0 ppm for the diphosphate linkage.⁹¹ Though care was taken to avoid presence of H_2O in the reaction, *N*-MIC was clearly hygroscopic and was a source of moisture leading to hydrolysis of **87** to afford GMP **88** (δ_{P} -0.7 ppm in D_2O). These conditions were not repeated, however it was reported in the literature that lyophilisation of *N*-MIC prior to use effectively reduces residual moisture.¹¹⁵

Synthesis of **4** was next attempted using DCI (Table 2.3, Entry 2) which was significantly less hygroscopic.⁸⁹ After 24 h, TLC analysis showed conversion to a

different lower R_f value spot than the previous attempt. Following removal of DMF, crude ^{31}P analysis (CDCl_3) showed two broad singlets in the expected region for a diphosphate linkage at $\delta_{\text{P}} -11.4$ and -14.6 ppm. Two other resonances were present in the spectrum at $\delta_{\text{P}} 0.2$ and -2.7 ppm, corresponding to **88** and **60** respectively. The resultant residue was reconstituted in MeOH/ H_2O and Et_3N added until pH = 9, until conversion to a lower R_f value spot was observed.

Several methods are described in the literature for the purification of sugar-nucleotides, primarily involving strong-anion exchange (SAX) chromatography. The first buffer attempted for sugar-nucleotide purification was triethylammonium bicarbonate (TEAB), which was prepared by bubbling CO_2 through a 1M aqueous solution of Et_3N until pH = 8.5.^{101,105} During methodology development, this buffer caused issues with the Bio-Rad purification system, including reduced flow rates and blockages as buffer concentration was increased.

Ammonium bicarbonate (NH_4HCO_3) was next evaluated, which presented fewer problems. Multiple flow rates, buffer gradients and injection concentrations/volumes were screened during optimisation, with the best protocol developed at a flow rate of 3.0 mL/min with a concentration gradient of 0 \rightarrow 100% 1.0 M NH_4HCO_3 over 33 min. Standards of GMP **88**, guanosine 5'-diphosphate (GDP) and GDP-Man **4** were collected for comparison.

When the crude residue was applied to the column, **4** was isolated in poor yield (<5%). During purification, a large UV peak co-eluted in the area of interest; after running a standard of DCI, this was confirmed to be the impurity. As the activator was being used in large excess, any entries using DCI were subjected to purification

via a HyperSep C18 column (eluting with H₂O) to remove most of the contaminant prior to application to the SAX column.

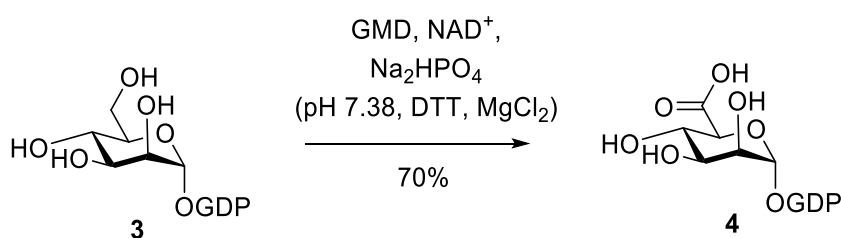
The pyrophosphorylation reaction was repeated using a variety of conditions, including reduced equivalents of DCI (1.0) to prevent purification problems and evaluation of DMF and pyridine as solvents. Reducing the equivalents of activator almost doubled the reaction time (Table 2.3, Entries 2 and 3). Changing the reaction solvent to pyridine provided the best improvement, furnishing **4** in 46% yield using 1.0 equivalents of DCI (Table 2.3, Entry 5). Whilst the uncatalysed reaction still afforded **4**, the yield was reduced by over half to 22% and the reaction time was very long (Table 2.3, Entry 4).

Synthesis of **4** was also attempted using fully deprotected glycosyl 1-phosphate **42**. The reaction was attempted in both DMF and pyridine (Table 2.3, Entries 6 and 7), however in both instances no reaction of **42** with **87** was observed. The addition of DCI did not improve conversion, and in all attempts unreacted GMP-morpholidate **87** could be observed by ³¹P NMR confirming that hydrolysis did not cause the failure of the reaction. This could be attributed to the poorer solubility of glycosyl 1-phosphate **42** in both DMF and pyridine.

2.2.2 Enzymatic synthesis

As discussed in Chapter 1.3, GDP-ManA **4** is produced *via* oxidation of GDP-Man **3** by GMD in the presence of NAD⁺. Access to a standard of **4** was desired as a reference to aid purification of chemically prepared crude mixtures of **4** by SAX chromatography. Prior to the reaction, standards of NAD⁺, NAD(H) and GDP-Man **3** were collected by SAX chromatography to permit facile monitoring of the reduction

of NAD^+ to NAD(H) by monitoring absence and appearance of the corresponding peaks. Recombinant GMD from *P. aeruginosa* was provided by the Field group, and incubation of GDP-Man **3** with GMD in the presence of NAD^+ at RT with gentle shaking afforded **4** (Scheme 2.14), however, conversion was only 20% in the first attempt. Re-expression of GMD to produce fresh aliquots for use in the enzymatic synthesis later improved conversion to 70%.



Scheme 2.14: Enzymatic synthesis of GDP-ManA **4** using GMD

The peak of interest was collected and lyophilised to afford GDP-ManA **4** which was characterised by ^1H , ^{31}P NMR and HRMS. The characteristic $J_{\text{H1-P}}$ was calculated as 8.0 Hz, and the smaller $J_{\text{H1-H2}}$ coupling constant identified at 1.7 Hz. ^{31}P analysis showed two resonances at δ_{P} -11.2, -13.7 ppm respectively and HRMS found the m/z ion of 618.0484 corresponding to $[\mathbf{4-H}]^-$.

2.3 Conclusions and Future Directions

In conclusion, this work presented efforts towards the synthesis of four differentially protected glycosyl 1-phosphates for evaluation in the chemical synthesis of GDP-ManA **4**. Of the routes attempted, two were successful, yielding **60** and **42**. The precursor, acetyl protected methyl uronate donor **68**, presented low reactivity and phenyl thioglycoside synthesis was hindered by competing orthoester formation. The optimum route towards these derivatives instead proceeded *via* a trichloroacetimidate donor, following removal of the anomeric acetate.

The same route was adopted for a benzyl protected uronate counterpart, with transformations towards its corresponding trichloroacetimidate donor largely straightforward. Unfortunately, target glycosyl 1-phosphate **62** could not be isolated due problems encountered during glycosylation of DBP. Despite use of multiple activation conditions, only a mixture of products, which may correspond to α/β anomers, were consistently formed in low yields.

The final route towards target **63** used benzoyl protected uronate donors, which showed further unreactivity compared to acetyl protected uronate donors. No reaction occurred with PhSH to form a phenyl thioglycoside, however use of the more reactive EtSH successfully yielded ethyl thioglycoside donor **85**, though only in moderate yield. No competing formation of an orthoester was observed during this synthesis. Formation of **63** *via* hydrogenolysis failed, thought to be attributed to solubility issues.

The optimum conditions for chemical sugar-nucleotide synthesis used protected glycosyl 1-phosphate **60** and DCI (1.0 equivalent) in pyridine, providing the best

balance between reaction time and isolated yield. Deprotected glycosyl 1-phosphate **42** was poorly soluble in the solvents screened and no conversion to GDP-ManA **4** was observed.

In contrast, the enzymatic route permitted fast access to **4** in a single step. However, this transformation is reliant upon expression of GMD and the sugar-nucleotide GDP-Man **3**, which is available commercially, but is expensive. The chemical methodology permitted access to multimilligram quantities of **4**, whereas the enzymatic route only generated milligram amounts; this was key however to aid analytical methodology development in the final purification of chemically synthesised GDP-ManA **4**.¹¹⁶

The approaches described compliment the P(III)-P(V) strategy published by Zhang *et al.*¹⁰⁵, providing a total of three routes to access **4**, the native sugar-nucleotide used for alginate biosynthesis in *P. aeruginosa*. Nevertheless, both chemical methodologies are multi-step routes that deliver the target material in overall yields of less than 10%. Exploration of transformations such as a C6 oxidation *post*-phosphate installation (TEMPO/NaOCl)¹¹⁷ or C6 oxidation (Pt, O₂)¹⁰⁴ *post* sugar-nucleotide formation would be logical steps to improve this in the future, as problems caused by low reactivity of uronate donors would be removed.

Chapter 3: Sugar-nucleotide tools for GMD

3.0 Introduction and aims

As outlined in Chapter 1.5, the synthesis of sugar-nucleotide probes for chemical biology applications is well established in the literature for elucidation of biochemical mechanisms amongst pathogenic bacteria. For *P. aeruginosa* alginate biosynthesis however, comparatively little research of this nature has been reported.

Following identification of GMD as a therapeutic target, recent work within the Miller group presented the synthesis of the first series of C6-modified GDP-Man analogues as tools to probe this enzyme.¹¹⁸ A series of five diastereomerically pure, isotopically enriched analogues bearing deuterium or methyl substituents (Figure 3.1) were accessed *via* functionalisation of a common C6-aldehyde building block. Transformation to the corresponding sugar-nucleotide was accomplished using GDP-ManPP from *S. enterica*.

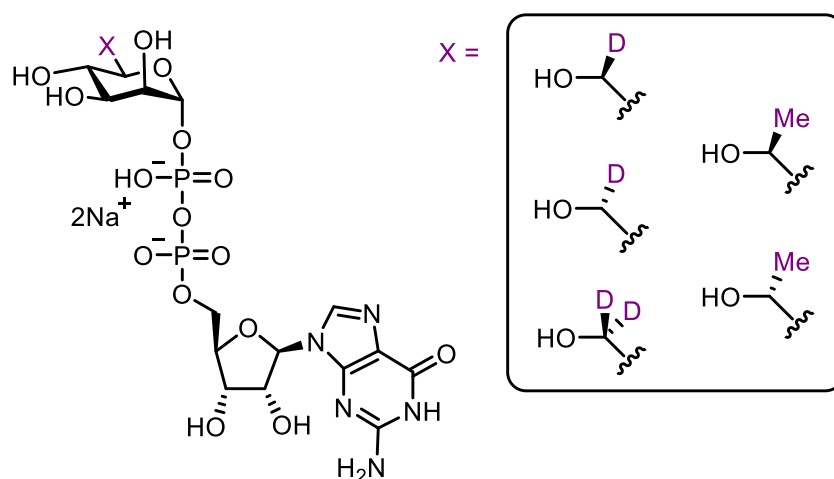
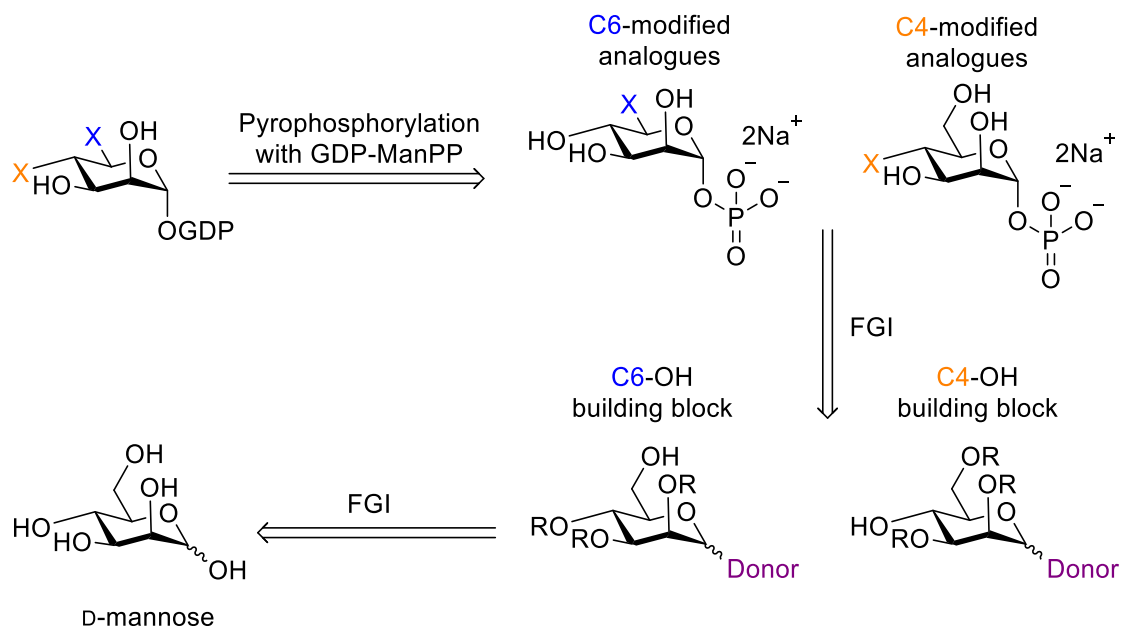


Figure 3.1: C6-modified GDP-Man analogues for use as structure-function tools of GMD.

The five analogues were evaluated as substrates of GMD, with C6-methyl analogues shown to reversibly inhibit GMD, *via* formation of a ketone during oxidation that could be identified by HRMS. This intermediate however, was not tightly bound, and upon spiking with the substrate, GDP-Man **3**, NAD(H) production was resumed.

To further this investigation, design and synthesis of structurally defined GDP-Man analogues to act as potential substrates of GMD was required. Access to these materials is crucial to advance knowledge of the GMD catalysed oxidation, with the view to gaining further insight into substrate specificity of this strategic enzyme. The analogues were proposed to bear electrophilic groups or present alternative electronic/structural properties and were categorised as follows: C6-modified, C4-modified and active site intermediate analogues.

Considering the recent literature detailing the synthesis of other sugar-nucleotide analogues discussed previously, the route towards these structure-function tools was proposed *via* a chemoenzymatic strategy, outlined in Scheme 3.1. First, modified glycosyl 1-phosphates were to be prepared chemically from protected C6-OH or C4-OH building blocks, where following a series of functional group interconversions, new analogues could be accessed. Several methodologies to install the anomeric phosphate were described in the literature, of which two will be evaluated in this work. Finally, formation of the corresponding GDP-Man analogues using GDP-ManPP from *S. enterica*, commonly utilised in the literature for syntheses of this nature, was to be evaluated.



Scheme 3.1: Retrosynthetic analysis for modified GDP-Man analogues.

3.1 C6-modified GDP-Man analogues

3.1.1 Biological rationale

Targeted covalent inhibition strategies retain importance across both areas of chemical biology and drug discovery, a recent example being Acalabrutinib. Approved by the FDA in 2017 for treatment of non-Hodgkin lymphoma, this tyrosine kinase inhibitor bears a Michael-acceptor in its structure. Furthermore, Amgen have recently reported the structure of AMG510, which was found to covalently inhibit a mutant form of the cancer target KRas. This proceeds through attack of a cysteine residue at an electrophilic Michael acceptor within AMG510. This discovery evolved from a sugar-nucleotide tool used in preliminary studies of the target enzyme.^{119,120}

With these recent examples in mind, the first series of sugar-nucleotide probes as structure function tools for GMD were designed to feature alternative functionalities at the C6-position of mannose (Figure 3.2). Inert to native oxidation, the first two probes in this category, featuring a chloride and a nitrile group, are intended to interact with the active site Cys²⁶⁸ residue of GMD through covalent attachment to the sugar-nucleotide analogue. The third probe, containing an azide moiety, was designed to investigate the substrate specificity of GMD and the final probe bearing a thio functionality was designed to investigate potential oxidation to a disulphide by GMD.

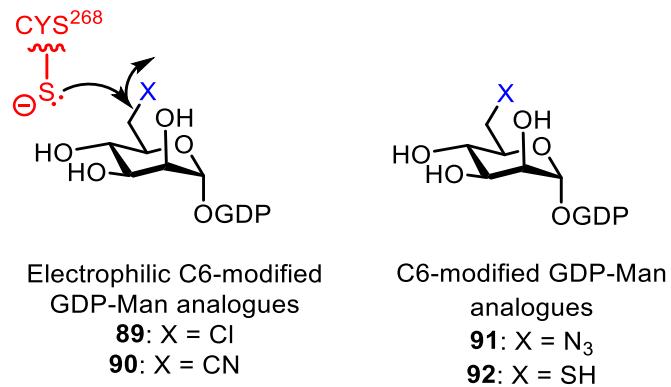
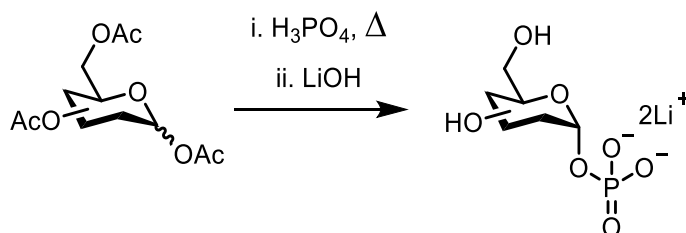


Figure 3.2: Chemical structures of C6-modified GDP-Man analogues.

3.1.2 Optimisation of MacDonald Phosphorylation

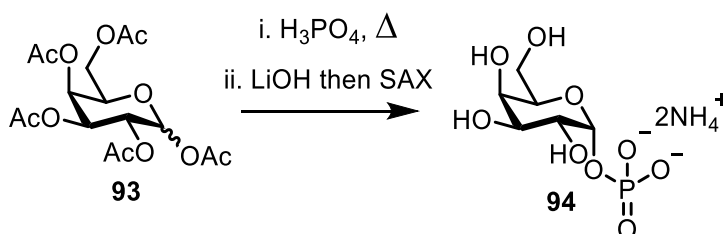
Originally published in 1962, the MacDonald phosphorylation procedure uses high temperature (50 °C) and low pressure to form a melt of crystalline H_3PO_4 and per-*O*-acetylated sugar, leading to glycosylation of the anomeric position and release of AcOH (Scheme 3.2).⁷⁵ The utility of this methodology has been demonstrated by several research groups^{95,101,121} to access both native and modified glycosyl 1-phosphates, however the procedure is often low yielding and requires a significant excess of H_3PO_4 (10.0 equivalents). Nevertheless, given the simplicity of this method, we sought to optimise and explore the scope of this reaction further in our synthesis of modified glycosyl 1-phosphates.¹²²



Scheme 3.2: General overview of MacDonald phosphorylation.

One of the main problems associated with MacDonald phosphorylation is undesired hydration of crystalline H_3PO_4 due to its hygroscopicity, where upon exposure to the atmosphere, the material quickly turns from an opaque crystalline solid to a paste. Presence of water leads to diminished yields of the desired glycosyl 1-phosphate, as it competes in the anomeric substitution reaction to form a hemiacetal by-product. Initial investigation began using per-*O*-acetylated galactose **93** (Scheme 3.3), where to overcome the issue of hydration, transfer of H_3PO_4 to a Schlenk tube containing **93** was performed in a glove box (or commercially available glove bag) under a N_2

atmosphere. The first attempt was performed on 500 mg scale with 10.0 equivalents of H_3PO_4 (Table 3.1, Entry 1). The melt was stirred for 3 h at 50 °C under vacuum, then saponified using 1M LiOH. Following filtration through a Whatman filter and neutralisation, the filtrate was concentrated *in vacuo* to afford a white solid.



Scheme 3.3: Optimisation of MacDonald phosphorylation to synthesise **94**.

Purification by strong anion exchange chromatography permitted facile removal of the uncharged hemiacetal by-product by initial washing with 3 column volumes (CV) of H_2O , followed by 3 CV of 1M NH_4HCO_3 to afford the desired glycosyl 1-phosphate **94** in improved yield of 68%. This presented an increased yield in comparison to the original publication by MacDonald in 1962, where **94** was isolated in 35% yield.

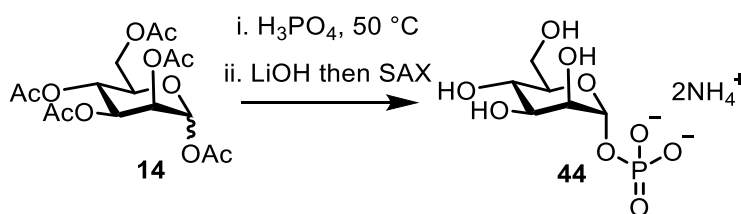
Entry	H_3PO_4 (equiv.)	Temperature (°C)*	Yield (%)	Scale (mg)	Time (h)
1	10.0	50	68	500	3
2	10.0	50	65	100	3
3	10.0	50	69	50	3
4	10.0	40	62	80	3
5	5.0	40	67	300	3

Table 3.1: Summary of optimised conditions for MacDonald phosphorylation.

*this refers to the heating block temperature not internal reaction temperature.

Subsequent reactions were performed on smaller scales to assess any effect on isolated yield, as in the synthesis of modified glycosyl 1-phosphates less material is generally available. When performed on 50-100 mg scales (Table 3.1, Entries 2 and 3), the desired glycosyl 1-phosphate was still isolated in pleasing yields exceeding 60%. Lowering the temperature to 40 °C also maintained the yield of **94** (Table 3.1, Entry 4), however, lowering the temperature further to 30 °C lead to inefficient formation of the melt. The final modification to the procedure investigated the effect of reducing the equivalents of H₃PO₄ from 10.0 to 5.0. This offered the best balance between reaction time and full conversion of the starting material by TLC at 40 °C (Table 3.1, Entry 5).

With an improved procedure available, per-*O*-acetylated mannose **14** was evaluated as a substrate, which was isolated in 55% yield (Scheme 3.4) following SAX chromatography. The structure was confirmed by ³¹P NMR analysis, where a resonance at δ_P 2.0 ppm (*J*_{H1-P} of 8.5 Hz) was observed. Having improved the yield for the synthesis of **44**, this provided scope to synthesise modified mannose 1-phosphate analogues using this methodology, discussed in further detail during this chapter.



Scheme 3.4: Synthesis of **44** via MacDonald phosphorylation.

3.1.3 Studies towards the synthesis of 6-chloro-6-deoxy- α -D-mannopyranosyl phosphate

Literature precedent and proposed mechanism of action

To further expand the toolkit and permit investigation of GMD mediated oxidation, we sought to synthesise sugar-nucleotide probes containing a C6-halogen substituent. Installation of such functionalities that act as leaving groups could lead to the formation of a covalent bond between Cys²⁶⁸ and the analogue, GDP-6-chloro-6-deoxy-mannose **89**, shown in Figure 3.3, with the potential to inhibit GMD mediated GDP-ManA production.

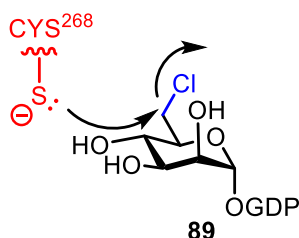


Figure 3.3: Proposed interaction of Cys²⁶⁸ with **89**.

To support the design of such probes molecular docking of an electrophilic GDP-Man analogue was completed with GMD. The corresponding covalent adduct formed following the proposed alkylation by Cys²⁶⁸ is illustrated in Figure 3.4.

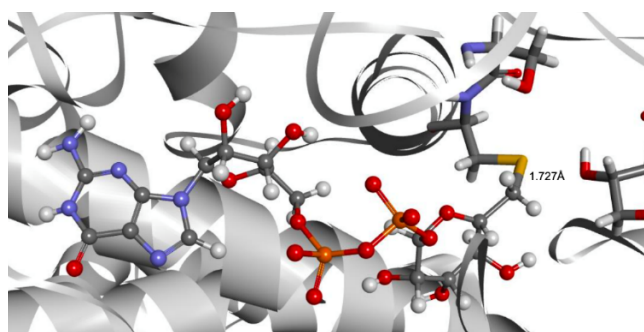
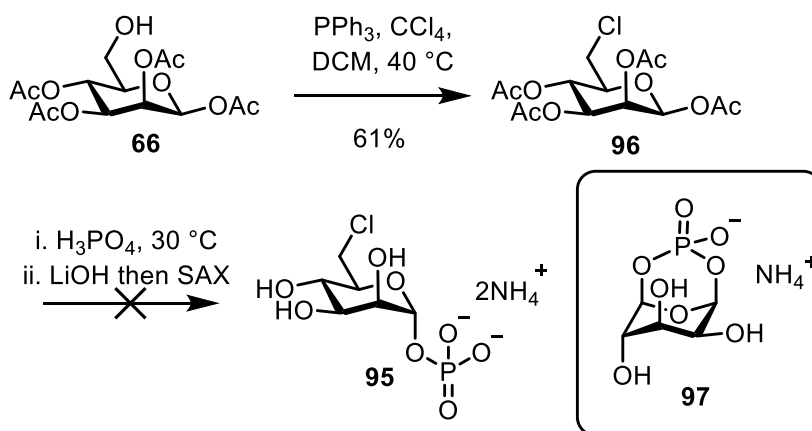


Figure 3.4: Covalent adduct formation following alkylation by Cys²⁶⁸.

Attempted synthesis of 6-Chloro-6-deoxy-mannopyranosyl phosphate

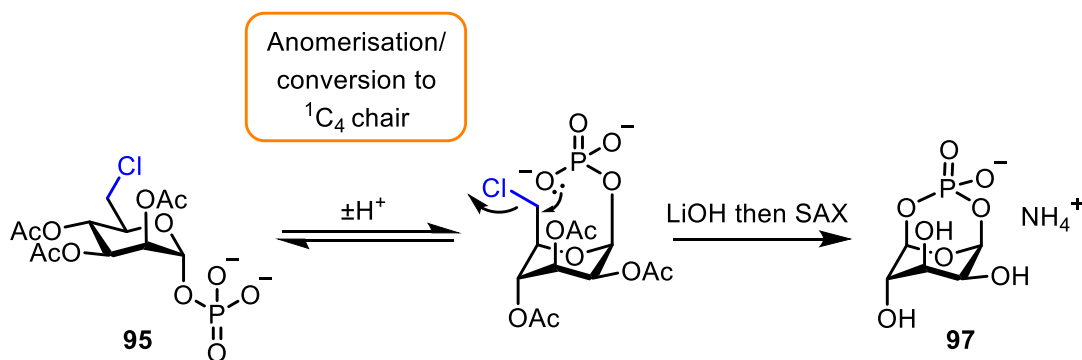
The route towards 6-Chloro-6-deoxy-mannopyranosyl phosphate **95** was designed from alcohol **66** (Scheme 3.5), that was transformed by Appel halogenation conditions (PPh_3 and CCl_4). After heating at reflux for 6 h, TLC analysis confirmed complete conversion of starting material and precursor **96** was isolated in 61% yield. Successful installation of the C6-Cl moiety could be confirmed by ^{13}C NMR, showing a new resonance that had shifted upfield to δ_{C} 42.9 ppm from δ_{C} 61.4 ppm.



Scheme 3.5: Attempted synthesis of glycosyl 1-phosphate **95**.

Following preparation of the reaction mixture in a glove box, the tube was heated to 35°C under vacuum. At this temperature, the melt did not form evenly hence temperature was increased to 45°C . After stirring gently for 4 h, two new R_f value spots could be observed *via* TLC, however the R_f value was higher than usually observed for a protected glycosyl 1-phosphate (0.50 as opposed to baseline). Following saponification and SAX chromatography, hemiacetal and the proposed product **95** were isolated.

Though ^{31}P NMR data showed only one resonance at δ_{P} 2.0 ppm, the anomeric proton resonance did not show the diagnostic doublet of doublets splitting pattern, instead appearing as an apparent triplet with $J = 6.8$ Hz. In the ^{13}C spectrum, coupling constants of $J_{\text{C1-P}} = 3.2$ Hz and $J_{\text{C2-P}} = 4.4$ Hz were observed. Analysis by HRMS confirmed displacement of the chloride functionality had occurred, with the major ion identified at m/z 241.0116, corresponding to species $[\mathbf{97}\text{-H}]^-$. It was proposed that during phosphorylation of **96**, intramolecular substitution of the C6-Cl through the anomeric oxygen afforded **97**, as shown in Scheme 3.6.



Scheme 3.6: Proposed mechanism for formation of **97**.

X-ray crystallographic data could not be obtained for **97**, therefore its anomeric configuration remains unconfirmed, however density functional theory (DFT) calculations suggest preference for the β -anomer, with a $\text{H}_1\text{-H}_2$ dihedral angle of 40.3° predicted (Figure 3.5). This supports assignment of **97** as the β -anomer, suggesting interconversion between α/β anomers may occur under the acidic conditions employed for this transformation. Consultation of the literature showed no previous reports of O^1, O^6 7-membered cyclic phosphate formation.

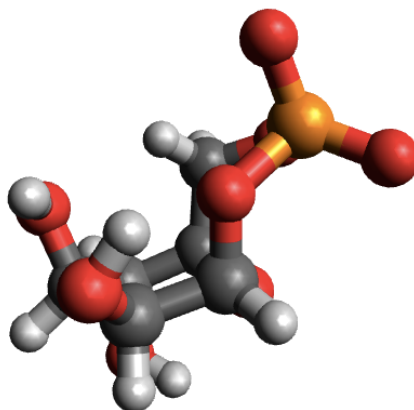
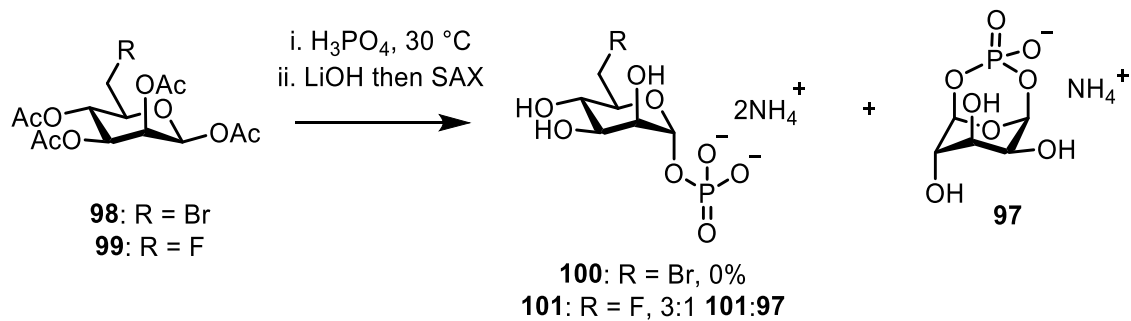


Figure 3.5: DFT energy minimised 3C_0 conformation of **97** (β -anomer).

The reaction was repeated at 35 °C and monitored every 30 min by TLC with the hope of isolating desired glycosyl 1-phosphate **95** prior to cyclisation. Unfortunately, within 1 h formation of **97** had occurred, and following saponification and work-up the resultant spectral data matched those previously obtained. It was concluded that **96** was an unsuitable substrate for MacDonald phosphorylation and the functionalised glycosyl 1-phosphate analogue could not be isolated using this methodology.

Work into the synthesis C6-halogenated glycosyl 1-phosphate analogues was continued by another member of the research group, with the results summarised in Scheme 3.7. Attempted synthesis C6-Br analogue **100** showed the same result, with exclusive formation of **97** observed. However, the C6-F analogue **101** could be isolated in a 3:1 ratio of **101:97** when the reaction was performed at 30 °C for 6-7 h. These findings followed the expected trend based on knowledge of leaving group capabilities of halogens.

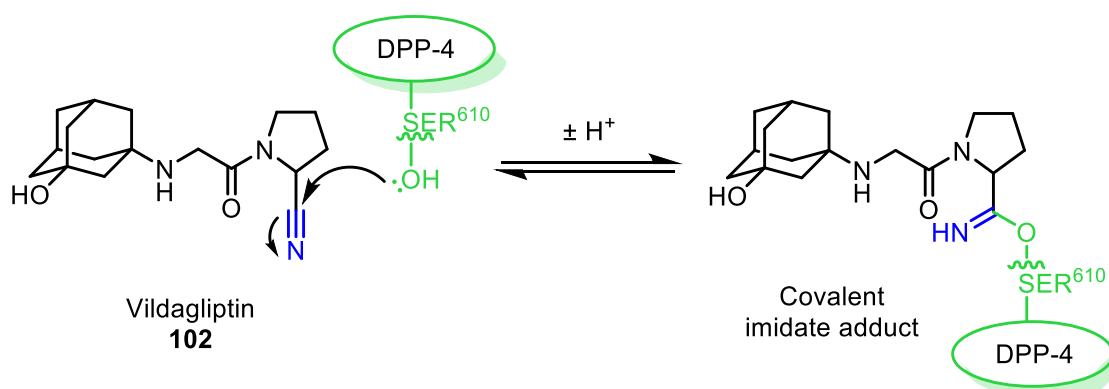


Scheme 3.7: Evaluation of **98** and **99** as substrates of MacDonald phosphorylation.

3.1.4 Studies towards the synthesis of α -D-mannopyranosylurononitrile phosphate

Literature precedent and proposed mechanism of action

Nitriles are known to react with both serine and cysteine residues of proteases to form imidate or thioimide covalent adducts, respectively. Relevant examples include Vildagliptin **102**^{123,124}, which interacts with an active site Ser⁶¹⁰ residue within DPP-4 for the treatment of Type 2 diabetes (Scheme 3.8) and Cathepsin K inhibitors that interact with active site cysteine residues as a treatment for osteoporosis.¹²⁵



Scheme 3.8: Proposed mechanism of action of Vildagliptin **102**. Attack of DPP-4 Ser⁶¹⁰ residue at the nitrile moiety forms a covalent imidate adduct.¹²⁴

Based on this information, it was proposed that novel analogue GDP-6-nitrile-mannose **90** may act as an inhibitor of GMD, providing a 'sink' for Cys²⁶⁸ by forming a covalent adduct with this key active site residue (Figure 3.6). In turn, this may lead to disruption of the oxidation of GDP-Man by GMD. Molecular docking of **90** with GMD supported a potential interaction, with a distance of 3.47 Å observed between Cys²⁶⁸ and C6 of **90**, comparable to 3.26 Å for the native product, GDP-ManA **4**.

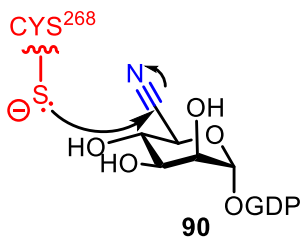
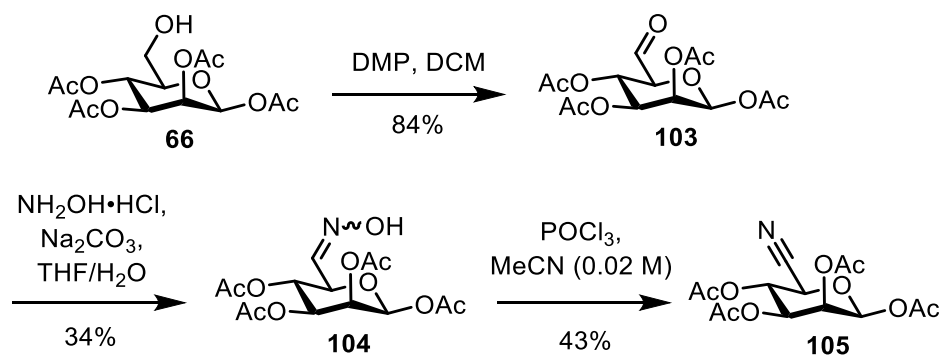


Figure 3.6: Proposed interaction of Cys²⁶⁸ with GDP-Man analogue **90**.

Synthesis of acetyl protected 6-mannopyranosylurionitrile derivatives

The strategy towards C6-nitrile derivatives was designed from work reported recently by Mende *et al.*¹²⁶, which proceeded from a C6-aldehyde *via* an oxime intermediate (Scheme 3.9). Alcohol **66** was treated with Dess-Martin periodinane (DMP), affording aldehyde **103** in 84% yield that was immediately reacted with hydroxylamine hydrochloride (NH₂OH·HCl) in the presence of Na₂CO₃ for 15 h. Following purification by column chromatography, **104** was successfully isolated in a moderate yield of 34%.



Scheme 3.9: Synthesis of **105**.

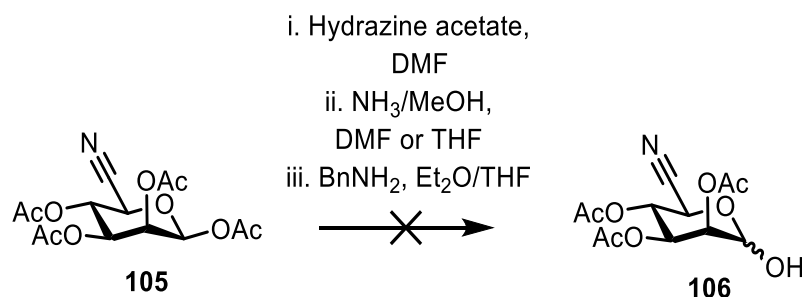
Oxime **104** was then subjected to treatment with phosphoryl chloride (POCl_3) at 65 °C, to produce nitrile **105**. It was noted that the concentration of the reaction mixture was 0.02 M (Table 3.2, Entry 1) in the original procedure, which made conversion of **104** slow, requiring a reaction time of 9 h.

Entry	[104] (M)	Time (h)	Isolated yield (%)
1	0.02	9.0	43
2	0.04	4.0	37
3	0.05	3.0	29
4	0.08	2.5	31
5	0.10	2.0	28

Table 3.2: Optimisation of POCl_3 mediated synthesis of nitrile **105**.

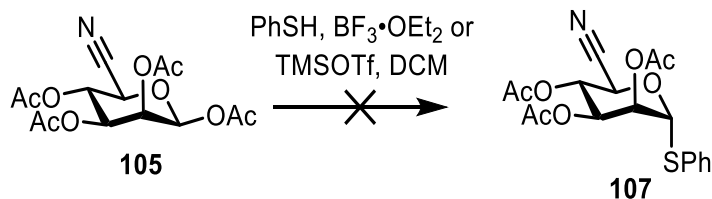
Following purification by column chromatography desired analogue **105** was isolated, however a small amount of **104** was also recovered. The experiment was repeated at higher concentration of 0.1 M with respect to starting material (Table 3.2, Entry 5), where conversion of **104** was complete within 2 h and ^{13}C NMR analysis revealed a resonance at δ_{C} 114.7 ppm, corresponding to $\text{C}\equiv\text{N}$. It was noted that the isolated yield decreased by 15% when the reaction was performed at 0.1 M, therefore the reaction was performed at a range of intermediate concentrations (Table 3.2, Entries 2, 3 and 4) to evaluate the effect on the isolated yield. The investigation showed a relationship between concentration and isolated yield, with the optimum conditions shown to be between 0.02-0.04 M (Table 3.2, Entries 1 and 2).

Following optimisation, nitrile **105** was subjected to anomeric acetate removal using established literature procedures (Scheme 3.10). Use of hydrazine acetate or NH_3/MeOH did not afford the desired hemiacetal, with TLC and NMR analysis showing no new product and only unreacted **105**, despite multiple optimisation attempts. Next, benzylamine (BnNH_2) anomeric acetate removal was attempted. This procedure uses Et_2O as the solvent, in which nitrile **105** was poorly soluble. THF was added to improve homogeneity, however no conversion of starting material was observed and only **105** was recovered.



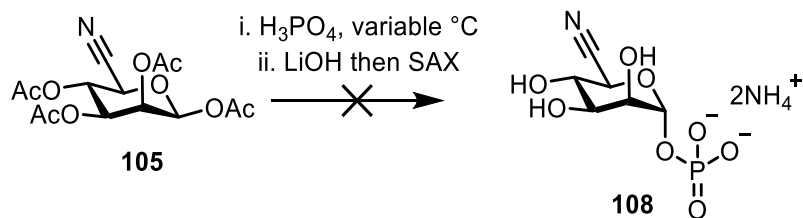
Scheme 3.10: Attempted anomeric acetate removal of **105**.

Given the difficulty faced in removal of the anomeric acetate group, next formation of thioglycoside **107** was attempted, illustrated in Scheme 3.11. This transformation was performed using $\text{BF}_3 \cdot \text{OEt}_2$ and TMSOTf, however in both instances, despite use of a large excess of Lewis acid (> 3.0 equivalents) and elongated reaction times (> 72 h) no conversion of starting material was observed and only **105** was recovered by column chromatography.



Scheme 3.11: Attempted synthesis of thioglycoside **107** using $\text{BF}_3 \cdot \text{OEt}_2$ and TMSOTf.

The final methodology screened to install the anomeric phosphate directly from **105** was MacDonald phosphorylation (Scheme 3.12). Several temperatures were attempted (see Table 3.3), however formation of a melt was difficult at lower temperatures.



Scheme 3.12: Attempted synthesis of **108** via MacDonald phosphorylation.

Entry	Scale (mg)	Temperature (°C)	Time (h)	Result
1	115	60	2.5	Decomposition
2	125	45	4	Decomposition
3	95	40	3	Hemiacetal formation

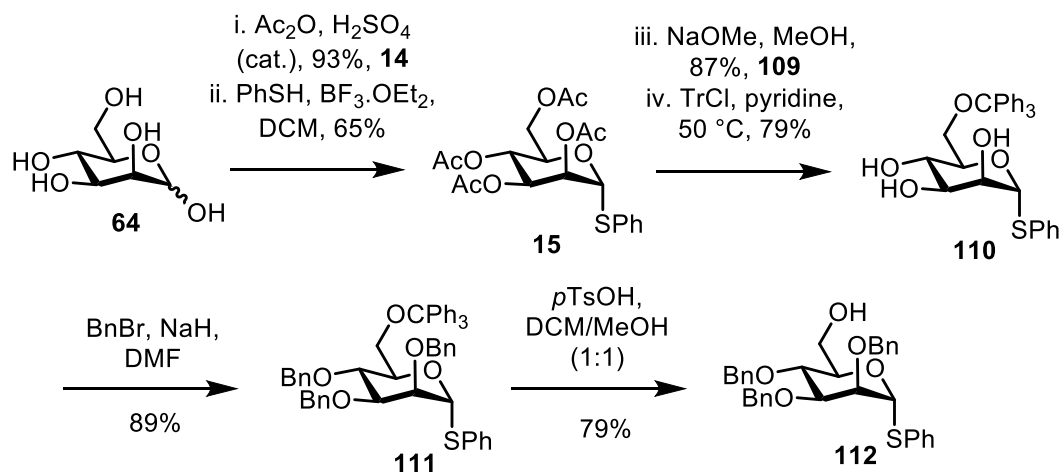
Table 3.3: Attempted conditions for synthesis of **108** via MacDonald phosphorylation.

In the first two attempts (Table 3.3, Entries 1 and 2), TLC analysis suggested some conversion of **105** was occurring, but following saponification and work-up no corresponding resonances were observed in the ^1H NMR or ^{31}P spectra, indicating decomposition to an unknown material. In the final attempt (Table 3.3, Entry 3), no conversion of starting material to a baseline R_f value spot was observed, and only hemiacetal was observed in the corresponding ^1H NMR spectrum indicated by observation of a doublet at δ_{H} 5.19 ppm.

The poor reactivity of acetyl protected C6-nitrile analogue **105** matched previous observations made in Chapter 2 during the synthesis of acetyl protected uronate donors. Whilst anomeric acetate removal could be achieved for uronate donor **68** (Chapter 2.1.1, page 67), the corresponding transformation on compound **105** failed using multiple reagents. Similarly, synthesis of a thioglycoside donor of **68** (Chapter 2.1.1, pages 64-66) was very slow and low yielding, with the equivalent reaction with **105** resulting in no formation of a thioglycoside. Even in the presence of H_3PO_4 , a strong Brønsted acid, no reaction at the anomeric centre was observed for **105**. The route towards **105** was not viable using this strategy and no further work was carried out using this series of acetyl-protected derivatives.

Synthesis of benzyl protected 6-mannopyranosyluronitrile derivatives

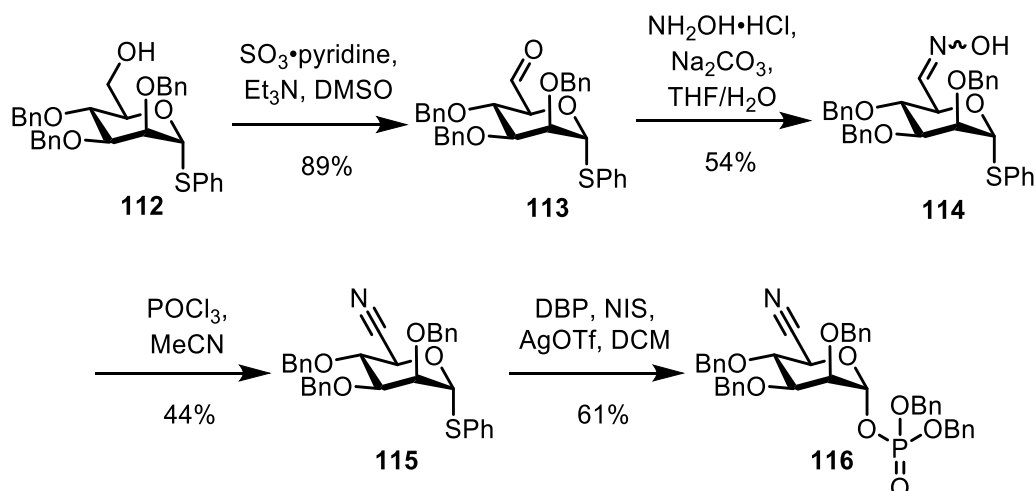
Accordingly, the route was changed to use benzyl protecting groups to produce a suitably armed donor. Starting from D-mannose **64**, successive per-O-acetylation and glycosylation of PhSH in the presence of $\text{BF}_3 \cdot \text{OEt}_2$ afforded **15**. Global deacetylation using sodium methoxide (NaOMe) and selective protection of C6-OH with a trityl group produced **110**, which was subsequently benzylated using BnBr in the presence of sodium hydride (NaH). Finally, the trityl group was cleaved using *p*TsOH in DCM/MeOH to furnish the desired C6-OH thioglycoside donor **112** in 29% yield over six steps on multigram scale (Scheme 3.13).



Scheme 3.13: Synthesis of thioglycoside donor **112** from D-mannose **64**.

Oxidation of **112** using Parikh-Doering conditions yielded aldehyde **113**; this was confirmed by ^1H NMR analysis, where a new singlet at δ_{H} 9.73 ppm was observed. This material was used immediately, without further purification, to form oxime **114**. Subsequent treatment with POCl_3 afforded the desired analogue **115** with the optimum conditions for this transformation using concentration of 0.025 M with respect to starting material to achieve a yield of 44%. Successful installation of the

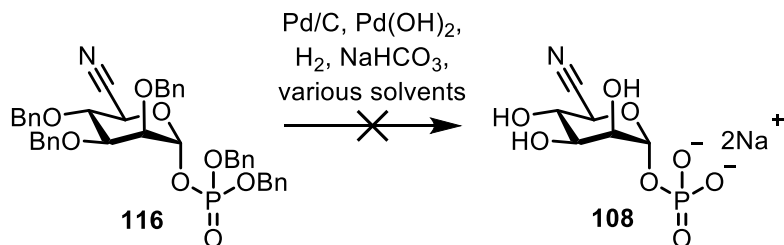
nitrile functionality was confirmed by ^{13}C NMR, with a resonance at δ_{C} 117.1 ppm corresponding to $\text{C}\equiv\text{N}$ identified (Scheme 3.14) and HRMS, where m/z 538.2055 was found corresponding to $[\mathbf{115}+\text{H}]^+$.



Scheme 3.14: Synthesis of protected glycosyl 1-phosphate analogue **116**.

Next, the phosphate functionality was introduced by reaction of **115** with DBP using NIS/AgOTf activation conditions. After stirring for 1.5 h at $-30\text{ }^\circ\text{C}$, TLC analysis showed complete conversion of **115** to a lower R_f value spot. Following purification by column chromatography, protected glycosyl 1-phosphate analogue **116** was isolated in a pleasing yield of 61%. $^{31}\text{P}\{^1\text{H}\}$ NMR analysis revealed a singlet at δ_{P} – 3.1 ppm, with the $J_{\text{H1-P}}$ calculated as 8.0 Hz.

Finally, protected glycosyl 1-phosphate **116** was subjected to hydrogenolysis using Pd/C and Pd(OH)₂/C catalysis (Scheme 3.15).



Scheme 3.15: Attempted synthesis of **108** via hydrogenolysis.

Following stirring of **116** under H₂ for 24 h in EtOH/THF, the reaction mixture was filtered over Celite™ and the solvent exchanged for MeOH/H₂O. After stirring for a further 48 h, ion-exchange and lyophilisation, NMR analysis still showed the presence of one benzyl group. The material was reconstituted in MeOH/H₂O with Pd(OH)₂/C and hydrogenolysis continued for a further 24 h, however no further benzyl removal was observed. Finally, the partially deprotected phosphate was dissolved in H₂O with Pd(OH)₂/C and stirred for a further 24 h. Unfortunately, following ion-exchange and lyophilisation, NMR analysis suggested that the compound had decomposed. In subsequent attempts, the same conditions were used with reaction times of up to 48 h, however ¹³C NMR analysis showed absence of the diagnostic C≡N resonance at ~ δ_c 115.0 ppm, at confirming that in addition to benzyl removal reduction of the nitrile moiety was occurring. To try and prevent undesired reduction, the reaction was monitored more closely by TLC (~ every 2 h) and the reaction time was shortened. Unfortunately, the same observation was made in this attempt.

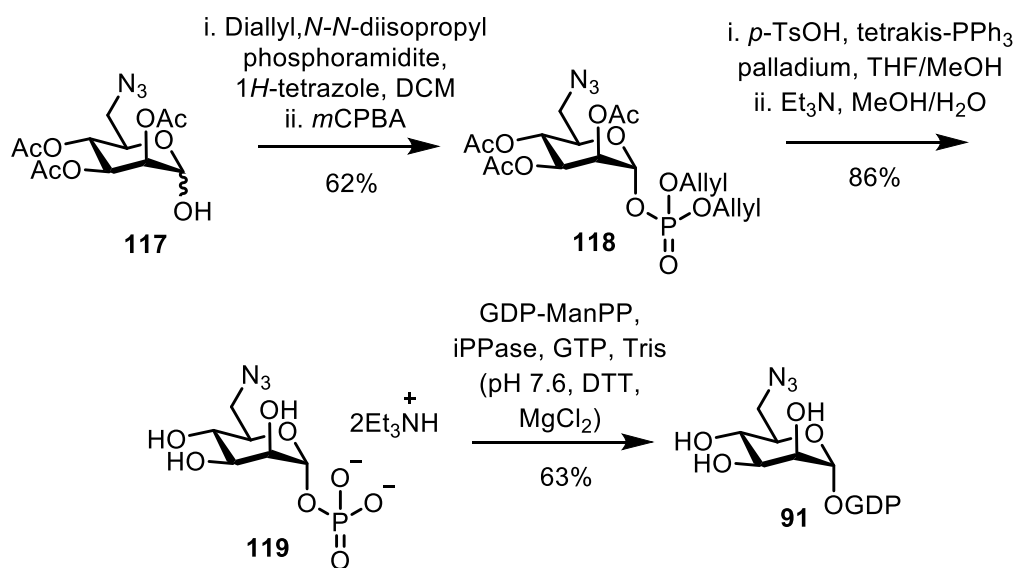
Hydrogenolysis was attempted using only Pd/C catalysis in EtOH/THF. After stirring for 9 h, conversion of starting material to lower R_f value spots was observed and the solvent was exchanged for MeOH/H₂O and stirred for a further 6 h. ³¹P NMR analysis showed 4 resonances, indicating presence of differentially benzylated compounds due to incomplete hydrogenolysis. In a final attempt, a new batch of Pd(OH)₂/C was used alongside Pd/C. Unfortunately, even after stirring in multiple solvents for 30 h, ³¹P NMR analysis still showed incomplete conversion of **116** to the deprotected glycosyl 1-phosphate **108**. Two singlets were observed at δ_P 2.6 and 0.4 ppm and resonances in the aromatic region (δ_H 7.80-7.30 ppm) were also present in the ¹H NMR spectrum.

Analogue **108** not be accessed using the Pd/C and Pd(OH)₂/C hydrogenolysis conditions described due to undesired reduction of the nitrile group. Consultation of the literature for chemoselective hydrogenolysis catalysts was unsuccessful. Sajiki *et al.* reported the use of Pd/C(en) for the selective hydrogenation of alkene and alkyne functionalities in the presence of nitriles^{127,128}, however no equivalent examples that permitted chemoselective benzyl group hydrogenolysis were found. Alternative conditions for this transformation such as oxidative debenylation (NaBrO₃/Na₂S₂O₄)¹²⁹ could not be attempted due to time constraints, and should be evaluated in future work.

3.1.5 Synthesis of 6-azido-6-deoxy- α -D-mannopyranosyl phosphate

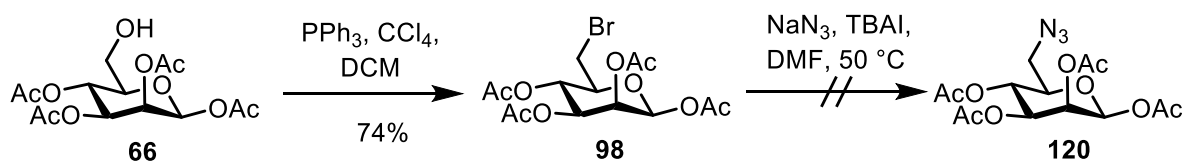
Literature precedent

For the purposes of our structure-function investigation, we wished to exploit the azido group to explore substrate specificity of GMD. Previous work by Marchesan *et al.* described the synthesis of a series of GDP-azido-mannose analogues to probe ManT activity.⁹⁶ In their synthesis of GDP-6-azido-6-deoxy-mannose **91**, the phosphate group was installed *via* a P(III) reagent, diallyl diisopropyl phosphoramidite upon reaction with hemiacetal **117**, which was oxidised to the corresponding P(V) species using 3-chloroperbenzoic acid (*m*CPBA). Deprotection was achieved using tetrakis(triphenylphosphine) palladium followed by Et₃N/MeOH/H₂O, affording **119** in an overall yield of 33%. Transformation to the corresponding GDP-sugar **91** was afforded using GDP-ManPP from *Salmonella enterica* in 63% yield (Scheme 3.16).



Scheme 3.16: Synthesis of GDP-6-azido-6-deoxy-mannose **91**.

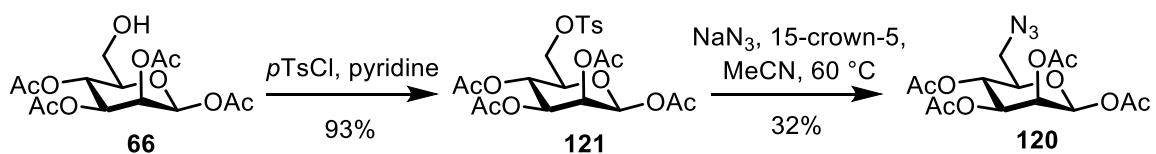
A new synthetic strategy towards 6-azido-6-deoxy mannopyranosyl phosphate **119** was devised from accessible alcohol **66** (Scheme 3.17) with the view of installing the phosphate moiety *via* the recently optimised MacDonald phosphorylation procedure. Alcohol **66** was first converted to a bromide using Appel halogenation conditions (PPh_3 and CBr_4), proceeding in a good yield of 74%. The characteristic C6-Br resonance could be observed at δ_{C} 30.3 ppm, an upfield shift in comparison to alcohol **66** (δ_{C} 61.4 ppm).



Scheme 3.17: Attempted synthesis of **120** *via* displacement of C6-bromide **98**.

Problems arose during displacement of **98** with NaN_3 in the presence of tetrabutylammonium iodide (TBAI). Despite being heated at elevated temperatures for up to 48 h, the reaction did not reach completion, with monitoring of the reaction difficult due to the almost indistinguishable R_f values of **98** and **120** in several solvent systems, which made purification difficult. NMR analysis of isolated fractions from column chromatography revealed three products: unreacted **98**, C6- N_3 **120** and an unidentified sugar, that may have corresponded to the C6-I counterpart of **66**. Alternative reaction conditions including reducing the equivalents and complete removal of TBAI were attempted. In both instances despite heating and reaction times of 72 h, incomplete conversion of **98** was observed, and the resultant mixture could not be purified successfully.

Next, the literature procedure was attempted, which utilised a tosylate leaving group for azide introduction (Scheme 3.18). Reaction of **66** with para-toluenesulfonyl chloride (*p*TsCl) in pyridine afforded **121** in an excellent yield of 93%. Unfortunately, displacement of the active sulfonyl ester with NaN₃ in DMF was initially unsuccessful, with minimal conversion to **120** observed despite long reaction times of up to 72 h and heating up to 40 °C (< 25% yield from crude NMR).



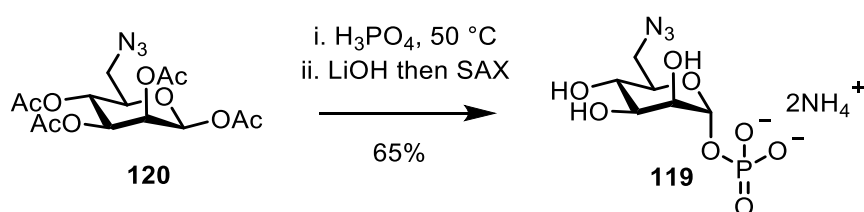
Scheme 3.18: Synthesis of **120** via displacement of tosylate **121**.

Consultation of literature for alternative conditions suggested the use of 15-crown-5 ether during azide formation.¹³⁰ The reaction was repeated at 60 °C in the presence of 15-crown-5 ether, in the hope of increasing the nucleophilicity of the azide ion through complexation of the sodium counterion. After 15 h, it appeared that most of **121** had been consumed, and isolation of the major product following column chromatography revealed the desired compound **120** but in a low yield of 29%.

Next, the solvent was changed to MeCN, to evaluate any differences in solubility or isolated yield. After stirring for 24 h at 60 °C, TLC analysis showed clear formation of a new R_f value spot and unreacted starting material. Pleasingly, no other products were isolated following column chromatography unlike in previous experiments. Whilst the isolated yield of **120** was only improved by 3%, the material was obtained in excellent purity compared to previous attempts, with the characteristic C6-N₃

resonance identified at δ_c 50.8 ppm. This was further supported by HRMS data, showing the major ion at m/z 396.1039 corresponding to $[\mathbf{120}+\text{Na}]^+$.

C6-N₃ **120** was subjected to MacDonald phosphorylation at 50 °C, as shown in Scheme 3.19. After stirring gently for 4 h, TLC analysis indicated formation of a baseline R_f value spot. Following saponification and work-up, the crude residue was applied to a SAX column affording the desired glycosyl 1-phosphate **119** as a white powder in 65% yield.



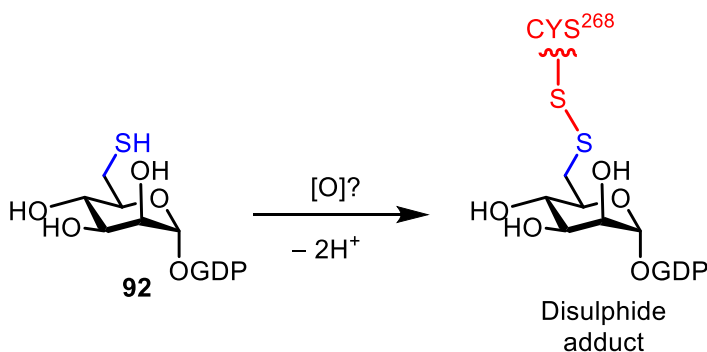
Scheme 3.19: Synthesis of **119** by MacDonald phosphorylation.

The resultant ¹H and ¹³C NMR spectra were difficult to interpret, as the ring protons had similar chemical shifts resulting in a series of multiplets that could not be characterised fully. These observations however did mirror those of previously observed data⁹⁶, and any attempted polishing of the sample, initially by repeated SAX chromatography followed by C18 chromatography, did not improve resolution. The anomeric proton was identified at δ_H 5.07 ppm, alongside the ³¹P resonance at δ_P 1.4 ppm, with the characteristic J_{H1-P} of 8.4 Hz observed. Confirmation of the structure was further supported by HRMS analysis, which found the ion at m/z 284.0288 corresponding to $[\mathbf{119}-\text{H}]^-$ as the major peak. This analogue was evaluated as a substrate of GDP-ManPP, discussed later in this chapter.

3.1.6 Synthesis of 6-deoxy-6-thio- α -D-mannopyranosyl phosphate

Literature precedent and proposed mechanism of action

The final analogue discussed in this chapter, GDP-6-deoxy-6-thio-mannose **92**, was designed to investigate the potential formation of a covalent bond between the thiol and Cys²⁶⁸ of GMD to form a disulphide adduct *via* oxidation (Scheme 3.20).



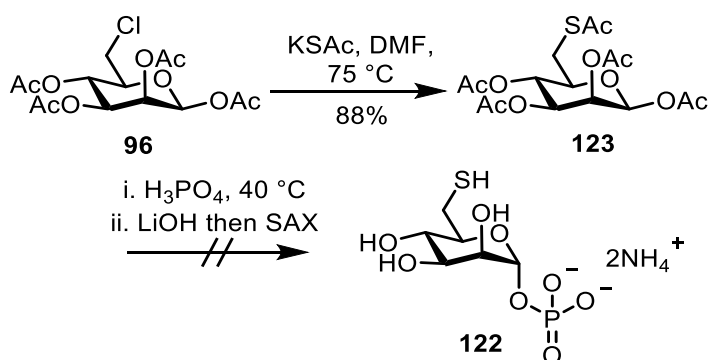
Scheme 3.20: Proposed reaction of Cys²⁶⁸ with **92** to form a disulphide adduct *via* oxidation.

This transformation would potentially prevent further turnover of GDP-ManA **4** as the key residue mediating this oxidation would be unavailable. The oxidation potential of a thiol in the active site of GMD is unknown, however disulphide probes to explore biosynthetic enzymes have been reported in the literature. An example is the synthesis of a 2-thiopyridyl containing UDP-3-deoxy-3-thio-galactose analogue used to probe the active site of β -1,4-galactosyltransferase which is involved in the biosynthesis of *N*-glycans.¹³¹

Attempted synthesis of 6-Deoxy-6-thio-mannopyranosyl phosphate

The strategy towards 6-Deoxy-6-thio-mannopyranosyl phosphate **122** was designed from per-*O*-acetylated starting materials as benzyl protected derivatives might have been incompatible during final deprotection stages, due to poisoning of palladium catalysts by sulphur.

Common leaving groups employed in the literature for the installation of the thioacetate moiety include tosylate or bromide.^{126,132} Owing to the material available at the time of synthesis, **96** was reacted with potassium thioacetate (KSAc) at elevated temperature (75 °C) in DMF. This successfully furnished protected C6-thioacetate derivative **123** in an excellent yield of 88% (Scheme 3.21).



Scheme 3.21: Attempted synthesis of glycosyl 1-phosphate analogue **122** via MacDonald phosphorylation.

Comparison of literature NMR data for the 6-deoxy-6-thio-glucose counterpart supported the NMR assignment of **123**, with key resonances identified at δ_{H} 2.32 ppm, corresponding to the diagnostic $\text{C}(\text{O})\text{CH}_3$ of the thioacetate group and δ_{C} 194.9 ppm for the thioacetate $\text{C}=\text{O}$.¹³³

With precursor **123** in hand, MacDonald phosphorylation was attempted at 40 °C. The reaction mixture was stirred gently for 5 h in total, forming a dark orange melt. TLC analysis indicated partial conversion of starting material to a baseline R_{f} value spot and as no further conversion was evident the mixture was saponified with 1M LiOH for 48 h. Following work-up and purification, two fractions were isolated, one corresponding to the hemiacetal and the other presumed to be **122**.

Initial ^1H NMR analysis of the latter fraction showed a mixture of a minimum of two products: anomeric resonances were identified at δ_{H} 5.34 and 5.16 ppm in a 2.5:1 ratio (shown in Figure 3.7) alongside corresponding resonances at δ_{P} 0.9 and 0.4 ppm in the ^{31}P spectrum. Analysis by HRMS identified two major ions at m/z 548.9910 and 469.0239. The first ion corresponded to disulphide [**124**-H]⁻, whilst the lower m/z ion correlated to the formation of a mixed disulphide containing **122** linked to the corresponding hemiacetal to afford [**125**-H]⁻.

Theoretically, as SAX separates analytes based upon overall charge, the two species would be expected to have different retention times (4- versus 2-, respectively), however the homodimerization may occur after purification whilst standing in solution or during lyophilisation. This reaction was very low yielding, and only 5 mg of **124** and **125** were isolated alongside 20 mg of hemiacetal.

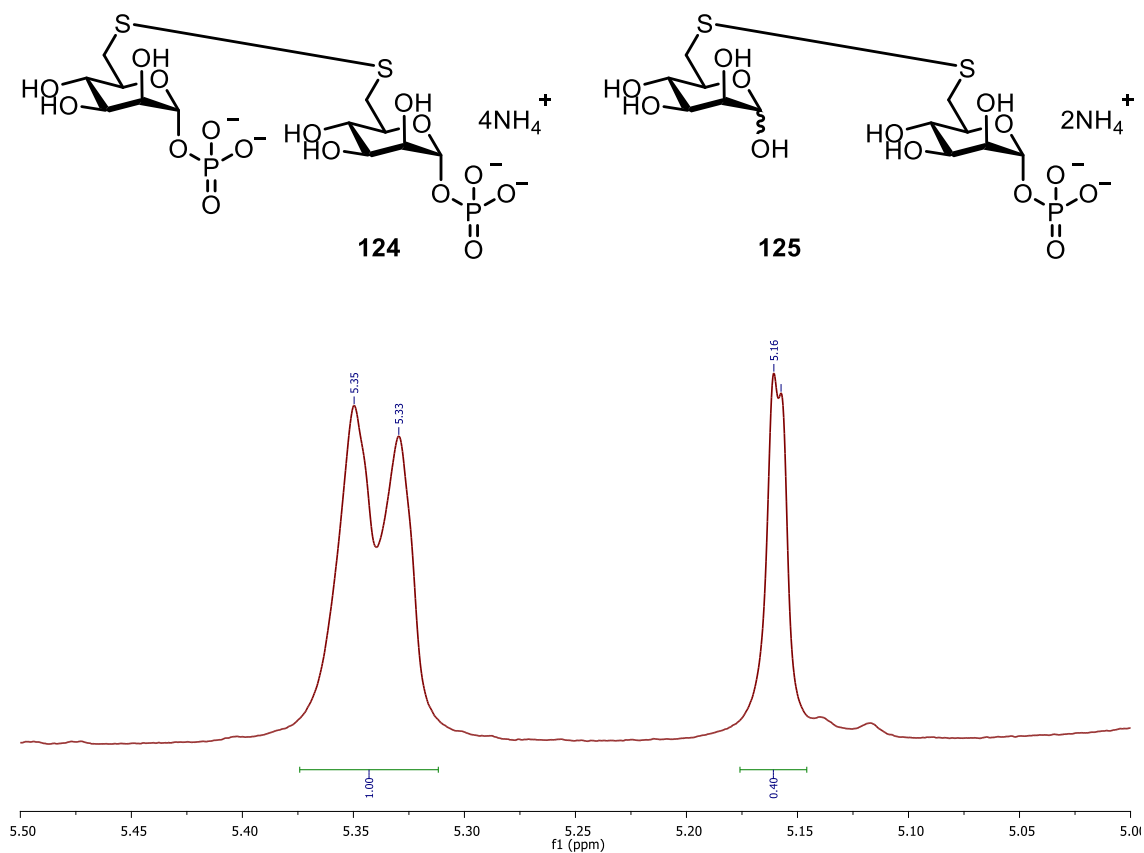
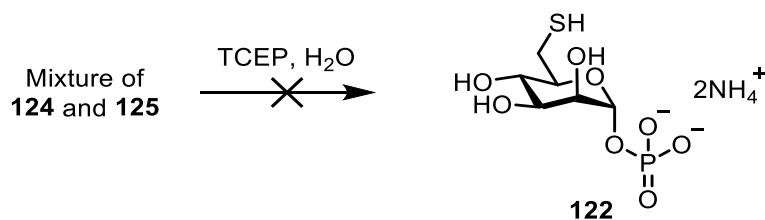


Figure 3.7: 400 MHz ¹H NMR spectrum of MacDonald phosphorylation of **122**, showing 2 anameric resonances and proposed structures of **124** and **125**.

The reaction was repeated on the same scale using the same procedure, where following SAX chromatography, 30 mg of the disulphide mixture was isolated, an improvement of 40%. As more material was available, the mixture was treated with tris(2-carboxyethyl)phosphine (TCEP), a common reagent for reducing disulphides (Scheme 3.22).



Scheme 3.22: Attempted reduction of disulphides using TCEP.

After stirring **124** and **125** with TCEP in H₂O for 6 h, the crude mixture was applied immediately to a SAX column and eluted with H₂O and 1M NH₄HCO₃ in a bid to isolate pure glycosyl 1-phosphate **122** opposed to a mixture of disulphides isolated in the previous attempt. Regrettably, this procedure did not lead to the isolation of pure **122** and no further work to access homogeneous samples of this analogue could be completed due to time constraints. The disulphide mixture was evaluated against GDP-ManPP, discussed later in this chapter.

3.2 C4-modified GDP-Man analogues

3.2.1 Biological rationale

The next series of analogues were modified at the C4-position of mannose, producing tools to evaluate the substrate specificity of GMD. Retaining the C6-OH group maintains the possibility of oxidation of these analogues by GMD, if accepted as substrates by the enzyme. If this were observed, evaluation of differences in respective rates of oxidation may identify potential competitive inhibitors of GMD.

3.2.2 Synthesis of 4-deoxy-4-fluoro- α -D-mannopyranosyl phosphate

Literature precedent and proposed mechanism of action

The introduction of fluorine to bioactive compounds is well documented in both medicinal chemistry and chemical biology. As the addition of fluorine does not result in a significant change from a steric perspective, interactions with enzyme active sites or receptor recognition sites are still possible. The greater electronegativity of fluorine, however, has the potential to notably alter biological responses.¹³⁴

As previously discussed, the use of fluorine-containing NDP-sugars as probes is common in the literature. Liu *et al.* reported the chemical synthesis of UDP-5-fluoro-Gal **57** to study the mechanism of action of UGM¹³⁵ and additionally, Schultz *et al.* published a chemoenzymatic synthesis of UDP-4-fluoro-Glc-NAc **126** and UDP-4-fluoro-Gal-NAc **127** (Figure 3.8) for their evaluation as chain terminators in glycosaminoglycan synthesis by GlmU uridylyltransferase.⁷⁷

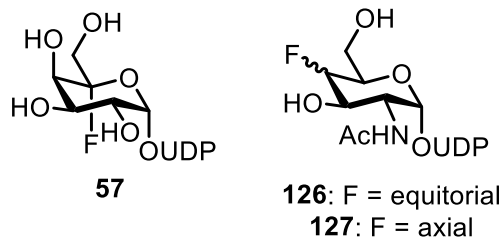
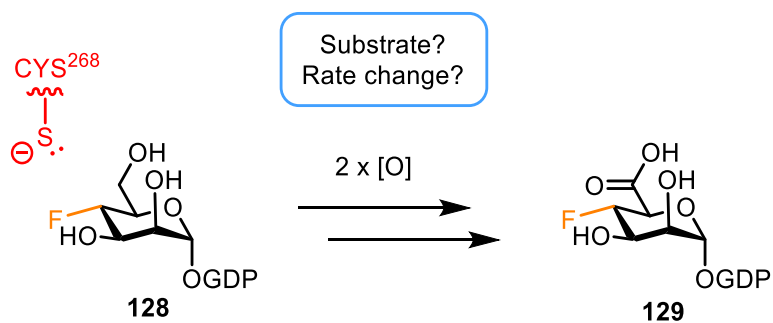


Figure 3.8: Chemical structures of fluorinated UDP-sugars **57**, **126** and **127** used as probes in chemical biology applications.

Given their importance in the elucidation of biochemical mechanisms, the novel sugar-nucleotide GDP-4-deoxy-4-fluoro-mannose **128** was chosen as a target, with a view to investigate binding potential and any electronic effects on the rate of oxidation (Scheme 3.23).

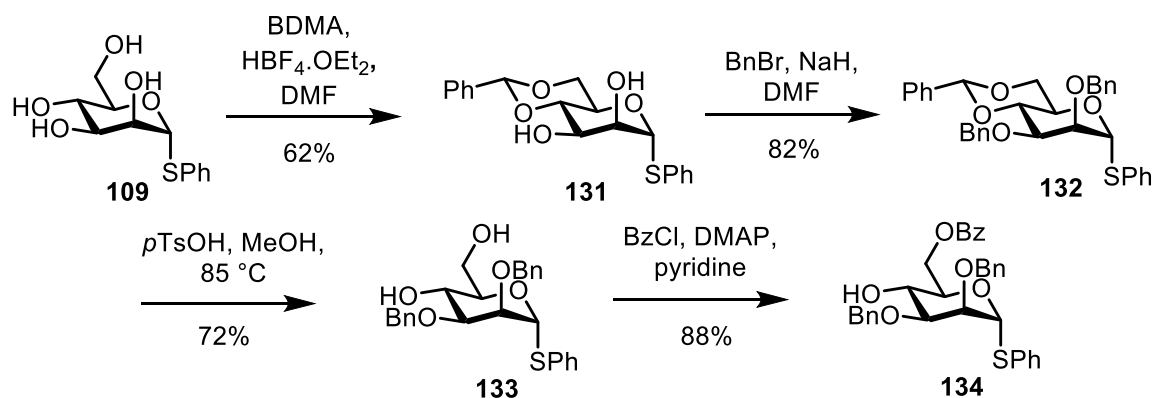


Scheme 3.23: Overview of proposed GMD catalysed oxidation of **128**.

Furthermore, if shown to be a substrate of GMD, this tool may be useful in the investigation of other areas of the alginate biosynthetic pathway such as polymerisation. In this application, if oxidised by GMD, the product GDP-4-deoxy-4-fluoro-ManA **129** may act as a chain terminator and prevent alginate polymerisation by enzymes such as *Alg44*.

Synthesis of 4-fluoro-mannopyranosyl derivatives: 6-O-benzoyl series

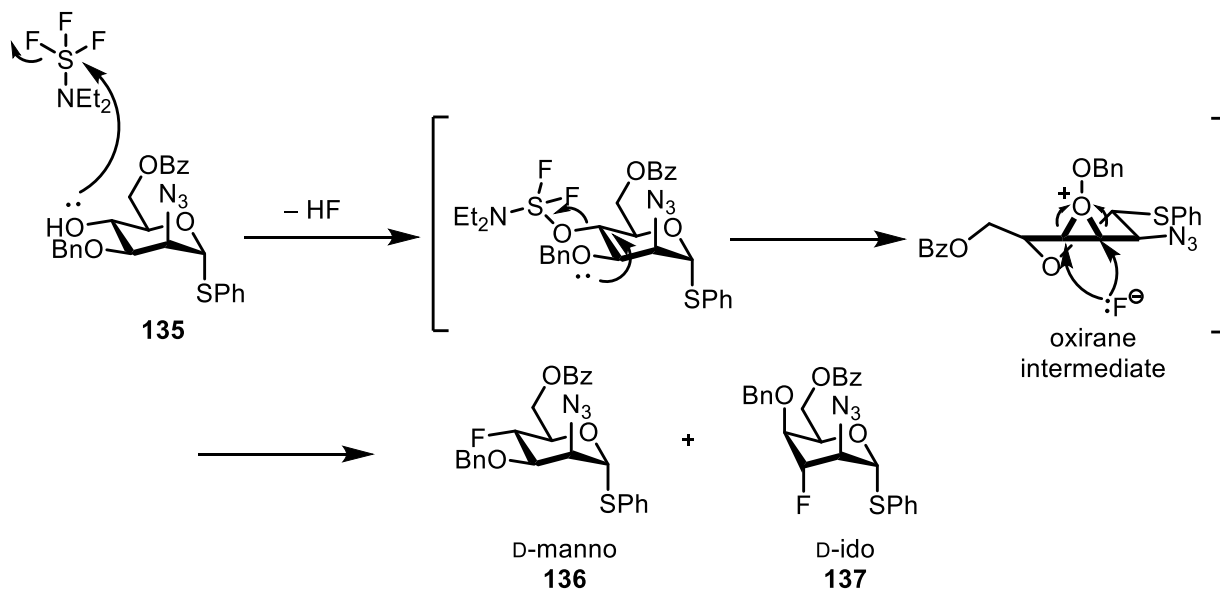
The synthetic strategy towards 4-deoxy-4-fluoro- α -D-mannopyranosyl phosphate **130** was derived from tetra-ol **109**, synthesised previously in this chapter (Scheme 3.24).



Scheme 3.24: Synthesis of C6-O-Bz building block **134**.

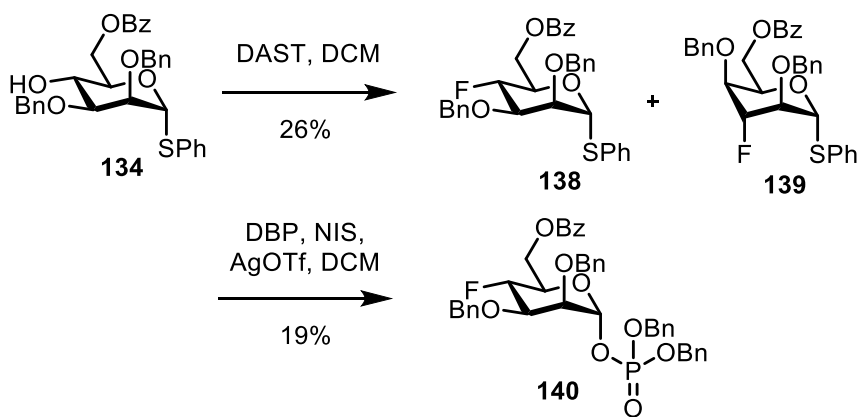
Formation of a benzylidene acetal at the C4 and C6 positions afforded **131** in 62% yield, which was subsequently benzylated using BnBr and NaH. Cleavage of the acetal was induced by *p*TsOH, before the C6-position was selectively benzoylated with benzoyl chloride (BzCl) in the presence of 4-dimethylaminopyridine (DMAP) to afford **134** in 88% yield.

Introduction of the C4-fluoro was performed using the nucleophilic fluorinating reagent diethylaminosulphur trifluoride (DAST) which had been reported in the literature for the synthesis of related compound **135**.¹³⁶ The proposed mechanism proceeds *via* an *O*-benzylated oxirane intermediate that can be opened to afford both the D-manno- and D-ido-configurations **136** and **137**, illustrated in Scheme 3.25.



Scheme 3.25: Proposed mechanism for C4-fluorination of **135** using DAST to produce **136** and **137** via an oxirane intermediate.

Initially, **134** was treated with 3.0 equivalents of DAST (Scheme 3.26). The reaction was stirred for 18 h at RT, whereby TLC analysis indicated complete conversion of **134** into a higher R_f value spot and two other minor spots, all of which were close in R_f.



Scheme 3.26: Synthesis of protected glycosyl 1-phosphate **140**.

Purification by column chromatography successfully separated this mixture, however following NMR analysis it was revealed that the higher R_f value spot still contained a mixture of both D-manno- and D-ido-configured products **138** and **139**. Separation of the regioisomers was attempted, however this was not successful despite evaluation of a range of solvent systems (hexane/Et₂O and Tol/acetone), and the crude mixture of regioisomers was isolated in a disappointing yield of 14%.

A literature procedure using 8.0 equivalents of DAST was attempted with a view to improving reaction yield. The reaction was complete by TLC within 18 h, however column chromatography was again unsuccessful in the separation of the regioisomers. Adoption of this procedure did however result in a modest yield improvement to 26%.

Given the difficulty in purification, the mixture of regioisomers was subjected to glycosylation with DBP under NIS/AgOTf activation conditions. Unlike in previous glycosylation reactions, this analogue required stirring at RT for 18 h to ensure complete conversion of **138/139**, likely attributed to the electron-withdrawing nature of the C4-fluoro group reducing anomeric reactivity.

Following work-up and column chromatography, characterisation of **140** by ¹H NMR confirmed the desired D-manno-configuration through observation of an apparent triplet with a J_{H3-H4} of 9.3 Hz, supporting the *trans* di-axial relationship between these protons (see Figure 3.9). Furthermore, the J_{H4-F} was calculated as 52.0 Hz, and a doublet at δ_F -202.9 ppm in the ¹⁹F spectrum showed a J_{C4-F} of 179 Hz. A resonance at δ_P -2.9 ppm was also observed in the ³¹P spectrum.

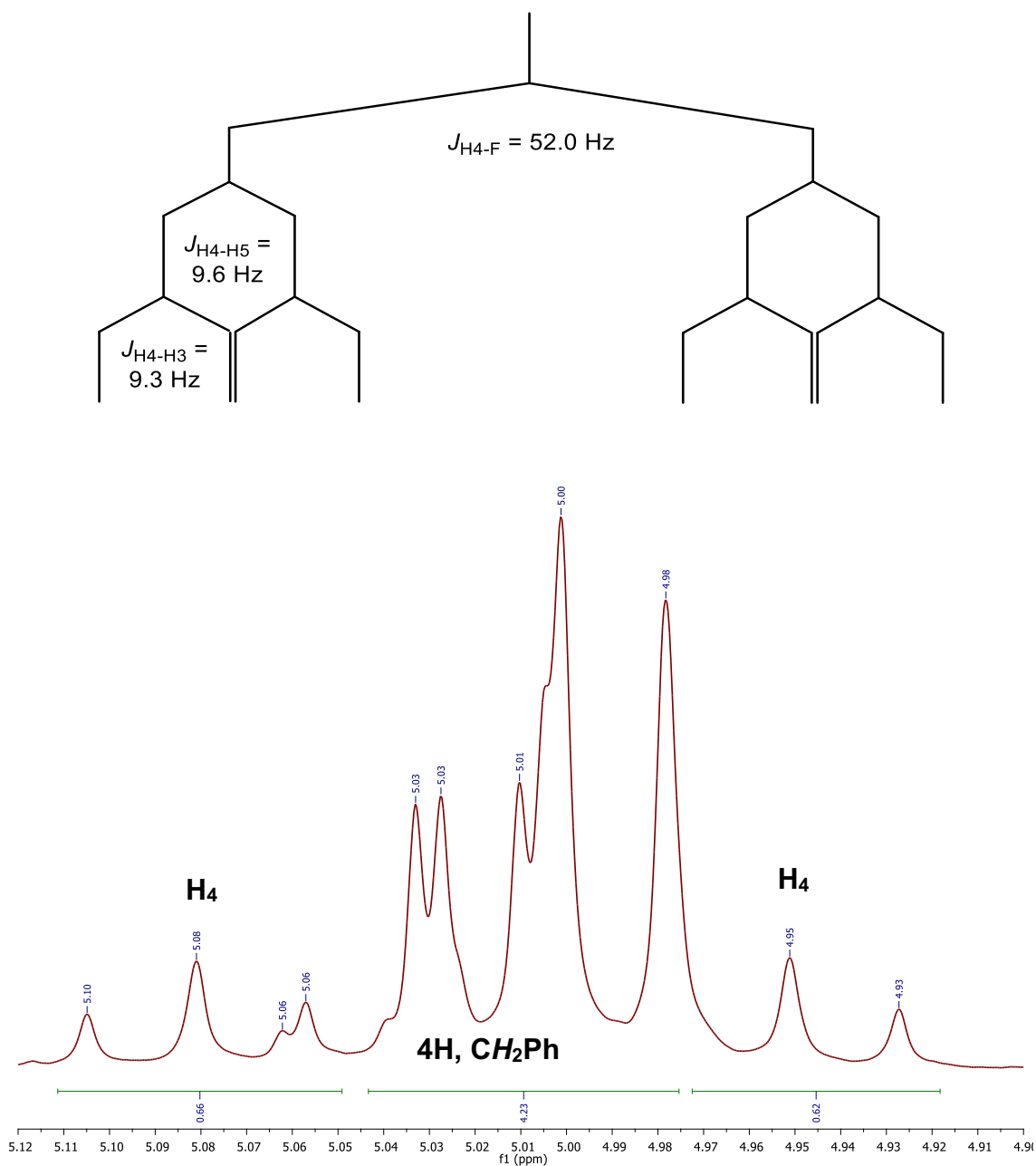
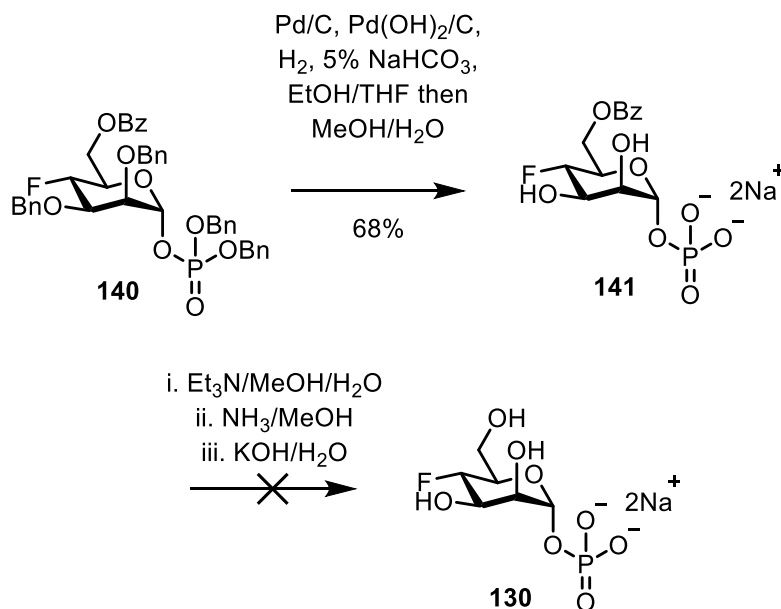


Figure 3.9: Tree diagram showing splitting of H₄ and 400 MHz ¹H NMR spectrum of **140** expanded at H₄.

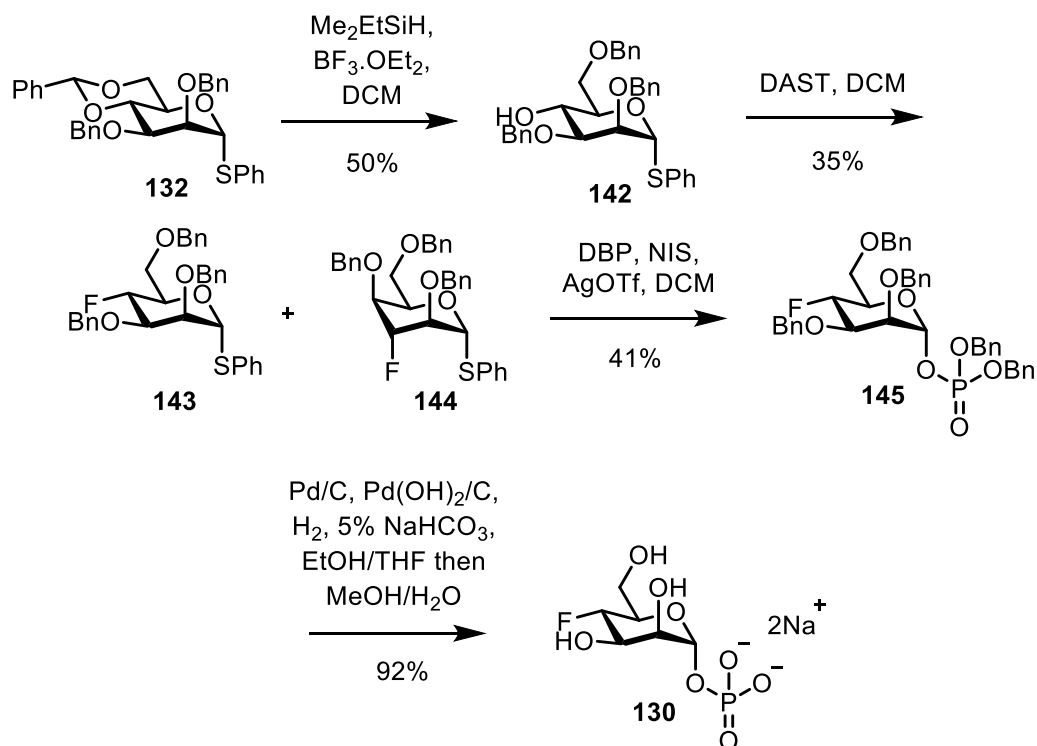
Next, deprotection of **140** was attempted using a mixture of EtOH/THF and NaHCO₃ (5% aq. solution) as reaction solvents (Scheme 3.27). After stirring for 24 h, the reaction was still incomplete by TLC, and the solvent was exchanged for MeOH/H₂O with NaHCO₃ (5% aq. solution) and hydrogenolysis continued for 36 h. NMR analysis confirmed that all benzyl groups had been removed, by the absence of the diagnostic CH₂Ph resonances by HSQC-DEPT analysis, yielding **141**. Unfortunately, saponification was challenging, and several conditions were attempted (Scheme 3.27). In all instances, benzoate cleavage was not observed despite addition of multiple equivalents of base and stirring for several days. Cleavage of the benzoate group was also attempted prior to hydrogenolysis; however this was also unsuccessful and no further conditions were screened to access **130** via this C6-O-Bz series of derivatives.



Scheme 3.27: Attempted synthesis of **130** from C6-O-Bz derivative **140**.

Synthesis of 4-fluoro-mannopyranosyl derivatives: 6-O-benzyl series

Given the difficulty in benzoate removal encountered, precursor **132** was returned to. Conditions were adopted to selectively open the benzylidene acetal to give the C6-O-Bn and C4-OH configured product **142**, with a view to permitting simultaneous hydrogenolysis of the benzyl ethers in one step, as illustrated in Scheme 3.28.



Scheme 3.28: Synthesis of modified glycosyl 1-phosphate **130**.

I_2 /sodium cyanoborohydride (NaBH_3CN) mediated reductive ring opening was reported to have high regioselectivity (> 95%) for the desired C6-OBn product in the literature.^{137,138} Unfortunately, these conditions gave rise to mostly benzylidene cleavage and **142** was only isolated in 10% yield. Alternative conditions of dimethylethylsilane (Me_2EtSiH) (5.0 equivalents) and $\text{BF}_3 \cdot \text{OEt}_2$ (2.0 equivalents) were evaluated next, which afforded the desired C6-O-Bn derivative **142** in an

improved yield of 41%, however a significant amount of diol **133** (18%) was still isolated. To optimise the method, the reaction was repeated with half the equivalents of Me₂EtSiH (2.5 equivalents) and BF₃•OEt₂ (1.0 equivalents). The reaction was complete within 1 h, and the yield of **142** improved to 50%.

With compound **142** in hand, DAST fluorination afforded a mixture of inseparable regioisomers **143** and **144**, however the crude yield was improved by 11% in comparison to the equivalent reaction with C6-OBz counterpart **134**. Glycosylation of DBP with **143/144** using NIS/AgOTf activation conditions afforded **145** in a satisfactory yield of 41%.

In the ¹H NMR spectrum of **145**, the H4 $J_{\text{H4-F}}$ and $J_{\text{H4-H3}}$ couplings were calculated as 52.0 and 9.3 Hz respectively, although this resonance was significantly overlapped by -CH₂Ph protons. In the ¹⁹F NMR spectrum, a doublet of doublets resonating at $\delta_{\text{F}} -202.5$ ppm revealed a $J_{\text{H4-F}}$ of 52.0 Hz and $J_{\text{H3-F}}$ of 12.7 Hz (Figure 3.10). Additional data revealed a $J_{\text{C4-F}}$ of 179 Hz, and the dibenzyl phosphate resonated at $\delta_{\text{P}} -2.8$ ppm, which agreed with spectroscopic data obtained for previously synthesised analogue **140** and supported the assignment of C6-OBn derivative **145**.

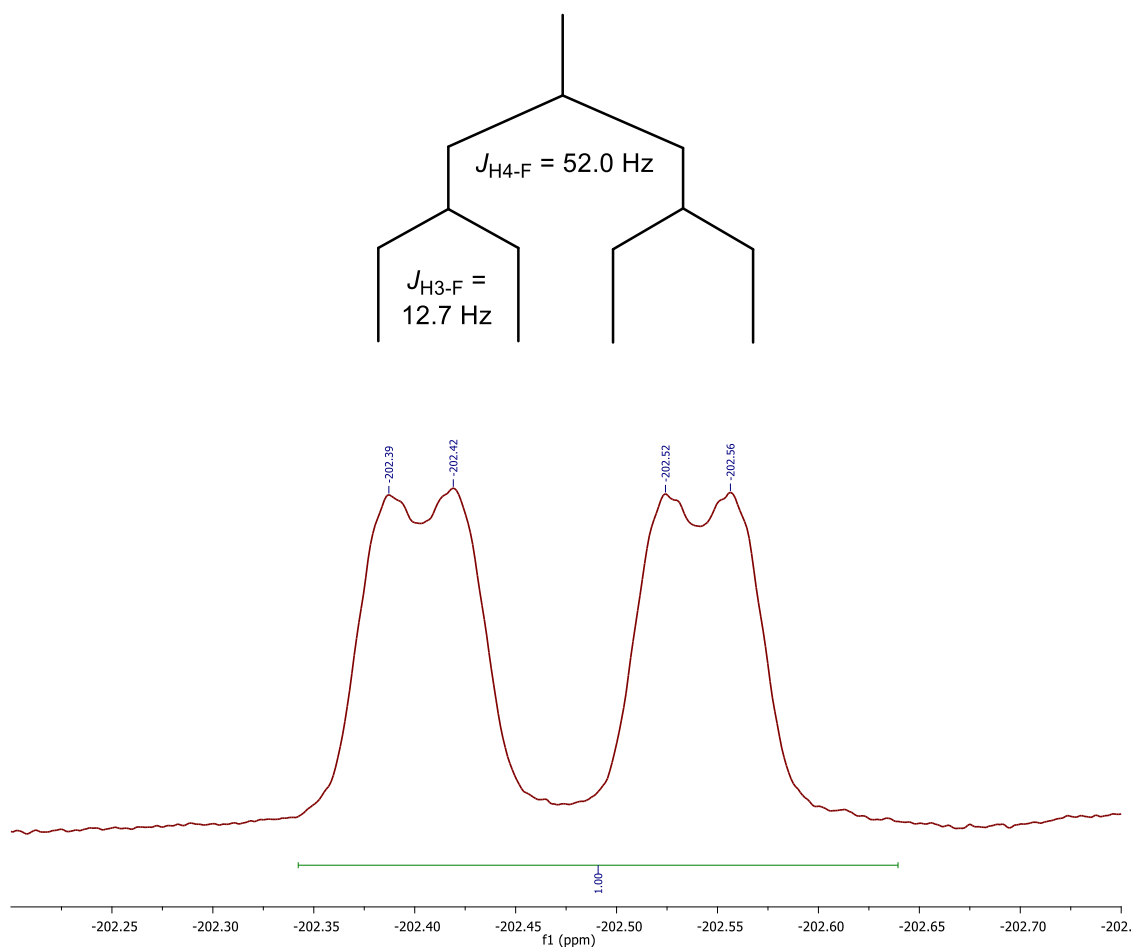


Figure 3.10: 376 MHz ^{19}F spectrum of **145**.

Finally, protected glycosyl 1-phosphate **145** was dissolved in EtOH/THF (2:1) with Pd/C and Pd(OH)₂/C and placed under a positive pressure of H₂. After stirring vigorously for 20 h at RT, TLC analysis indicated that deprotection was complete. Standard purification afforded target glycosyl 1-phosphate **130** as a white solid in 85% yield. ^{19}F NMR analysis confirmed the structure of the product, with a doublet of doublets resonating at $\delta_{\text{F}} -205.3$ ppm ($J_{\text{H4-F}} = 52.0$ Hz, $J_{\text{H3-F}} = 13.3$) identified. This was further supported by ^{31}P NMR ($\delta_{\text{P}} -2.2$ ppm) and HRMS data, where m/z 261.0182 was identified, corresponding to [**130-H**]⁻. This analogue was evaluated as a substrate of GDP-ManPP, discussed later in this chapter.

3.2.3 Studies towards the synthesis of 4-deoxy- α -D-manno-hex-4-eno-1,5-pyranosyl phosphate

Literature precedent

The final target in this category designed to probe GMD substrate specificity featured a double bond between the C4 and C5 positions of mannose, creating a 4,5-unsaturated system (Figure 3.11). This analogue could be used investigate binding within the active site of GMD, as it would be expected to adopt an alternative conformation to a 4C_1 chair. As oxidation of **146** would produce a conjugated system, it would be interesting to evaluate the rate of this transformation if accepted as a substrate. Furthermore, it would be of interest to explore **149** as a potential chain terminator of alginate production by inhibition of polymerisation.

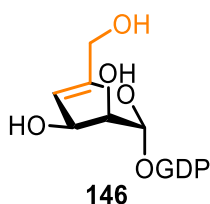
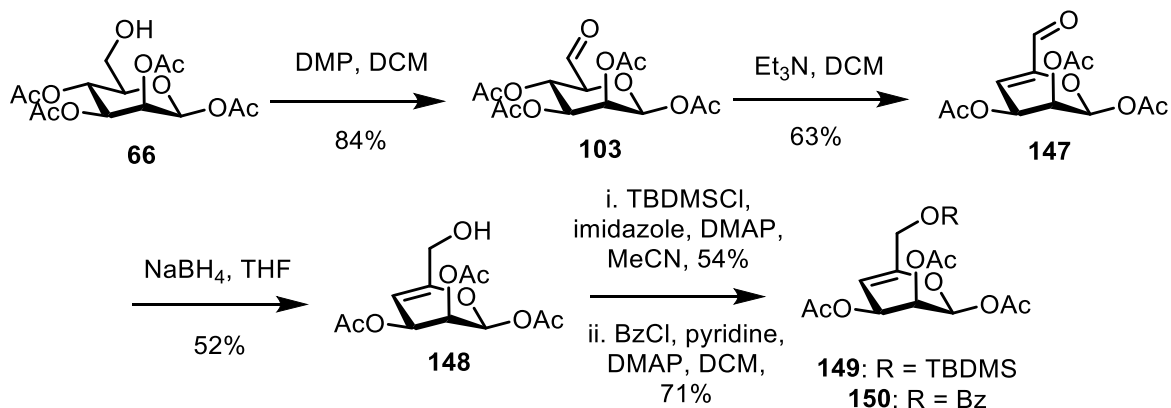


Figure 3.11: Chemical structures of alkene containing GDP-Man analogue **146**.

Anomeric acetate series

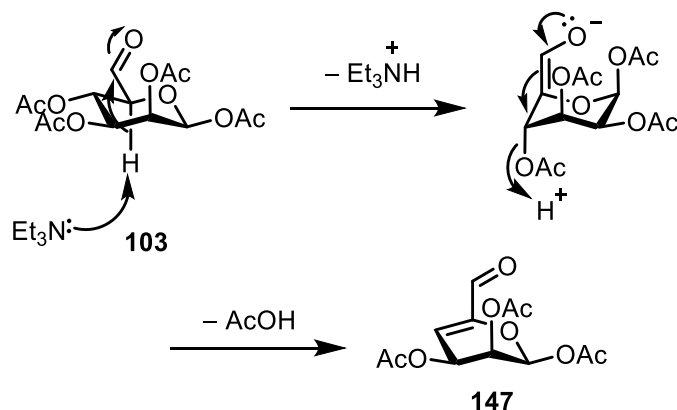
The route towards this analogue was derived from alcohol **66**, as shown in Scheme 3.29. As used in studies towards the synthesis of C6-nitrile containing analogues, DMP mediated oxidation afforded aldehyde **103** in 84% yield. Elimination of the C4-acetate was successfully induced by the addition of Et_3N , where upon stirring for 2 h at RT, compound **147** was isolated in 63% yield. The structure was confirmed by NMR analysis, showing absence of H5 and a $\text{C}(\text{O})\text{CH}_3$ singlet. The ${}^{13}\text{C}$ chemical

shifts of C₄ and C₅ could also be easily identified at δ_c 114.3 and 150.2 ppm, respectively, lying within the expected region for an alkene.



Scheme 3.29: Synthesis of protected 4,5-unsaturated analogues **149** and **150**.

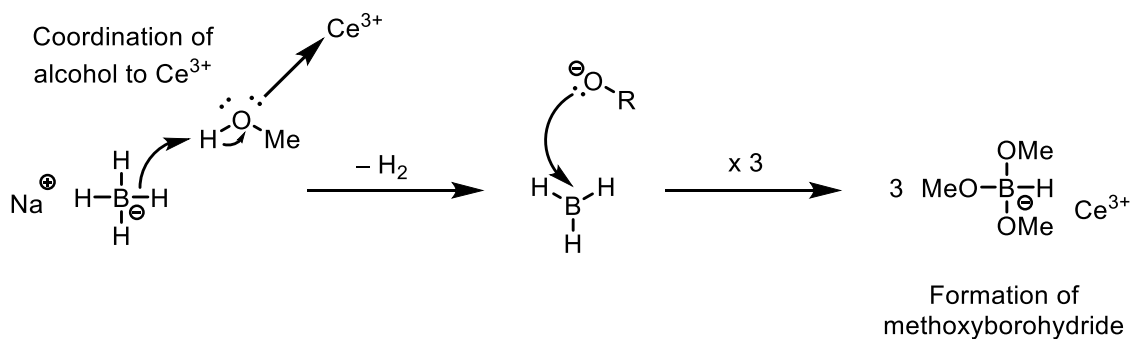
This step proceeds *via* an E₁cB mechanism, with the acidic H₅ proton of **103** easily removed by Et₃N as it can be stabilised by conjugation into the carbonyl. Following a conformational change to a ¹C₄ chair, elimination of the C₄-acetate affords derivative **147**, as shown in Scheme 3.30.



Scheme 3.30: Formation of **147** *via* an E₁cB reaction.

Following elimination of the C₄-acetate, sodium borohydride (NaBH₄) mediated reduction successfully yielded allylic alcohol **148**. Success of this transformation was

confirmed by NMR, through disappearance of the aldehyde proton at δ_{H} 9.29 ppm and replacement by a multiplet at δ_{H} 4.07 ppm integrating for 2H, corresponding to H_6 and H_6' . The desired reduction product was only isolated in 52% yield, therefore Luche reduction conditions were evaluated.^{139,140} In this procedure, cerium trichloride heptahydrate ($\text{CeCl}_3 \cdot 7\text{H}_2\text{O}$) acts as a Lewis acid catalyst to generate methoxyborohydride *in-situ*, outlined in Scheme 3.31. This species is a harder reducing agent than NaBH_4 , therefore would have greater selectivity towards the harder 1,2-addition site in accordance to hard soft acid base (HSAB) theory.

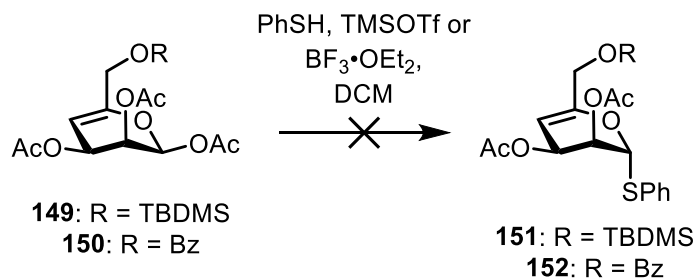


Scheme 3.31: Summary of Luche reduction conditions.

Unfortunately, in both reduction attempts using these conditions, the isolated yields were further reduced to 41 and 10%, hence the original conditions were used. Finally, allylic alcohol **148** was protected with two different protecting groups: *tert*-Butyldimethylsilyl (TBDMS) and benzoyl. Each structure was confirmed by NMR, where for **149** five new resonances were identified at δ_{C} 25.9, 25.8 and 25.6 ppm ($-\text{SiC}(\text{CH}_3)_3$), 18.3 ppm ($-\text{SiC}(\text{CH}_3)_3$) and -5.4 ppm ($2 \times -\text{SiCH}_3$). For **150**, a new resonance at δ_{C} 165.7 ppm corresponding to the benzoyl $\text{C}=\text{O}$ was observed.

Attempted synthesis of a glycosyl donor

Next, synthesis of a suitable glycosyl donor was attempted using PhSH in the presence of two different Lewis acids (Scheme 3.32).

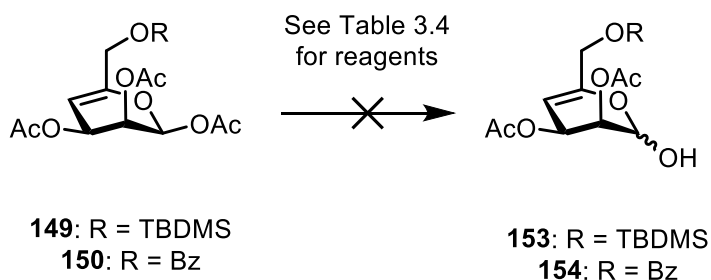


Scheme 3.32: Attempted synthesis of thioglycoside donors **151** and **152**.

In a first attempted synthesis of thioglycoside **151** from **149**, TMSOTf was used but ¹H NMR analysis of the isolated product showed absence of the singlet at δ_H 0.83 ppm, confirming an undesired cleavage of the 6-O-TBDMS group. Use of BF₃·OEt₂ was also evaluated, where after 1.5 h TLC analysis showed that the starting material had been consumed. However, akin to the previous reaction, the major product showed no resonance at δ_H 0.83 ppm indicating an undesired silyl group cleavage.

Next, glycosylation of PhSH with **150** was performed using BF₃·OEt₂ and TMSOTf activation on small scale (~ 50 mg). Unfortunately, TLC analysis did not show any conversion of starting material in either reaction, and this was the only material identified by NMR, with no upfield shift of the anomeric proton observed (previously δ_H 6.40 ppm in **150**). The experiments were repeated on larger scales (~ 100 mg), however no change to the anomeric proton/carbon chemical shifts were observed in the resultant NMR spectra of either attempt.

As thioglycoside synthesis was unsuccessful, both substrates were screened against anomeric acetate removal conditions towards the synthesis of a trichloroacetimidate donor (Scheme 3.33). In the case of 6-O-TBDMS protected derivative **149**, the reagent scope was limited due to its acid sensitivity, however more conditions could be trialled on 6-O-Bz compound **150**. The results of the attempted transformations are summarised in Table 3.4.



Scheme 3.33: Attempted synthesis of hemiacetals **153** and **154**.

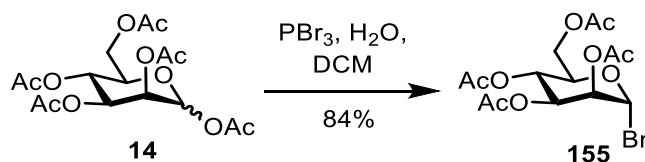
Substrate	Entry	Reagent	Time (h)	Result
6-O-TBDMS 149	1	Hydrazine acetate	24	No conversion
	2	BnNH ₂	24	No conversion
6-O-Bz 150	3	Hydrazine acetate	24	No conversion
	4	EDA/AcOH	24	No conversion
	5	BnNH ₂	24	No conversion
	6	Nd(OTf) ₃	36	No conversion

Table 3.4: Summary of conditions attempted for anomeric acetate removal.

Hydrazine acetate and EDA/AcOH, both evaluated previously in Chapter 2.1.1, failed to remove the anomeric acetate on either substrate (Table 3.4, Entries 1, 3 and 4). Anomeric acetate removal of **149** and **150** was also unsuccessful using BnNH₂¹⁴¹, confirmed by NMR analysis (Table 3.4, Entries 2 and 5). Further literature consultation revealed an alternative procedure employing Nd(OTf)₃ for anomeric

acetate removal. Tran *et al.*¹⁴² reported optimum results when using 5% mol Nd(OTf)₃, however adoption of this procedure did not result in conversion of **150**. In the second attempt, up to 50 mol% of catalyst was added, however no conversion of **150** was observed after 30 h. In a final attempt to induce conversion, 1.0 equivalent of Nd(OTf)₃ was added and heated at 50 °C overnight. Once again, no conversion of **153** was observed by TLC and the starting material was recovered (Table 3.4, Entry 6). Given the failure to synthesise desired hemiacetal **154** to produce a handle for further functionalisation, this route was abandoned.

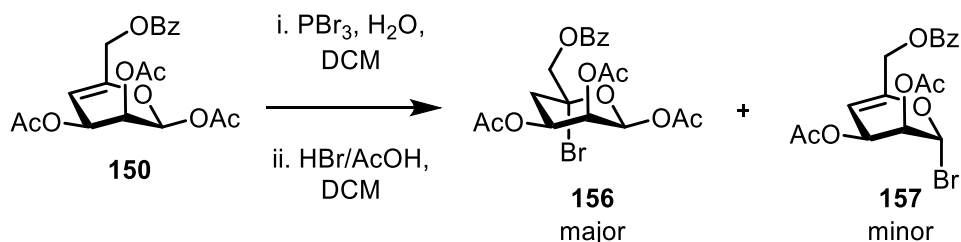
As the anomeric acetate could not be cleaved, the strategy was changed to evaluate synthesis of a glycosyl bromide, previously employed by Schultz *et al.*¹⁰¹ Use of phosphorus tribromide (PBr₃)/H₂O in DCM was first attempted on per-*O*-acetylated mannopyranose **14** (Scheme 3.34) to confirm reproducibility of the procedure. ¹H NMR data of the isolated compound matched reported values, with successful formation of the α-anomer confirmed by the small vicinal *J*_{H1-H2} of 1.3 Hz.¹⁴³



Scheme 3.34: Synthesis of glycosyl bromide **155** using PBr₃ and H₂O.

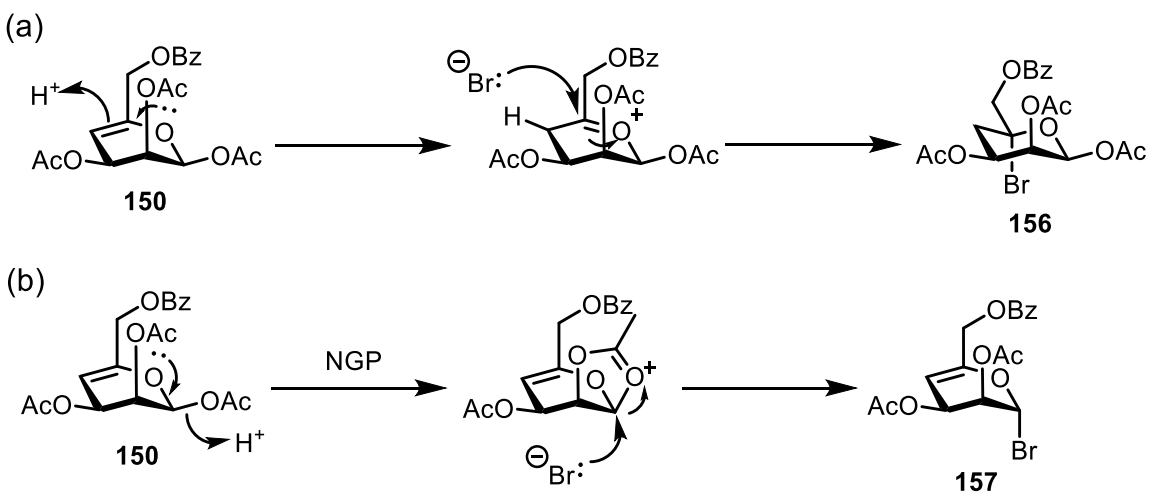
The procedure was then performed on **150** (Scheme 3.35), where within 3 h, complete conversion of starting material to two new R_f value spots was observed by TLC. Crude ¹H NMR analysis showed three products in a ratio of 1.0:0.4:0.2. The major product was confirmed as an undesired C5-Br product **156** (δ_H 6.30 ppm). This was confirmed by ¹H NMR, with the two C4 protons observed as a multiplet at

δ_{H} 2.0-2.5 ppm, consistent with a change in hybridisation from sp^2 to sp^3 following addition of HBr. The minor product was desired glycosyl bromide **157** (δ_{H} 6.49 ppm) and the remaining material was unreacted **150** (δ_{H} 6.40 ppm).



Scheme 3.35: Attempted synthesis of **157** from protected allylic alcohol **150**. The major product of the reaction was **156**.

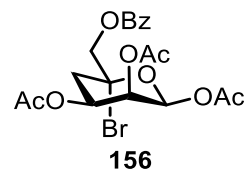
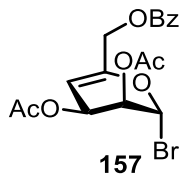
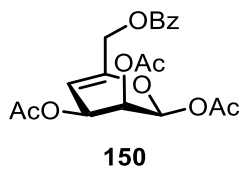
The proposed mechanisms for the formation of these products are shown in Scheme 3.36, where following *in-situ* generation of HBr, two competing pathways are presented. In pathway (a), C5-Br compound **156** is produced following competing addition of HBr to the double bond whereas in pathway (b) minor product **157** is generated through glycosylation of bromide at the anomeric centre.



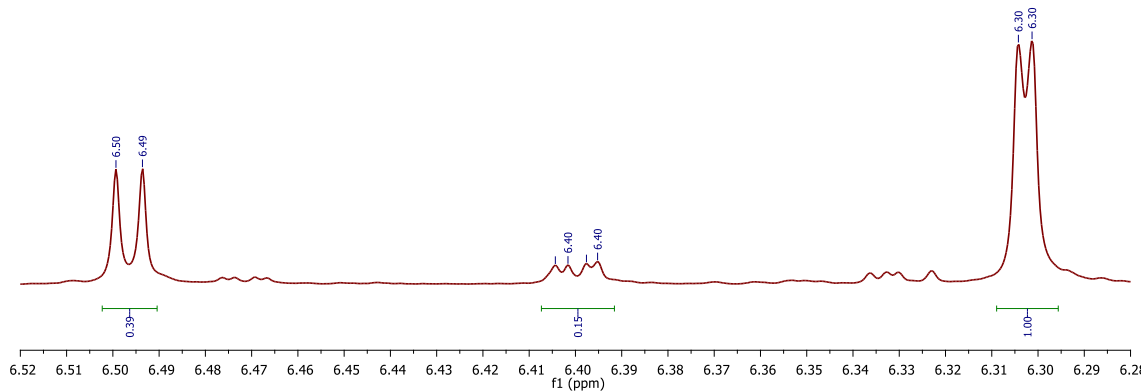
Scheme 3.36: Mechanisms for formation of **156** and **157**.

Also common for the synthesis of glycosyl bromides, the reaction of **150** with HBr/AcOH in DCM at 0 °C was complete within 1 h. NMR analysis showed the same resonances observed in the previous attempt using PBr₃/H₂O, however the ratio of C5-Br product **156** to glycosyl bromide **157** was 1.0:0.2. Given that this method showed high selectivity for production of **156**, these conditions were not repeated. A comparison of ¹H NMR spectra of both conditions attempted for this transformation is shown in Figure 3.12.

Attempted modifications of the PBr₃/H₂O procedure to favour formation of **157** were unsuccessful. The reaction was performed with half the equivalents of H₂O (3.0 equiv. instead of 6.0 equivalents), then repeated and held at 0 °C for the duration. Within 1.5 h, **150** was completely consumed in both instances and NMR analysis of the product revealed that the major product was the undesired C5-Br product **156**, and little improvement to the ratio was observed (1.0:0.3). No further optimisation of this procedure was attempted.



Method 1: $\text{PBr}_3/\text{H}_2\text{O}$ in DCM



Method 2: HBr/AcOH in DCM

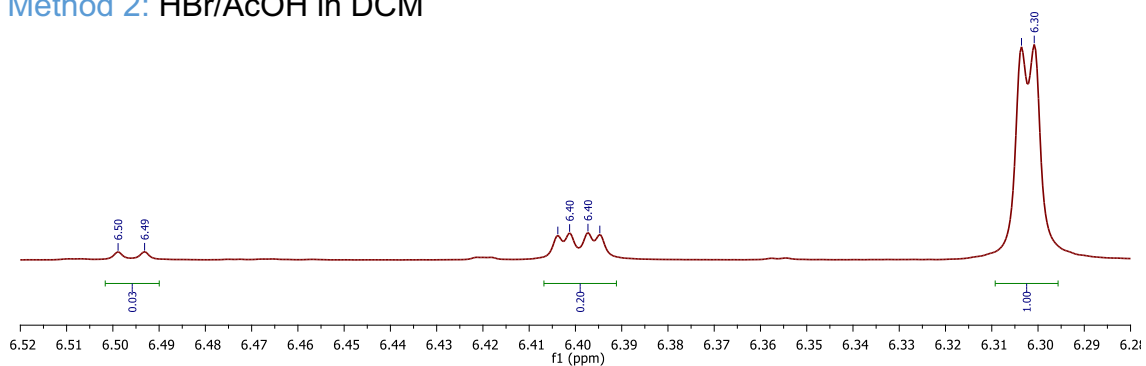
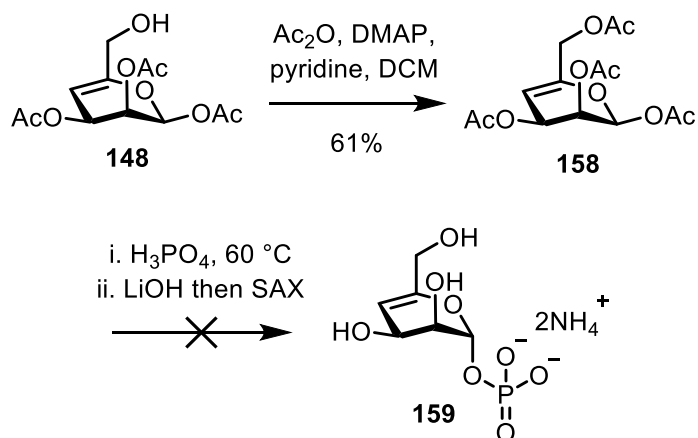


Figure 3.12: Comparative 400 MHz ^1H NMR spectra of attempted syntheses of **157**, showing variable ratios of **150:167:156**.

MacDonald phosphorylation

Next, compound **158** was prepared from allylic alcohol **148** for evaluation against the recently optimised MacDonald phosphorylation procedure (Scheme 3.37).



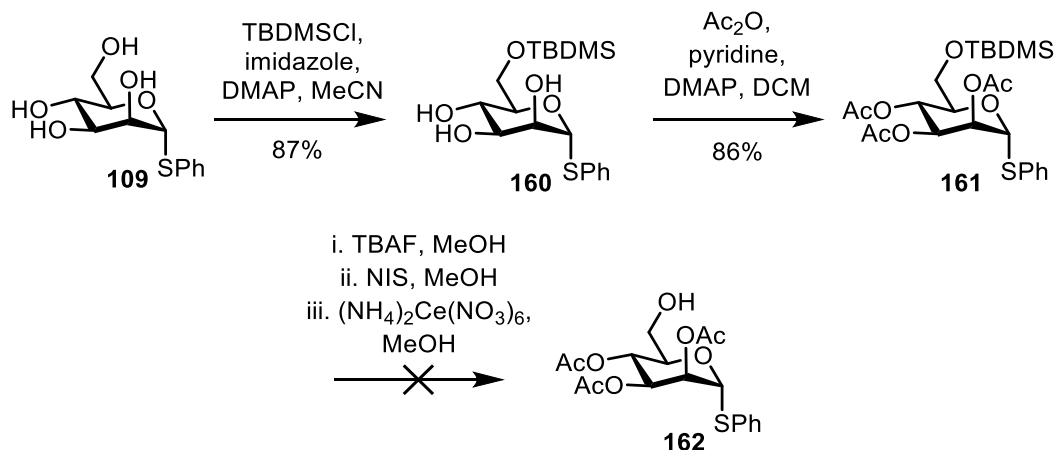
Scheme 3.37: Attempted synthesis of **159**.

Following preparation of the reaction mixture (50 mg scale) in a glove box, the Schlenk tube was heated at 60 °C under vacuum and a dark brown melt was afforded after 1.5 h. TLC analysis showed partial conversion of **158** to a lower R_f value spot. Following work-up and purification by SAX chromatography, analysis by ^{31}P NMR showed one resonance at δ_{P} 2.6 ppm, with a corresponding $J_{\text{H1-P}}$ of 8.0 Hz. It was noted that the ^1H spectrum was unusually messy compared to spectra obtained for other glycosyl 1-phosphates following SAX chromatography, and only the anomeric proton (δ_{H} 5.32 ppm) could be assigned. Though appearing promising by NMR, subsequent HRMS analysis did not detect any ions correlating to the proposed molecular formula, which may indicate limited stability of glycosyl 1-phosphate **159**.

The procedure was repeated on a larger scale (130 mg) at a reduced temperature of 45 °C however formation of the melt was impeded and resulted in a brown/black tar after 2 h. Crude NMR data suggested only decomposition of the material, with no ^{31}P data successfully obtained. Disappointingly, a final attempt employing the first set of reaction conditions (60 °C) also failed to reproduce the first result and no further work on this procedure could be completed during the timeframe available.

Pre-installed anomeric thioglycoside series

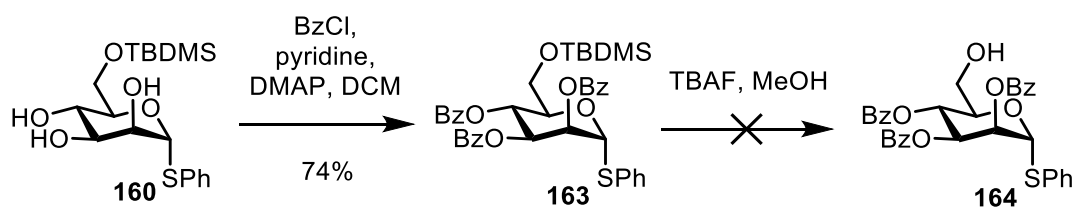
As problems were encountered during installation of a glycosyl donor, the synthetic strategy was altered to proceed *via* a substrate that already contained a pre-installed thioglycoside donor, detailed in Scheme 3.38. Tetra-ol **109** was selectively protected at the C6-position with a TBDMS group then per-O-acetylated to afford **161** in an overall yield of 75% over 2 steps.



Scheme 3.38: Attempted synthesis of C6-OH derivative **162** *via* TBAF mediated silyl deprotection.

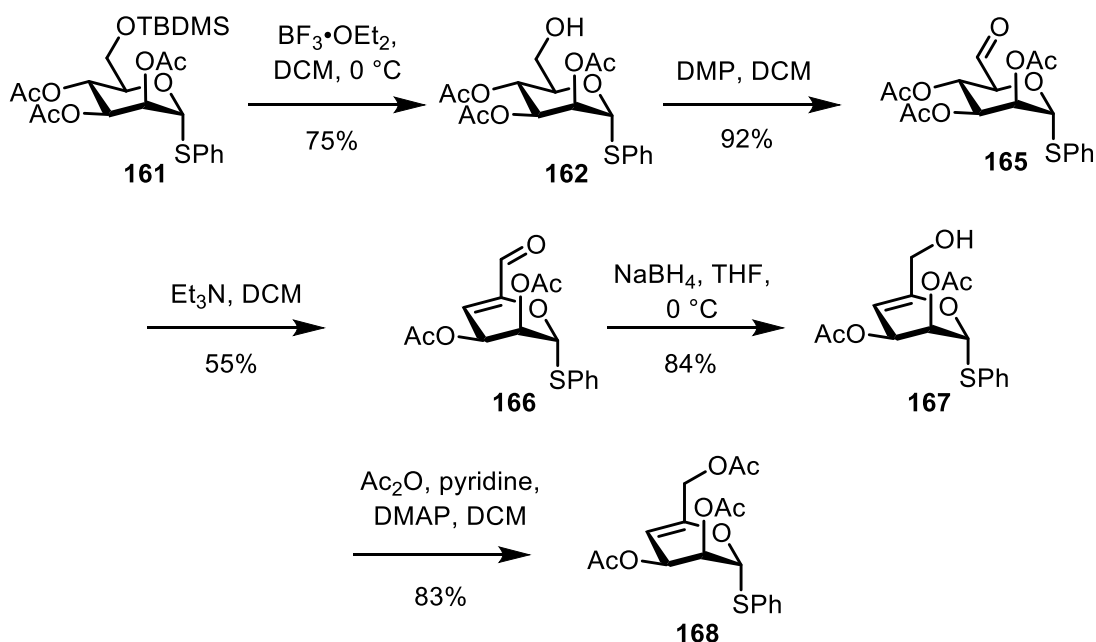
The use of fluoride reagents such as tetra-*N*-butylammonium fluoride (TBAF) is the most common methodology for the deprotection of silyl ethers.¹⁴⁴ This transformation is driven by the formation of a strong Si-F bond, that is on average 30 kcal/mol stronger than that of Si-O, *via* an S_NSi mechanism. Owing to this, cleavage of the 6-O-TBDMS group of **161** was attempted using TBAF, but despite use of only 1.2 equivalents at 0 °C, formation of multiple products was observed by TLC. Separation of the products was achieved by column chromatography, however ¹H NMR analysis confirmed that undesired acetyl cleavage had occurred, with absence of three singlets at δ_H 2.08, 2.02 and 1.98 ppm observed in the ¹H NMR spectrum. The reaction was repeated with only 0.5 equivalents of TBAF, however the same result was observed. Other methods reported in the literature for the removal of silyl ethers included catalytic NIS in MeOH and ceric ammonium nitrate (CAN) in MeOH, of which both were attempted.^{145,146} Unfortunately, neither of these methods showed any conversion of **161** by TLC.

With the aim of having increased stability to TBAF, **163** was also synthesised in 74% yield (Scheme 3.39), before being subjected to silyl deprotection with TBAF towards the synthesis of **164**. However, undesired benzoyl cleavage was also observed with this substrate.



Scheme 3.39: Failed synthesis of **164** *via* TBAF mediated silyl deprotection.

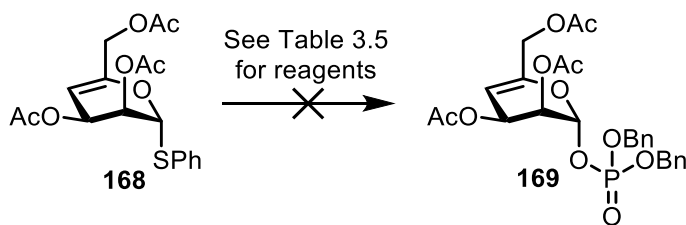
During a previous reaction, it was observed that 6-O-TBDMS group cleavage occurred in the presence of Lewis acids when attempting to form a thioglycoside. These conditions were attempted on **161**, and 6-O-TBDMS cleavage was successfully induced within 1 h using 0.5 equivalents of $\text{BF}_3 \cdot \text{OEt}_2$ at 0 °C. The desired alcohol **162** was isolated in 75% yield, scaled up to 3.5 g (Scheme 3.40).



Scheme 3.40: Synthesis of acetyl protected thioglycoside donor **168**.

With the desired thioglycoside donor in hand, **162** was oxidised to the corresponding aldehyde **165** using DMP and the C4-acetate was eliminated under basic conditions, as described previously. Enal **166** was reduced using NaBH_4 and protected with an acetate at the C6-position to give protected thioglycoside donor **168** available for phosphate addition. The structure was confirmed by ^1H NMR analysis, where an additional resonance corresponding to the acetate group was identified as a singlet integrating for 3H at δ_{H} 1.99 ppm.

With donor **168** in hand, the next stage was attempted glycosylation with DBP to afford protected glycosyl 1-phosphate **169**, as shown in Scheme 3.41. A summary of conditions attempted for this transformation can be found in Table 3.5.



Scheme 3.41: Attempted synthesis of protected glycosyl 1-phosphate **169**.

Entry	Activation conditions (equiv.)	Scale (mg)	Time (h)
1	NIS (1.5), AgOTf (1.5)	68	2
2	NIS (1.5), AgOTf (1.5)	230	1
3	PhIO (1.2), TMSOTf (0.4)	95	1
4	TTBP (2.5), Ph ₂ SO (1.3), Tf ₂ O (1.3)	95	1.5

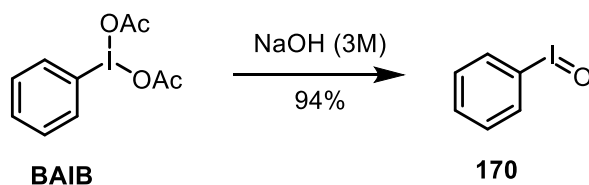
Table 3.5: Summary of conditions attempted for the synthesis of **169**.

Synthesis of **169** was initially attempted using NIS/AgOTf activation conditions (Table 3.5, Entry 1). TLC analysis appeared to show conversion of **168** to a baseline R_f value spot within 2 h at $-10\text{ }^\circ\text{C}$, however isolation of this compound proved difficult as the compound did not stain well with $\text{H}_2\text{SO}_4/\text{MeOH}$ and was only weakly UV visible. Following column chromatography, two sets of fractions were isolated however only 15 mg of material was collected. ^1H and ^{31}P NMR analysis of the fractions confirmed that multiple products were present, with two resonances observed at $\delta_{\text{P}} -2.5$ and -2.7 ppm in the ^{31}P spectrum.

This suggested formation of an anomeric mixture, or the possibility of addition of the acceptor to an alternative position. The reaction was repeated on a larger scale

(Table 3.5, Entry 2) but the reaction was sluggish requiring a temperature of 10 °C to initiate conversion of **168**. After stirring for 4 h, the reaction mixture was quenched and purified. Analysis of the material by NMR corresponded to previously obtained data, and regrettably it could not be established if addition was occurring at a different position as the product(s) formed were unstable, rapidly decomposing to form black oils.

Wakao *et al.* reported the use of iodosobenzene (PhIO) and TMSOTf as a promoter system for the chemoselective activation of thioglycosides in the presence of allyl glycosides.¹⁴⁷ PhIO **170** was easily prepared by treatment of BAIB with 3M NaOH, illustrated in Scheme 3.42. The resultant solid was dried in a desiccator overnight over P₂O₅ to remove H₂O.



Scheme 3.42: Preparation of PhIO **170** from BAIB and NaOH (3M).

To a solution of **168** was added sequentially DBP and freshly dried PhIO **170** (Table 3.5, Entry 3). After stirring for 1 h, the solution was cooled to -30 °C and TMSOTf was added dropwise. After stirring at this temperature for 30 min, TLC analysis indicated conversion of **168** to at least two lower R_f value spots. The reaction mixture was warmed to -15 °C, and after 1 h the reaction was deemed complete.

Attempted isolation of the products by chromatography was once again unsuccessful. Though the ¹H NMR spectrum was cleaner than previous attempts, it

still contained at least two products, neither of which corresponded to the starting material. However, ^{31}P analysis only showed one resonance at $\delta_{\text{P}} -0.9$ ppm which neither corresponds to dibenzyl phosphate or an anomeric dibenzyl phosphate (typically observed between $\delta_{\text{P}} -3.0$ and -4.0 ppm in previous analogues).

Finally, conditions reported by Crich *et al.*¹⁴⁸ were attempted. **168** was pre-activated with 2,4,6-Tri-*tert*-butylpyrimidine (TTBP) and diphenyl sulphoxide (Ph_2SO) for 1 h, cooled to -78 °C and Tf_2O added dropwise. DBP was then added and the reaction mixture was stirred for 1.5 h. The reaction mixture was quenched and concentrated *in vacuo* before being columned immediately. Once again, ^1H NMR analysis revealed several products however ^{31}P NMR analysis could not be obtained in this attempt and the material quickly decomposed. No further attempts to access **169** were performed using donor **168**.

Conclusions

Installation of an endocyclic 4,5-double bond was shown to dramatically alter the anomeric reactivity of the analogues investigated. Attempted removal of the anomeric acetate and thioglycoside donor synthesis both failed, and anomeric reactivity was only observed under strong Brønsted acid conditions. However, the desired glycosyl bromide **157** was still only a minor product of this reaction and the major product was determined as C5-bromo analogue **159**. The reactivity of these derivatives was comparable to glycals (1,2-unsaturated sugars) which are excellent glycosyl donors, and readily undergo electrophilic addition across the double bond (Figure 3.13).¹⁴⁹

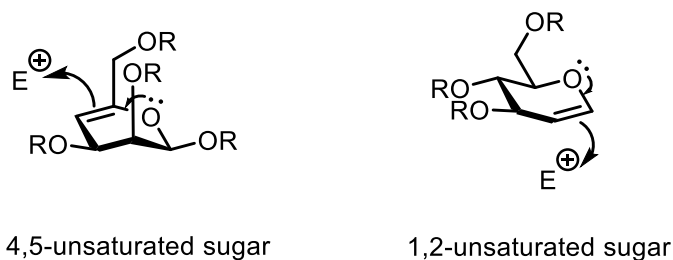


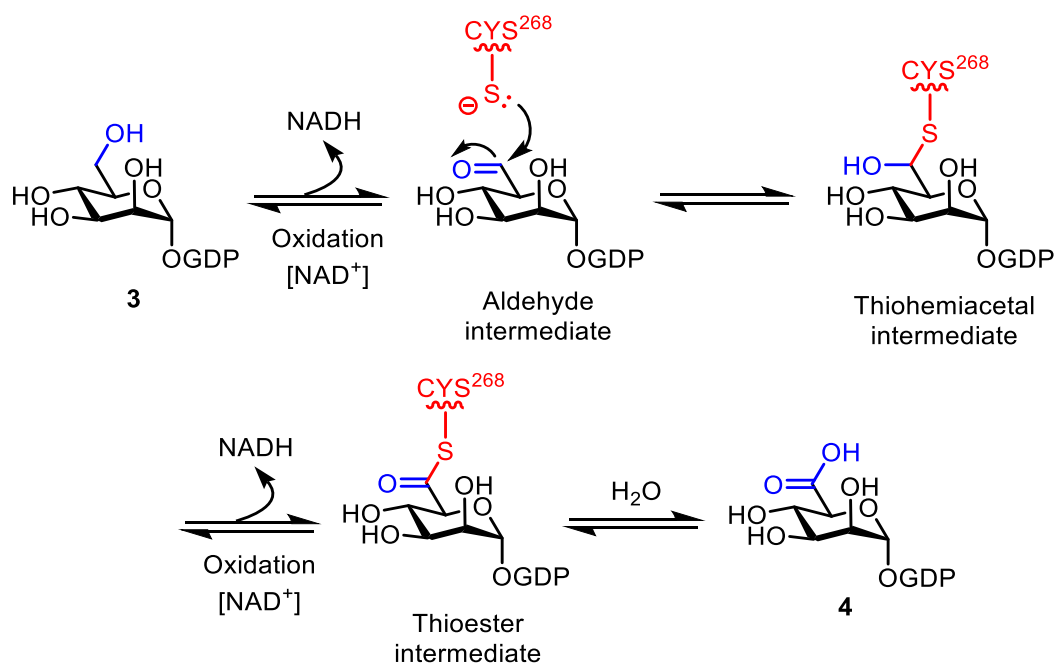
Figure 3.13: Reactivity comparison between 4,5- and 1,2-unsaturated sugars.

Results obtained using the pre-installed thioglycoside series of analogues afforded mixtures of products, consistent with the varying methods of reactivity presented by the installation of a 4,5-double bond. Unfortunately, characterisation of the products formed was impossible as decomposition was observed in all attempts. MacDonald phosphorylation was the most promising method towards synthesis of **159**, but regrettably the results obtained from the first attempt could not be reproduced in the time available. Despite all efforts described, target **159** could not be isolated.

3.3 Active site intermediate analogues

3.3.1 Biological rationale

The next series of analogues were designed as active site intermediates with the potential to be oxidised by GMD, by the mechanism previously described in Chapter 1.3.2, recapped in Scheme 3.43.



Scheme 3.43: Proposed mechanism of GMD catalysed oxidation of GDP-Man **3** to GDP-ManA **4**.⁶⁶

Members of this category of tools were structurally similar to the native substrate and product of GMD. It was hoped that these analogues may provide information regarding key binding requirements within the active site, or potentially provide interesting kinetic data surrounding the rate of oxidation of these analogues if they are accepted as substrates of GMD. If the latter is observed, then these analogues could be evaluated as competitive inhibitors.

Literature precedent and proposed mechanism of action

The use of amine-containing probes for structure-function investigations is not well documented in the literature. However, incorporation of a 1° or 2° amine functionality into a sugar-nucleotide probe to afford GDP-6-amino-6-deoxy-mannose **171** and GDP-6-deoxy-6-methoxyamino-mannose **172** (Figure 3.14) would be useful to explore the mechanism of action.

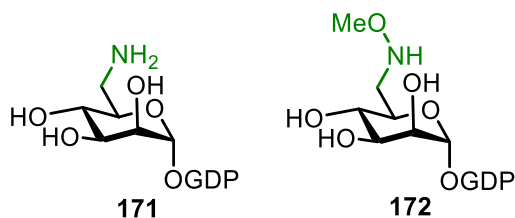
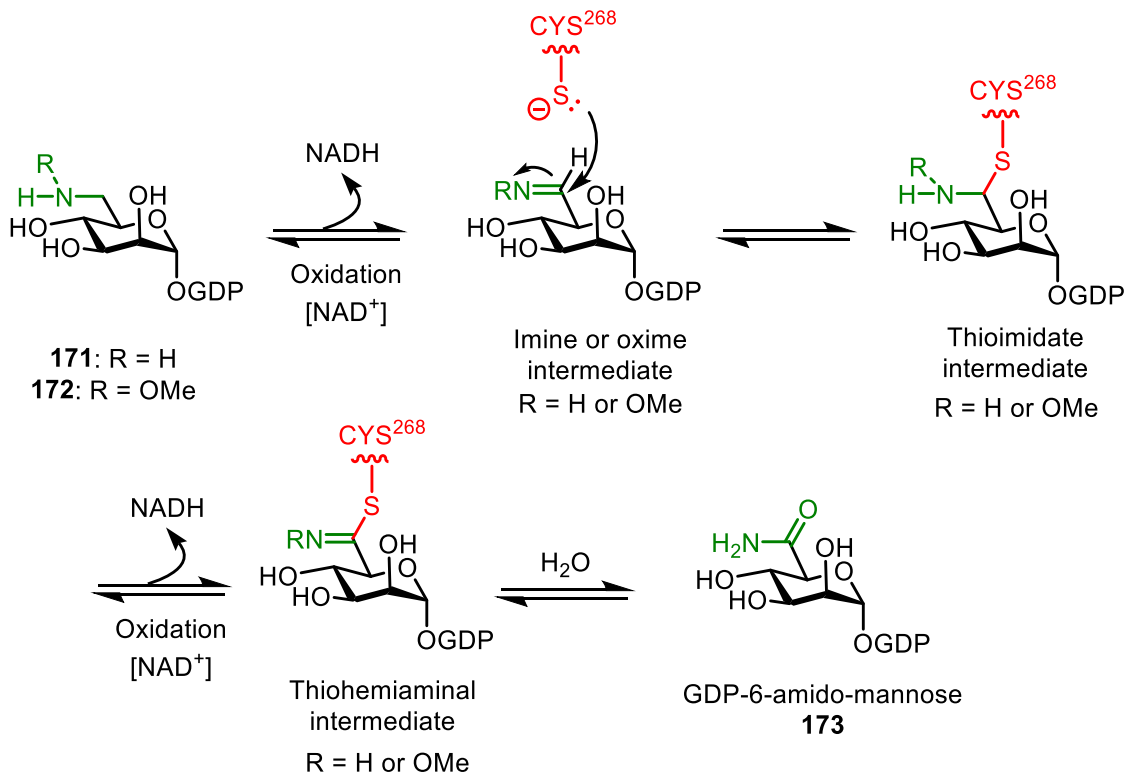


Figure 3.14: Chemical structures of GDP-Man analogues **171** and **172**.

Evaluation of **171** and **172** as substrates of GMD could provide new information regarding this putative oxidation step, where if the analogues were accepted formation of imine or oxime intermediates may be possible. The oxidation potentials of C-O to C=O and C-N to C=N are different, with C-N to C=N expected to be slower.¹⁵⁰ Nevertheless, formation of such Schiff bases as intermediates in enzyme mechanisms is well documented in the literature, with examples including QueF, a nitrile reductase, and *N*-acetylneuraminate lyase.^{151–153}

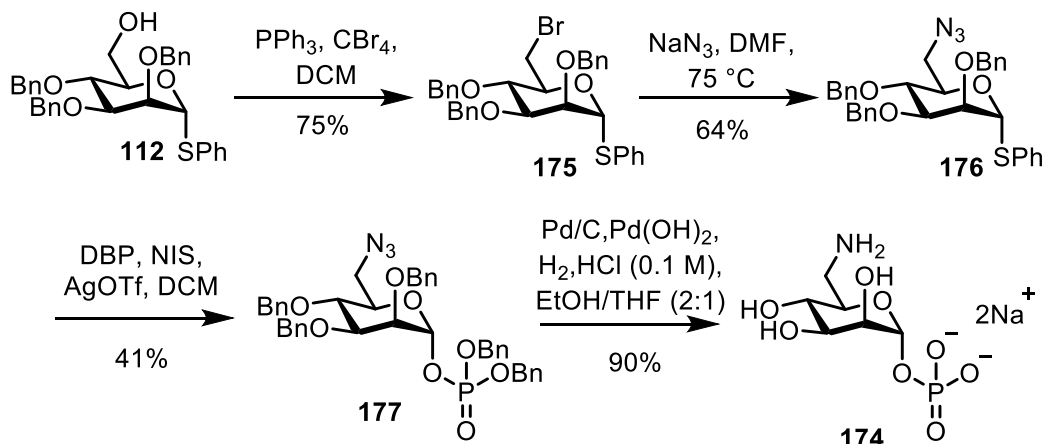
This study would provide useful information about substrate binding in the active site of GMD, in addition to the possibility of the analogues acting as inhibitors to reduce turnover of **4** if they are able to proceed in the proposed mechanism outlined in Scheme 3.44.



Scheme 3.44: Proposed mechanism of GMD mediated oxidation of **171** or **172** to afford GDP-6-amido-mannose **173**.

3.3.2 Synthesis of 6-amino-6-deoxy- α -D-mannopyranosyl phosphate

The route towards glycosyl 1-phosphate **174** was designed from building block **112**, as shown in Scheme 3.45. Alcohol **112** was successfully converted to a bromide using Appel halogenation conditions (PPh_3 and CBr_4), which was subsequently displaced with NaN_3 at elevated temperature (75°C). Conversion from a bromide to an azide could be easily confirmed by ^{13}C NMR, with the C6 carbon shifting significantly downfield from δ_{C} 33.4 ppm to δ_{C} 51.6 ppm.



Scheme 3.45: Synthesis of **174**.

Following this, DBP was glycosylated with C6-azide **176** using NIS/AgOTf activation conditions, which proceeded in a good yield of 65%. Presence of the dibenzyl phosphate was confirmed by NMR analysis, with a resonance at δ_{P} -2.8 ppm observed in the ^{31}P NMR spectrum and a $J_{\text{H1-P}}$ coupling constant of 6.1 Hz.

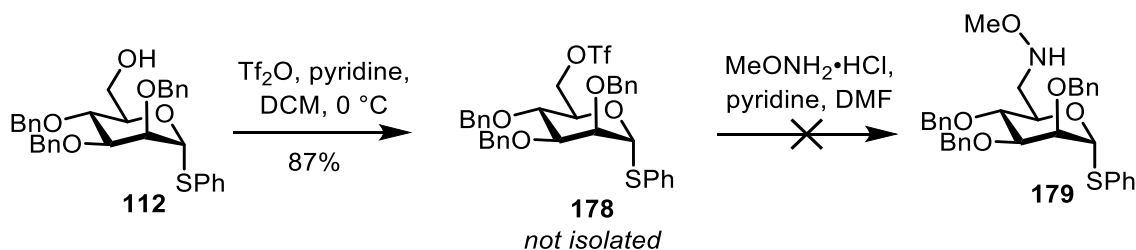
The final step was deprotection of protected glycosyl 1-phosphate **177** by hydrogenolysis using Pd/C and Pd(OH)₂/C catalysis. The first attempt was performed in EtOH/THF (2:1) with 1.0 equivalent of 0.1 M HCl, to minimise deactivation/poisoning of the palladium catalysts by the newly formed amine moiety.

After stirring for 18 h, TLC analysis (MeCN/H₂O, 3:1) indicated conversion of starting material to a lower R_f value spot. However, following work-up and HSQC-DEPT analysis, the presence of 3 benzyl groups could still be observed. The reaction solvent was changed to MeOH/H₂O (2:1) and hydrogenolysis continued, however no further conversion was observed by TLC. The catalyst and solvent were changed once again however the reaction still did reach completion. The ¹H NMR spectrum was now difficult to interpret due to a messy baseline, indicating that the material was beginning to decompose.

At this time, other members of the research group were experiencing similar issues surrounding incomplete hydrogenolysis when using Pd(OH)₂/C. Therefore, the catalyst was exchanged for a new batch. The reaction was performed akin to the first attempt, except for addition of 1.2 equivalents of 0.1 M HCl opposed to 1.0 equivalent. The reaction mixture was stirred for 15 h, where TLC analysis (MeCN/H₂O, 3:1) showed conversion of starting material to a baseline R_f value spot. Following work-up, NMR analysis indicated full hydrogenolysis had been successful, affording **174** as the disodium salt in 90% yield. The anomeric proton at δ_H 5.42 ppm displayed a *J*_{H1-P} of 5.6 Hz and HRMS analysis found [**174**-H]⁻ as the major ion at *m/z* 258.0388 compared to the theoretical *m/z* of 258.0378. This analogue was evaluated as a substrate of GDP-ManPP, discussed later in this chapter.

3.3.3 Studies towards the synthesis of 6-deoxy-6-methoxyamino- α -D-mannopyranosyl phosphate

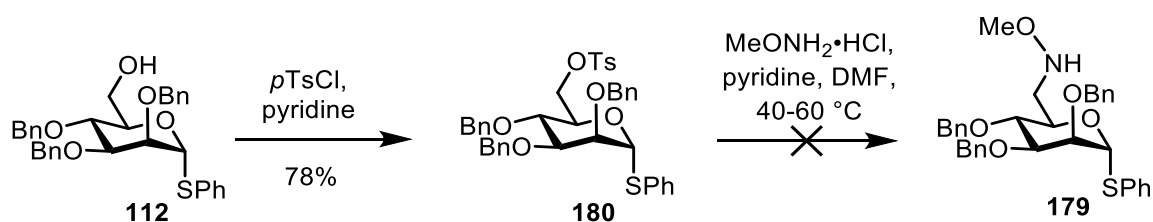
The route towards a C6-methoxyamine functionalised analogue was devised from **112**, and the initial route proceeded *via* formation of a triflate and displacement with methoxyamine hydrochloride ($\text{MeONH}_2 \cdot \text{HCl}$) in the presence of pyridine (Scheme 3.46).



Scheme 3.46: Attempted synthesis of C6-methoxyamine functionalised donor **179** *via* displacement of a C6-triflate.

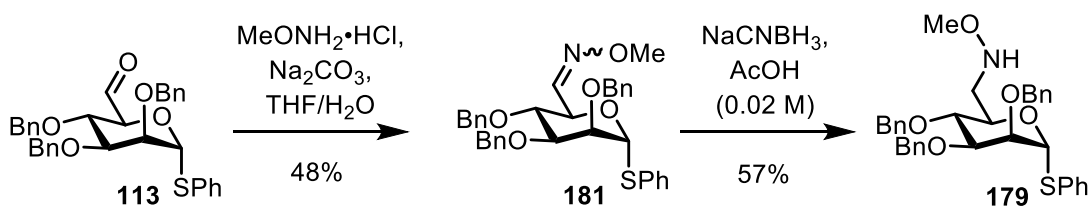
Reaction of **112** with Tf_2O in the presence of pyridine at 0 °C afforded triflate **178** which was used crude in immediate reaction with $\text{MeONH}_2 \cdot \text{HCl}$. The reaction mixture was stirred for 18 h, whereupon a new R_f value spot could be observed by TLC. Crude NMR analysis of the material did not appear promising, with the diagnostic $-\text{OCH}_3$ singlet corresponding to the methoxyamine functionality absent from the spectrum. Purification by column chromatography only lead to the isolation of 7 mg of material (from 290 mg), and the resultant NMR spectrum could not be interpreted, suggesting decomposition of triflate **178** to an unidentified material.

Given the success using a tosylate group in previous syntheses, **180** was prepared instead for use in the displacement reaction (Scheme 3.47). However, upon stirring for 18 h at elevated temperature (up to 60 °C) with MeONH₂•HCl, TLC analysis showed that no reaction had taken place and only **112** could be identified.



Scheme 3.47: Attempted synthesis C6-methoxyamine functionalised donor **179** via displacement of a C6-tosylate.

Though requiring additional steps, a new route was designed *via* an oxime, as shown in Scheme 3.48. Accessed *via* Parikh-Doering oxidation, aldehyde **113** was reacted with MeONH₂•HCl in the presence of Na₂CO₃ to form oxime **181**. The resultant ¹H NMR spectra was complex with significant overlap between the ring protons making assignment challenging, however a diagnostic singlet corresponding to the methoxyamine OCH₃ could be identified at δ_H 3.83 ppm.



Scheme 3.48: Synthesis of methoxyamine functionalised donor **179** *via* an oxime.

In 2006, Peri *et al.* reported the use of NaBH₃CN (5.0 equivalents) in glacial AcOH for the reduction of a related substrate in their studies towards the synthesis of novel Lipid A antagonists.¹⁵⁴ Their procedure was initially attempted using 2.5 equivalents of NaCNBH₃, however slow formation of a new R_f value spot was observed and the remaining 2.5 equivalents were added after 3 hours. After 6 h the reaction mixture was concentrated *in vacuo*, and immediately purified by column chromatography to afford desired compound **179** in 42% yield. When the reaction was repeated, 5.0 equivalents was added from the beginning and stirred for a total of 15 h, resulting in a yield improvement to 57%. The desired reduction product could be identified by NMR, with new H₆ and H₆' protons at 3.38 and 3.02 ppm and presence of the methoxyamine OCH₃ singlet at δ_H 3.46 ppm (Figure 3.15). The molecular ion corresponding to [**179**+H]⁺ was identified at *m/z* 572.2478, in good agreement with the required *m/z* of 572.2471.

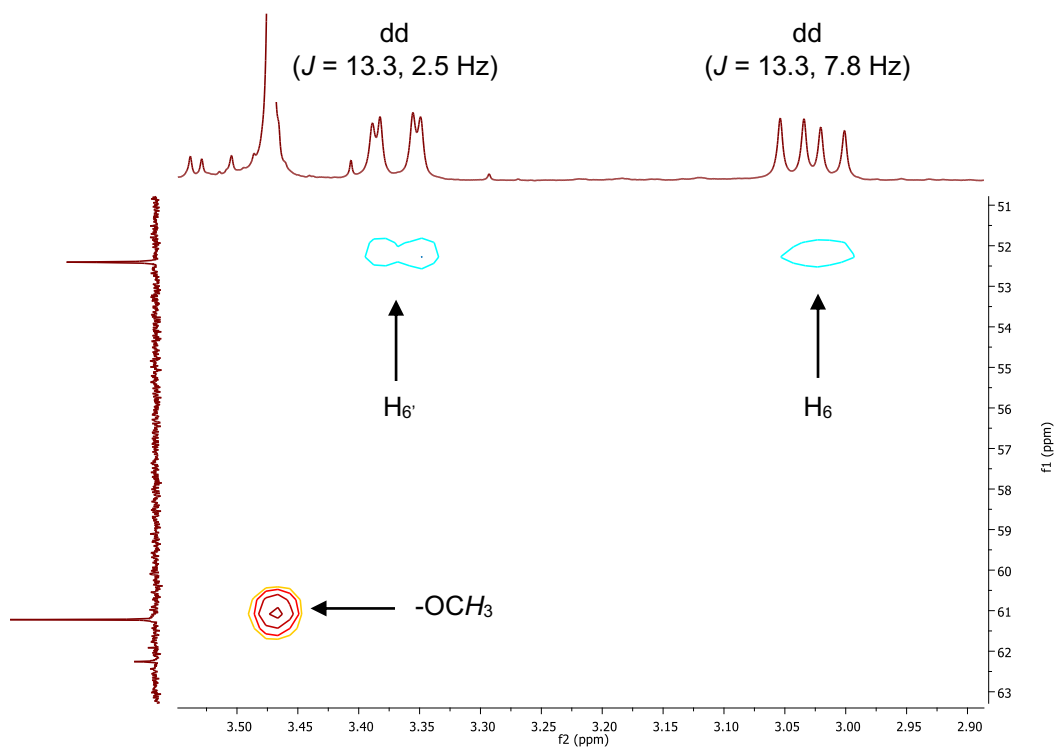
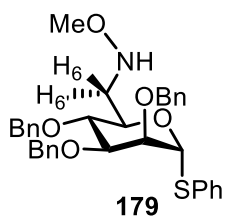
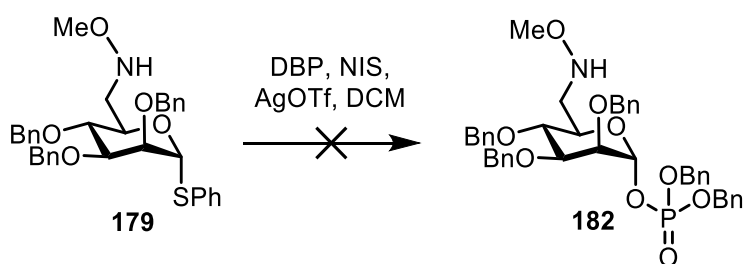


Figure 3.15: 400 MHz HSQC-DEPT spectrum of **179**, showing H_{6'}, H₆ (blue) following reduction and -OCH₃ (red).

Next, DBP was glycosylated with donor **179** (Scheme 3.49) in attempted formation of protected glycosyl 1-phosphate **182** on small scale (50 mg). Monitoring of the reaction by TLC showed no formation of a new R_f value spot and 6 mg of material was isolated, for analysis by ^1H and ^{31}P NMR.



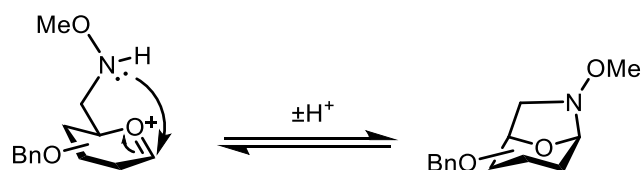
Scheme 3.49: Attempted synthesis of **182**.

The ^1H spectrum was very noisy, and whilst the $-\text{OCH}_3$ of the methoxyamine group could still be observed as a singlet at δ_{H} 3.88 ppm the anomeric doublet of doublets could not be identified. Promisingly, the $^{31}\text{P}\{^1\text{H}\}$ spectrum showed a resonance in the previously observed region for the dibenzyl phosphate moiety in other analogues, at δ_{P} -2.8 ppm. However, analysis of the sample by HRMS revealed no ion corresponding to the proposed molecular formula.

The reaction was repeated using the same activation conditions. After stirring for 2 h at $0\text{ }^\circ\text{C}$, TLC analysis suggested partial conversion to a lower R_f value spot. Following work up and purification, NMR analysis was directly comparable to the previous attempt. The sample was re-purified, however no improvement in resolution of the resultant NMR spectra was observed and the data was of insufficient quality to permit full assignment.

The procedure was repeated for a third time on a larger scale (112 mg) where, following work-up, the material was submitted for crude NMR analysis. In this attempt, $^{31}\text{P}\{^1\text{H}\}$ data showed only a singlet at $\delta_{\text{P}} -2.8$ ppm however the anomeric doublet of doublets could still not be observed.

A competing reaction may occur during attempted synthesis of **182**, through attack of nitrogen at the anomeric centre of the oxocarbenium ion intermediate to form a system comparable to that of 1,6-anhydro sugar, illustrated in Scheme 3.50. A similar cyclisation product was observed previously by a member the research group during the synthesis of other C6-nitrogen containing building blocks.



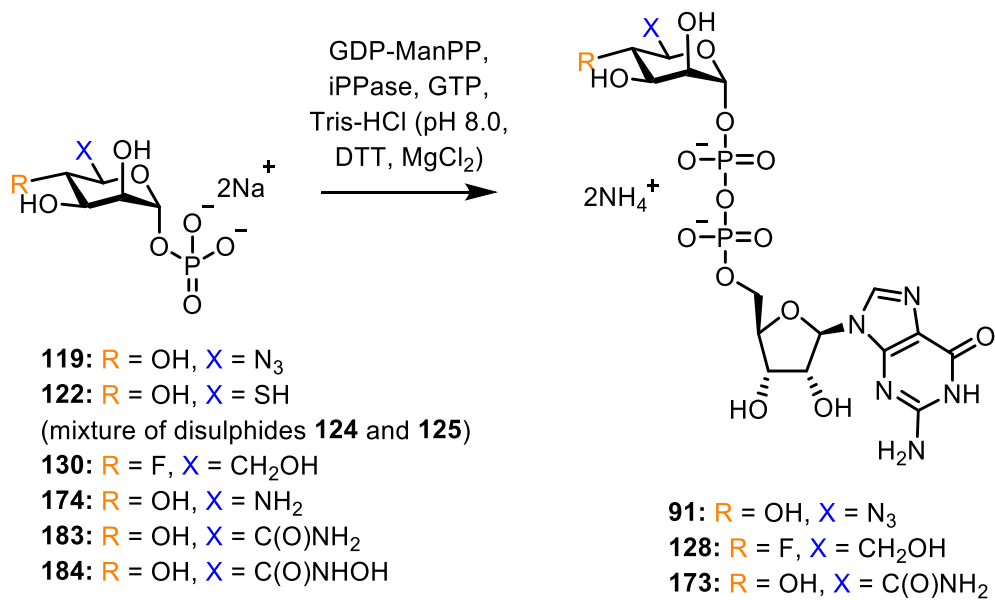
Scheme 3.50: Proposed competing mechanism of nitrogen cyclisation.

Before the reaction is repeated, the amine should be protected to evaluate the difference on outcome of the glycosylation reaction. Whilst use of a benzyl group would permit simultaneous hydrogenolysis with the benzyl ethers, the removal of benzyl amine protecting groups can be challenging and it may be more appropriate to use a base labile protecting group such as acetyl or fluorenylmethoxycarbonyl (Fmoc).

3.4 Evaluating the substrate specificity of GDP-ManPP: chemoenzymatic synthesis of modified GDP-Man analogues

Enzymatic synthesis of GDP-sugars is well established in the literature, predominantly utilising GDP-ManPP from *S. enterica*. This methodology enables facile access to these important precursors, with the enzyme generally displaying low substrate specificity, providing scope to synthesise modified GDP-Man analogues, crucial to this project.

Four modified glycosyl 1-phosphates synthesised chemically were evaluated as substrates of GDP-ManPP. Two additional glycosyl 1-phosphates, **183** and **184** that were synthesised by another member of the research group were also screened (see Table 3.6). Assays were performed on small quantities of glycosyl 1-phosphate (< 5 mg), which were incubated with GDP-ManPP, inorganic pyrophosphatase (iPPase) and guanosine 5'-triphosphate (GTP) in Tris-HCl (pH 8.0) buffer containing MgCl₂ and dithiothreitol (DTT) (Scheme 3.51). Conversion to the corresponding sugar-nucleotide could be easily monitored *via* SAX chromatography, which saw disappearance of GTP and introduction of a new peak corresponding to the GDP-sugar.



Scheme 3.51: General procedure for enzymatic synthesis of sugar-nucleotide analogues using GDP-ManPP.

Category	Substrate	Scale (mg)	Time (h)	Conversion (%)
C6-modified analogues	 119	4.2	16	55
	 122 (mixture of disulphides 124 and 125)	0.5	35	0
C4-modified analogues	 130	1.4	27	96

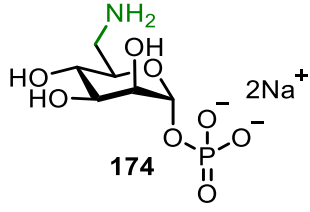
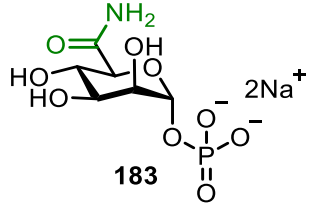
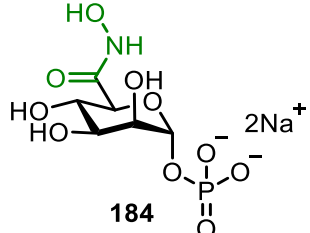
Active site intermediate analogues	 174	0.5	35	< 5
	 183	1.7	27	79
	 184	1.3	27	0

Table 3.6: Summary of glycosyl 1-phosphate analogues evaluated as substrates of GDP-ManPP.

Three glycosyl 1-phosphates were accepted as substrates by GDP-ManPP, permitting isolation of the respective GDP-Man analogues. 6-azido-6-deoxy-mannopyranosyl phosphate **119** showed 55% conversion to its corresponding GDP-sugar **91** after 35 h, and GDP-4-deoxy-4-fluoro-mannose **128** and GDP-6-amido-mannose **173** were also successfully synthesised from **130** and **183**, showing 96 and 79% conversion after 27 h, respectively (Table 3.7). Each sugar-nucleotide was characterised by ^1H and ^{31}P NMR and HRMS, with the diagnostic δ_{P} resonances for each analogue shown in Table 3.7.

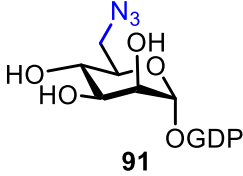
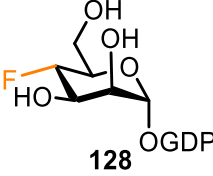
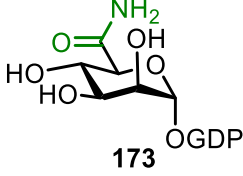
Category	GDP-Man analogue	Isolated yield after SAX (%)	³¹ P NMR δ _P (ppm)
C6-modified analogues	 <p style="text-align: center;">91</p>	16	-11.5, -14.0
C4-modified analogues	 <p style="text-align: center;">128</p>	53	-12.0, -14.0
Active site intermediate analogues	 <p style="text-align: center;">173</p>	41	-11.5, -14.0

Table 3.7: Summary of GDP-Man analogues synthesised enzymatically using GDP-ManPP.

The NDP-sugars of the three remaining substrates were unsuccessfully synthesised using this protocol. The mixture of disulphide products **124** and **125** were incubated under the described conditions for 35 h, hoping that the reducing conditions used for the assay would permit isolation of GDP-6-deoxy-6-thio-mannose **92**. Unfortunately, no conversion to a GDP-sugar was observed by SAX, with only GTP and GDP observed.

C6-amino functionalised glycosyl 1-phosphate **174** was screened against GDP-ManPP, however after incubation for 35 h minimal conversion to GDP-6-amino-6-deoxy-mannose **171** (< 5%) was observed. As the buffer used is pH = 8.0, the amine would be expected to be protonated (pK_a = ~ 11.0) hence this species may exist as a zwitterion. This would lead to an overall charge of 1- for **174** (opposed to 2- for

other GDP-sugars) and theoretically alter the retention time of **174** in SAX chromatography which may be misleading during purification. Whilst the buffer pH cannot be changed, other possible routes to access this sugar-nucleotide could proceed *via* the reduction of GDP-6-azido-6-deoxy-mannose **91** using the Staudinger procedure *post* sugar-nucleotide synthesis.

Finally, glycosyl 1-phosphate **184** bearing a C6-hydroxamate functionality was screened against GDP-ManPP. Regrettably, no conversion to a GDP-sugar could be observed by SAX chromatography; instead, only the products of GTP hydrolysis, GMP and GDP could be observed.

3.4.1 Discussion

Evaluation of GDP-ManPP substrate specificity towards the modified glycosyl 1-phosphates synthesised in this chapter presented new findings that supplemented prior research efforts in this area by the groups of Macmillan and Lowary.^{76,96} As expected from previous literature, C6-azido functionalised glycosyl 1-phosphate **119** was a moderate substrate of GDP-ManPP, but 6-amido glycosyl 1-phosphate **183** was demonstrated to be a good substrate of the enzyme. These results supported previous findings that the C6-OH is not required for substrate binding.

Conversely, the C4-OH was suggested to interact with GDP-ManPP, being tightly bound within the active site. Replacement of C4-OH with C4-F in analogue **130** was well tolerated by GDP-ManPP, and the highest percentage conversion to GDP-sugar was observed with this substrate.

During this study, it was observed that C6-modified glycosyl 1-phosphates bearing positive or negative charges under the described assay conditions (pH = 8.0), C6-amino **174** and C6-hydroxamate **184** respectively, were both poor substrates of GDP-ManPP. This supported earlier findings by another member of the research group that showed α -D-mannopyranuronic acid **42**, which would also be negatively charged at this pH, was also a poor substrate of GDP-ManPP.

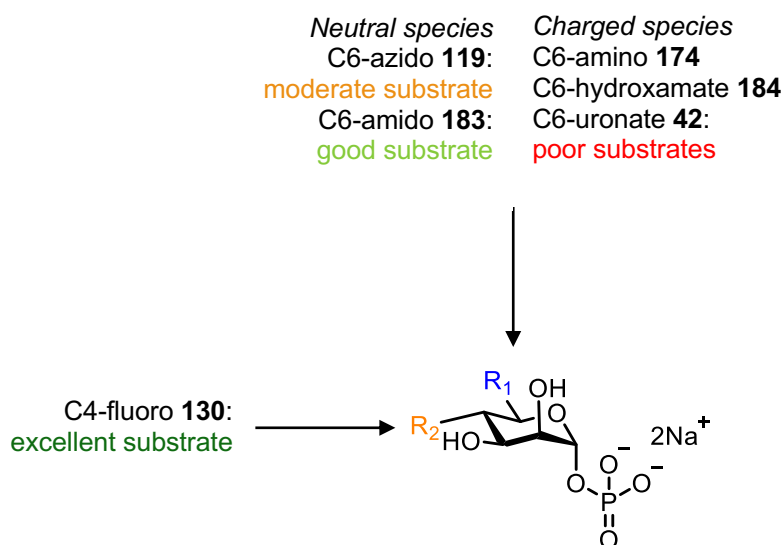


Figure 3.16: Summary of substrate specificity of GDP-ManPP.

3.5 Conclusions and Future Directions

This chapter describes efforts towards the synthesis GDP-Man analogues that were designed to probe a nucleophilic Cys²⁶⁸ residue in GMD and are categorised as C6-modified, C4-modified and active site intermediate analogues.

The first section detailed synthetic routes towards eight modified glycosyl 1-phosphates, of which four were successful. Installation of new functionalities to C6-modified and active site intermediate analogues proceeded *via* a common C6-OH building block, protected with acetyl or benzyl groups. Introduction of an azide was afforded by displacement of a tosylate towards the synthesis of glycosyl 1-phosphate **119** compared to displacement of a chloride with KSAc for the synthesis of C6-thio functionalised glycosyl 1-phosphate **122**. Synthesis of a C6-amino containing glycosyl 1-phosphate **174** was accomplished *via* successive Appel halogenation and azide displacement reactions, whereby simultaneous azide reduction and benzyl ether hydrogenolysis then afforded the target compound. An alternative protecting group strategy was required to access C4-fluoro functionalised glycosyl 1-phosphate **130**, and the optimum route proceeded *via* reductive ring opening of a C4-C6 benzylidene acetal to reveal the C4-OH for DAST mediated fluorination. Incorporation of the anomeric phosphate group was performed using two different strategies. Optimisation of the MacDonald phosphorylation procedure proved crucial, permitting access to modified glycosyl 1-phosphates **119** and **122**, bearing C6-azido and C6-thio functionalities, from acetylated precursors in good yields. Synthesis of **122** was complicated by the formation of two disulphides **124** and **125**, which could not be separated or reduced successfully. Benzylated

thioglycoside donors were converted to their corresponding glycosyl 1-phosphates through reaction with DBP followed by hydrogenolysis, to afford analogues **130** and **174**, bearing C4-fluoro and C6-amino groups respectively.

Synthesis of the remaining four glycosyl 1-phosphate analogues was unsuccessful. During the synthesis of C6-chloro glycosyl 1-phosphate **95**, cyclic compound **97** was formed as the major product from MacDonald phosphorylation. Access to **95** could next be attempted using benzyl protected derivatives, where during hydrogenolysis it would be of interest to evaluate if isolation of **95** is possible and whether formation of by-product **97** is observed under the non-acidic conditions used for this transformation.

Despite evaluation of multiple strategies, α -D-mannopyranosyluronitrile phosphate **108** was not isolated. Acetyl protected C6-nitrile donors showed poor anomeric reactivity, comparable to that of uronate donors discussed in Chapter 2.1.1. The most promising route proceeded using benzylated derivatives that had increased anomeric reactivity, but unfortunately the route failed at the final hydrogenolysis step, due to undesired reduction of the nitrile moiety. In future experiments, alternative conditions for this transformation such as oxidative debenylation ($\text{NaBrO}_3/\text{Na}_2\text{S}_2\text{O}_4$) could be attempted.

Installation of a protected anomeric phosphate to a C6-methoxyamine donor failed and synthesis of protected glycosyl 1-phosphate analogue **182** could not be completed. In all attempts, a mixture of products was formed, proposed to arise from a competing reaction through the unprotected amine which should be suitably protected before repeating this procedure.

The final target **159**, containing an endocyclic C4,5-alkene, was also not completed during this project. Work towards this analogue was both challenging and time-consuming, with a range of routes attempted. It was observed that analogues bearing this functionality behaved in a similar manner to glycols, with anomeric reactivity not observed unless using a strong Brønsted acid. Installation of the protected phosphate *via* a pre-installed thioglycoside donor also failed, with only mixtures of products formed that were unstable. Access to this target *via* MacDonald phosphorylation appeared to be the most promising route, however during the timeframe available the results could not be reproduced, and further work on this step should be completed in future.

The second section described the evaluation of six modified glycosyl 1-phosphates as substrates of GDP-ManPP. Three analogues, bearing C4-fluoro, C6-amido and C6-azido functionalities, were shown to be excellent to moderate substrates, respectively. This chemoenzymatic strategy provided fast access to modified GDP-Man analogues on milligram scales for biochemical evaluation against GMD. No conversion of the remaining three glycosyl 1-phosphates, bearing C6-thio, C6-amino and C6-hydroxamate functionalities respectively, to their corresponding GDP-sugar was observed.

Nevertheless, this study provided new information surrounding structure activity relationships of GDP-ManPP, where it was shown that turnover of 6-position modified glycosyl 1-phosphates bearing positive or negative charges was not tolerated by the enzyme. In order to access these analogues in the future, chemical synthesis should be attempted.

Chapter 4: Biochemical evaluation of GDP-Man analogues

4.0 Introduction and aims

As discussed in Chapter 3.0, the use of sugar-nucleotide probes to investigate GMD mediated oxidation of GDP-Man **3** has not been widely investigated to date. Several small molecule inhibitors of GMD have been identified in the literature, the most notable being erythromycin A **5** and penicillic acid **6**, as mentioned in Chapter 1.3.2. However, these compounds are only mM inhibitors (IC_{50} of 1.2 and 2.4 mM, respectively)⁶⁸ and **6** is not selective for the catalytic Cys²⁶⁸ residue.⁷⁰ Determination of GMD inhibition is most commonly achieved using a spectrophotometric assay that monitors NAD(H) production.

Following chemoenzymatic synthesis of three modified GDP-Man analogues, their activities towards GMD were to be investigated using a colorimetric assay monitoring NAD(H) formation. Evaluation of the analogues as substrates and/or inhibitors of GMD was envisaged to provide insight into substrate specificity and binding interactions, to identify functionalities capable of interacting with the Cys²⁶⁸ residue.

4.1 GDP-6-azido-6-deoxy-mannose

4.1.1 Evaluation as a substrate of GMD

To assess the viability of GDP-6-azido-6-deoxy-mannose **91** as a substrate of GMD, a 3-well assay was prepared as follows: negative control, GDP-Man (10 μ M) and a well containing **91** (50 μ M) with GDP-Man **3** (10 μ M). After incubation for 45 min, data showed analogue **91** had little influence on the oxidation of **3**, with conversion reaching 89% within this time period. The experiment was repeated, however the inhibitor was pre-incubated with GMD on ice for 2 h prior to the addition of **3**. This made little difference to the rate of NAD(H) formation, with conversion reaching 83% within 50 min (Figure 4.1). As this analogue showed only 11-16% inhibition of GDP-ManA **4** production at 50 μ M, no further experiments were performed. GDP-6-azido-6-deoxy-mannose **91** was shown not to be a substrate of GMD.

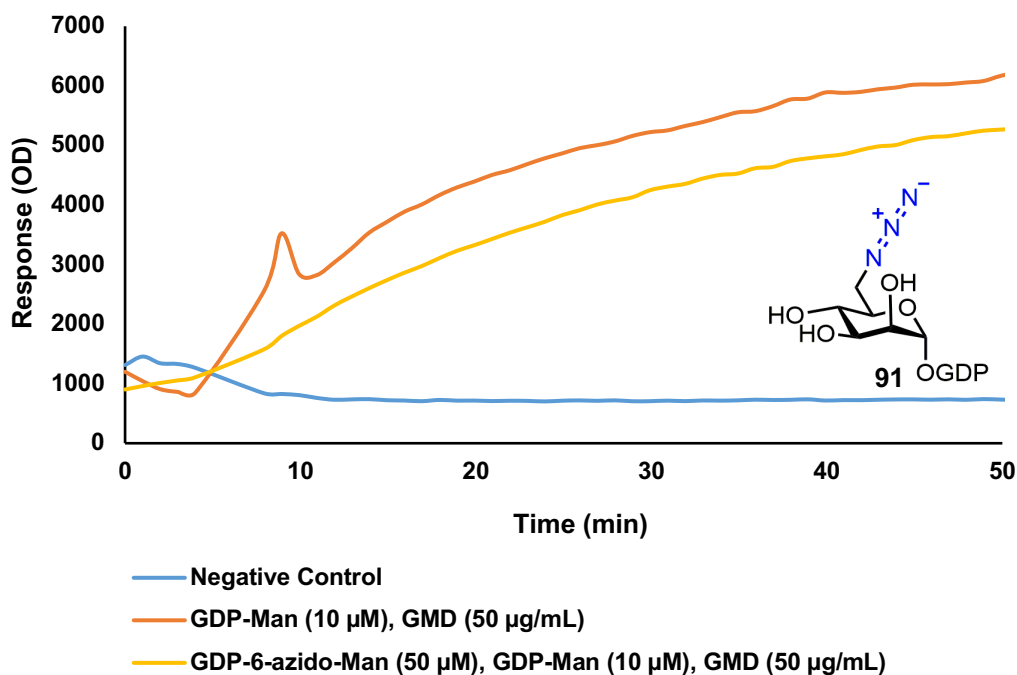


Figure 4.1: Evaluation of **91** as a substrate of GMD following pre-incubation.

4.2 GDP-4-deoxy-4-fluoro-mannose

4.2.1 Evaluation as a substrate of GMD

The potential of GDP-4-deoxy-4-fluoro-mannose **128** as a substrate of GMD was first evaluated by incubation of the analogue (50 μM) with GMD (50 $\mu\text{g}/\text{mL}$) for 60 min. During this time, no production of NAD(H) was observed. The experiment was repeated, but after 40 min the well containing analogue **133** was spiked with GDP-Man **3** and production of NAD(H) began (Figure 4.2).

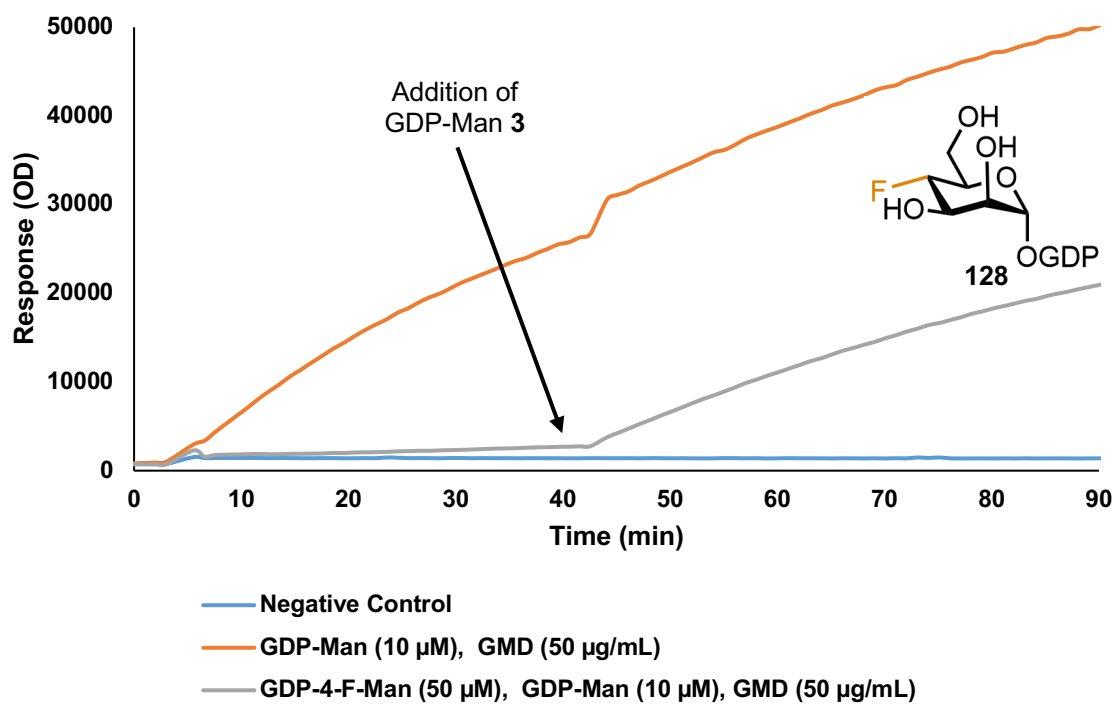


Figure 4.2: Incubation of **128** with GMD showing NAD(H) production after spiking with GDP-Man **3** after 40 min.

4.2.2 Discussion

This data suggested that analogue **128** is either oxidised by GMD very slowly or is not a substrate of GMD and is unable to bind in the active site. This implies that the C4-OH group is essential for substrate binding, as replacement by 4-F may remove hydrogen bond donor capability and would appear to disrupt this process. Referring to the PDB structure of GMD shown in Figure 4.3 (PDB ID: 1MV8, Ligand [GDX]2005:A), within the active site it is observed that the C4-OH of **4** appears to make up to three hydrogen bond contacts with the carboxylate groups of proximal Leu¹⁵⁹ and Glu¹⁵⁷ residues, suggesting this to be disrupted by analogue **128**.

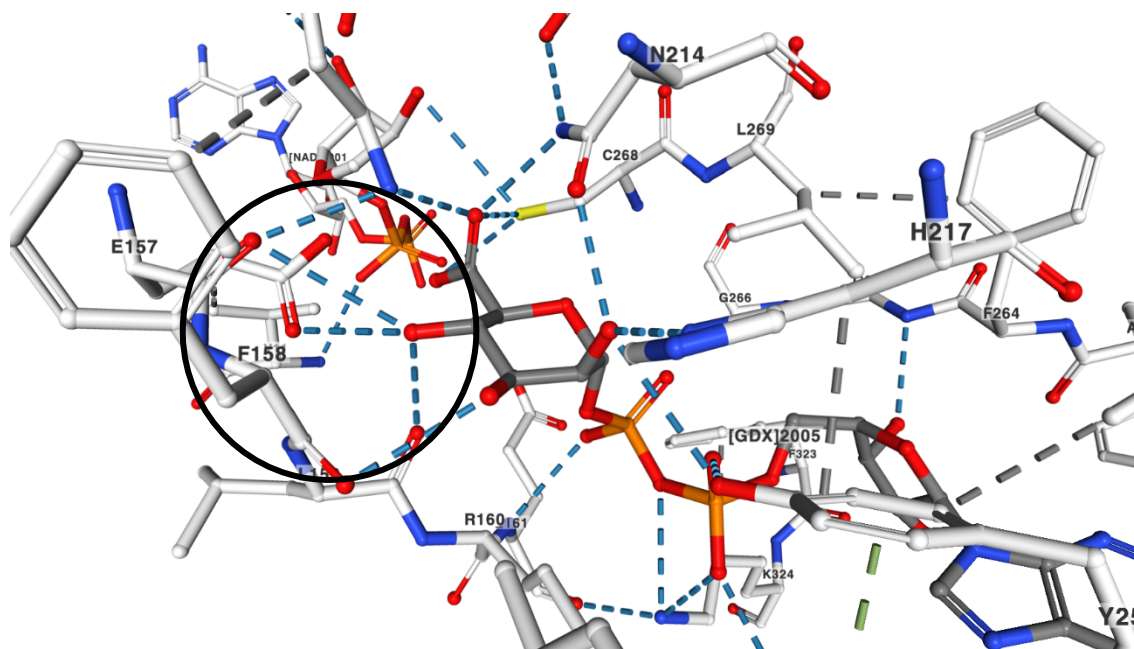


Figure 4.3: GDP-ManA **4** bound in GMD active site showing three hydrogen bonding contacts between C4-OH and carboxylate groups of Leu¹⁵⁹ and Glu¹⁵⁷. (PDB ID: 1MV8, Ligand [GDX]2005:A).

Unfortunately, analogue **128** could not be used as a competitive inhibitor of GMD because it was not oxidised. It has however provided new information surrounding substrate binding specificities within the active site of GMD. It would be of interest to evaluate other C4-modified sugar-nucleotides against GMD, such as GDP-4-methoxy-mannose, which was previously synthesised by Lou *et al.*⁷⁶ and GDP-4-deoxy-mannose. Testing of such analogues with varying hydrogen bond donor and acceptor capabilities could provide further information into substrate binding within the active site GMD and evaluate whether oxidation is facilitated.

4.3 GDP-6-amido-6-deoxy-mannose

4.3.1 Evaluation as an inhibitor of GMD

GDP-6-amido-6-deoxy-mannose **173** was first evaluated as a substrate of GMD. A 3-well assay was prepared as follows: negative control, GDP-Man (10 μ M) and a well containing **173** (50 μ M) with GDP-Man **3** (10 μ M) and monitored for 45 min. Interestingly, this analogue only showed 14% conversion of **3** at 50 μ M (Figure 4.4).

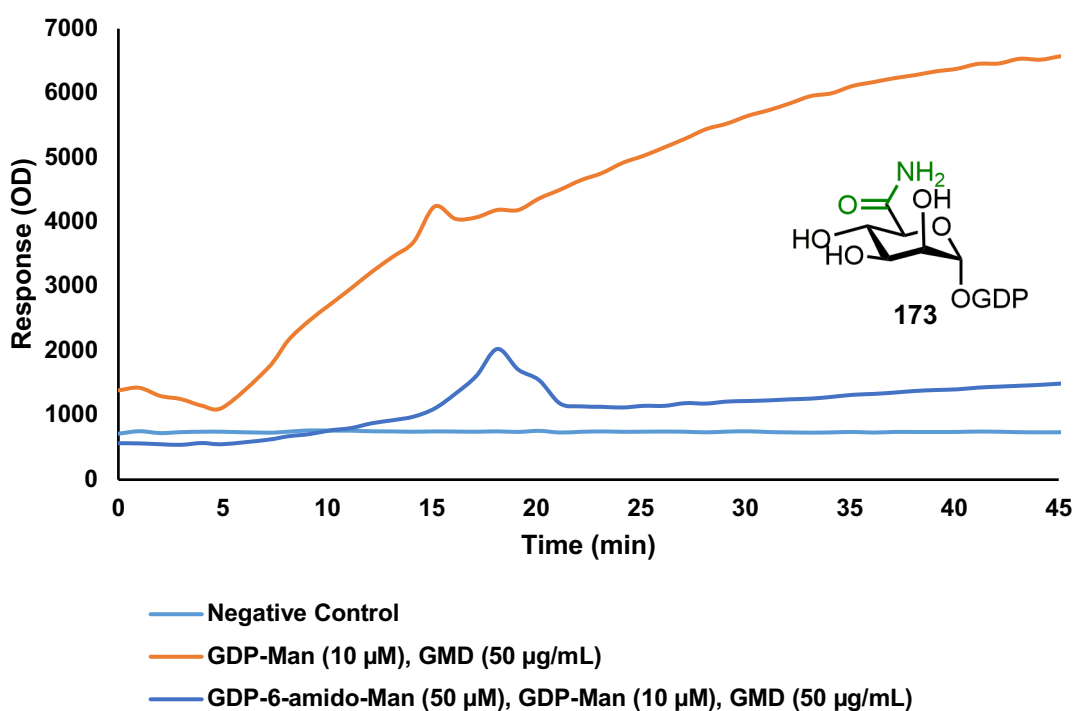


Figure 4.4: Initial evaluation of **173** (50 μ M) as a substrate of GMD.

Next, the assay was performed in triplicate using 7 different concentrations of **173** (200-1 μM). The expected relationship between increased conversion and decreased inhibitor concentration was clearly observed, as shown in Figure 4.5.

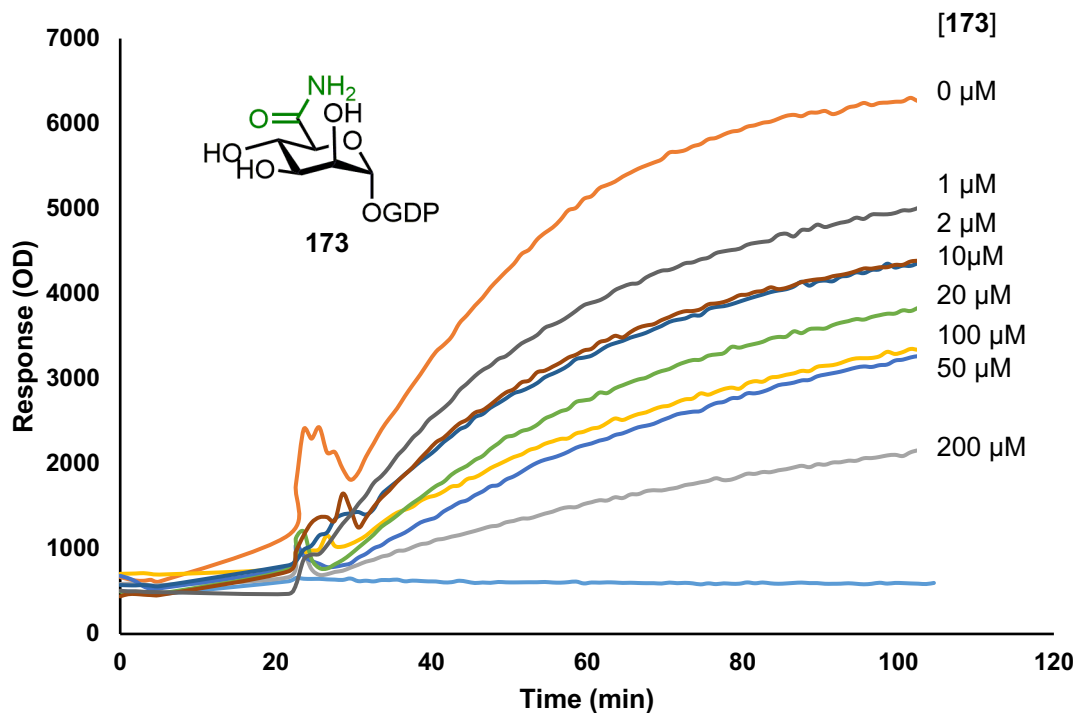


Figure 4.5: Evaluation of variable concentrations of **173** as an inhibitor of GMD.

Figure 4.6 shows the average inhibition (%) observed at variable concentrations of **173**. The data suggests that the IC_{50} value lies between 20 and 100 μM , however this could not be determined accurately as a wider range of inhibitor concentrations are required to produce a full curve. Due to time constraints, these could not be collected.

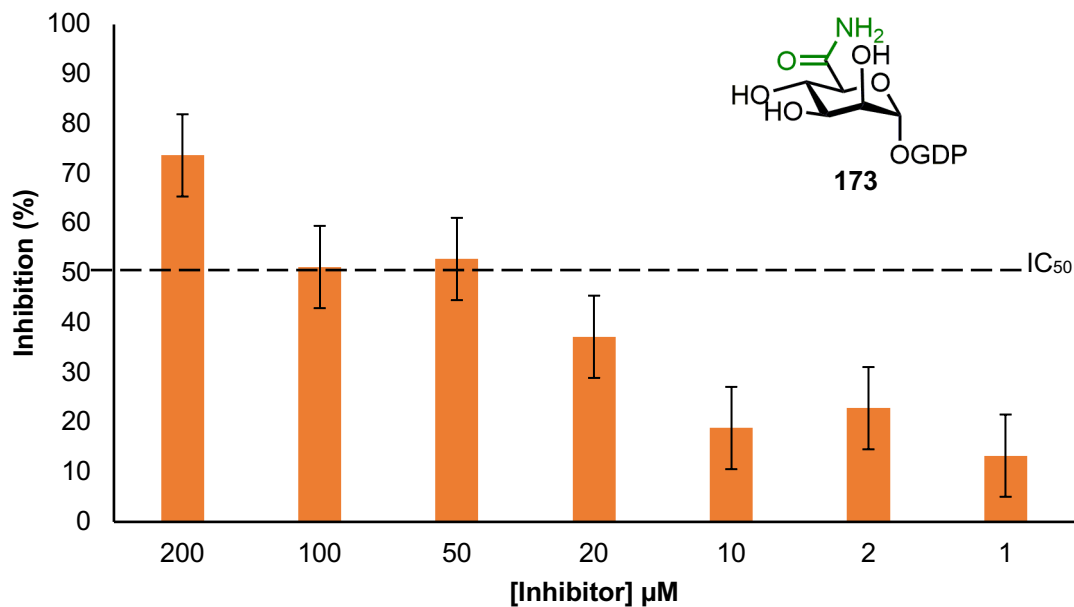


Figure 4.6: Average inhibition (%) at variable concentrations of **173**.

4.3.2 Evaluating potential hydrolysis of GDP-6-amido-6-deoxy-mannose by GMD

Finally, we sought to investigate whether GDP-6-amido-mannose **173** was being hydrolysed by GMD to form the native product of oxidation, GDP-ManA **4**. Evaluation of **4** as an inhibitor was performed using the same assay, where incubation with GMD for 50 min showed 44% inhibition of NAD(H) production at 50 μM , shown in Figure 4.7, lying within a similar range to that observed for analogue **173**. This observation confirmed GDP-ManA **4** acts as a feedback inhibitor of GMD, where if abundant in high concentration, it prevents oxidation of GDP-Man by remaining bound in the active site.

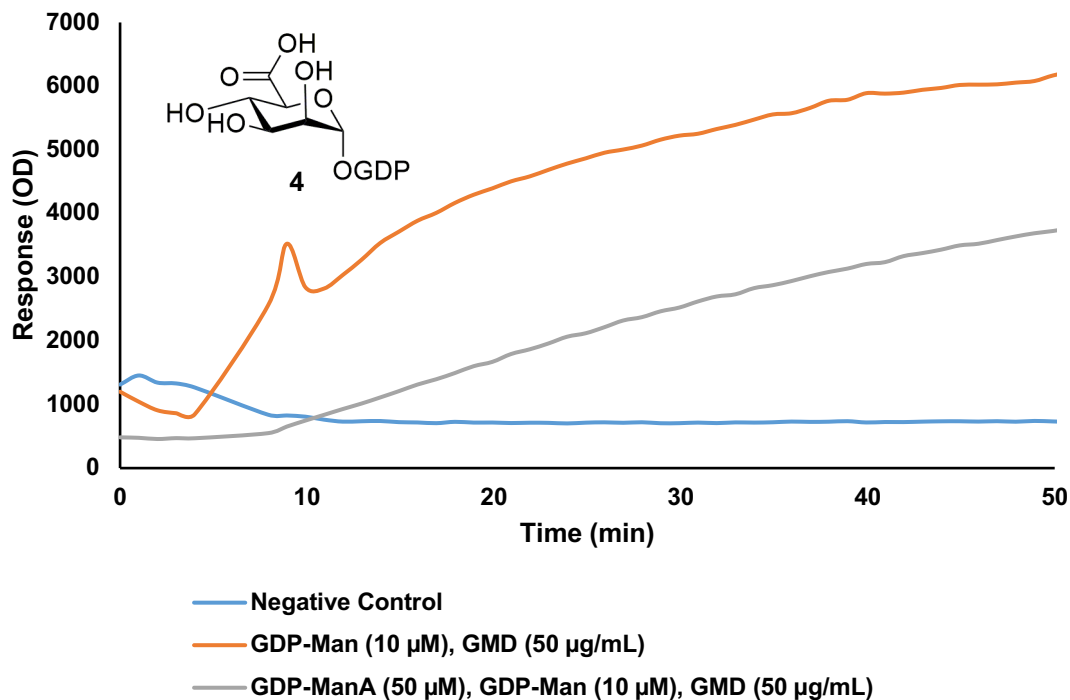
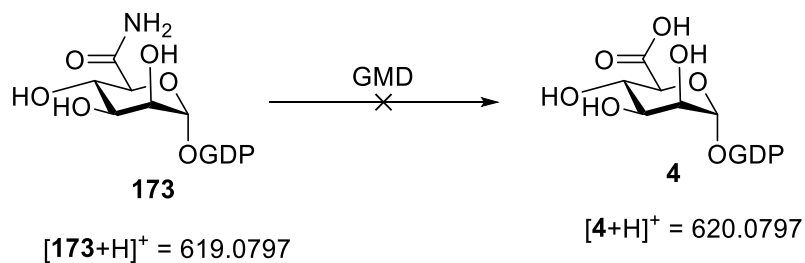


Figure 4.7: Evaluation of GDP-ManA **4** as a feedback inhibitor of GMD.

To rule out a feedback inhibition mechanism for analogue **173**, two experiments were performed, and the resultant mixtures analysed by HRMS, outlined in Scheme 4.1. Two reactions were prepared containing **173**: one control without GMD (Sample A) and one with GMD (Sample B). Each mixture was incubated for 3 h on ice, then MeOH was added. The reaction containing GMD was vortexed, centrifuged, then the supernatant was removed and filtered.



Scheme 4.1: Is GDP-6-amido-mannose **173** hydrolysed by GMD to **4**?

For Sample A, the major ion was identified at m/z 619.0797 corresponding to $[173+H]^+$. If hydrolysis was occurring, a peak at m/z 620.0797 corresponding to GDP-ManA $[4+H]^+$ would be observed, however in Sample B only the m/z corresponding to $[176+H]^+$ could be observed. This suggests no hydrolysis, or a very minimal amount of hydrolysis of **173** is induced by GMD under these conditions.

4.3.3 Discussion

GDP-6-amido-6-deoxy-mannose **173** was identified as a μM inhibitor of GMD, with an IC_{50} value in the range of 20 to 50 μM . HRMS analysis confirmed that no hydrolysis of this analogue to the native product GDP-ManA **4** was induced by GMD, ruling out **4** acting as a feedback inhibitor *via* this mechanism. It is thus proposed that **173** may act as a competitive inhibitor of GMD, with molecular docking studies of **173** in the active site of GMD revealing that the $\text{C}(\text{O})\text{NH}_2$ may establish two hydrogen bonds with a proximal Glu¹⁵⁷ residue and the key Cys²⁶⁸ residue (Figure 4.9), proposed to permit strong binding of this analogue.

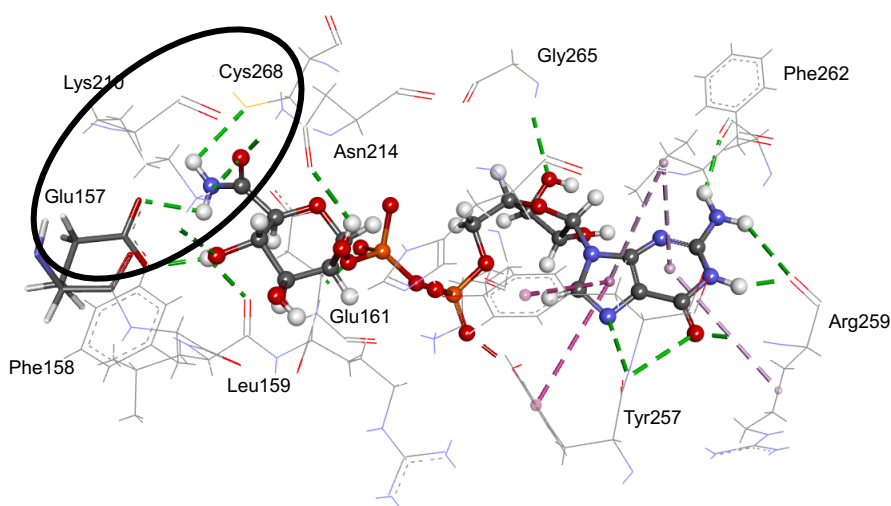


Figure 4.9: Molecular docking of **173** in the active site of GMD showing two hydrogen bond contacts between $\text{C}(\text{O})\text{NH}_2$ with Glu¹⁵⁷ and Cys²⁶⁸.

4.4 Conclusions and Future Directions

In conclusion, three GDP-Man analogues were evaluated as substrates of GMD. GDP-6-azido-6-deoxy-mannose **91** was not a substrate of the enzyme, with conversion of GDP-Man **3** to GDP-ManA **4** only reduced by 14%. GDP-4-deoxy-4-fluoro-mannose **128** was also shown not to be a substrate of GMD. This has been proposed to originate through disruption of key hydrogen bonding contacts between C4-OH and the carboxylate group of neighbouring Leu¹⁵⁸ and Glu¹⁵⁷ residues, suggesting that the C4-OH is required for substrate binding.

Serendipitously, GDP-6-amido-6-deoxy-mannose **173**, which was not originally designed as a tool to probe GMD, was demonstrated to be a μM inhibitor of the enzyme. The mechanism of inhibition is not yet determined, however feedback inhibition through hydrolysis of the analogue to GDP-ManA **4** has been excluded. From inspection of molecular docking data, it appears that the amide group of **173** may be able to form a hydrogen bonding network with a proximal Glu¹⁵⁷ residue and the key Cys²⁶⁸ residue, proposed to result in strong binding of this analogue within the active site of GMD. This suggests a competitive inhibition mechanism may be exhibited by **173**, and this hypothesis could be strengthened by performing further kinetic analysis and obtaining a crystal structure of **173** bound in the GMD active site.

The data collected from biochemical evaluation can be used as a guide for the design of new analogues to further supplement understanding of GMD catalysed oxidation. More analogues exhibiting structural similarities to the native substrate/product should be designed and evaluated to compare with the interesting

inhibition profile exhibited by **173**. Evaluation of GDP-6-hydroxamate-6-deoxymannose **185** is now of interest, and an alternative strategy to access this material *via* chemical sugar-nucleotide synthesis would be beneficial to this investigation. Furthermore, the tetrazole group, a commonly employed carboxylic acid bioisostere in medicinal chemistry, would be interesting to incorporate into a GDP-Man analogue, affording **186** to further explore interactions within the binding pocket of GMD. The structures of these proposed analogues are shown in Figure 4.10.

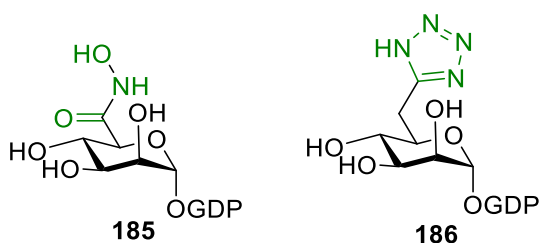


Figure 4.10: Proposed structures of GDP-Man analogues **185** and **186**.

Evaluation of electrophilic GDP-Man analogues, capable of alkylating Cys²⁶⁸, as substrates of GMD should be completed next, with a view of identifying new covalent inhibitors. Further work to complete the synthesis of electrophilic GDP-Man analogues **89** and **90**, bearing C6-chloro and C6-nitrile functionalities respectively, that were described in Chapter 3 could be supplemented by synthesis of a GDP-Man analogue featuring a C6-C8 Michael acceptor (Figure 4.11). Preliminary molecular docking has shown such homologues to fit in the GMD active site, with a distance of 3.39 Å calculated between C6 and Cys²⁶⁸, again comparable to that of the native product GDP-ManA **4**.

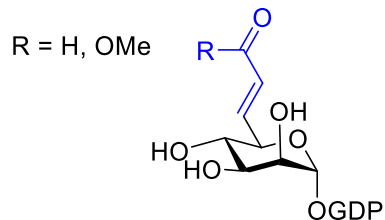


Figure 4.11: Generic structure of a GDP-Man analogue bearing a C6-C8 Michael acceptor.

When evaluating potential covalent adducts, it will be important to ensure selectivity for the active site Cys²⁶⁸ residue, to provide tools with high efficacy. This could be achieved by retaining the sugar-nucleotide backbone, which ensures specific binding interactions within the active site are retained. Whilst this approach is applicable for the preliminary exploration of functionalities capable of inhibiting GMD, future work will require synthesis of cell-permeable probes to facilitate monitoring of such ligands beyond *in vitro* studies. Rationalising a cell-permeable GMD probe with inhibitor activity would open a pathway to the design of ‘drug-like’ molecules that retain the glyco-warhead but replace the highly charged nucleotide component in future investigations.

Chapter 5: Overall Conclusions and Future Directions

In conclusion, two complementary routes to synthesise GDP-ManA, the constituent sugar-nucleotide building block for alginate biosynthesis, were evaluated. For the chemical synthesis, the final pyrophosphorylation step was optimised to produce GDP-ManA in 46% yield using DCI as the activator on multi-milligram scales. In contrast, an enzymatic route using GMD permitted facile access to this key sugar-nucleotide, albeit in lower quantities for use as an analytical standard.

Studies towards the synthesis of modified GDP-Man analogues for use as structure function tools of GMD proceeded with varying success. Following chemical synthesis of modified glycosyl 1-phosphates, a total of six analogues were screened against GDP-ManPP, of which three were successfully converted to the corresponding GDP-Man analogue. Although the remaining three sugar-nucleotide analogues could not be accessed *via* the proposed chemoenzymatic strategy, this study supplemented prior studies into GDP-ManPP by providing new insights into the substrate specificity of this enzyme. The information obtained can be used to guide future synthetic routes towards the remaining GDP-sugar targets described and other related analogues.

Screening of the GDP-Man analogues synthesised against GMD provided important new details surrounding substrate specificity of this strategic enzyme. Notably, a GDP-Man analogue bearing a C6-amido group was identified as a μM inhibitor. Further work to determine the IC_{50} value and confirm the proposed competitive inhibition mechanism are now required, however this finding provides a guide for the future design of similar analogues that may also act as inhibitors of GMD.

Chapter 6: Experimental

6.0 General experimental details

All reagents and solvents which were available commercially were purchased from Acros, Alfa Aesar, Fisher Scientific, Sigma Aldrich or TCI. All reactions in non-aqueous solvents were conducted in oven dried glassware with a magnetic stirring device under an inert atmosphere of nitrogen passed through molecular sieves using a vacuum manifold. Solvents were purified by passing through activated alumina columns and used directly from a Pure Solv-MD solvent purification system and were transferred under nitrogen. Reactions requiring low temperatures used the following cooling baths: $-78\text{ }^{\circ}\text{C}$ (dry ice/acetone), $-30\text{ }^{\circ}\text{C}$ (dry ice/acetone), $-15\text{ }^{\circ}\text{C}$ (NaCl/ice/water) and $0\text{ }^{\circ}\text{C}$ (ice/water).

Reactions were followed by thin layer chromatography (TLC) using Merck silica gel 60F254 analytical plates (aluminium support) and were developed using standard visualising agents: short wave UV radiation (245 nm) and 5% sulfuric acid in methanol/ Δ or orcinol/ Δ .

Purification *via* flash column chromatography was conducted using silica gel 60 (0.043-0.063 mm) under positive pressure of compressed air.

Purification by C18 chromatography was conducted using a ThermoScientific X30 SPE column (HyperSep C18, 6 mL) eluting with H_2O .

Purification *via* strong ion exchange (SAX) chromatography was conducted on a Bio-Rad Biologic LP system using a Bio-Scale Mini UNOsphere Q (strong anion exchange) cartridge (5 mL): flow rate (3.0 mL/min), $0 \rightarrow 100\%$ 1.0 M NH_4HCO_3 over 33 min or a ThermoFisher Dionex UltiMate 3000 HPLC system using a Poros HQ

50 (strong anion exchange) column (5 mL): flow rate (7.0 mL/min), 5 → 250 mM NH_4HCO_3 over 15 min with on-line UV detector to monitor @265nm.

Infra-red spectra were recorded neat on a Thermo Scientific Nicolet iS10 spectrometer; selected absorption frequencies (ν_{max}) are reported in cm^{-1} .

Optical activities were recorded on automatic Rudolph Autopol I or Bellingham and Stanley ADP430 polarimeters (concentration in g/100mL).

pH measurements were recorded using a Hanna[®] pH 20 meter.

^1H NMR spectra were recorded at 600, 400 or 300 MHz, ^{13}C NMR spectra at 150, 100 or 75 MHz, ^{19}F NMR spectra at 376 MHz and ^{31}P NMR spectra at 161 MHz respectively using Bruker AV-III spectrometers. ^1H NMR resonances were assigned with the aid of gDQCOSY. ^{13}C NMR resonances were assigned with the aid of gHSQCAD. Coupling constants are reported in Hertz. Chemical shifts (δ , in ppm) are standardised against the deuterated solvent peak. NMR data were analysed using Mestrenova software. ^1H NMR splitting patterns were assigned as follows: brs (broad singlet), s (singlet), d (doublet), dd (doublet of doublets), ddd (doublet of doublet of doublets), appt (apparent triplet), t (triplet), quartet (q) or m (multiplet and/or multiple resonances). Assignment in NMR analysis follows the generic ring numbering system shown in Figure 6.1.

LRMS and HRMS (ESI) were obtained on Agilent 6530 Q-TOF, LQT Orbitrap XL1 or Waters (Xevo, G2-XS TOF or G2-S ASAP) Micromass LCT spectrometers using a methanol mobile phase in positive/negative ionisation modes as appropriate. HRMS was obtained using a lock-mass to adjust the calibrated mass.

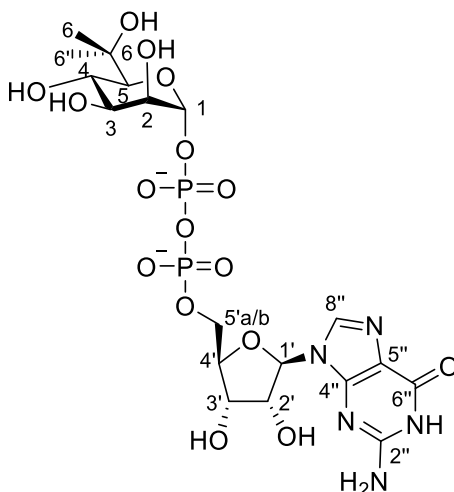


Figure 6.1: Ring numbering system for NMR assignment.

DFT calculations were performed by Dr. Jóhannes Reynisson as follows: The geometry optimisations were performed with Gaussian 16 software¹⁵⁵ using restricted density functional theory. The B3LYP functional hybrid method was employed and the 6-311+G(2df, p) with diffused basis set was used for the geometry optimisation and frequency analysis in vacuum. The normal modes revealed no imaginary frequencies indicating that they represent minima on the potential energy surface.^{156–158}

Molecular docking was performed by Dr. Ayesha Zafar and Dr. Jóhannes Reynisson as follows: The Scigress Ultra version F.J 2.6 program¹⁵⁹ was used for the modelling of the ligands in the crystal structures of GMD (PDB ID: 1MV8).⁶⁶ Hydrogen atoms were added to the structures and the ligands were built into the binding pocket based on GDX, the co-crystallised ligand. The ligands were first structurally optimised followed by a short 10 ps molecular dynamic (MD) run using the MM2.¹⁶⁰

6.1 General experimental procedures

A. Glycosylation of thioglycoside using NIS/AgOTf activation

Thioglycoside (1.0 equiv.) was dissolved in DCM (0.1 M) and stirred with powdered 4 Å MS for 1 h. DBP (1.5 equiv.) was added and the reaction mixture was stirred for a further 30 min before being cooled to $-30\text{ }^{\circ}\text{C}$. NIS (1.5 equiv.) and AgOTf (0.3 equiv.) were added successively and the reaction was stirred until TLC analysis indicated the reaction was complete. The reaction mixture was quenched with Et₃N, filtered over Celite™ then diluted with DCM. The organic layer was washed with saturated aqueous Na₂S₂O₃ solution (20 mL), saturated aqueous NaHCO₃ solution (20 mL), H₂O (20 mL), brine (20 mL), dried (MgSO₄), filtered and concentrated *in vacuo*.

B. Glycosylation of trichloroacetimidate using TMSOTf activation

Crude trichloroacetimidate (1.0 equiv.) was dissolved in DCM (0.1 M) and stirred with powdered 4 Å MS for 1 h. DBP (1.7 equiv.) was added and the reaction mixture was stirred for a further 30 min before being cooled to $-10\text{ }^{\circ}\text{C}$. TMSOTf (0.5 equiv.) was added dropwise and the reaction mixture allowed to warm to RT over 1 h with stirring until TLC analysis indicated the reaction was complete. The reaction mixture was quenched with Et₃N, filtered over Celite™ then diluted with DCM. The organic layer was washed with saturated aqueous NaHCO₃ solution (25 mL), H₂O (25 mL), brine (25 mL), dried (MgSO₄), filtered and concentrated *in vacuo*.

C. DAST fluorination

A solution of DAST (8.0 equiv.) in DCM (1 M) was cooled to $-78\text{ }^{\circ}\text{C}$ in a TeflonTM flask and a solution of C4-OH sugar (1.0 equiv.) in anhydrous DCM (0.1 M) was added dropwise. The reaction mixture was warmed to RT and stirred until TLC analysis indicated the reaction was complete. The reaction mixture was quenched with saturated aqueous NaHCO_3 solution (10 mL) under positive pressure of N_2 and diluted with DCM (25 mL). The organic layer was washed with saturated aqueous NaHCO_3 solution (20 mL), H_2O (2×20 mL), brine (20 mL), dried (MgSO_4), filtered and concentrated *in vacuo*.

D. MacDonald phosphorylation

Per-O-acetylated sugar (1.0 equiv.) was weighed into a pre-dried Schlenk tube and dried under high vacuum for 1 h. H_3PO_4 (5.0 equiv.) was weighed inside a glove box or glove bag, transferred to the Schlenk tube and the tube sealed under nitrogen. The tube was placed under nitrogen on a double manifold and then heated under high vacuum at the given temperature with gentle stirring to form a melt. The reaction was monitored by TLC analysis (Pet. ether/EtOAc, 1/2) for formation of a baseline ($R_f = 0$) spot corresponding to the glycosyl 1-phosphate (hemiacetal by-product observed at R_f 0.5) until the reaction was complete. The resultant melt was cooled to RT, reconstituted in anhydrous THF then added to a stirred solution of 1 M LiOH (concentration = 25 mM with respect to starting material) at $0\text{ }^{\circ}\text{C}$ then warmed to RT and stirred until saponification was complete by TLC analysis (MeCN/ H_2O /AcOH, 3/1/0.1), typically 48-72 h. The reaction mixture was filtered through a Whatman GA

filter under vacuum and rinsed with H₂O. The filtrate was neutralised through the addition of Amberlite™ 120 ion-exchange resin (H⁺ form) to pH = 7, filtered and concentrated *in vacuo*. The crude residue was then triturated with MeOH, centrifuged and the supernatant removed before purification or directly applied to a Bio-Scale Mini UNOsphere Q (SAX) cartridge (CV = 5 mL), eluting with 3 CV of H₂O and 3 CV of 1.0 M NH₄HCO₃ solution. Fractions containing the glycosyl 1-phosphate were collected and lyophilised repeatedly to remove residual NH₄HCO₃ and deliver the target material.

E. Chemical synthesis of sugar-nucleotides

Glycosyl 1-phosphate and GMP-morpholidate were exchanged to their *bis*-triethylammonium salt forms prior to the reaction and lyophilised. Glycosyl 1-phosphate (*bis*-triethylammonium salt, 1.0 equiv.), GMP-morpholidate (*bis*-triethylammonium salt, 1.5 equiv.) and activator were each co-evaporated with Tol or pyridine (3 × 2 mL) and then dissolved in DMF or pyridine (0.05 M), respectively. The reaction mixture was stirred at room temperature and conversion monitored by TLC analysis (IPA/NH₄OH/H₂O, 6/3/1). The reaction mixture was concentrated under reduced pressure (water bath temperature not exceeding 30 °C) and dried under high vacuum before analysis by crude ¹H and ³¹P NMR to confirm presence of an NDP-sugar.

F. Deprotection of sugar-nucleotides

The crude reaction mixture was suspended in a mixture of MeOH and H₂O (1:1) then Et₃N was added until pH = 9. The reaction mixture was stirred for 24 h at room

temperature or until TLC analysis (IPA/NH₄OH/H₂O, 6/3/1) indicated conversion of starting material to a lower R_f value spot. The reaction mixture was concentrated under reduced pressure (water bath temperature not exceeding 30 °C) to give a dark yellow residue. The resultant residue was dissolved in H₂O and if using DCI, passed down a Thermo Scientific™ X30 SPE column (HyperSep C18, 6 mL), eluting with H₂O to remove DCI. The resulting aliquots were purified by SAX chromatography as described in the general experimental procedures.

G. Enzymatic synthesis of sugar-nucleotides using GDP-ManPP

The assay for enzymatic synthesis of sugar-nucleotides by GDP-ManPP was prepared as follows: The assay buffer was Tris-HCl (pH 8.0, 100 μM) containing MgCl₂ (12.8 mM) and DTT (1.6 mM). The final concentration of assay components were as follows: glycosyl 1-phosphate (1.0 equiv., 14.7 μM) and GTP (0.93 equiv., 15 μM). The enzyme concentrations were as follows: GDP-ManPP (0.1 mg/mL) and inorganic pyrophosphatase (iPPase, 2.70 U/mL). The reaction was incubated with shaking at ambient temperature until formation of an NDP-sugar was observed by SAX. MeOH (2 mL) was added and the mixture was centrifuged (5000 RPM) for 5 min to remove insoluble protein, passed through a syringe filter (0.4 μM, PTFE) and purified by SAX chromatography as described in the general experimental procedures.

6.2 Enzyme production

6.2.1 GDP-mannose pyrophosphorylase (GDP-ManPP)

Expression and purification of GDP-ManPP from *S. enterica* (the clone was kindly donated by T. L. Lowary) was performed by the Field group using the following procedure: The transformant was grown according to the literature.¹⁶¹ 1 L of transformant in LB medium containing appropriate antibiotic (kanamycin, 25 µg/mL) was incubated at 37 °C with gentle shaking until an OD600 of about 0.6. Heterologous protein expression was induced by adding isopropyl β-D-1-thiogalactopyranoside (IPTG) at 0.5 mM final concentration, followed by incubation at 18 °C overnight at 180 rpm. Afterwards, cells were harvested by centrifugation (4000 × g, 4 °C, 20 min) and stored at –80 °C until use. Frozen cells were thawed in 50 mM Tris-HCl pH 8.0, 500 mM NaCl, 20 mM imidazole supplemented with DNase (10 µg/mL, Sigma) and proteinase inhibitor cocktail (Roche), then lysed by sonication in ice. After centrifugation (20,000 × g, 4 °C, 20 min) to remove the cell debris, the crude protein solution was purified at 4 °C using an ÄKTA pure FPLC system (GE Healthcare). The supernatant was passed through a HisTrap™ HP column (5 ml, GE healthcare), pre-equilibrated with buffer A (50 mM Tris-HCl pH 8.0, 500 mM NaCl, 20 mM imidazole). Unbound proteins were washed with five column volumes of buffer A, followed by elution with buffer B (50 mM Tris-HCl pH 8, 500 mM NaCl, 500 mM imidazole). GDP-ManPP comprising fractions were pulled together to give a final 7 mg/mL concentrated solution (concentration determined by Bradford assay, Sigma). Concentrated GDP-ManPP was then divided into aliquots and stored at –80°C until required.

6.2.2 GDP-mannose dehydrogenase (GMD)

Expression and purification of GMD from *P. aeruginosa* (the recombinant plasmid pET-3a containing the algD gene encoding for GMD was kindly donated by P. Tipton) was performed by the Field group using the following procedure: The transformant was grown according to the literature.¹⁶² 1 L of transformant in LB medium containing appropriate antibiotic (carbenicillin, 100 µg/mL) was incubated at 37 °C with gentle shaking until an OD600 of about 0.6. Heterologous protein expression was induced by adding isopropyl β-D-1-thiogalactopyranoside (IPTG) at 0.4 mM final concentration, followed by incubation at 37 °C for 4 hours at 180 rpm. Afterwards, cells were harvested by centrifugation (4000 × g, 4 °C, 20 min) and stored at -80 °C until use. Frozen cells were thawed in 20 mM HEPES pH 7.5, 150 mM NaCl supplemented with DNase (10 µg/mL, Sigma) and proteinase inhibitor cocktail (Roche), then lysed by sonication in ice. After centrifugation (20,000 × g, 4 °C, 20 min), protamine sulfate was added to the supernatant to precipitate nucleic acid. After removal of precipitated nucleic acid by centrifugation, the crude protein solution was fractionated with ammonium sulfate, with GMD precipitating between 45 and 60% saturation. Protein pellets were re-dissolved in 20 mM HEPES pH 7.5, 150 mM NaCl and purified using an ÄKTA pure FPLC system (GE Healthcare) by gel filtration chromatography using a Superdex S200 16/600 column (GE Healthcare). Proteins were eluted with 20 mM HEPES (pH 7.5) and 150 mM NaCl at the flow rate of 1 mL/min. GMD comprising fractions were pulled together to give a final 4.5 mg/mL concentrated solution (concentration determined by Bradford

assay, Sigma). Concentrated GMD was then divided into aliquots and stored at -80°C until required.

6.3 Determination of GMD activity and assay

Fluorescence assays were performed in black NUNC 96 plates on a BMG Labtech FLUOstar Omega microplate reader equipped with suitable excitation and emission filters at 355 and 460 nm, respectively. The fluorescence assay showed an increase in fluorescence at 460 nm compared to the negative control, indicating formation of NAD(H) hence activity of GMD. Four concentrations of GMD were evaluated: 200, 100, 50 and 20 $\mu\text{g}/\text{mL}$, with the optimum concentration found to be 50 $\mu\text{g}/\text{mL}$, which was adopted for all assays described in this thesis (Figure 6.2).

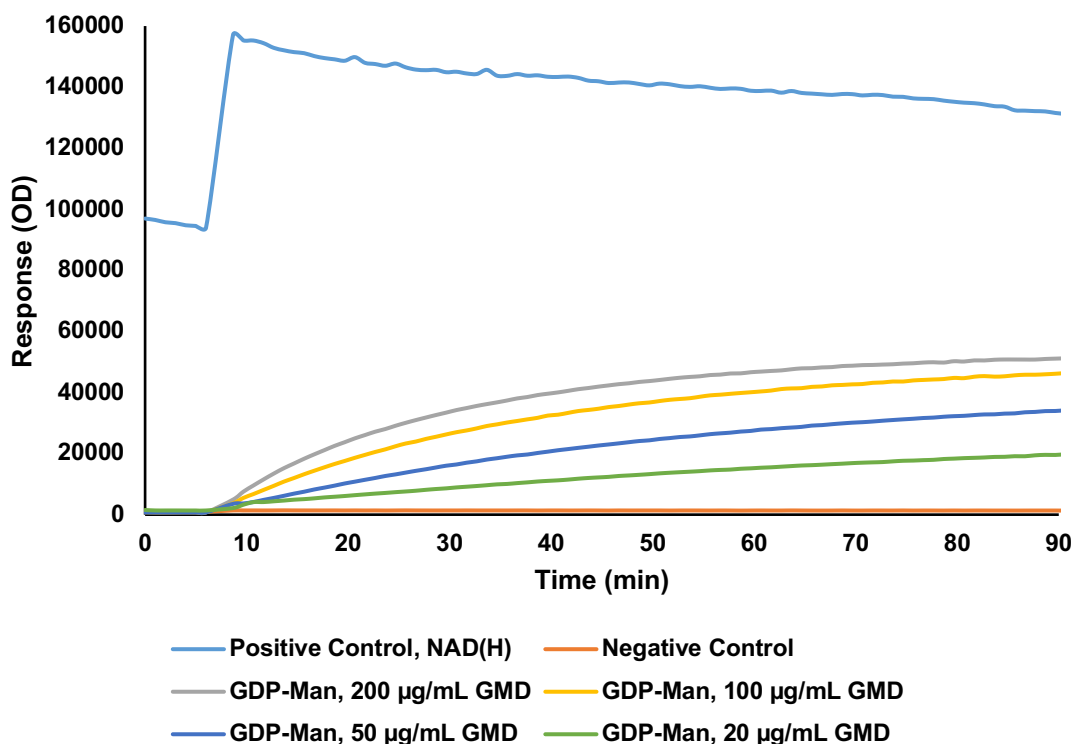


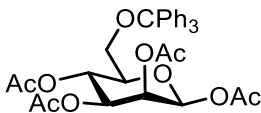
Figure 6.2: Evaluation of GMD activity and concentration.

The assay for GMD activity against GDP-Man analogues was prepared as follows:
The assay buffer was sodium phosphate (pH 7.38, 200 μM) containing MgCl_2 (5 μM) and DTT (10 μM). The final concentration of assay components were as follows: NAD^+ (200 μM), GDP-Man **3** (10 μM), GDP-Man analogue (50 μM). The enzyme concentration was as follows: GMD (50 $\mu\text{g}/\text{mL}$).

6.4 Experimental details for Chapter 2

6.4.1 α -D-mannopyranuronic acid derivatives: acetyl protected methyl uronate series

1,2,3,4-Tetra-O-acetyl-6-O-trityl- β -D-mannopyranose **65**



D-mannose **64** (25.8 g, 142 mmol, 1.0 equiv.) and TrCl (40.1 g, 143 mmol, 1.1 equiv.) were suspended in pyridine (125 mL) and stirred at 50 °C for 3 h. The solution was cooled to 0 °C and Ac₂O (75 mL) was added *via* a dropping funnel over 30 min before being warmed to RT. After stirring for 18 h, the reaction mixture was poured onto ice (750 mL) and stirred vigorously for 1.5 h to afford a white solid (H₂O was exchanged twice during this time to remove pyridine). The solid was collected by vacuum filtration and washed with ice-cold H₂O (250 mL) and dried for 2.5 h. The solid was recrystallized from the minimum amount of hot EtOH collected by filtration and dried (P₂O₅) in a vacuum desiccator, affording **65** as a white solid (39.0 g, 66.0 mmol, 46% β -anomer). These data were in good agreement with literature values.^{163,164}

R_f 0.38 (Hex/EtOAc, 3/1);

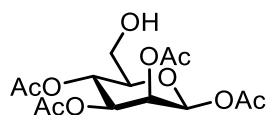
¹H NMR (300 MHz, CDCl₃) δ _H 7.47-7.45 (7H, m, Ar-H), 7.30-7.23 (8H, m, Ar-H), 5.87 (1H, d, *J* = 1.1 Hz, H₁), 5.48 (1H, dd, *J* = 3.3, 1.1 Hz, H₂), 5.38 (1H, appt, *J* = 9.9 Hz, H₄), 5.07 (1H, dd, *J* = 9.9, 3.3 Hz, H₃), 3.70-3.63 (1H, m, H₅), 3.35 (1H, dd, *J* = 10.6, 2.8 Hz, H₆), 3.17 (1H, dd, *J* = 10.6, 4.5 Hz, H₆), 2.25 (3H, s, C(O)CH₃), 2.15 (3H, s, C(O)CH₃), 1.99 (3H, s, C(O)CH₃), 1.76 (3H, s, C(O)CH₃);

^{13}C NMR (100 MHz, CDCl_3) δ_{C} 170.5 (C=O), 170.1 (C=O), 169.4 (C=O), 168.7 (C=O), 143.9 (Ar-C), 129.0 (Ar-C), 128.0 (Ar-C), 127.3 (Ar-C), 90.8 (C_1), 87.0 (OCPh_3), 75.0 (C_5), 71.2 (C_3), 68.7 (C_2), 66.3 (C_4), 62.5 (C_6), 21.1 (C(O)CH_3), 21.0 (C(O)CH_3), 20.8 (2C, C(O)CH_3);

LRMS m/z (ES^+) 613 ($[\text{M}+\text{Na}]^+$, 100%);

HRMS m/z (ESI^+) [Found: ($\text{M}+\text{Na}$) $^+$ 613.2035 $\text{C}_{33}\text{H}_{34}\text{O}_{10}\text{Na}$ requires $\text{M}+\text{Na}^+$, 613.2044].

1,2,3,4-Tetra-O-acetyl- β -D-mannopyranose **66**



65 (10.2 g, 17.3 mmol, 1.0 equiv.) was dissolved in AcOH (120 mL) at 40 °C with stirring. The solution was cooled to 15 °C and HBr/AcOH (33% w/w in acetic acid, 5 mL, 20 mmol, 1.2 equiv.) was added dropwise, inducing a yellow precipitate. After 10 s, the solution was filtered through CeliteTM onto H_2O (250 mL) and the solid washed with AcOH (10 mL) under vacuum. HBr/AcOH was quenched with saturated aqueous NaHCO_3 solution (250 mL) forming an opaque white suspension which was extracted with CHCl_3 (2 \times 200 mL). The organic layer was washed with saturated aqueous NaHCO_3 solution (100 mL), H_2O (100 mL), dried (MgSO_4), filtered and concentrated *in vacuo*. The resultant residue was dissolved in the minimum amount of hot CHCl_3 and induced to crystallise with Et_2O . The crystals were collected by filtration and dried *in vacuo*, affording **66** as a white solid (3.6 g, 10 mmol, 60%). These data were in good agreement with literature values.¹⁶³

R_f 0.33 (Hex/EtOAc, 1/1);

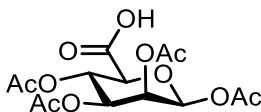
¹H NMR (300 MHz, CDCl₃) δ_H 5.88 (1H, d, *J* = 1.2 Hz, H₁), 5.50 (1H, dd, *J* = 3.2, 1.2 Hz, H₂), 5.27 (1H, appt, *J* = 9.9 Hz, H₄), 5.18 (1H, dd, *J* = 9.9, 3.2 Hz, H₃), 3.82-3.58 (3H, m, H₅, H₆, H_{6'}), 2.22 (3H, s, C(O)CH₃), 2.11 (3H, s, C(O)CH₃), 2.10 (3H, s, C(O)CH₃), 2.02 (3H, s, C(O)CH₃);

¹³C NMR (100 MHz, CDCl₃) δ_C 170.6 (C=O), 170.4 (C=O), 170.0 (C=O), 168.7 (C=O), 90.7 (C₁), 75.7 (C₅), 70.8 (C₃), 68.5 (C₂), 65.9 (C₄), 61.4 (C₆), 20.9 (C(O)CH₃), 20.9 (C(O)CH₃), 20.8 (C(O)CH₃), 20.7 (C(O)CH₃);

LRMS *m/z* (ES⁺) 366 ([M+NH₄]⁺, 100%);

HRMS *m/z* (ES⁺) [Found: (M+NH₄)⁺ 366.1397 C₁₄H₂₀O₁₀NH₄ requires M+NH₄⁺, 366.1395].

1,2,3,4-Tetra-O-acetyl-β-D-mannopyranosiduronic acid **67**



To a vigorously stirred solution of **66** (1.5 g, 4.3 mmol, 1.0 equiv.) in DCM/H₂O (2:1, 30 mL) was added TEMPO (0.3 g, 2.2 mmol, 0.5 equiv.) and BAIB (6.9 g, 22 mmol, 5.0 equiv.). After 5 h, the reaction was quenched with 10% aqueous Na₂S₂O₃ solution (30 mL), the organic layer removed and the aqueous layer acidified to pH 2-3 using 1M HCl. The aqueous layer was extracted with EtOAc (2 × 30 mL), dried (MgSO₄), filtered and concentrated *in vacuo* affording **67** as a white solid (1.2 g, 3.3 mmol, 75%).

R_f 0.81 (DCM/MeOH, 9/1);

[α]_D²⁶ -20.0 (c = 0.50, MeOH);

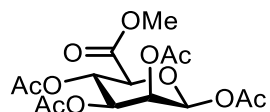
¹H NMR (300 MHz, CDCl₃) δ_H 5.96 (1H, d, *J* = 1.5 Hz, H₁), 5.50 (1H, dd, *J* = 3.2, 1.5 Hz, H₂), 5.48 (1H, appt, *J* = 9.2 Hz, H₄), 5.21 (1H, dd, *J* = 9.2, 3.2 Hz, H₃), 4.2 (1H, d, *J* = 8.9 Hz, H₅), 2.21 (3H, s, C(O)CH₃), 2.13 (3H, s, C(O)CH₃), 2.10 (3H, s, C(O)CH₃), 2.04 (3H, s, C(O)CH₃);

¹³C NMR (100 MHz, CDCl₃) δ_C 169.9 (C=O, uronic acid), 169.7 (C=O), 169.5 (C=O), 169.4 (C=O), 168.2 (C=O), 89.4 (C₁), 72.3 (C₅), 69.3 (C₃), 66.9 (C₂), 65.9 (C₄), 20.4 (C(O)CH₃), 20.4 (C(O)CH₃), 20.3 (C(O)CH₃), 20.2 (C(O)CH₃);

LRMS *m/z* (ES⁻) 361 ([M-H]⁻, 100%);

HRMS *m/z* (ES⁻) [Found: (M-H)⁻ 361.0767 C₁₄H₁₇O₁₁ requires *M-H*⁻, 361.0776].

Methyl 1,2,3,4-tetra-*O*-acetyl-β-D-mannopyranosyluronate **68**



To a solution of **67** (0.60 g, 1.7 mmol, 1.0 equiv.) in DMF (8 mL) was added methyl iodide (250 μL, 4.02 mmol, 2.4 equiv.) and K₂CO₃ (0.16 g, 1.1 mmol, 1.5 equiv.). After stirring for 72 h, the reaction was quenched with MeOH (5 mL), extracted with EtOAc (25 mL) and washed with H₂O (15 mL) and brine (15 mL). The organic layer was dried (MgSO₄), filtered and concentrated *in vacuo*. The resultant yellow solid was triturated with MeOH to afford **68** as a white solid (480 mg, 1.3 mmol, 77%).

R_f 0.23 (Hex/EtOAc, 3/1);

[α]_D²⁶ -16.0 (c = 0.50, CHCl₃);

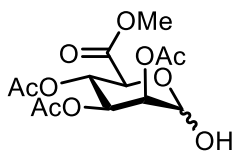
¹H NMR (300 MHz, CDCl₃) δ_H 5.91 (1H, d, J = 1.3 Hz, H₁), 5.50 (1H, dd, J = 3.5 Hz, 1.2, H₂), 5.42 (1H, appt, J = 9.4 Hz, H₄), 5.19 (1H, dd, J = 9.6, 3.2 Hz, H₃), 4.15 (1H, d, J = 9.4 Hz, H₅), 3.74 (3H, s, C(O)OCH₃), 2.21 (3H, s, C(O)CH₃), 2.12 (3H, s, C(O)CH₃), 2.07 (3H, s, C(O)CH₃), 2.03 (3H, s, C(O)CH₃);

¹³C NMR (100 MHz, CDCl₃) δ_C 170.6 (C=O, uronate), 170.0 (C=O), 170.0 (C=O), 168.8 (C=O), 167.2 (C=O), 90.1 (C₁), 73.6 (C₅), 70.0 (C₃), 67.8 (C₂), 66.7 (C₄), 53.3 (C(O)OCH₃), 21.1 (C(O)CH₃), 21.1 (C(O)CH₃), 21.0 (C(O)CH₃), 20.9 (C(O)CH₃);

LRMS *m/z* (ES⁺) 394 ([M+NH₄]⁺, 100%);

HRMS *m/z* (ES⁺) [Found: (M+NH₄)⁺ 394.1337 C₁₅H₂₀O₁₁NH₄ requires M+NH₄⁺, 394.1344].

Methyl 2,3,4-tri-O-acetyl-α/β-D-mannopyranosyluronate **71**



To a solution of **68** (100 mg, 0.3 mmol, 1.0 equiv.) in DMF (2 mL) was added hydrazine acetate (38 mg, 0.41 mmol, 1.5 equiv.). After stirring for 3 h, the solvent was removed *in vacuo* and the residue reconstituted in EtOAc (10 mL) and washed with H₂O (10 mL) and brine (10 mL). The organic layer was dried (MgSO₄), filtered and concentrated *in vacuo*. Purification by silica gel column chromatography eluting

with Hex/EtOAc (3/1, 1/1) afforded **71** as a colourless oil (58 mg, 0.17 mmol, 64%, 95% α -anomer).

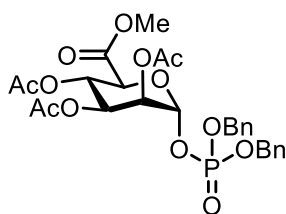
R_f 0.47 (Hex/EtOAc, 1/1);

^1H NMR (400 MHz, CDCl_3) δ_{H} 5.45 (1H, d, $J = 3.2$ Hz, H_3), 5.41 (1H, appt, $J = 8.9$ Hz, H_4), 5.34 (1H, d, $J = 2.5$ Hz, H_1), 5.26-5.25 (1H, m, H_2), 4.58 (1H, d, $J = 8.9$ Hz, H_5), 3.77 (3H, s, C(O)OCH_3), 2.15 (3H, s, C(O)CH_3), 2.07 (3H, s, C(O)CH_3), 2.02 (3H, s, C(O)CH_3);

^{13}C NMR (100 MHz, CDCl_3) δ_{C} 170.2 (C=O, uronate), 169.7 (C=O), 168.6 (C=O), 162.8 (C=O), 92.1 (C_1), 69.7 (C_2), 69.6 (C_5), 68.3 (C_3), 67.2 (C_4), 54.7 (C(O)OCH_3), 20.9 (C(O)CH_3), 20.7 (C(O)CH_3), 20.6 (C(O)CH_3);

HRMS m/z (ES^+) [Found: $(\text{M}+\text{NH}_4)^+$ 352.1246 $\text{C}_{13}\text{H}_{18}\text{O}_{10}\text{NH}_4$ requires $\text{M}+\text{NH}_4^+$, 352.1283].

Dibenzyl methyl 2,3,4-tri-O-acetyl- α -D-mannopyranosyluronate phosphate **73**



To a solution of **71** (550 mg, 1.7 mmol, 1.0 equiv.) and oven dried anhydrous K_2CO_3 (360 mg, 2.6 mmol, 1.6 equiv.) in DCM (5.5 mL) was added trichloroacetonitrile (0.37 mL, 4.62 mmol, 2.8 equiv.). After stirring for 18 h, the solution was filtered over CeliteTM, washed with DCM (15 mL) and concentrated *in vacuo* to afford **72** as a brown oil (774 mg, 1.62 mmol, 88%). Prepared as per Procedure B using crude **72**,

DBP (770 mg, 2.8 mmol, 1.7 equiv.) and TMSOTf (0.15 mL, 0.81 mmol, 0.5 equiv.) in DCM (15 mL). Reaction time: 1 h. Purification by silica gel column chromatography, eluting with Tol/acetone (10/1, 7/1, 3/1) afforded **73** as a colourless oil (369 mg, 0.62 mmol, 38%). These data were in good agreement with literature values.¹⁰⁵

R_f 0.30 (Hex/EtOAc, 1/1);

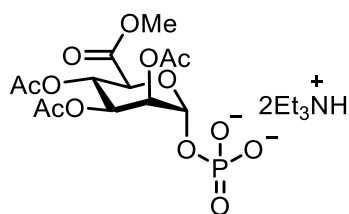
¹H NMR (400 MHz, CDCl₃) δ_H 7.35-7.34 (8H, m, Ar-H), 7.19-7.17 (2H, m, Ar-H), 5.70 (1H, dd, J_{H1-P} = 6.4 Hz, J_{H1-H2} = 2.0 Hz, H₁), 5.41-5.31 (2H, m, H₃, H₄), 5.24 (1H, d, J = 2.0 Hz, H₂), 5.10-5.08 (4H, m, CH₂Ph), 4.39 (1H, d, J = 8.8 Hz, H₅), 3.69 (3H, s, C(O)OCH₃), 2.13 (3H, s, C(O)CH₃), 2.05 (3H, s, C(O)CH₃), 2.01 (3H, s, C(O)CH₃);

¹³C NMR (100 MHz, CDCl₃) δ_C 169.6 (C=O, uronate), 169.5 (C=O), 169.5 (C=O), 167.2 (C=O), 129.1 (Ar-C), 128.7 (Ar-C), 128.7 (Ar-C), 128.2 (Ar-C), 128.1 (Ar-C), 94.7 (C₁), 70.8 (C₅), 70.1 (CH₂Ph), 69.9 (CH₂Ph), 68.2 (C₂), 67.6 (C₃), 66.4 (C₄), 52.8 (C(O)OCH₃), 21.5 (C(O)CH₃), 20.7 (C(O)CH₃), 20.6 (C(O)CH₃);

³¹P NMR (161 MHz, CDCl₃) δ_P -3.2 (1P, d, J_{H1-P} = 6.4 Hz);

HRMS *m/z* (ASAP) [Found: (M+H) 595.1586, C₂₇H₃₁O₁₃P requires *M+H*⁺, 595.1586].

Methyl 2,3,4-tri-O-acetyl- α -D-mannopyranosyluronate phosphate
(bis-triethylammonium salt) **60**



A suspension of **73** (200 mg, 0.3 mmol, 1.0 equiv.) and 10% Pd/C (0.2 eq. per benzyl group) in MeOH (5 mL) was stirred vigorously under an atmosphere of H₂ for 5 h. The reaction mixture was filtered over Celite™, washed with MeOH (20 mL), the filtrate treated with Et₃N (95 μL, 0.68 mmol, 2.0 equiv.) and concentrated *in vacuo* to afford **60** as a white solid (148 mg, 0.24 mmol, 71%). Data previously reported for the *bis*-tetrabutylammonium salt.¹⁰⁵

R_f 0.45 (EtOAc/MeOH/H₂O, 5/3/1);

[α]_D²⁶ +16.1 (c = 0.30, MeOH);

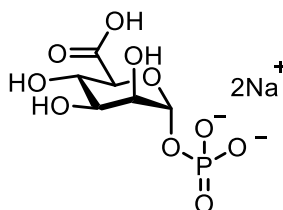
¹H NMR (400 MHz, CDCl₃) δ_H 5.62 (1H, d, J_{H1-P} = 7.0 Hz, H₁), 5.47 (1H, d, J = 9.9 Hz, H₃), 5.37-5.30 (2H, m, H₂, H₄), 4.70 (1H, d, J = 10.0 Hz, H₅), 3.70 (3H, s, C(O)OCH₃), 2.93 (12H, q, J = 6.6 Hz, [CH₃CH₂]₃NH⁺), 2.13 (3H, s, C(O)CH₃), 2.03 (3H, s, C(O)CH₃), 1.96 (3H, s, C(O)CH₃), 1.25 (18H, t, J = 6.9 Hz, [CH₃CH₂]₃NH⁺);

¹³C NMR (100 MHz, CDCl₃) δ_C 169.9 (2C, C=O), 169.6 (C=O), 168.6 (C=O), 93.6 (C₁), 69.6 (C₂), 69.5 (C₅), 68.6 (C₃), 67.1 (C₄), 52.5 (C(O)OCH₃), 45.6 ([CH₃CH₂]₃NH⁺), 20.9 (C(O)CH₃), 20.7 (C(O)CH₃), 20.6 (C(O)CH₃), 9.2 ([CH₃CH₂]₃NH⁺);

³¹P NMR (161 MHz, CDCl₃) δ_P -0.9 (1P, d, J_{H1-P} = 7.0 Hz);

HRMS *m/z* (ES⁻) [Found: (M-H)⁻ 413.0495 C₁₃H₁₉O₁₃P requires *M-H*⁻, 413.0484].

α -D-mannopyranuronic acid (disodium salt) **42**



To a solution of **60** (130 mg, 0.21 mmol, 1.0 equiv.) in MeOH/H₂O (2:1, 3 mL/1.5 mL) was added Et₃N (3 mL). The solution was stirred for 18 h then concentrated *in vacuo* (water bath temperature did not exceed 30 °C). Purification by ion-exchange chromatography (Dowex[®] 50W-X8 resin, Na⁺ form) followed by repeated lyophilisation afforded **42** as a cream solid (53 mg, 0.19 mmol, 90%).

R_f 0.33 (MeCN/H₂O with 3 drops NH₄OH, 2/1);

[α]_D²⁶ +22.2 (*c* = 0.45, H₂O);

¹H NMR (400 MHz, D₂O) δ _H 5.28 (1H, d, *J*_{H1-P} = 8.6 Hz, H₁), 4.02 (1H, d, *J* = 10.0 Hz, H₅), 3.89-3.83 (2H, m, H₂, H₃), 3.75-3.65 (1H, m, H₄);

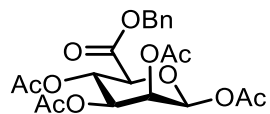
¹³C NMR (100 MHz, D₂O) δ _C 177.4 (C=O), 95.2 (C₁), 72.9 (C₄), 71.0 (C₂), 70.0 (C₃), 69.0 (C₅);

³¹P NMR (161 MHz, D₂O) δ _P 1.4 (1P, d, *J*_{H1-P} = 8.6 Hz);

HRMS *m/z* (ES⁻) [Found: (M-H)⁻ 273.0013 C₆H₁₁O₁₀P requires M-H⁻, 273.0012].

6.4.2 α -D-mannopyranuronic acid derivatives: acetyl protected benzyl uronate series

Benzyl 1,2,3,4-tetra-O-acetyl- β -D-mannopyranosyluronate **74**



To a solution of **66** (0.43 g, 1.2 mmol, 1.0 equiv.) in DMF (6 mL) was added BnBr (0.34 mL, 2.9 mmol, 2.4 equiv.) and K_2CO_3 (0.25 g, 1.8 mmol, 1.5 equiv.). After stirring for 24 h, the solvent was removed *in vacuo* and the residue reconstituted in EtOAc (25 mL), washed with H_2O (25 mL) and brine (25 mL). The organic layer was dried ($MgSO_4$), filtered and concentrated *in vacuo*. Purification by silica gel column chromatography, eluting in Hex/EtOAc (3/1, 1/1) afforded **74** as a white solid (481 mg, 1.06 mmol, 88%). These data were in good agreement with literature values.¹⁶⁵

R_f 0.85 (Hex/EtOAc, 1/1);

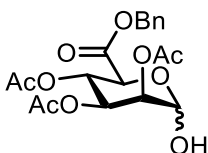
1H NMR (400 MHz, $CDCl_3$) δ_H 7.36 (5H, m Ar-*H*), 5.92 (1H, brs, H_1), 5.48 (1H, d, $J = 2.7$ Hz, H_2), 5.42 (1H, appt, $J = 9.4$ Hz, H_4), 5.19 (1H, d, $J = 3.4$ Hz, H_3), 5.15 (2H, d, $J = 8.9$ Hz, CH_2Ph), 4.19 (1H, d, $J = 9.4$ Hz, H_5), 2.20 (3H, s, $C(O)CH_3$), 2.10 (3H, s, $C(O)CH_3$), 1.99 (3H, s, $C(O)CH_3$), 1.79 (3H, s, $C(O)CH_3$);

^{13}C NMR (100 MHz, $CDCl_3$) δ_C 170.2 (C=O, uronate), 169.6 (C=O), 169.5 (C=O), 168.4 (C=O), 166.3 (C=O), 134.7 (Ar-C), 128.8 (Ar-C), 128.7 (Ar-C), 128.6 (Ar-C), 89.9 (C_1), 73.3 (C_5), 69.7 (C_4), 67.9 (CH_2Ph), 67.5 (C_2), 66.4 (C_4), 20.7 ($C(O)CH_3$), 20.7 ($C(O)CH_3$), 20.5 ($C(O)CH_3$), 20.4 ($C(O)CH_3$);

LRMS m/z (ES^+) 475 ($[M+Na]^+$, 100%);

HRMS m/z (ES^+) [Found: $(M+Na)^+$ 475.1211 $C_{21}H_{24}O_{11}Na$ requires $M+Na^+$, 475.1217].

Benzyl 2,3,4-tri-*O*-acetyl- α/β -D-mannopyranosyluronate **75**



To a solution of **74** (100 mg, 0.22 mmol, 1.0 equiv.) in DMF was added hydrazine acetate (24 mg, 0.36 mmol, 1.2 equiv.). After stirring for 4 h, the solvent was removed *in vacuo* and the residue reconstituted in EtOAc (10 mL), washed with H_2O (10 mL) and brine (10 mL). The organic layer was dried ($MgSO_4$), filtered and concentrated *in vacuo*. Purification by silica gel column chromatography eluting with Hex/EtOAc (3/1, 1/1) afforded **75** as a colourless oil (74 mg, 0.18 mmol, 82%). These data were in good agreement with literature values.¹⁶⁵

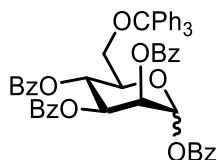
R_f 0.66 (Hex/EtOAc, 1/1);

1H NMR (400 MHz, $CDCl_3$) δ_H 7.36 (5H, s, Ar-*H*), 5.45 (1H, dd, $J = 9.5, 3.0$ Hz, H_3), 5.41 (1H, appt, $J = 9.1$ Hz, H_4), 5.31 (1H, brs, H_1), 5.24 (1H, s, H_2), 5.17 (1H, s, CH_2Ph), 5.11 (1H, s, CH_2Ph), 4.62 (1H, d, $J = 9.0$ Hz, H_5). 2.14 (3H, s, $C(O)CH_3$), 1.97 (3H, s, $C(O)CH_3$), 1.78 (3H, s, $C(O)CH_3$);

^{13}C NMR (100 MHz, $CDCl_3$) δ_C 170.3 (C=O, uronate), 169.8 (C=O), 168.3 (C=O), 162.9 (C=O), 128.7 (Ar-C), 128.6 (Ar-C), 92.1 (C_1), 69.9 (C_2), 69.4 (C_5), 68.5 (C_3), 67.7 (OCH_2Ph), 67.2 (C_4), 20.9 ($C(O)CH_3$), 20.6 ($C(O)CH_3$), 20.4 ($C(O)CH_3$).

6.4.3 α -D-mannopyranuronic acid derivatives: benzoyl protected uronate series

1,2,3,4-Tetra-O-benzoyl-6-O-trityl- α/β -D-mannopyranose **78**



D-mannose **64** (1.5 g, 8.3 mmol, 1.0 equiv.) and TrCl (2.39 g, 8.58 mmol, 1.03 equiv.) were suspended in pyridine (12 mL) and stirred at 50 °C for 3 h. The solution was cooled to 0 °C, then BzCl (4.85 mL, 41.7 mmol, 5.0 equiv.) was added *via* a dropping funnel over 30 min before being warmed to RT then to 50 °C to aid solubility. After stirring for 18 h, the reaction mixture was poured onto H₂O/ice (75 mL), extracted with EtOAc (100 mL), washed with H₂O (3 × 75 mL), dried (MgSO₄), filtered and concentrated *in vacuo*. Purification by Reveleris® automated silica gel column chromatography, eluting in Pet. Ether/EtOAc (4/1, 3/1) afforded **78** (5.8:1 α/β mixture) as a yellow oil (6.47 g, 7.71 mmol, 93%).

R_f 0.31 (Hex/EtOAc, 3/1);

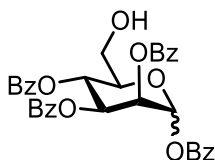
¹H NMR (400 MHz, CDCl₃) δ _H α -anomer 8.26-8.08 (10H, m, Ar-H), 7.99-7.85 (6H, m, Ar-H), 7.76 (3H, d, *J* = 8.4, 2.5 Hz, Ar-H), 7.70-7.62 (4H, m, Ar-H), 7.59-7.04 (17H, m, Ar-H), 6.70 (1H, d, *J* = 1.4 Hz, H₁), 6.37 (1H, appt, *J* = 10.1 Hz, H₄), 4.64-4.48 (1H, m, H₂), 4.30 (1H, dd, *J* = 10.1, 2.7 Hz, H₃), 3.56-3.50 (2H, m, H₆, H_{6'}), 3.20 (1H, dd, *J* = 10.7, 3.5 Hz, H₅);

¹³C NMR (100 MHz, CDCl₃) δ _C α -anomer 165.9 (C=O), 165.5 (C=O), 165.0 (C=O), 164.0 (C=O), 143.7 (2C, Ar-C), 134.0 (Ar-C), 133.8 (Ar-C), 133.4 (Ar-C), 133.2 (Ar-C), 130.2 (Ar-C), 130.0 (Ar-C), 129.8 (Ar-C), 129.1 (Ar-C), 128.9 (2C, Ar-C), 128.8

(2C, Ar-C), 128.7 (Ar-C), 128.5 (Ar-C), 128.3 (Ar-C), 128.1 (Ar-C), 127.8 (Ar-C), 127.4 (Ar-C), 127.0 (Ar-C), 91.8 (C₁), 72.3 (C₃), 67.1 (C₂), 66.2 (C₄), 63.2 (C₆), 61.6 (C₅);

HRMS m/z (ES⁺) [Found: (M+Na)⁺ 861.2697 C₅₃H₄₂O₁₀ requires M+Na⁺, 861.2676].

1,2,3,4-Tetra-O-benzoyl- α/β -D-mannopyranose **79**



To a solution of **78** (2.0 g, 2.4 mmol, 1.0 equiv.) in DCM: MeOH (1:1, 7 mL each) was added *p*-TsOH monohydrate (0.49 g, 0.52 mmol, 1.0 equiv.). After stirring at RT for 18 h, the reaction mixture was quenched with Et₃N until pH = 7 then concentrated *in vacuo*. Purification by silica gel column chromatography, eluting in Pet. Ether/EtOAc (4/1, 3/1, 2/1, 1/1) afforded **79** (4:1 α/β mixture) as a colourless oil (0.82 g, 1.5 mmol, 61%).

R_f 0.01 (Pet. Ether/EtOAc, 2/1);

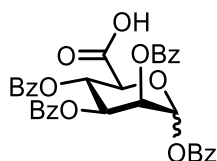
¹H NMR (400 MHz, CDCl₃) δ _H α -anomer 8.22-8.08 (6H, m, Ar-*H*), 8.02-7.90 (3H, m, Ar-*H*), 7.88-7.82 (2H, m, Ar-*H*), 7.71-7.31 (16H, m, Ar-*H*), 6.62 (1H, d, *J* = 2.1 Hz, H₁), 6.12 (1H, dd, *J* = 10.2, 3.4 Hz, H₃), 6.01 (1H, appt, *J* = 10.2 Hz, H₄), 5.88 (1H, dd, *J* = 3.3, 2.1 Hz, H₂), 4.24 (1H, ddd, *J* = 10.0, 3.6, 2.3 Hz, H₅), 3.85 (1H, dd, *J* = 12.9, 2.2 Hz, H₆'), 3.80 (1H, dd, *J* = 12.9, 3.9 Hz, H₆);

¹³C NMR (100 MHz, CDCl₃) δ _C α -anomer 166.3 (C=O), 165.8 (C=O), 165.4 (C=O), 164.1 (C=O), 134.2 (Ar-C), 133.9 (Ar-C), 133.7 (Ar-C), 133.6 (Ar-C), 130.3 (Ar-C),

130.2 (Ar-C), 130.1 (Ar-C), 129.9 (Ar-C), 128.9 (2C, Ar-C), 128.7 (2C, Ar-C), 128.6 (Ar-C), 128.5 (Ar-C), 91.5 (C₁), 73.5 (C₅), 69.7 (C₂ or C₃), 69.6 (C₂ or C₃), 66.6 (C₄), 61.3 (C₆);

HRMS *m/z* (ES⁺) [Found: (M+NH₄)⁺ 614.2032 C₃₄H₂₈O₁₀NH₄ requires M+NH₄⁺, 614.2065].

1,2,3,4-Tetra-O-benzoyl- α/β -D-mannopyranosiduronic acid **80**



To a vigorously stirred solution of **79** (240 mg, 0.4 mmol, 1.0 equiv.) in DCM/H₂O (2:1, 4.2 mL) was added successively TEMPO (13 mg, 80 μ mol, 0.2 equiv.) and BAIB (322 mg, 1.0 mmol, 2.5 equiv.). After 5 h, the reaction mixture was quenched with 10% aqueous Na₂S₃O₃ solution (10 mL) and the organic layer was separated. The aqueous layer was acidified to pH 2 through the addition of 1M HCl, then extracted with EtOAc (50 mL), dried (MgSO₄), filtered and concentrated *in vacuo*. The two organic layers were combined for purification by silica gel column chromatography, eluting in Pet. Ether/EtOAc with 2% v/v AcOH, affording **80** (3:1 α/β mixture) as a colourless oil (100 mg, 0.16 mmol, 41%).

R_f 0.10 (Pet. Ether/EtOAc, 1/2 with 2% v/v AcOH);

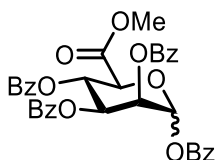
¹H NMR (400 MHz, CDCl₃) δ _H 8.12-8.06 (2H, m, Ar-H), 8.05-7.99 (2H, m, Ar-H), 7.92-7.88 (2H, m, Ar-H), 7.55 (2H, td, *J* = 7.4, 3.3 Hz, Ar-H), 7.49-7.37 (6H, m, Ar-H), 7.26 (4H, ddd, *J* = 9.7, 7.1, 5.0 Hz, Ar-H), 7.16 (2H, dd, *J* = 5.0, 4.4 Hz, Ar-H),

6.60 (1H, d, $J = 2.0$ Hz, H₁), 5.86 (1H, dd, $J = 9.3, 3.3$ Hz, H₃), 5.80-5.76 (1H, m, H₂), 4.60 (1H, appt, $J = 9.3$ Hz, H₄), 4.53 (1H, d, $J = 9.4$ Hz, H₅);

¹³C NMR (100 MHz, CDCl₃) δ_c 171.8 (C=O, uronic acid), 166.1 (2C, 2 × C=O), 165.3 (C=O), 164.2 (C=O), 137.9 (Ar-C), 134.3 (Ar-C), 133.8 (Ar-C), 133.6 (Ar-C), 130.2 (Ar-C), 130.0 (Ar-C), 129.9 (Ar-C), 129.1 (Ar-C), 129.0 (Ar-C), 128.8 (2C, Ar-C), 128.7 (Ar-C), 128.5, (Ar-C), 128.4 (Ar-C), 128.3 (Ar-C), 128.2 (Ar-C), 125.3 (Ar-C), 91.1 (C₁), 72.9 (C₅), 70.9 (C₃), 68.9 (C₂), 67.0 (C₄);

HRMS m/z (ES⁻) [Found: (M-H)⁻ 609.1405 C₃₄H₂₆O₁₁ requires $M-H^-$, 609.1402].

Methyl 1,2,3,4-tetra-O-benzoyl- α/β -D-mannopyranosyluronate **81**



To a solution of **80** (0.22 g, 0.36 mmol, 1.0 equiv.) in DMF (3.6 mL) was added MeI (53 μ L, 0.86 mmol, 2.4 equiv.) and K₂CO₃ (77 mg, 0.54 mmol, 1.5 equiv.). After 12 h, the reaction mixture was quenched with MeOH (3 mL) then extracted with EtOAc (50 mL), washed with H₂O (2 × 30 mL) and brine (30 mL). The organic layer was dried (MgSO₄), filtered and concentrated *in vacuo*. Purification by silica gel column chromatography, eluting in Pet. Ether/EtOAc (4/1) afforded **81** (6:1 α/β mixture) as a colourless oil (95 mg, 0.15 mmol, 42%).

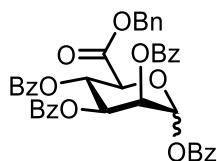
R_f 0.72 (Pet. Ether/EtOAc, 1/1);

¹H NMR (400 MHz, CDCl₃) δ_H 8.19-8.15 (2H, m, Ar-H), 8.09 (2H, dd, $J = 6.4, 2.1$ Hz), 8.05-8.01 (2H, m, Ar-H), 7.92-7.88 (2H, m, Ar-H), 7.68-7.32 (12H, m, Ar-H),

6.81 (1H, d, $J = 3.4$ Hz, H₁), 6.10-6.02 (2H, m, H₃, H₄), 5.89 (1H, dd, $J = 6.5, 3.4$ Hz, H₂), 4.79 (1H, d $J = 7.7$ Hz, H₅), 3.68 (3H, s, C(O)OCH₃);

¹³C NMR (100 MHz, CDCl₃) δ_c 167.9 (C=O, uronate), 166.0 (C=O), 65.8 (C=O), 165.72 (C=O), 164.24 (C=O), 134.6 (Ar-C), 134.2 (Ar-C), 134.1 (2C, Ar-C), 130.7 (Ar-C), 130.5 (Ar-C), 130.3 (2C, Ar-C), 129.2 (Ar-C), 129.1 (2C, Ar-C), 129.0 (2C, Ar-C), 128.9 (Ar-C), 91.1 (C₁), 72.6 (C₅), 69.5 (C₃ or C₄), 69.2 (C₃ or C₄), 68.2 (C₂), 53.4 (C(O)OCH₃).

Benzyl 1,2,3,4-tetra-O-benzoyl- α/β -D-mannopyranosyluronate **82**



To a solution of **80** (0.33 g, 0.54 mmol, 1.0 equiv.) in DMF (5.4 mL) was added BnBr (0.32 mL, 1.3 mmol, 2.4 equiv.) and K₂CO₃ (0.11 g, 0.81 mmol, 1.5 equiv.). After 18 h, the solvent was removed *in vacuo* and the resultant residue extracted with EtOAc (50 mL), washed with H₂O (2 × 30 mL) and brine (30 mL). The organic layer was dried (MgSO₄), filtered and concentrated *in vacuo*. Purification by silica gel column chromatography, eluting in Pet. Ether/EtOAc (4/1) afforded **82** (3:1 α/β mixture) as a white solid (0.19 g, 0.27 mmol, 50%).

R_f 0.82 (Pet. Ether/EtOAc, 1/1);

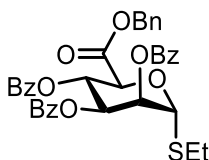
¹H NMR (400 MHz, CDCl₃) δ_H 8.18-8.06 (5H, m, Ar-H), 7.96-7.84 (6H, m, Ar-H), 7.57-7.43 (5H, m, Ar-H), 7.40-7.28 (5H, m, Ar-H), 7.24-7.11 (4H, m, Ar-H), 6.79 (1H, d, $J = 2.9$ Hz, H₁), 6.10 (1H, appt, $J = 8.0$ Hz, H₄), 6.05 (1H, dd, $J = 3.3, 1.2$ Hz, H₃),

5.89 (1H, appt, $J = 3.0$ Hz, H₂), 5.20 (1H, d, $J = 12.1$ Hz, CH₂Ph), 4.97 (1H, d, $J = 12.1$ Hz, CH₂Ph), 4.81 (1H, d, $J = 8.1$ Hz, H₅);

¹³C NMR (100 MHz, CDCl₃) δ_c 167.1 (C=O, uronate), 165.5 (C=O), 165.4 (C=O), 165.3 (C=O), 163.9 (C=O), 134.5 (Ar-C), 134.2 (Ar-C), 133.9 (Ar-C), 133.7 (Ar-C), 130.3 (Ar-C), 130.2 (Ar-C), 130.1 (Ar-C), 130.0 (Ar-C), 128.9 (Ar-C), 128.8 (Ar-C), 128.7 (Ar-C), 128.56 (Ar-C), 90.9 (C₁), 72.4 (C₅), 69.3 (C₂, C₃ or C₄), 68.9 (C₂, C₃ or C₄), 68.2 (CH₂Ph), 67.8 (C₂, C₃ or C₄);

HRMS m/z (ESI⁺) [Found: (M+Na)⁺ 723.1843 C₄₁H₃₂O₁₁ requires M+Na⁺, 723.1843].

Benzyl ethyl 2,3,4-tri-O-benzoyl- α -D-1-thio-mannopyranosyluronate **85**



To a solution of **82** (1.19 g, 1.52 mmol, 1.0 equiv.) in DCE (15.2 mL) at RT was added dropwise EtSH (0.18 mL, 2.6 mmol, 1.7 equiv.) and BF₃•Oet₂ (0.38 mL, 3.0 mmol, 2.0 equiv.). The reaction mixture was heated to 50 °C for 24 h, then the reaction mixture was cooled to RT and quenched with saturated aqueous NaHCO₃ solution (15 mL) and diluted with DCM (100 mL). The organic layer was washed with saturated aqueous NaHCO₃ solution (50 mL), H₂O (75 mL), brine (75 mL) then dried (MgSO₄), filtered and concentrated *in vacuo*. Purification by silica gel column chromatography, eluting with Pet. Ether/EtOAc (6/1) afforded **85** as a yellow oil (0.40 g, 0.62 mmol, 41%).

R_f 0.82 (Pet. Ether/EtOAc, 2/1);

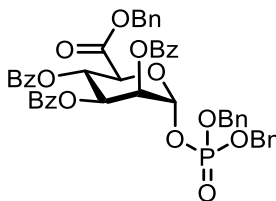
$[\alpha]_D^{26} -17.5$ ($c = 0.25$, CHCl_3);

$^1\text{H NMR}$ (400 MHz, CDCl_3) δ_{H} 8.18-8.04 (3H, m, Ar-H), 7.98-7.92 (2H, m, Ar-H), 7.90-7.80 (2H, m, Ar-H), 7.68-7.41 (8H, m, Ar-H), 7.40-7.27 (5H, m, Ar-H), 7.24-7.09 (5H, m, Ar-H), 6.03 (1H, appt, $J = 8.8$ Hz, H₄), 5.82 (1H, dd, $J = 8.8, 3.3$ Hz, H₃), 5.77 (1H, appt, $J = 3.3$ Hz, H₂), 5.71 (1H, d, $J = 2.6$ Hz, H₁), 5.21 (1H, d, $J = 12.2$ Hz, CH₂Ph), 5.04 (1H, d, $J = 8.3$ Hz, H₅), 4.96 (1H, 12.2 Hz, CH₂Ph), 2.78 (2H, q, $J = 8.0$ Hz, -SCH₂CH₃), 1.36 (3H, t, $J = 8.0$ Hz, -SCH₂CH₃);

$^{13}\text{C NMR}$ (100 MHz, CDCl_3) δ_{C} 167.9 (C=O, uronate), 165.6 (C=O), 165.4 (C=O), 165.3 (C=O), 136.2 (Ar-C), 134.6, 134.3 (Ar-C), 134.0 (Ar-C), 133.9 (Ar-C), 133.7 (Ar-C), 133.6 (Ar-C), 130.4 (Ar-C), 130.3 (Ar-C), 130.1 (Ar-C), 130.0 (Ar-C), 129.9 (Ar-C), 129.3 (Ar-C), 129.0 (2C, Ar-C), 128.9 (Ar-C), 128.7 (Ar-C), 128.6 (2C, Ar-C), 128.5 (2C, Ar-C), 81.9 (C₁), 71.0 (C₂), 69.8 (C₅), 68.5 (C₃), 68.4 (C₄), 67.9 (CH₂Ph), 25.7 (-SCH₂CH₃), 15.0 (-SCH₂CH₃);

HRMS m/z (ESI⁺) [Found: (M+Na)⁺ 663.1628 C₃₆H₃₂O₉S requires M+Na⁺, 663.1665].

Tri-O-benzyl 2,3,4-tri-O-benzoyl- α -D-mannopyranosyluronate phosphate **86**



Prepared as per Procedure A using thioglycoside **85** (90 mg, 0.14 mmol, 1.0 equiv.), DBP (67 mg, 0.24 mmol, 1.7 equiv.), NIS (47 mg, 0.21 mmol, 1.5 equiv.) and AgOTf

(11 mg, 42 μ mol, 0.3 equiv.). Reaction time: 1.5 h. Purification by silica gel column chromatography, eluting with Pet. Ether/EtOAc (4/1, 3/1) afforded **86** as a colourless oil (35 mg, 41 μ mol, 29%).

R_f 0.51 (Pet. Ether/EtOAc, 2/1);

$[\alpha]_D^{26} -76.7$ ($c = 1.25$, CHCl₃);

¹H NMR (400 MHz, CDCl₃) δ_H 8.12 (7H, m, Ar-H), 7.65-7.28 (21H, m, Ar-H), 7.21-7.06 (4H, m, Ar-H), 6.02 (1H, dd, $J_{H1-P} = 7.3$ Hz, $J_{H1-H2} = 3.1$ Hz, H₁), 5.97 (1H, appt, $J = 9.4$ Hz, H₄), 5.87 (1H, dd, $J = 9.4, 2.7$ Hz, H₃), 5.66 (1H, appt, $J = 2.7$ Hz, H₂), 5.16-5.09 (5H, m, CH₂Ph), 4.96 (1H, d, $J = 12.1$ Hz, CH₂Ph), 4.74 (1H, d, $J = 9.4$ Hz, H₅);

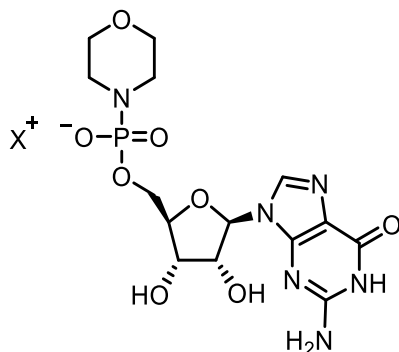
¹³C NMR (100 MHz, CDCl₃) δ_C 170.0 (C=O, uronate), 165.3 (C=O), 165.2 (2 \times C=O), 135.5 (Ar-C), 135.4 (2C, Ar-C), 135.3 (Ar-C), 134.5 (Ar-C), 133.9 (Ar-C), 133.6 (2C, Ar-C), 130.2 (Ar-C), 130.0 (Ar-C), 129.9 (2C, Ar-C), 128.9 (2C, Ar-C), 128.8 (2C, Ar-C), 128.6 (Ar-C), 128.5 (2C, Ar-C), 128.4 (Ar-C), 128.3 (Ar-C), 95.0 (C₁), 71.4 (C₅), 70.3 (CH₂Ph), 69.4 (C₂), 68.7 (C₃), 68.1 (2C, CH₂Ph), 67.4 (C₄);

³¹P NMR (161 MHz, CDCl₃) $\delta_P -3.1$ (1P, d, $J_{H1-P} = 7.3$ Hz);

HRMS m/z (ES⁺) [Found: (M+NH₄)⁺ 874.2625 C₄₈H₄₁O₁₃P requires M+NH₄⁺, 874.2623].

6.4.4 Synthesis of guanosine diphosphate-mannuronic acid (GDP-ManA)

Guanosine-5'-phosphoromorpholidate **87**



Method 1 (Khorana): Dowex[®] 50W-X8 resin (H⁺ form, 17 × 700 mm column) was exchanged to its morpholine form by passing a 10% aqueous morpholine solution through the column (200 mL). Exchange was indicated through a basic pH of the eluate (pH 10.87). Guanosine 5'-monophosphate disodium salt **88** (407 mg, 1.0 mmol, 1.0 equiv.) in H₂O (50 mL) was applied to the column and eluates containing sodium morpholine-GMP were concentrated *in vacuo* to a final volume of 10 mL. Morpholine (210 μL, 2.4 mmol, 2.4 equiv.) and *t*BuOH (10 mL) were added and the solution was heated to 100 °C at reflux, whilst a solution of DCC (825 mg, 4.0 mmol, 4.0 equiv.) in *t*-BuOH (15 mL) was added dropwise over 2 h. The solution was heated at reflux for a further 3 h, where TLC analysis) showed two spots ($R_f = 0.52 + 0.93$), and the R_f value of **87** is reported as 0.45.¹¹³ The yellow solution cooled to RT and was left for 72 h whereupon a white crystalline by-product (dicyclohexylurea) had formed. The suspension was filtered and concentrated *in vacuo* to half its original volume and extracted with Et₂O (2 × 20 mL). The combined organic layers were washed with H₂O (120 mL) and the aqueous phase was purified by Sephadex[®] G-25 column chromatography, eluting with a linear gradient of TEAB (0.005 → 0.5 M).

Fractions containing **87** were visualised, collected and concentrated *in vacuo*. The residue was dissolved in MeOH (10 mL), 4-morpholine-*N,N'*-dicyclohexylcarboxamidine (600 mg, 2.0 mmol, 2.0 equiv.) was added then the solution concentrated *in vacuo*. The residue was dissolved in MeOH (5 mL) and Et₂O (25 mL) was added to form a white precipitate. The liquid was decanted and the precipitate was washed with Et₂O (2 × 10 mL), re-dissolved in H₂O and lyophilized to afford guanosine 5'-phosphormorpholidate (*N,N'*-dicyclohexylcarboamidinium salt) **87** as a white solid (198 mg, 0.27 mmol, 27%). R_f 0.52 (IPA/NH₄OH/H₂O, 7/1/2); ³¹P (161 MHz, D₂O) δ_P – 7.4 (1P, s).

Method B (Mukaiyama): Sodium morpholine-GMP was prepared as per the above procedure. To a solution of morpholine-GMP in DMSO (10 mL) was added morpholine (0.58 mL, 6.6 mmol, 5.4 equiv.) to form an opaque white solution. After stirring for 5 min at RT, dipyriddy disulphide (0.89 g, 4.1 mmol, 3.3 equiv.) was added slowly to the solution followed by Ph₃P (1.06 g, 4.1 mmol, 3.3 equiv.). The resultant bright yellow solution was stirred for 4 h at RT and a solution of NaI (0.1 M in acetone) was then added until a precipitate formed. This was collected by filtration, dissolved in H₂O and purified by Sephadex[®] G-25 column chromatography, eluting with a gradient of TEAB (0.005 → 0.5 M). Fractions containing **87** were visualised, collected and concentrated *in vacuo*. Repeated lyophilisation afforded guanosine 5'-phosphormorpholidate (sodium salt) **87** as a white solid (161 mg, 0.37 mmol, 30%).

R_f 0.52 (IPA/NH₄OH/H₂O, 7/1/2);

[α]_D²⁶ –16.0 (c = 0.50, H₂O);

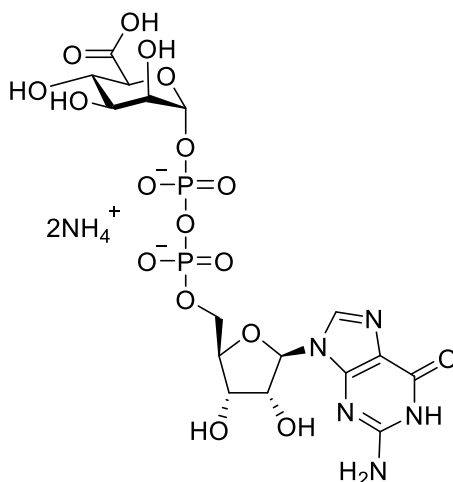
^1H NMR (400 MHz, D_2O) δ_{H} 7.93 (1H, s, H_8), 5.79 (1H, d, $J = 5.0$ Hz, $\text{H}_{1'}$), 4.67 (1H, t, $J = 5.1$ Hz, $\text{H}_{2'}$), , 4.41 (1H, t, $J = 4.8$ Hz, $\text{H}_{3'}$), 4.20 (1H, brs, $\text{H}_{4'}$), 3.95-3.88 (2H, m, $\text{H}_{5'a}$, $\text{H}_{5'b}$), 3.47 (4H, t, $J = 4.5$ Hz, CH_2 morpholine), 2.85-2.82 (4H, m, CH_2 morpholine);

$^{13}\text{C}\{^{31}\text{P}\}$ NMR (101 MHz, D_2O) δ_{C} 159.5 (guanine C), 154.5 (guanine C), 151.68 (guanine C), 137.25 (C_8), 116.4 (guanine C), 87.3 ($\text{C}_{1'}$), 83.7 ($\text{C}_{4'}$), 83.7 ($\text{C}_{1'}$), 73.7 ($\text{C}_{2'}$), 70.4 ($\text{C}_{3'}$), 66.9 (CH_2 morpholine), 64.1 ($\text{C}_{5'}$), 44.7 (CH_2 morpholine);

$^{31}\text{P}\{^1\text{H}\}$ (161 MHz, D_2O) δ_{P} -7.5 (1P, s);

HRMS m/z (ES^-) [Found: $(\text{M}-\text{H})^-$ 431.1080 $\text{C}_{14}\text{H}_{21}\text{N}_6\text{O}_8\text{P}$ requires $\text{M}-\text{H}^-$, 431.1079].

Guanosine diphosphate-mannuronic acid (*bis*-ammonium salt) **4**



Chemical Synthesis: Prepared as per Procedure E using **59** (22 mg, 53 μmol , 1.0 equiv.), GMP-morpholidate **97** (36 mg, 84 μmol , 1.5 equiv.) and DCI (6 mg, 53 μmol , 1.0 equiv.) in pyridine (1 mL). Reaction time: 120 h. Deprotected as per Procedure F. Purification by C18 chromatography and strong-anion exchange chromatography as described in the general experimental details afforded **4** as a white solid (*bis*-

ammonium salt, 15 mg, 24 μmol , 46%). These data were in good agreement with literature values.¹⁰⁵

Enzymatic Synthesis: GDP-mannose **3** (1.6 mg, 2.5 μmol , 1.0 equiv.) and NAD^+ (3.5 mg, 5.25 μmol , 2.1 equiv.) were dissolved in buffer (0.9 mL, 200 mM sodium phosphate, pH 7.4, 1 mM DTT, 0.5 mM MgCl_2) and GMD (0.8 mg/mL) was added. Final reaction volume: 1 mL. The mixture was incubated at room temperature with gentle shaking. After 21 h, the enzymatic transformation was stopped by addition of MeOH (1 mL) and the mixture was vortexed and centrifuged (5000 RPM). The supernatant was filtered through a syringe disc filter (0.45 μm , PTFE) and purified by strong-anion exchange chromatography as described in as described in the general experimental details to afford **4** as a white solid (*bis*-ammonium salt, 1.17 mg, 1.9 μmol , 70%). These data were in good agreement with literature values.¹⁰⁵ R_f 0.19 (isopropyl alcohol/ NH_4OH /water, 6/3/1);

^1H NMR (400 MHz, D_2O) δ_{H} 7.96 (1H, s, $\text{H}_{8''}$), 5.79 (1H, d, $J = 6.1$ Hz, $\text{H}_{1'}$), 5.39 (1H, dd, $J_{\text{H}_{1'-\text{P}}} = 8.0$, $J_{\text{H}_{1'-\text{H}_2}} = 1.7$ Hz, H_1), 4.64 (1H, hidden, $\text{H}_{2'}$), 4.35 (1H, dd, $J = 4.8$, 3.3 Hz, $\text{H}_{3'}$), 4.34-4.29 (1H, m, $\text{H}_{4'}$), 4.18 (2H, dd, $J = 5.2$, 3.5 Hz, $\text{H}_{5'b}$), 3.95 (1H, d, $J = 10.0$ Hz, $\text{H}_{5'a}$), 3.88 (1H, dd, $J = 2.2$, 3.3 Hz, H_2), 3.78 (1H, dd, $J = 9.6$, 3.3 Hz, H_3), 3.64 (1H, t, $J = 9.7$ Hz, H_4);

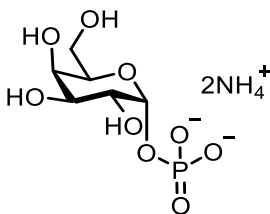
$^{31}\text{P}\{^1\text{H}\}$ NMR (101 MHz, D_2O) δ_{P} -11.2 (1P, s), -13.7 (1P, s);

HRMS m/z (ES^-) [Found: $(\text{M}-\text{H})^-$ 618.0484 $\text{C}_{16}\text{H}_{22}\text{N}_5\text{O}_{17}\text{P}_2$ requires $\text{M}-\text{H}^-$, 618.0491].

6.5 Experimental details for Chapter 3

6.5.1 Optimisation of MacDonald Phosphorylation

α -D-galactopyranosyl phosphate **94**



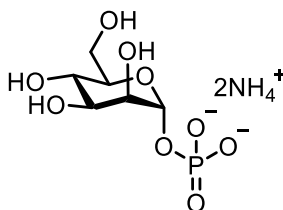
Prepared as per Procedure D using **93** (300 mg, 0.77 mmol, 1.0 equiv.) and H_3PO_4 (377 mg, 3.85 mmol, 5.0 equiv.) at 50 °C. Reaction time: 4 h. **94** was afforded as a white solid (152 mg, 0.52 mmol, 67%). These data were in good agreement with literature values.¹⁶⁶

^1H NMR (400 MHz, D_2O) δ_{H} 5.31 (1H, dd, $J_{\text{H1-P}} = 7.3$ Hz, $J_{\text{H1-H2}} = 3.6$ Hz, H₁), 4.01 (1H, dd, $J = 7.0, 4.9$ Hz, H₅), 3.82 (1H, d, $J = 2.7$ Hz, H₄), 3.74 (1H, dd, $J = 10.2, 3.4$ Hz, H₃), 3.57 (3H, m, H₂, H₆, H_{6'});

^{13}C NMR (101 MHz, D_2O) δ_{C} 94.1 (C₁), 71.0 (C₅), 69.6 (C₃), 69.0 (C₄), 68.7 (C₂), 61.4 (C₆);

^{31}P NMR (162 MHz, D_2O) δ_{P} 2.6 (1P, d, $J_{\text{H1-P}} = 7.3$ Hz).

α -D-mannopyranosyl phosphate **44**



Prepared as per Procedure D using **14** (250 mg, 0.64 mmol, 1.0 equiv.) and H₃PO₄ (313 mg, 3.20 mmol, 5.0 equiv.) at 45 °C. Reaction time: 4 h. **44** was afforded as a white solid (91 mg, 0.35 mmol, 55%). These data were in good agreement with literature values.⁹⁸

R_f 0.40 (MeCN/H₂O and 3 drops NH₄OH, 2/1);

[α]_D²⁶ +22.2 (*c* = 0.45, H₂O);

¹H (400 MHz, D₂O) δ _H 5.23 (1H, d, *J*_{H1-P} = 8.5 Hz, H₁), 3.87-3.74 (4H, m, H₂, H₃, H₅, H₆), 3.66-3.59 (1H, m, H₆') 3.50 (1H, appt, *J* = 9.6 Hz, H₄);

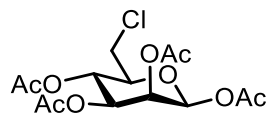
¹³C (100 MHz, D₂O) δ _C 95.0 (C₁), 73.0, 71.2 (C₂), 70.2, 67.2 (C₄), 61.3 (C₆);

³¹P (161 MHz, D₂O) δ _P 2.0 (1P, d, *J*_{H1-P} = 8.5 Hz);

HRMS *m/z* (ES⁻) [Found: (M-H)⁻ 259.0224 C₆H₁₁O₉ requires M-H⁻, 259.0231].

6.5.2 6-Chloro-6-deoxy- α -D-mannopyranose derivatives

1,2,3,4-Tetra-O-acetyl-6-chloro-6-deoxy- β -D-mannopyranose **96**



To a solution of **66** (0.50 g, 1.4 mmol, 1.0 equiv.) and Ph_3P (0.64 g, 2.5 mmol, 1.7 equiv.) in DCM (14 mL) was added dropwise CCl_4 (0.24 mL, 2.5 mmol, 1.7 equiv.). The reaction mixture was heated at 40 °C with stirring for 9 h, before being cooled to RT, poured onto H_2O (30 mL) and diluted with DCM (35 mL). The organic layer was washed with H_2O (2 \times 30 mL), brine (30 mL), dried (MgSO_4), filtered and concentrated *in vacuo*. Purification by silica gel column chromatography, eluting with Pet. ether/EtOAc (4/1, 3/1, 1/1) afforded **96** as a white foam (0.32 g, 0.82 mmol, 61%).

R_f 0.78 (Pet. ether/EtOAc, 1/1);

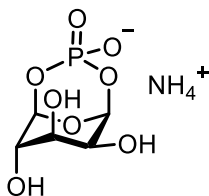
$[\alpha]_D^{26} -13.3$ ($c = 0.75$, CHCl_3);

^1H NMR (400 MHz, CDCl_3) δ_{H} 5.87 (1H, d, $J = 1.2$ Hz, H_1), 5.44 (1H, dd, $J = 3.3, 1.2$ Hz, H_2), 5.26 (1H, appt, $J = 9.8$ Hz, H_4), 5.12 (1H, dd, $J = 9.8, 3.3$ Hz, H_3), 3.84-3.78 (1H, m, H_5), 3.64 (1H, dd, $J = 12.2, 2.9$ Hz, H_6'), 3.57 (1H, dd, $J = 12.2, 5.8$ Hz, H_6), 2.16 (3H, s, C(O)CH_3), 2.07 (3H, s, C(O)CH_3), 2.04 (3H, s, C(O)CH_3), 1.96 (3H, s, C(O)CH_3);

^{13}C NMR (100 MHz, CDCl_3) δ_{C} 170.2 (C=O), 169.8 (C=O), 169.6 (C=O), 168.4 (C=O), 90.3 (C_1), 74.7 (C_5), 70.5 (C_3), 68.2 (C_2), 66.9 (C_4), 42.9 (C_6), 20.8 (C(O)CH_3), 20.7 (2C, C(O)CH_3), 20.6 (C(O)CH_3);

HRMS m/z (ESI⁺) [Found: (M+Na)⁺ 389.0633 C₁₄H₁₉ClO₉ requires M+Na⁺, 389.0616].

O¹,O⁶-Hydroxyphosphoryl-D-mannopyranose (*bis*-ammonium salt) **97**



Prepared as per Procedure D using **96** (150 mg, 0.41 mmol, 1.0 equiv.) and H₂PO₄ (200 mg, 2.1 mmol, 5.0 equiv.). Reaction time: 3 h. **97** was afforded as a white solid (15 mg, 71 μmol, 17%).

R_f 0.30 (MeCN/H₂O + 3 drops AcOH);

¹H NMR (400 MHz, D₂O) δ_H 5.29 (1H, appt, J_{H1-P} = 6.8 Hz, H₁), 4.39 (1H, s, H₅), 4.30 (1H, dd, J = 5.9, 2.4 Hz, H₄), 4.21 (2H, dd, J = 13.6, 8.5 Hz, H₃, H₆), 4.05 (1H, dd, J = 10.8, 2.5 Hz, H_{6'}), 3.85 (1H, d, J_{H2-P} = 6.5 Hz, H₂);

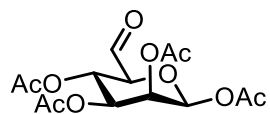
¹³C NMR (100 MHz, D₂O) δ_C 96.6 (d, J_{C1-P} = 3.2 Hz, C₁), 77.0 (C₃), 75.4 (C₅), 70.2 (d, J_{C2-P} = 4.4 Hz C₂), 70.1 (C₄), 69.0 (C₆);

³¹P{¹H} NMR (161 MHz, D₂O) δ_P 2.0 (1P, s);

HRMS m/z (ES⁻) [Found: (M-H)⁻ 241.0116 C₆H₁₀O₈P requires M-H⁻, 241.0119].

6.5.3 α -D-mannopyranosylurononitrile derivatives

1,2,3,4-Tetra-O-acetyl- β -D-manno-hexodialdo-1,5-pyranoside **103**



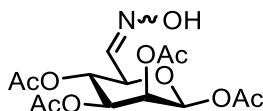
To a solution of **66** (1.5 g, 4.3 mmol, 1.0 equiv.) in DCM (16 mL) was added DMP (2.18 g, 5.2 mmol, 1.2 equiv.). After stirring for 6 h, the reaction mixture was diluted with DCM (50 mL) and washed with saturated aqueous $\text{Na}_2\text{S}_2\text{O}_3$ (50 mL), saturated aqueous NaHCO_3 solution (50 mL) and H_2O (50 mL). The organic layer was dried (MgSO_4), filtered and concentrated *in vacuo* to afford **103** as a white solid which was used without any further purification (1.25 g, 3.61 mmol, 84%).

R_f 0.37 (Hex/EtOAc, 1/3);

^1H NMR (400 MHz, CDCl_3) δ_{H} 9.64 (1H, s, CHO), 6.07 (1H, d, $J = 2.0$ Hz, H_1), 5.48 (1H, dd, $J = 3.3, 2.0$ Hz, H_2), 5.44 (1H, appt, $J = 8.0$ Hz, H_4), 5.20 (1H, dd, $J = 8.0$ Hz, 3.3 Hz, H_3), 4.07 (1H, d, $J = 8.0$ Hz, H_5), 2.17 (3H, s, C(O)CH_3), 2.14 (3H, s, C(O)CH_3), 2.10 (3H, s, C(O)CH_3), 2.03 (3H, s, C(O)CH_3);

^{13}C NMR (100 MHz, CDCl_3) δ_{C} 195.6 (CHO), 169.9 (C=O), 169.6 (C=O), 169.6 (C=O), 168.5 (C=O), 89.6 (C_1), 77.7 (C_5), 68.7 (C_3), 66.8 (C_4), 65.4 (C_2), 20.8 (C(O)CH_3), 20.7 (C(O)CH_3), 20.7 (C(O)CH_3), 20.6 (C(O)CH_3).

1,2,3,4-Tetra-O-acetyl- β -D-mannopyranosyl 6-oxime **104**



To a solution of **103** (0.50 g, 1.4 mmol, 1.0 equiv.) in THF (14 mL) was added dropwise a solution of $\text{NH}_2\text{OH}\cdot\text{HCl}$ (0.10 g, 1.4 mmol 1.0 equiv.) in H_2O (2.90 mL). After cooling to 0 °C, a solution of Na_2CO_3 (0.18 g, 1.7 mmol 1.2 equiv.) in H_2O (1.73 mL) was added dropwise at 0 °C before being slowly warmed to RT. After stirring for 18 h, the reaction mixture was poured onto H_2O (100 mL) and extracted EtOAc (3 \times 75 mL), dried (MgSO_4), filtered and concentrated *in vacuo*. Purification by silica gel column chromatography, eluting in Hex/EtOAc (1/2) afforded **104** as a colourless oil (0.26 g, 0.73 mmol, 51%).

R_f 0.74 (Hex/EtOAc, 1/2);

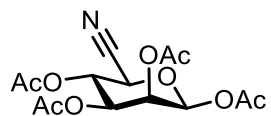
$[\alpha]_D^{26} -17.4$ ($c = 1.25$, CHCl_3);

^1H NMR (400 MHz, CDCl_3) δ_{H} 7.39 (1H, d, $J = 6.7$ Hz, $\text{HC}=\text{N}$), 5.93 (1H, d, $J = 1.2$ Hz, H_1), 5.51 (1H, dd, $J = 3.2, 1.2$ Hz, H_2), 5.33 (1H, d, $J = 9.9$ Hz, H_5), 5.19 (1H, dd, $J = 9.9, 3.2$ Hz, H_3), 4.20 (1H, appt, $J = 9.9$ Hz, H_4), 2.22 (3H, s, $\text{C}(\text{O})\text{CH}_3$), 2.11 (3H, s, $\text{C}(\text{O})\text{CH}_3$), 2.04 (3H, s, $\text{C}(\text{O})\text{CH}_3$), 2.02 (3H, s, $\text{C}(\text{O})\text{CH}_3$);

^{13}C NMR (101 MHz, CDCl_3) δ_{C} 170.4 (C=O), 169.9 (C=O), 169.8 (C=O) 168.3 (C=O), 146.4 (C=N), 90.2 (C_1), 73.1 (C_5), 70.1 (C_3), 68.1 (C_2), 66.6 (C_4), 20.7 (2C, $\text{C}(\text{O})\text{CH}_3$), 20.4 ($\text{C}(\text{O})\text{CH}_3$), 20.5 ($\text{C}(\text{O})\text{CH}_3$);

HRMS m/z (ES^+) [Found: $(M+NH_4)^+$ 379.1363 $C_{14}H_{19}NO_{10}$ requires $M+NH_4^+$, 379.1392].

1,2,3,4-Tetra-O-acetyl- β -D-mannopyranosylurononitrile **105**



To a solution of **104** (500 mg, 1.38 mmol, 1.0 equiv.) in MeCN (34 mL) was added $POCl_3$ (0.13 mL, 1.4 mmol, 1.0 equiv.). After 5 min the solution was heated to 65 °C and after stirring for 5 h, the reaction mixture was cooled to RT and quenched with saturated aqueous $NaHCO_3$ solution (20 mL). The reaction mixture was extracted with EtOAc (50 mL), washed with H_2O (2 \times 30 mL), dried ($MgSO_4$), filtered and concentrated *in vacuo*. Purification by silica gel column chromatography, eluting with Hex/EtOAc (1/1) afforded **105** as a colourless oil (170 mg, 0.51 mmol, 37%).

R_f 0.9 (Hex/EtOAc, 1/2);

$[\alpha]_D^{26}$ -49.6 ($c = 1.65$, $CHCl_3$);

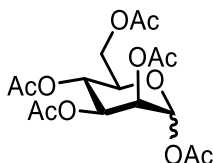
1H NMR (400 MHz, $CDCl_3$) δ_H 6.10 (1H, d, $J = 2.9$ Hz, H_1), 5.40 (1H, appt, $J = 3.1$ Hz, H_2), 5.34 (1H, appt, $J = 9.0$ Hz, H_4), 5.24 (1H, dd, $J = 6.3, 3.3$ Hz, H_3), 4.63 (1H, d, $J = 6.0$ Hz, H_5), 2.20 (3H, s, $C(O)CH_3$), 2.17 (3H, s, $C(O)CH_3$), 2.15 (6H, s, $C(O)CH_3$);

^{13}C NMR (101 MHz, $CDCl_3$) δ_C 169.7 (C=O), 169.6 (C=O), 168.9 (C=O), 168.8 (C=O), 114.7 (C \equiv N), 88.7 (C_1), 67.6 (C_4), 66.9 (C_3), 65.1 (C_2), 61.0 (C_5), 20.64 (2C, $C(O)CH_3$), 20.59 (2C, $C(O)CH_3$);

HRMS m/z (ES^+) [Found: $(M+NH_4)^+$ 361.1252 $C_{14}H_{17}NO_9$ requires $M+NH_4^+$, 361.1286];

ν_{max}/cm^{-1} 2240 ($C\equiv N$ stretching), 1748 ($C=O$ stretching), 1204 ($C-O$ stretching).

1,2,3,4,6-Penta-O-acetyl- α/β -D-mannopyranose **14**



D-mannose **64** (5.0 g, 28 mmol, 1.0 equiv.) was suspended in Ac_2O (27.0 mL, 290 mmol, 10.3 equiv.) and cooled to 0 °C before H_2SO_4 (2 drops) was added. The reaction mixture was warmed to RT over 1 h, before being diluted with H_2O /ice (100 mL) and extracted with EtOAc (100 mL). The organic layer was washed with saturated aqueous $NaHCO_3$ solution (2 \times 100 mL), H_2O (2 \times 100 mL) dried ($MgSO_4$), filtered and concentrated *in vacuo*. Repeated co-evaporation to remove residual AcOH afforded **14** (3.6:1 α/β) as a colourless oil (10.1 g, 26 mmol, 93%). These data were in good agreement with literature values.¹⁶⁷

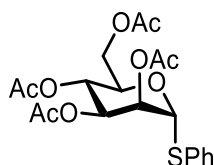
R_f 0.58 (Hex/EtOAc, 1/1);

1H NMR (400 MHz, $CDCl_3$) δ_H (α -anomer) 6.09 (1H, d, $J = 2.1$ Hz, H_1), 5.36-5.35 (2H, m, H_3, H_4), 5.27 (1H, d, $J = 2.1$ Hz, H_2), 4.34-4.27 (1H, m, H_6), 4.17-4.03 (2H, m, H_5, H_6'), 2.19 (3H, s, $C(O)CH_3$), 2.18 (3H, s, $C(O)CH_3$), 2.10 (3H, s, $C(O)CH_3$), 2.06 (3H, s, $C(O)CH_3$), 2.02 (3H, s, $C(O)CH_3$);

^{13}C NMR (100 MHz, CDCl_3) δ_{c} (α -anomer) 170.6 (C=O), 169.9 (C=O), 169.7 (C=O), 168.0 (C=O), 166.4 (C=O), 90.63 (C_1), 70.6 (C_5), 68.8 (C_3), 68.4 (C_2), 65.6 (C_4), 62.1 (C_6), 20.8 (C(O)CH₃), 20.7 (2C, C(O)CH₃), 20.6 (2C, C(O)CH₃);

HRMS m/z (ES⁺) [Found: (M+NH₄)⁺ 408.1496 C₁₆H₂₂O₁₁ requires M+NH₄⁺, 408.1500].

Phenyl 2,3,4,6-tetra-O-acetyl-1-thio- α -D-mannopyranose **15**



To a solution of **14** (5.0 g, 12 mmol, 1.0 equiv.) in DCM (10 mL) was added PhSH (1.96 mL, 19 mmol, 1.5 equiv.) and $\text{BF}_3 \cdot \text{OEt}_2$ (7.58 mL, 61 mmol, 4.8 equiv.) dropwise. After 48 h, the reaction mixture was diluted with DCM (20 mL), washed with saturated aqueous NaHCO_3 solution (3 \times 30 mL), 5% aqueous NaOH solution (3 \times 30 mL), H_2O (3 \times 30 mL) and brine (30 mL). The organic layer was dried (MgSO_4), filtered and concentrated *in vacuo*. Recrystallisation from the minimum amount of absolute EtOH afforded **15** as a yellow solid (3.66 g, 8.3 mmol, 65%). These data were in good agreement with literature values.¹⁶⁷

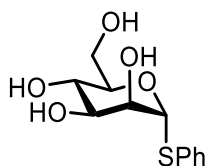
R_f 0.73 (Hex/EtOAc, 1/1);

^1H NMR (400 MHz, CDCl_3) δ_{H} 7.50-7.48 (2H, m, Ar-H), 7.35-7.30 (3H, m, Ar-H), 5.51-5.50 (2H, m, H₁, H₃), 5.34-5.33 (2H, m, H₂, H₄), 4.58-4.52 (1H, m, H₅), 4.31 (1H, dd, J = 12.2, 5.9 Hz, H₆), 4.11 (1H, dd, J = 12.2, 2.4 Hz, H_{6'}), 2.16 (3H, s, C(O)CH₃), 2.08 (3H, s, C(O)CH₃), 2.05 (3H, s, C(O)CH₃), 2.02 (3H, s, C(O)CH₃);

^{13}C NMR (100 MHz, CDCl_3) δ_{C} 170.5 (C=O), 169.9 (C=O), 169.8 (C=O), 169.7 (C=O), 134.5 (Ar-C), 132.7 (Ar-C), 132.1 (Ar-C), 129.2 (Ar-C), 128.1 (Ar-C), 85.7 (C_1), 70.9 (C_3), 69.6 (C_5), 69.4 (C_2), 66.4 (C_4), 62.5 (C_6), 20.8 ($\text{C}(\text{O})\text{CH}_3$), 20.7 ($\text{C}(\text{O})\text{CH}_3$), 20.6 ($\text{C}(\text{O})\text{CH}_3$).

HRMS m/z (ES^+) [Found: ($\text{M}+\text{NH}_4$) $^+$ 458.1475 $\text{C}_{20}\text{H}_{24}\text{O}_9\text{S}$ requires $\text{M}+\text{NH}_4^+$, 458.1479].

Phenyl 1-thio- α -D-mannopyranoside **109**



To a solution of **15** (1.0 g, 2.3 mmol, 1.0 equiv.) in MeOH (10 mL) was added dropwise a solution of NaOMe in MeOH (1M, 2 mL total). After stirring for 2 h, the reaction mixture was neutralised through addition of AmberliteTM 120 ion-exchange resin (H^+ form) pH = 7, filtered and concentrated *in vacuo*. Drying over P_2O_5 in a vacuum desiccator afforded **109** as a white foam which was used without any further purification (0.54 g, 2.0 mmol, 87%). These data were in good agreement with literature values.¹⁶⁸

R_f 0.05 (Hex/EtOAc, 1/2);

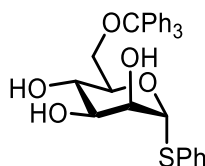
^1H NMR (400 MHz, $\text{DMSO-}d_6$) δ_{H} 7.52-7.48 (2H, m, Ar-H), 7.35-7.24 (3H, m, Ar-H), 5.34 (1H, d, J = 1.4 Hz, H_1), 5.14 (1H, d, J = 4.2 Hz, $\text{C}_2\text{-OH}$), 4.89 (1H, d, J = 5.4 Hz, $\text{C}_3\text{-OH}$), 4.80 (1H, d, J = 5.4 Hz, $\text{C}_4\text{-OH}$), 4.52 (1H, d, J = 6.0 Hz, $\text{C}_6\text{-OH}$) 3.90-3.87

(1H, m, H₂), 3.76 (1H, dd, *J* = 10.8, 4.2 Hz, H₅), 3.66 (1H, ddd, *J* = 11.8, 5.7, 2.1 Hz, H_{6'}), 3.55-3.43 (3H, m, H₃, H₄, H₆);

¹³C NMR (100 MHz, DMSO-*d*₆) δ_c 135.4 (Ar-C), 131.5 (Ar-C), 129.5 (Ar-C), 127.5 (Ar-C), 89.4 (C₁), 75.9 (C₅), 72.4 (C₂), 72.0 (C₃), 67.5 (C₄), 61.4 (C₆).

HRMS *m/z* (ES⁺) [Found: (M+NH₄)⁺ 290.1061 C₁₂H₁₆O₅S requires M+NH₄⁺, 290.1062].

Phenyl 6-O-trityl mannopyranoside **110**



To a solution of **109** (13.5 g, 49 mmol, 1.0 equiv.) in pyridine (245 mL) was added TrCl (15.0 g, 53 mmol, 1.1 equiv.). The reaction mixture was heated to 50 °C and stirred for 18 h, before the reaction mixture was cooled to RT then concentrated *in vacuo*. The resultant orange oil was co-evaporated with toluene (2 × 30 mL) then purified by Reveleris® automated silica gel flash column chromatography, eluting with Pet. ether/EtOAc (8/2) to afford **110** as a yellow oil (20.0 g, 39 mmol, 79%). These data were in good agreement with literature values.¹¹⁸

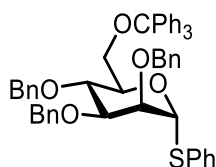
R_f 0.4 (Pet. Ether/EtOAc, 1/1);

¹H NMR (400 MHz, MeOD-*d*₄) δ_H 7.71-7.67 (2H, m, Ar-*H*), 7.48-7.42 (5H, m, Ar-*H*), 7.29-7.18 (13H, m, Ar-*H*), 5.54 (1H, d, *J* = 1.2 Hz, H₁), 4.39-4.33 (1H, m, H₅), 4.12-4.02 (1H, m, H₂), 3.68 (1H, dd, *J* = 9.3, 3.3 Hz, H₃), 3.56 (1H, appt, *J* = 9.6 Hz, H₄), 3.51 (1H, dd, *J* = 9.9, 1.7 Hz, H_{6'}), 3.36-3.29 (1H, m, H₆);

^{13}C NMR (100 MHz, MeOD- d_4) δ_{c} 145.5 (Ar-C), 136.2 (Ar-C), 132.6 (Ar-C), 130.1 (Ar-C), 130.0 (Ar-C), 128.7 (Ar-C), 128.3 (Ar-C), 128.0 (Ar-C), 89.9 (C₁), 74.8 (C₅), 73.5 (C₂), 73.4 (C₃), 69.4 (C₄), 65.4 (C₆);

HRMS m/z (ESI⁺) [Found: (M+Na)⁺ 537.1733 C₃₁H₃₀O₅S requires M+Na⁺, 537.1712].

Phenyl 2,3,4-tri-O-benzyl-6-O-trityl mannopyranoside **111**



NaH (60% in mineral oil, 3.74 g, 156 mmol, 6.0 equiv.) was washed with hexane (3 × 10 mL), decanted, dried under high vacuum for 10 min and dissolved in DMF (35 mL). To this solution was added dropwise at 0 °C a solution of **110** (13.5 g, 26 mmol, 1.0 equiv.) in DMF (135 mL) over 30 min. The reaction mixture was stirred for 30 min before BnBr (15.44 mL, 130 mmol, 5.0 equiv.) was added dropwise at 0 °C before warming to RT. After stirring for 18 h, the reaction mixture was quenched with MeOH (40 mL) then concentrated *in vacuo*. Purification by Reveleris® automated silica gel flash column chromatography, eluting with Pet. ether/EtOAc (8/2) afforded **111** as a yellow oil (14.2 g, 23 mmol, 89%). These data were in good agreement with literature values.¹¹⁸

R_f 0.79 (Pet. ether/EtOAc, 3/1);

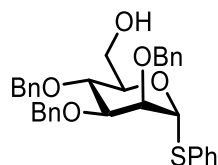
^1H NMR (400 MHz, CDCl₃) δ_{H} 144.2 (Ar-C), 138.4 (Ar-C), 138.2 (Ar-C), 135.1 (Ar-C), 131.2 (Ar-C), 129.1 (Ar-C), 129.0 (Ar-C), 128.6 (Ar-C), 128.5 (Ar-C), 128.4 (Ar-

C), 128.3 (Ar-C), 128.0 (Ar-C), 127.9 (3C, Ar-C), 127.7 (2C, Ar-C), 127.7 (Ar-C), 127.2 (Ar-C), 127.0 (Ar-C), 5.68 (1H, d, $J = 1.4$ Hz, H₁), 4.76-4.61 (6H, m, CH₂Ph), 4.31-4.25 (1H, m, H₅), 4.15-4.07 (1H, m, H₄), 4.02 (1H, dd, $J = 3.0, 1.7$ Hz, H₂), 3.83 (1H, dd, $J = 9.3, 3.1$ Hz, H₃), 3.54 (1H, dd, $J = 10.0, 1.8$ Hz, H_{6'}), 3.31, 1H, dd, $J = 10.0, 4.8$ Hz, H₆);

¹³C NMR (100 MHz, CDCl₃) δ_c 144.2 (Ar-C), 138.4 (Ar-C), 138.2 (Ar-C), 135.2(Ar-C), 135.1 (Ar-C), 131.2 (Ar-C), 129.1 (Ar-C), 129.0 (Ar-C), 128.6(Ar-C), 128.5 (Ar-C), 128.4 (Ar-C), 128.3 (Ar-C), 128.0 (Ar-C), 127.9 (3C, Ar-C), 127. (3C, Ar-C), 127.2 (Ar-C), 127.0 (Ar-C), 85.5 (C₁), 80.4 (C₃), 77.3 (C₄), 75.4 (C₂), 75.2 (CH₂Ph), 72.9 (C₅), 72.5 (CH₂Ph), 72.2 (CH₂Ph), 63.0 (C₆);

HRMS m/z (ESI⁺) [Found: (M+Na)⁺ 807.3154 C₅₂H₄₈O₅S requires M+Na⁺, 807.3120].

Phenyl 2,3,4-tri-O-benzyl mannopyranoside **112**



To a solution of **111** (14.0 g, 18 mmol, 1.0 equiv.) in dichloromethane and methanol (180 mL total, 1:1) was added *p*-TsOH monohydrate (1.73 g, 9 mmol, 0.5 equiv.) at RT. The reaction mixture was stirred for 4 h, quenched with Et₃N until pH = 7 and concentrated *in vacuo*. The resultant yellow residue was purified by Reveleris® automated silica gel flash column chromatography, eluting with Pet. ether/EtOAc

(9/1, 3/1), to afford **112** as a yellow oil (7.82 g, 14 mmol, 79%). These data were in good agreement with literature values.¹¹⁸

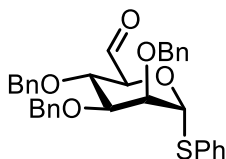
R_f 0.46 (Pet. ether/EtOAc, 3/1);

¹H NMR (400 MHz, CDCl₃) δ_H 7.44-7.28 (20H, m, Ar-H), 5.54 (1H, d, *J* = 1.5 Hz, H₁), 4.99 (1H, d, *J* = 10.9 Hz, CH₂Ph), 4.72-4.62 (5H, CH₂Ph), 4.18-4.13 (2H, m, H₅), 4.08 (1H, appt, *J* = 9.4 Hz, H₄), 4.03 (1H, dd, *J* = 3.0, 1.8 Hz, H₂), 3.92 (1H, dd, *J* = 9.1, 3.0 Hz, H₃), 3.87-3.81 (2H, m, H₆, H_{6'});

¹³C NMR (100 MHz, CDCl₃) δ_C 138.4 (Ar-C), 138.2 (Ar-C), 137.9 (Ar-C), 134.0 (Ar-C), 132.0 (Ar-C), 129.2 (Ar-C), 128.5 (Ar-C), 128.2 (Ar-C), 128.0 (Ar-C), 127.9 (3C, Ar-C), 127.8 (Ar-C), 86.1 (C₁), 80.2 (C₃), 76.5 (C₂), 75.4 (CH₂Ph), 74.9 (C₄), 73.4 (C₅), 72.4 (CH₂Ph), 72.3 (CH₂Ph), 62.3 (C₆);

HRMS *m/z* (ESI⁺) [Found: (M+Na)⁺ 565.2035 C₃₃H₃₄O₅S requires M+Na⁺, 565.2025].

Phenyl 2,3,4-tri-O-benzyl-1-thio- α -D-manno-hexodialdo-1,5-pyranoside **113**



To a solution of **112** (2.0 g, 3.7 mmol, 1.0 equiv.) in DMSO (37 mL) was added successively Et₃N (1.53 mL, 11.0 mmol, 3.0 equiv.) and SO₃•pyridine (1.75 g, 11.0 mmol, 3.0 equiv.). After stirring for 3 h, the reaction mixture was extracted with EtOAc (100 mL) and washed with H₂O (3 × 50 mL) and brine (3 × 50 mL). The organic layer was dried (MgSO₄), filtered and concentrated *in vacuo* to afford **113**

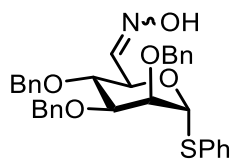
as a yellow oil which was used without any further purification (1.8 g, 3.3 mmol, 89%). These data were in good agreement with literature values.¹¹⁸

R_f 0.24 (Hex/EtOAc, 2/1);

¹H NMR (400 MHz, CDCl₃) δ_H 9.73 (1H, s, CHO), 7.34-7.27 (20H, m, Ar-H), 5.61 (1H, d, *J* = 4.1 Hz, H₁), 4.66 (2H, d, *J* = 11.7 Hz, CH₂Ph), 4.58-4.48 (5H, m, CH₂Ph, H₅), 4.16-4.10 (1H, m, H₄), 3.94-3.92 (1H, m, H₂), 3.87 (1H, dd, *J* = 7.6, 2.9 Hz, H₃);

¹³C NMR (100 MHz, CDCl₃) δ_C 197.6 (CHO), 137.7 (Ar-C), 137.6 (4C, Ar-C), 129.1 (Ar-C), 128.5 (Ar-C), 128.4 (Ar-C), 128.1 (Ar-C), 128.0 (Ar-C), 127.9 (3C, Ar-C), 127.6 (Ar-C), 84.9 (C₁), 80.4 (C₃), 76.2 (C₂), 75.3 (CH₂Ph), 74.1 (C₄), 73.8 (C₅), 72.8 (CH₂Ph), 72.3 (CH₂Ph).

Phenyl 2,3,4-tri-O-benzyl-1-thio- α -D-mannopyranosyl oxime **114**



To a solution of **113** (1.0 g, 1.9 mmol, 1.0 equiv.) in THF (18.5 mL) was added dropwise solution of hydroxylamine hydrochloride (0.13 g, 1.9 mmol, 1.0 equiv.) in H₂O (3.7 mL). The solution was cooled to 0 °C before a solution of Na₂CO₃ (0.24 g, 2.2 mmol, 1.2 equiv.) in H₂O (2.22 mL) was added dropwise. The solution was stirred for 30 min at 0 °C before being warmed to RT. After stirring for 18 h, the reaction mixture was poured onto H₂O (50 mL) then extracted with EtOAc (50 mL), washed with H₂O (3 × 50 mL), brine (50 mL), dried (MgSO₄), filtered and concentrated *in*

vacuo. Purification by silica gel column chromatography, eluting in Pet. ether/EtOAc (5/1) afforded **114** as a yellow oil (0.56 g, 1.0 mmol, 56%).

R_f 0.52 (Hex/EtOAc, 3/1);

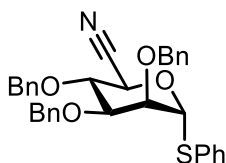
[α]_D²⁶ +42.3 (*c* = 4.10, CHCl₃);

¹H NMR (400 MHz, CDCl₃) δ_H 7.65 (1H, brs, HC=N), 7.46 (1H, d, *J* = 6.5 Hz, Ar-H), 7.40-7.23 (19H, m, Ar-H), 5.49 (1H, d, *J* = 1.6 Hz, H₁), 4.85 (1H, m, CH₂Ph), 4.76-4.71 (1H, m, H₃), 4.70-4.58 (5H, m, CH₂Ph), 4.03-3.97 (2H, m, H₂, H₄), 3.88-3.85 (1H, m, H₅);

¹³C NMR (100 MHz, CDCl₃) δ_C 148.5 (C=N), 138.1 (Ar-C), 138.0 (Ar-C), 137.7 (Ar-C), 133.9 (Ar-C), 131.7 (Ar-C), 129.1 (Ar-C), 128.4 (2C, Ar-C), 128.2 (Ar-C), 128.0 (Ar-C), 127.8 (2C, Ar-C), 127.6 (Ar-C), 86.1 (C₁), 79.5 (C₅), 76.4 (C₂ or C₄), 76.3 (C₂ or C₄), 75.1 (CH₂Ph), 72.4 (CH₂Ph), 72.3 (CH₂Ph), 70.7 (C₃);

HRMS *m/z* (ES⁺) [Found: (M+H)⁺ 556.2166 C₃₃H₃₃NO₅S requires *M+H*⁺, 556.2158].

Phenyl 2,3,4-tri-*O*-benzyl-1-thio-α-D-mannopyranosylurononitrile **115**



To a solution of **114** (0.14 g, 0.25 mmol, 1.0 equiv.) in MeCN (10 mL) was added dropwise POCl₃ (38 μL, 0.25 mmol, 1.0 equiv.). The solution was stirred for 5 min at RT, before being heated to 65 °C. After stirring for 5 h, the reaction mixture was cooled to RT, quenched with saturated aqueous NaHCO₃ solution (20 mL) and

extracted with EtOAc (30 mL). The organic layer was washed with H₂O (2 × 30 mL), dried (MgSO₄), filtered and concentrated *in vacuo*. Purification by silica gel column chromatography, eluting with Pet. ether/EtOAc (4/1) afforded **115** as a colourless oil (59 mg, 0.11 mmol, 44%).

R_f 0.77 (Pet. ether/EtOAc, 3/1);

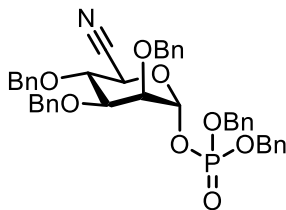
[α]_D²⁶ +67.7 (c = 0.95, CHCl₃);

¹H NMR (400 MHz, CDCl₃) δ_H 7.39-7.26 (20H, m, Ar-H), 5.49 (1H, d, J = 2.2 Hz H₁), 4.91-4.87 (3H, m, H₅, CH₂Ph), 4.69-4.62 (4H, m, CH₂Ph), 4.20 (1H, appt, J = 9.1 Hz, H₄), 3.94 (1H, appt, J = 2.6 Hz, H₂), 3.74-3.67 (1H, dd, J = 9.1, 2.9 Hz, H₃);

¹³C NMR (100 MHz, CDCl₃) δ_C 137.6 (Ar-C), 137.4 (Ar-C), 137.2 (Ar-C), 132.8 (Ar-C), 131.5 (Ar-C), 129.4 (Ar-C), 128.6 (2C, Ar-C), 128.5 (Ar-C), 128.2 (Ar-C), 128.1 (3C, Ar-C), 127.9 (Ar-C), 117.1 (C≡N), 86.2 (C₁), 78.4 (C₃), 76.1 (C₄), 75.8 (2C, C₂, CH₂Ph) 72.7 (CH₂Ph), 72.6 (CH₂Ph), 62.2 (C₅);

HRMS *m/z* (ES⁺) [Found: (M+H)⁺ 538.2055 C₃₃H₃₁NO₄S requires *M+H*⁺, 538.2053].

Dibenzyl phenyl 2,3,4-tri-O-benzyl-α-D-mannopyranosylurononitrile phosphate **116**



Prepared as per Procedure A using thioglycoside **115** (76 mg, 0.14 mmol, 1.0 equiv.), DBP (58 mg, 0.21 mmol, 1.5 equiv.), NIS (47 mg, 0.21 mmol, 1.5 equiv.) and AgOTf (10 mg, 42 μmol, 0.3 equiv.) in DCM (2 mL). Reaction time: 1 h.

Purification by silica gel column chromatography, eluting with Pet. ether/EtOAc (3/1) afforded **116** as a colourless oil (55 mg, 78 μ mol, 56%).

R_f 0.27 (Pet. ether/EtOAc, 3/1);

$[\alpha]_D^{26} +10.8$ ($c = 3.25$, CHCl_3);

^1H NMR (400 MHz, CDCl_3) δ_{H} 7.39-7.27 (25H, m, Ar-H), 5.40 (1H, dd, $J_{\text{H1-P}} = 8.0$ Hz, $J_{\text{H1-H2}} = 1.9$ Hz, H₁), 5.12 (2H, dd, $J = 6.4, 4.8$ Hz, CH_2Ph), 5.01 (2H, m, CH_2Ph), 4.75 (2H, m, CH_2Ph), 4.65-4.56 (4H, m, CH_2Ph), 4.26 (1H, d, $J = 7.2$ Hz, H₅), 4.10 (1H, appt, $J = 7.4$ Hz, H₄), 3.79 (1H, dd, $J = 2.8, 1.9$ Hz, H₂), 3.55 (1H, dd, $J = 7.4, 2.8$ Hz, H₃);

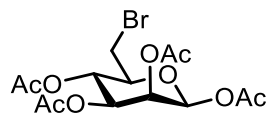
$^{13}\text{C}\{^{31}\text{P}\}$ NMR (100 MHz, CDCl_3) δ_{C} 137.7 (Ar-C), 137.5 (Ar-C), 136.8 (Ar-C), 135.7 (Ar-C), 135.6 (Ar-C), 132.6 (Ar-C), 130.1 (Ar-C), 129.5 (Ar-C), 128.7 (Ar-C), 128.6 (Ar-C), 128.5 (Ar-C), 128.3 (Ar-C), 128.2 (Ar-C), 128.1 (Ar-C), 128.0 (Ar-C), 127.8 (Ar-C), 116.11 ($\text{C}\equiv\text{N}$), 95.9 (C₁), 77.4 (C₃), 75.3 (C₄), 75.0 (CH_2Ph), 73.3 (C₂), 72.7 (CH_2Ph), 69.9 (CH_2Ph), 69.8 (CH_2Ph), 69.7 (CH_2Ph), 63.1 (C₅);

^{31}P NMR (161 MHz, CDCl_3) δ_{P} -3.1 (1P, d, $J_{\text{H1-P}} = 8.0$ Hz);

HRMS m/z (ES^+) [Found: $(\text{M}+\text{H})^+$ 706.2536 $\text{C}_{41}\text{H}_{40}\text{NO}_3\text{P}$ requires $\text{M}+\text{H}^+$, 706.2571].

6.5.4 6-Azido-6-deoxy- α -D-mannopyranose derivatives

1,2,3,4-Tetra-O-acetyl-6-bromo-6-deoxy- β -D-mannopyranose **98**



To a solution of **66** (0.40 g, 1.2 mmol, 1.0 equiv.) and Ph_3P (0.51 g, 2.0 mmol, 1.7 equiv.) in DCM (8 mL) at 0 °C was added dropwise a solution of CBr_4 (0.65 g, 2.0 mmol, 1.7 equiv.) in DCM (3 mL) before warming to RT. After 5 h, the reaction mixture was poured onto H_2O (20 mL), diluted with DCM (20 mL), washed with H_2O (20 mL), brine (20 mL), dried (MgSO_4), filtered and concentrated *in vacuo*. Purification by silica gel column chromatography, eluting with Pet. Ether/EtOAc (4/1, 3/1, 1/1) afforded **98** as a white solid (0.35 g, 0.85 mmol, 74%). Data previously reported for the α -anomer.¹⁶⁹

R_f 0.77 (Pet. Ether/EtOAc, 1/1);

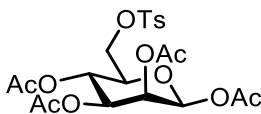
$[\alpha]_D^{26} -14.6$ ($c = 0.55$, CHCl_3);

^1H NMR (400 MHz, CDCl_3) δ_{H} 5.89 (1H, d, $J = 1.2$ Hz, H_1), 5.47 (1H, dd, $J = 3.2, 1.2$ Hz, H_2), 5.27 (1H, appt, $J = 9.7$ Hz, H_4), 5.13 (1H, ddd, $J = 9.7, 3.2, 1.2$ Hz, H_3), 3.82 (1H, ddd, $J = 9.4, 6.3, 3.0$ Hz, H_5), 3.50 (1H, dd, $J = 11.4, 3.0$ Hz, H_6'), 3.42 (1H, dd, $J = 11.4, 6.3$ Hz, H_6), 2.20 (3H, s, C(O)CH_3), 2.10 (3H, s, C(O)CH_3), 2.07 (3H, s, C(O)CH_3), 1.99 (3H, s, C(O)CH_3);

^{13}C NMR (100 MHz, CDCl_3) δ_{C} 170.3 (C=O), 169.9 (C=O), 169.7 (C=O), 168.5 (C=O), 90.4 (C_1), 74.5 (C_5), 70.6 (C_3), 68.3 (C_2), 68.1 (C_4), 30.3 (C_6), 20.9 (2C, C(O)CH_3), 20.8 (C(O)CH_3), 20.6 (C(O)CH_3);

HRMS m/z (ESI⁺) [Found: (M+Na)⁺ 433.0115 C₁₄H₁₉BrO₉ requires M+Na⁺, 433.0110].

1,2,3,4-Tetra-O-acetyl-6-O-tosyl- β -D-mannopyranose **121**



To a solution of **98** (0.25 g, 0.72 mmol, 1.0 equiv.) in pyridine (4.8 mL) was added *p*TsCl (0.47 g, 2.5 mmol, 3.4 equiv.). After stirring for 7 h, the reaction mixture was poured onto H₂O (10 mL) and diluted with CHCl₃ (30 mL). The organic layer was washed with saturated aqueous NaHCO₃ solution (2 × 20 mL), H₂O (2 × 20 mL), brine (20 mL), dried (MgSO₄), filtered and concentrated *in vacuo*. Drying under high vacuum afforded **121** as a colourless syrup (0.34 g, 0.67 mmol, 93%). Data previously reported for the α -anomer.¹⁶⁹

R_f 0.82 (Pet. Ether/EtOAc, 1/2);

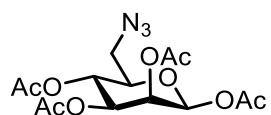
[α]_D²⁶ -6.7 (*c* = 1.65, CHCl₃);

¹H NMR (400 MHz, CDCl₃) δ _H 7.78-7.74 (2H, m, Ar-*H*), 7.33 (2H, d, *J* = 8.0 Hz, Ar-*H*), 7.30-7.27 (1H, m, Ar-*H*), 5.79 (1H, d, *J* = 1.2 Hz, H₁), 5.42 (1H, dd, *J* = 3.2, 1.2 Hz, H₂), 5.20 (1H, appt, *J* = 9.8 Hz, H₄), 5.08 (1H, *J* = 9.8, 3.2 Hz, H₃), 4.13 (2H, d, *J* = 4.3 Hz, H₆, H_{6'}), 3.79 (1H, dd, *J* = 9.6, 4.3 Hz, H₅), 2.43 (3H, s, -OphCH₃), 2.16 (3H, s, C(O)CH₃), 2.06 (3H, s, C(O)CH₃), 2.00 (3H, s, C(O)CH₃), 1.98 (3H, s, C(O)CH₃);

^{13}C NMR (100 MHz, CDCl_3) δ_{c} 170.3 (C=O), 169.9 (C=O), 169.7 (C=O), 168.3 (C=O), 149.9 (Ar-C), 145.2 (Ar-C), 136.1 (Ar-C), 132.6 (Ar-C), 130.0 (Ar-C), 128.2 (Ar-C), 90.3 (C_1), 70.9 (C_5), 70.5 (C_4), 68.1 (C_3), 67.6 (C_2), 65.8 (C_6), 21.8 (-Oph CH_3), 20.8 (C(O) CH_3), 20.7 (2C, C(O) CH_3), 20.6 (C(O) CH_3);

HRMS m/z (ESI $^+$) [Found: ($\text{M}+\text{Na}$) $^+$ 525.1073 $\text{C}_{21}\text{H}_{26}\text{O}_{12}\text{S}$ requires $\text{M}+\text{Na}^+$, 525.1043].

1,2,3,4-Tetra-O-acetyl-6-azido-6-deoxy- β -D-mannopyranose



To a solution of **121** (0.20 g, 0.39 mmol, 1.0 equiv.) in DMF (3.9 mL) was added successively 15-crown-5 ether (0.23 mL, 1.20 mmol, 3.0 equiv.) and NaN_3 (78 mg, 1.20 mmol, 3.0 equiv.). The reaction mixture was heated to 60 $^\circ\text{C}$ and after stirring for 24 h, the reaction mixture was cooled to RT, poured onto H_2O (20 mL) and extracted with EtOAc (25 mL). The organic layer was washed with 10% aqueous $\text{Na}_2\text{S}_2\text{O}_3$ solution (20 mL), H_2O (20 mL), brine (20 mL), dried (MgSO_4), filtered and concentrated *in vacuo*. Purification by silica gel column chromatography, eluting with Tol/EtOAc (5/1, 4/1) afforded **120** as a colourless oil (31 mg, 83 μmol , 32%). Data previously reported for the α -anomer.¹⁶⁹

R_f 0.33 (Tol/acetone, 4/1)

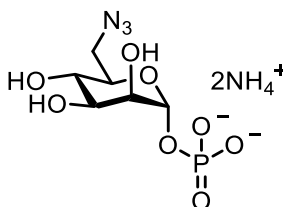
$[\alpha]_D^{26} -13.5$ ($c = 1.55$, CHCl_3);

^1H NMR (400 MHz, CDCl_3) δ_{H} 5.86 (1H, d, $J = 1.2$ Hz, H_1), 5.47 (1H, dd, $J = 3.2, 1.2$ Hz, H_2), 5.25 (1H, appt, $J = 10.0$ Hz, H_4), 5.11 (1H, dd, $J = 10.0, 3.2$ Hz, H_3), 3.78-3.72 (1H, m, H_5), 3.38 (2H, dd, $J = 13.4, 4.5$ Hz, H_6, H_6'), 2.21 (3H, s, $\text{C}(\text{O})\text{CH}_3$), 2.09 (3H, s, $\text{C}(\text{O})\text{CH}_3$), 2.05 (3H, s, $\text{C}(\text{O})\text{CH}_3$), 1.99 (3H, s, $\text{C}(\text{O})\text{CH}_3$);

^{13}C NMR (100 MHz, CDCl_3) δ_{C} 170.3 (C=O), 169.9 (C=O), 169.8 (C=O), 168.5 (C=O), 90.3 (C_1), 74.5 (C_5), 70.7 (C_3), 68.2 (C_2), 66.5 (C_4), 50.8 (C_6), 20.9 ($\text{C}(\text{O})\text{CH}_3$), 20.8 (2C, $\text{C}(\text{O})\text{CH}_3$), 20.6 ($\text{C}(\text{O})\text{CH}_3$);

HRMS m/z (ESI $^+$) [Found: $(\text{M}+\text{Na})^+$ 396.1039 $\text{C}_{14}\text{H}_{19}\text{N}_3\text{O}_9$ requires $\text{M}+\text{Na}^+$, 396.1019].

6-Azido-6-deoxy- α -D-mannopyranosyl phosphate (bis-ammonium salt) **119**



Prepared as per Procedure D using **120** (100 mg, 0.27 mmol, 1.0 equiv.) and H_3PO_4 (127 mg, 1.30 mmol, 5.0 equiv.). Reaction time: 4 h. **119** was afforded as a white solid (48 mg, 0.17 mmol, 65%). Data previously reported for the bis-triethylammonium salt.⁹⁶

R_f 0.28 (MeCN/ H_2O , 3/1 plus 3 drops AcOH);

$[\alpha]_D^{26} +3.6$ ($c = 0.71$, H_2O);

^1H NMR (400 MHz, D_2O) δ_{H} 5.07 (1H, dd, $J_{\text{H}_1-\text{P}} = 8.4$ Hz, $J_{\text{H}_1-\text{H}_2} = 1.9$ Hz, H_1), 3.72-3.67 (3H, m, $\text{H}_5, \text{H}_2, \text{H}_4$), 3.50-3.45 (1H, m, H_6), 3.42-3.37 (2H, m, H_3, H_6');

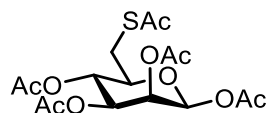
^{13}C NMR (101 MHz, D_2O) δ_{C} 94.9 (C_1), 72.4, 71.1, 69.7, 67.2 (C_3), 51.0 (C_6);

^{31}P NMR (162 MHz, D_2O) δ_{P} 1.4 (1P, d, $J_{\text{H}_1-\text{P}} = 8.4$ Hz);

HRMS m/z (ESI $^-$) [Found: ($\text{M}-\text{H}$) $^-$ 284.0288, $\text{C}_6\text{H}_{11}\text{N}_3\text{O}_8\text{P}$ requires $\text{M}-\text{H}^-$, 284.0284].

6.5.5 6-Deoxy-6-thio- α -D-mannopyranose derivatives

1,2,3,4-Tetra-O-acetyl-6-S-acetyl-6-deoxy- β -D-mannopyranose **123**



To a solution of **96** (58 mg, 0.16 mmol, 1.0 equiv.) in DMF (1.6 mL) was added KSAc (54 mg, 0.48 mmol, 3.0 equiv.). The reaction mixture was heated to 75 °C and stirred for 24 h, cooled to RT then poured onto H_2O (10 mL) and extracted with EtOAc (20 mL). The organic layer was washed with saturated aqueous NaHCO_3 solution (15 mL), H_2O (15 mL), brine (15 mL), dried (MgSO_4), filtered and concentrated *in vacuo*. Purification by silica gel column chromatography, eluting with Pet. Ether/EtOAc (2/1) afforded **123** as an orange oil (55 mg, 0.14 mmol, 88%).

R_f 0.38 (Pet. Ether/EtOAc, 2/1);

$[\alpha]_D^{26} -7.3$ ($c = 1.45$, CHCl_3);

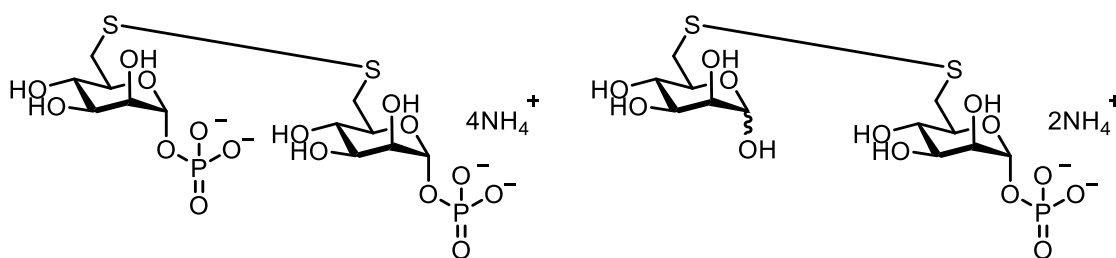
^1H NMR (400 MHz, CDCl_3) δ_{H} 5.80 (1H, d, $J = 1.2$ Hz, H_1), 5.45-5.43 (1H, dd, $J = 3.2, 1.1$ Hz, H_2), 5.18 (1H, appt, $J = 9.8$, H_4), 5.07 (1H, dd, $J = 9.8, 3.2$ Hz, H_3), 3.68 (1H, ddd, $J = 9.8, 7.5, 2.7$ Hz, H_5), 3.28, 1H, dd, $J = 14.3, 2.5$ Hz, H_6'), 3.03 (1H, dd, $J = 14.3, 7.4$ Hz, H_6), 2.32 (3H, s, $\text{SC}(\text{O})\text{CH}_3$), 2.19 (3H, s, $\text{C}(\text{O})\text{CH}_3$), 2.10 (3H, s, $\text{C}(\text{O})\text{CH}_3$), 2.08 (3H, s, $\text{C}(\text{O})\text{CH}_3$), 1.98 (3H, s, $\text{C}(\text{O})\text{CH}_3$);

^{13}C NMR (100 MHz, CDCl_3) δ_{C} 194.9 (SC=O), 170.3 (C=O), 170.1 (C=O), 169.9 (C=O), 168.4 (C=O), 90.5 (C_1), 74.7 (C_5), 70.7 (C_3), 68.4 (C_2), 67.8 (C_4), 30.5 (SC(O)CH₃), 30.2 (C_6), 20.9 (2C, C(O)CH₃), 20.8 (C(O)CH₃), 20.6 (C(O)CH₃);

HRMS m/z (ESI⁺) [Found: ($\text{M}+\text{NH}_4$)⁺ 424.1284 $\text{C}_{16}\text{H}_{22}\text{O}_{10}\text{S}$ requires $\text{M}+\text{NH}_4$ ⁺, 424.1317].

6-Deoxy-6-thio- α -D-mannopyranosyl phosphate disulphide (*tetra*-ammonium salt)

124 and 6-Deoxy-6-thio- α -D-mannopyranosyl phosphate mixed disulphide (*bis*-ammonium salt) **125**



Prepared as per Procedure D using **123** (100 mg, 0.25 mmol, 1.0 equiv.) and H_3PO_4 (240 mg, 2.50 mmol, 5.0 equiv.). Reaction time: 4 h. A mixture of **124** and **125** were afforded as white solids (5 mg, 18 μmol , 7%).

R_f 0.15 (MeCN/ H_2O , 3/1 plus 3 drops AcOH);

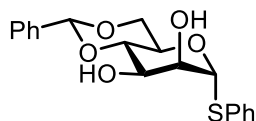
^1H NMR (400 MHz, D_2O) δ_{H} 5.34 (1H, d, $J_{\text{H1-P}} = 8.1$ Hz, disulphide **124**), 5.16 (0.40H, d, $J = 1.3$ Hz, mixed disulphide **125**), ratio: 2.5:1;

$^{31}\text{P}\{^1\text{H}\}$ NMR (162 MHz, D_2O) δ_{P} 0.9 (0.40P, s, mixed disulphide **125**), 0.4 (1P, s, disulphide **124**);

HRMS m/z (ESI⁻) Disulphide **124**: [Found: (M-H)⁻ 548.9910, C₁₂H₂₃O₁₆P₂S₂ requires M-H⁻, 548.9908]. Mixed disulphide **125**: [Found: (M-H)⁻ 469.0239 C₁₂H₂₂O₁₃PS₂ requires M-H⁻, 469.0240].

6.5.6 4-Deoxy-4-fluoro- α -D-mannopyranose derivatives

Phenyl 4,6-O-benzylidene-1-thio- α -D-mannopyranoside **131**



To a solution of **109** (13.5 g, 49 mmol, 1.0 equiv.) in DMF (150 mL) was added successively at 0 °C BDMA (7.5 mL, 50 mmol, 1.02 equiv.) and HBF₄•OEt₂ (6.9 mL, 51 mmol, 1.03 equiv.) before warming to RT. After stirring for 18 h, the reaction mixture was quenched with Et₃N until pH = 7 then concentrated *in vacuo*. The resultant yellow residue was recrystallized from absolute EtOH to afford **131** as a white solid (11.0 g, 30 mmol, 62%). These data were in good agreement with literature values.¹⁶⁸

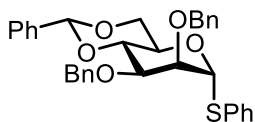
R_f 0.79 (Pet. ether/EtOAc, 1/2);

¹H NMR (400 MHz, DMSO-d₆) δ _H 7.51-7.29 (12H, m, Ar-H), 5.63 (1H, s, benzylidene-H), 5.55 (1H, d, J = 4.1 Hz, C₂-OH), 5.47 (1H, d, J = 0.9 Hz, H₁), 5.22 (1H, d, J = 6.0 Hz, C₃-OH), 4.10-4.03 (1H, m, H₅, H₆), 4.01 (1H, s, H₂), 3.94 (1H, appt, J = 9.3 Hz, H₄), 3.81-3.73 (2H, m, H₃, H₆);

¹³C NMR (100 MHz, DMSO-d₆) δ _C 137.8 (Ar-C), 133.7 (Ar-C), 131.3 (2C, Ar-C), 129.3 (2C, Ar-C), 128.9 (Ar-C), 128.0 (2C, Ar-C), 127.5 (Ar-C), 126.4 (2C, Ar-C), 101.2 (benzylidene-C), 89.3 (C₁), 78.5 (C₄), 72.4 (C₂), 68.1 (C₃), 67.6 (C₆), 65.3 (C₅);

HRMS m/z (ESI⁺) [Found: (M+Na)⁺ 383.0948 C₁₉H₂₀O₅S requires M+Na⁺, 383.0929].

Phenyl 2,3-di-O-benzyl-4,6-O-benzylidene-1-thio- α -D-mannopyranoside **132**



NaH (60% in mineral oil, 0.20 g, 8.2 mmol, 2.7 equiv.) was washed with hexane (3 × 20 mL) and decanted, dried under high vacuum and dissolved in DMF (2.5 mL). A solution of **131** (1.09 g, 3.0 mmol, 1.0 equiv.) in DMF (15 mL) was added dropwise to the suspension of NaH at 0 °C over 15 min. BnBr (0.97 mL, 8.2 mmol, 2.7 equiv.) was then added dropwise over 15 min, before the reaction mixture was warmed to RT. After stirring for 18 h, the reaction mixture was quenched with MeOH (40 mL), concentrated *in vacuo* and the residue reconstituted in DCM (100 mL). The organic layer was washed with H₂O (2 × 50 mL), brine (2 × 50 mL), dried (MgSO₄), filtered and concentrated *in vacuo*. Purification by silica gel column chromatography, eluting with Pet. ether/EtOAc (4/1) afforded **132** as a white solid (1.35 g, 2.5 mmol, 82%). These data were in good agreement with literature values.¹⁷⁰

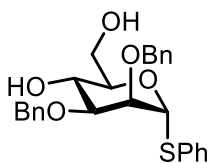
R_f 0.90 (Pet. ether/EtOAc, 2/1);

¹H NMR (400 MHz, CDCl₃) δ_{H} 7.54 (2H, dd, J = 7.6, 1.9 Hz, Ar- H), 7.41-7.35 (18H, m, Ar- H), 5.67 (1H, s, benzylidene- H), 5.53 (1H, d, J = 1.4 Hz, H₁), 4.85 (1H, d, J = 12.2 Hz, CH₂Ph), 4.74 (1H, s, CH₂Ph), 4.68 (1H, d, J = 12.2 Hz, CH₂Ph), 4.37-4.22 (3H, m, H₄, H₅, H₆), 4.07 (1H, dd, J = 3.2, 1.4 Hz, H₂), 3.99 (1H, dd, J = 9.5, 3.2 Hz, H₃), 3.91 (1H, d, J = 9.8 Hz, H_{6'});

^{13}C NMR (100 MHz, CDCl_3) δ_{c} 138.5 (Ar-C), 138.4 (Ar-C), 137.8 (Ar-C), 137.7 (Ar-C), 133.9 (Ar-C), 132.6 (Ar-C), 131.8 (Ar-C), 129.3 (2C, Ar-C), 129.0 (Ar-C), 128.6 (Ar-C), 128.5 (2C, Ar-C), 128.4 (Ar-C), 128.3 (2C, Ar-C), 128.0 (Ar-C), 127.9 (Ar-C), 127.8 (2C, Ar-C), 126.4 (Ar-C), 126.2 (2C, Ar-C), 101.6 (benzylidene-C), 87.3 (C_1), 79.2 (C_4), 78.2 (C_2), 76.4 (C_3), 73.2 (CH_2Ph), 72.3 (CH_2Ph), 68.6 (C_6), 65.6 (C_5);

HRMS m/z (ESI $^+$) [Found: ($\text{M}+\text{Na}$) $^+$ 563.1896 $\text{C}_{33}\text{H}_{32}\text{O}_5\text{S}$ requires $\text{M}+\text{Na}^+$, 563.1868].

Phenyl 2,3-di-O-benzyl-1-thio- α -D-mannopyranoside **133**



To a solution of **132** (2.8 g, 5.2 mmol, 1.0 equiv.) in MeOH (21 mL) was added *p*-TsOH (0.2 g, 1.0 mmol, 0.2 equiv.). The reaction mixture was heated at reflux (85 °C) for 2 h, cooled to RT, quenched with Et_3N (2 mL) and concentrated *in vacuo*. The residue was reconstituted in DCM (80 mL), washed with saturated aqueous NaHCO_3 solution (2 x 50 mL), H_2O (2 x 50 mL), brine (50 mL), dried (MgSO_4), filtered and concentrated *in vacuo*. Purification by Reveleris® automated silica gel flash column chromatography (liquid injection onto column), eluting with Hex/EtOAc (1/0, 7/3, 1/1, 0/1) afforded **133** as a white solid (1.7 g, 3.8 mmol, 72%). These data were in good agreement with literature values.¹⁷¹

R_f 0.09 (Hex/EtOAc, 2/1);

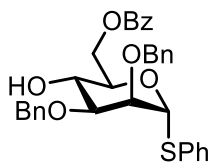
^1H NMR (300 MHz, CDCl_3) δ_{H} 7.43-7.20 (15 H, m, Ar-H), 5.51 (1 H, d, $J = 1.2$ Hz, H₁), 4.60 (1 H, d, $J = 12.2$ Hz, CH_2Ph), 4.50 (2 H, s, CH_2Ph), 4.49 (1 H, d, $J = 12.1$ Hz, CH_2Ph), 4.18-4.10 (1 H, m, H₄), 4.09-4.02 (1 H, m, H₅), 3.92 (1 H, dd, $J = 2.9, 1.5$ Hz, H₂), 3.80 (2 H, m, H₆, H_{6'}), 3.67 (1 H, dd, $J = 9.2, 3.0$ Hz, H₃), 3.59 (1 H, d, $J = 3.2$ Hz, C₄-OH), 2.86 (1 H, t, $J = 5.7$ Hz, C₆-OH);

^{13}C NMR (75 MHz, CDCl_3) δ_{C} 138.0 (Ar-C), 137.8 (Ar-C), 134.2, (Ar-C) 131.9 (Ar-C), 129.2 (Ar-C), 128.6 (Ar-C), 128.5 (Ar-C), 128.2 (Ar-C), 128.1 (Ar-C), 128.0 (Ar-C), 127.9 (Ar-C), 127.7 (Ar-C), 86.1 (C₁), 79.6 (C₃), 75.9 (C₂), 73.8 (C₅), 72.3 (CH₂Ph), 72.1 (CH₂Ph), 67.0 (C₄), 62.3 (C₆);

LRMS (ES^+) m/z 470 [(M+NH₄)⁺, 100%];

HRMS (ES^+) m/z [Found: (M+NH₄)⁺ 470.1993 C₂₆H₂₈O₅S requires M+NH₄⁺, 470.1996].

Phenyl 6-O-benzoyl-2,3-di-O-benzyl-1-thio- α -D-mannopyranoside **134**



To a solution of **133** (1.0 g, 2.2 mmol, 1.0 equiv.) in pyridine (12 mL) at 0 °C was added successively DMAP (0.13 g, 1.1 mmol, 0.5 equiv.) and BzCl (0.31 mL, 2.7 mmol, 1.2 equiv.). The reaction mixture was warmed to RT and after stirring for 24 h was extracted with DCM (40 mL). The organic layer was washed with 0.5 M HCl (40 mL), saturated aqueous NaHCO₃ solution (40 mL), H₂O (40 mL), brine (40 mL), dried (MgSO₄), filtered and concentrated *in vacuo*. Purification by silica gel column

chromatography, eluting with Hex/EtOAc (5/1, 3/1) afforded **134** as a colourless oil (1.08 g, 1.9 mmol, 88%).

R_f 0.93 (Hex/EtOAc, 1/1);

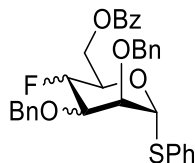
[α]_D²⁶ +8.9 (c = 4.05, CHCl₃);

¹H (400 MHz, CDCl₃) δ_H 8.01-7.98 (1H, m, Ar-H), 7.55-7.17 (20H, m, Ar-H), 5.65 (1H, d, J = 1.4 Hz, H₁), 4.71 (6H, m, H₆, H_{6'}, CH₂Ph), 4.43 (1H, d, J = 9.6 Hz, H₅), 4.15 (1H, appt, J = 9.6 Hz, H₄), 4.04 (1H, dd, J = 3.0, 1.4 Hz, H₂), 3.73 (1H, dd, J = 9.6, 3.0 Hz, H₃);

¹³C (100 MHz, CDCl₃) δ_C 166.7 (C=O), 137.8 (Ar-C), 134.1 (Ar-C), 133.0 (Ar-C), 131.6 (Ar-C), 130.1 (Ar-C), 129.9 (Ar-C), 129.1 (Ar-C), 128.7 (Ar-C), 128.5 (Ar-C), 128.3 (Ar-C), 128.1 (Ar-C), 128.1 (Ar-C), 127.8 (Ar-C), 127.8 (Ar-C), 127.6 (Ar-C), 85.7 (C₁), 79.6 (C₃), 75.7 (C₂), 72.0 (CH₂Ph), 71.9 (CH₂Ph), 71.8 (C₅), 66.9 (C₄), 64.2 (C₆);

HRMS m/z (ES⁺) [Found: (M+NH₄)⁺ 574.2292 C₃₃H₃₂O₆S requires M+NH₄⁺, 574.2303].

Phenyl 6-O-benzoyl-2,3-di-O-benzyl-4-deoxy-4-fluoro-1-thio- α -D-mannopyranoside **138** and Phenyl 6-O-benzoyl-2,3-di-O-benzyl-4-deoxy-4-fluoro-1-thio- α -D-idopyranoside **139**



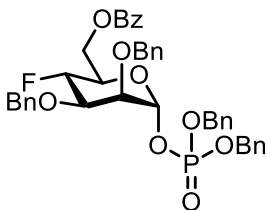
Prepared as per Procedure C using thioglycoside **134** (240 mg, 0.43 mmol, 1.0 equiv.) in DCM (3 mL) and DAST (0.45 mL, 3.4 mmol, 8.0 equiv.) in DCM (2.25 mL). Reaction time: 18 h. Purification by silica gel column chromatography, eluting in Hex/EtOAc (9/1, 7/1) afforded a mixture of regioisomers **138** and **139** (59 mg, 0.11 mmol, 26%).

R_f 0.7 (Hex/EtOAc, 3/1);

¹⁹F NMR{¹H} (376 MHz, CDCl₃) δ_F -197.0 (1F, s);

HRMS m/z (ES⁺) [Found: (M+NH₄)⁺ 576.2233 C₃₃H₃₁FO₅S requires M+NH₄⁺, 576.2259].

Dibenzyl 6-O-benzoyl-2,3-di-O-benzyl-4-deoxy-4-fluoro- α -D-mannopyranosyl phosphate **140**



Prepared as per Procedure A using crude thioglycosides **138/139** (56 mg, 0.1 mmol, 1.0 equiv.), DBP (42 mg, 0.15 mmol, 1.5 equiv.), NIS (34 mg, 0.15 mmol, 1.5 equiv.)

and AgOTf (8 mg, 31 μmol , 0.3 equiv.) in DCM (2 mL). Reaction time: 18 h. Purification by silica gel column chromatography, eluting in Hex/EtOAc (3/1, 2/1) afforded **140** as a colourless oil (14 mg, 19 μmol , 19%).

R_f 0.23 (Hex/EtOAc, 3/1);

$[\alpha]_D^{26} +6.6$ ($c = 0.95$, CHCl_3);

^1H NMR (400 MHz, CDCl_3) δ_{H} 7.99-7.95 (2H, m, Ar-H), 7.51-7.47 (1H, m, Ar-H), 7.38-7.27 (22H, m, Ar-H), 5.68-5.64 (1H, m, H₁), 5.04-4.97 (4H, m, CH₂Ph), 5.01 (1H, ddd, $J_{\text{H4-F}} = 52.0$ Hz, $J_{\text{H4-H5}} = 9.6$ Hz, $J_{\text{H4-H3}} = 9.3$ Hz, H₄), 4.67 (2H, d, $J = 11.6$ Hz, CH₂Ph), 4.56 (2H, dd, $J = 11.9$, 6.4 Hz, CH₂Ph), 4.49 (1H, dd, $J = 10.4$, 1.9 Hz, H_{6'}), 4.40 (1H, ddd, $J = 12.3$, 4.1, 1.3 Hz, H₆), 4.06-3.99 (1H, m, H₅), 3.85 (1H, ddd, $J_{\text{H3-F}} = 12.6$, $J_{\text{H3-H4}} = 9.3$, $J_{\text{H3-H2}} = 3.2$ Hz, H₃), 3.72 (1H, dd, $J = 5.1$, 2.8 Hz, H₂);

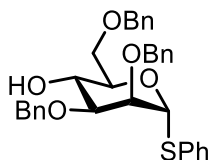
^{13}C NMR (100 MHz, CDCl_3) δ_{C} 166.2 (C=O), 137.9 (Ar-C), 137.6 (Ar-C), 135.5 (Ar-C), 135.4 (Ar-C), 133.0 (Ar-C), 129.7 (Ar-C), 128.8 (Ar-C), 128.7 (2C, Ar-C), 128.4 (2C, Ar-C), 128.3 (Ar-C), 128.1 (2C, Ar-C), 127.8 (Ar-C), 127.7 (Ar-C), 127.6 (Ar-C), 95.9 (C₁), 88.7 (d, $J_{\text{C4-F}} = 179$ Hz, C₄), 76.0 (C₃), 75.9 (C₂), 73.3 (CH₂Ph), 72.9 (CH₂Ph), 70.5 (C₅), 69.8 (CH₂Ph), 69.7 (CH₂Ph), 62.5 (C₆);

$^{19}\text{F}\{^1\text{H}\}$ NMR (376 MHz, CDCl_3) δ_{F} -202.9 (1F, s);

$^{31}\text{P}\{^1\text{H}\}$ NMR (161 MHz, CDCl_3) δ_{P} -2.9 (1P, s);

HRMS m/z (ES⁺) [Found: (M+H)⁺ 727.2497 C₄₁H₄₀FO₉P requires $M+H^+$, 727.2473].

Phenyl 2,3,6-tri-O-benzyl-1-thio- α -D-mannopyranoside **142**



A solution of **132** (0.26 g, 0.48 mmol, 1.0 equiv.) in DCM (4.8 mL) was cooled to 0 °C. Me₂EtSiH (0.16 mL, 1.20 mmol, 2.5 equiv.) was added dropwise and stirred for 10 min, before BF₃•OEt₂ (59 μL, 0.48 mmol, 1.0 equiv.) was added dropwise. After stirring for 2 h, the reaction mixture was quenched with saturated aqueous NaHCO₃ solution (5 mL) and diluted with DCM (50 mL). The organic layer was washed with saturated aqueous NaHCO₃ solution (25 mL), H₂O (25 mL), brine (25 mL), dried (MgSO₄), filtered and concentrated *in vacuo*. Purification by silica gel column chromatography, eluting with Tol/acetone (8/1, 6/1, 5/1) afforded **142** as a colourless oil (0.13 g, 0.24 mmol, 50%). These data were in good agreement with literature values.¹⁷²

R_f 0.52 (Pet. ether/EtOAc, 3/1);

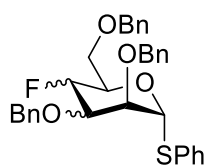
¹H NMR (400 MHz, CDCl₃) δ_H 7.48-7.43 (2H, m, Ar-H), 7.37-7.19 (18H, m, Ar-H), 5.60 (1H, d, *J* = 1.4 Hz, H₁), 4.68 (1H, d, *J* = 12.1 Hz, CH₂Ph), 4.62-4.47 (5H, m, CH₂Ph), 4.28 (1H, ddd, *J* = 9.1, 5.3, 3.5 Hz, H₅), 4.12 (1H, appt, *J* = 9.4 Hz, H₄), 4.00 (1H, dd, *J* = 3.1, 1.4 Hz, H₂), 3.85-3.76 (2H, m, H₆, H_{6'}), 3.68 (1H, dd, *J* = 9.4, 3.1 Hz, H₃);

¹³C NMR (100 MHz, CDCl₃) δ_C 138.4 (Ar-C), 137.9 (2C, Ar-C), 134.4 (Ar-C), 131.8 (Ar-C), 129.1 (Ar-C), 128.5 (2C, Ar-C), 128.4 (Ar-C), 128.3 (Ar-C), 128.0 (Ar-C),

127.9 (Ar-C), 127.7 (Ar-C), 127.6 (2C, Ar-C), 85.9 (C₁), 79.7 (C₃), 77.2 (C₂), 75.7 (CH₂Ph), 73.5 (CH₂Ph), 72.5 (C₅), 72.0 (CH₂Ph), 70.2 (C₆), 67.9 (C₄);

HRMS *m/z* (ES⁺) [Found: (M+NH₄)⁺ 560.2499 C₃₃H₃₄O₅S requires M+NH₄⁺, 560.2510].

Phenyl 2,3,6-tri-O-benzyl-4-deoxy-4-fluoro-1-thio- α -D-mannopyranoside **143** and Phenyl 2,3,6-tri-O-benzyl-4-deoxy-4-fluoro-1-thio- α -D-idopyranoside **144**



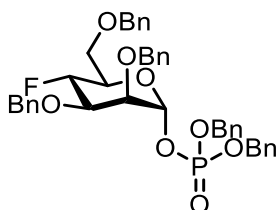
Prepared as per Procedure C using thioglycoside **142** (70 mg, 0.13 mmol, 1.0 equiv.) in DCM (1.3 mL) and DAST (0.13 mL, 1.0 mmol, 8.0 equiv.) in DCM (1 mL). Reaction time: 16 h. Purification by silica gel column chromatography, eluting with Tol/acetone (9/1) afforded a mixture of regioisomers **143** and **144** (33 mg, 59 μ mol, 45%).

R_f 0.86 (Pet. Ether/EtOAc, 3/1);

¹⁹F NMR{¹H} (376 MHz, CDCl₃) δ_F -201.8 (1F, s);

HRMS *m/z* (ES⁺) [Found: (M+Na)⁺ 567.1956 C₃₃H₃₁FO₅S requires M+Na⁺, 567.1982].

Dibenzyl 2,3,6-tri-O-benzyl-4-deoxy-4-fluoro- α -D-mannopyranosyl phosphate **145**



Prepared as per Procedure A using crude thioglycosides **143/144** (100 mg, 0.18 mmol, 1.0 equiv.), DBP (75 mg, 0.27 mmol, 1.5 equiv.), NIS (61 mg, 0.27 mmol, 1.5 equiv.) and AgOTf (14 mg, 54 μ mol, 0.3 equiv.) in DCM (2 mL). Reaction time: 2.5 h. Purification by silica gel column chromatography, eluting with Pet. Ether/EtOAc (5/1, 3/1, 1/1) afforded **145** as a yellow oil (52 mg, 73 μ mol, 41%).

R_f 0.17 (Pet. Ether/EtOAc, 3/1);

$[\alpha]_D^{26} +0.7$ ($c = 0.25$, CHCl_3);

^1H NMR (400 MHz, CDCl_3) δ_H 7.35-7.21 (25H, m, Ar-H), 5.71-5.67 (1H, m, H₁), 5.00-4.93 (4H, m, CH_2Ph), 4.89 (1H, ddd, $J_{\text{H}_4-\text{F}} = 52.0$ Hz, $J_{\text{H}_4-\text{H}_5} = 10.0$ Hz, $J_{\text{H}_4-\text{H}_3} = 9.3$ Hz), 4.66-4.59 (4H, m, CH_2Ph), 4.58-4.46 (2H, CH_2Ph), 3.94 (1H, dtd, $J = 9.8, 5.2, 1.9$ Hz, H₅), 3.81 (1H, ddd, $J_{\text{H}_3-\text{F}} = 12.7$ Hz, $J_{\text{H}_3-\text{H}_4} = 9.3$ Hz, $J_{\text{H}_3-\text{H}_2} = 3.2$ Hz, H₃), 3.69 (1H, dt, $J = 5.4, 2.5$ Hz, H₂), 3.67-3.58 (2H, m, H₆, H_{6'});

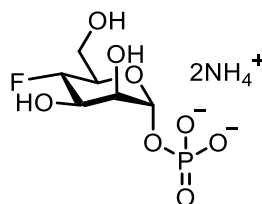
^{13}C NMR (100 MHz, CDCl_3) δ_C 138.1 (2C, Ar-C), 137.6 (Ar-C), 135.6 (Ar-C), 128.8 (2C, Ar-C), 128.7 (Ar-C), 128.4 (Ar-C), 128.1 (Ar-C), 128.0 (Ar-C), 127.9 (Ar-C), 127.8 (Ar-C), 127.7 (2C, Ar-C), 96.1 (C₁), 87.8 (d, $J_{\text{C}_4-\text{F}} = 179$ Hz, C₄), 76.2 (C₃), 75.5 (C₂), 73.6 (CH_2Ph), 73.2 (CH_2Ph), 72.8 (CH_2Ph), 72.1 (C₅), 69.7 (2C, CH_2Ph), 68.3 (C₆);

^{19}F NMR (376 MHz, CDCl_3) δ_{F} -202.5 (1F, dd, $J_{\text{H4-F}} = 52.0$ Hz, $J_{\text{H3-F}} = 12.7$ Hz);

$^{31}\text{P}\{^1\text{H}\}$ NMR (161 MHz, CDCl_3) δ_{P} -2.8 (1P, s);

HRMS m/z (ESI $^+$) [Found: $(\text{M}+\text{Na})^+$ 719.2152 $\text{C}_{40}\text{H}_{40}\text{O}_7\text{S}_2$ requires $\text{M}+\text{Na}^+$, 719.2113].

4-Deoxy-4-fluoro- α -D-mannopyranosyl phosphate (bis-ammonium salt) **130**



A suspension of **145** (48 mg, 67 μmol , 1.0 equiv.) and Pd/C (10% loading, 11 mg, 10 μmol , 0.03 equiv. per benzyl group) and Pd(OH) $_2$ /C (20% loading, 7 mg, 10 μmol , 0.03 equiv. per benzyl group) in EtOH//THF (2:1, 0.9:0.45 mL) with 5% aqueous NaHCO_3 solution (250 μL) was stirred vigorously under an atmosphere of H_2 for 20 h. The reaction mixture was filtered over Celite $^{\text{TM}}$, washed with MeOH/ H_2O (2:1, 15 mL) and MeOH/ H_2O (1:1, 20 mL) then concentrated *in vacuo*. The residue was reconstituted in H_2O and purified by strong anion exchange chromatography, eluting with H_2O (3 column volumes, 15 mL) and 1M NH_4HCO_3 (3 column volumes, 15 mL). This afforded **130** as a white solid (*bis*-ammonium salt, 15 mg, 57 μmol , 85%).

R_f 0.38 (MeCN/ H_2O , 3/1 with 3 drops AcOH);

$[\alpha]_D^{26} +20.8$ ($c = 0.45$, H_2O);

^1H NMR (400 MHz, D_2O) δ_{H} 5.41 (1H, brs, H_1), 4.60 (1H, dd, $J_{\text{H4-F}} = 52.0$ Hz, $J_{\text{H4-H3}} = 10.0$ Hz, H_4), 4.17 (1H, m, H_3), 4.03 (2H, brs, H_2 , H_5), 3.83 (2H, m, H_6 , H_6');

^{13}C NMR (100 MHz, D_2O) δ_{C} 95.7 (C_1), 87.9 (d, $J_{\text{C}_4\text{-F}} = 176.0$ Hz, C_4), 70.9 (d, $J_{\text{C}_3\text{-F}} = 24.4$ Hz, C_3), 68.4 (C_2 or C_5), 68.2 (C_2 or C_5), 60.11 (C_6);

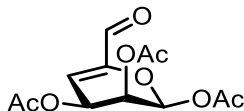
^{19}F NMR (376 MHz, D_2O) δ_{F} -205.3 (1F, dd, $J_{\text{F-H}_4} = 52.0$ Hz, $J_{\text{F-H}_3} = 13.3$ Hz);

$^{31}\text{P}\{^1\text{H}\}$ NMR (161 MHz, D_2O) δ_{P} -2.2 (1P, s);

HRMS m/z (ES^-) [Found: $(\text{M-H})^-$ 261.0182 $\text{C}_6\text{H}_{12}\text{FO}_8\text{P}$ requires M-H^- , 261.0181].

6.5.7 4-Deoxy- α -D-manno-hex-4-eno-1,5-pyranose derivatives

1,2,3-Tri-O-acetyl-4-deoxy- β -D-manno-hex-4-enodialdo-1,5-pyranoside **147**



To a solution of **103** (1.0 g, 2.9 mmol, 1.0 equiv.) in DCM (28 mL) was added Et_3N (0.48 mL, 3.5 mmol, 1.2 equiv.) dropwise. After stirring for 2 h the reaction mixture was diluted with DCM (50 mL) and washed with 1M HCl (50 mL), saturated aqueous NaHCO_3 solution (50 mL), H_2O (50 mL) and brine. The organic layer was dried (MgSO_4), filtered and concentrated *in vacuo*. Purification by silica gel column chromatography, eluting in Hex/EtOAc (1/2) afforded **147** as a yellow oil (0.52 g, 1.8 mmol, 63%).

R_f 0.45 (Hex/EtOAc, 1/3);

$[\alpha]_D^{26} +39.5$ ($c = 0.55$, CHCl_3);

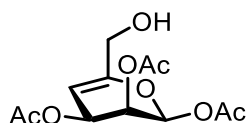
^1H NMR (400 MHz, CDCl_3) δ_{H} 9.29 (1H, s, CHO), 6.48 (1H, dd, $J = 2.1$ Hz, 1.1 Hz, H_1), 5.94 (1H, d, $J = 4.2$ Hz, H_4), 5.79 (1H, dd, $J = 4.2$, 1.1 Hz, H_2), 5.42 (1H, dd, J

= 4.2 Hz, 2.1 Hz, H₃), 2.15 (3H, s, C(O)CH₃), 2.13 (3H, s, C(O)CH₃), 2.12 (3H, s, C(O)CH₃);

¹³C NMR (100 MHz, CDCl₃) δ_c 184.9 (CHO), 170.0 (C=O), 169.7 (C=O), 168.6 (C=O), 150.2 (C₅), 114.3 (C₄), 88.4 (C₁), 65.0 (C₃), 62.1 (C₂), 20.7 (C(O)CH₃), 20.6 (C(O)CH₃), 20.5 (C(O)CH₃);

HRMS *m/z* (ES⁺) [Found: (M+NH₄)⁺ 304.1039 C₁₂H₁₄O₈ requires M+NH₄⁺, 304.1072].

1,2,3-Tri-O-acetyl-4-deoxy-β-D-manno-hex-4-eno-1,5-pyranoside **148**



To a solution of **147** (1.29 g, 4.5 mmol, 1.0 equiv.) in THF (45 mL) at 0 °C was added NaBH₄ (0.20 g, 5.4 mmol, 1.2 equiv.) before warming to RT. After 2 h, the reaction mixture was quenched with saturated aqueous NH₄Cl solution (30 mL), extracted with EtOAc (40 mL) and washed with H₂O (50 mL) and brine (50 mL). The organic layer was dried (MgSO₄), filtered and concentrated *in vacuo*. Purification by silica gel column chromatography, eluting in Hex/EtOAc (1/2) afforded **148** as a colourless oil (0.89 g, 3.1 mmol, 68%).

R_f 0.63 (Hex/EtOAc, 1/3);

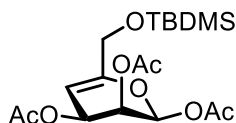
[α]_D²⁶ +16.8 (*c* = 4.60, CHCl₃);

^1H NMR (400 MHz, CDCl_3) δ_{H} 6.36 (1H, d, $J = 2.6$ Hz, H_1), 5.55 (1H, appt, $J = 4.9$ Hz, H_3), 5.34 (1H, dd, $J = 4.9, 2.6$ Hz, H_2), 5.13 (1H, d, $J = 4.9$ Hz, H_4), 4.07 (2H, brs, H_6, H_6'), 2.16 (3H, s, $\text{C}(\text{O})\text{CH}_3$), 2.10 (3H, s, $\text{C}(\text{O})\text{CH}_3$), 2.09 (3H, s, $\text{C}(\text{O})\text{CH}_3$);

^{13}C NMR (100 MHz, CDCl_3) δ_{C} 170.6 (C=O), 169.9 (C=O), 169.5 (C=O), 154.2 (C_5), 95.0 (C_4), 87.9 (C_1), 65.9 (C_2), 61.7 (C_3 or C_6), 61.6 (C_3 or C_6), 20.9 (2C, $\text{C}(\text{O})\text{CH}_3$), 20.6 ($\text{C}(\text{O})\text{CH}_3$);

HRMS m/z (ES^+) [Found: $(\text{M}+\text{NH}_4)^+$ 306.1197 $\text{C}_{12}\text{H}_{16}\text{O}_8$ requires $\text{M}+\text{NH}_4^+$, 306.1228].

1,2,3-Tri-O-acetyl-4-deoxy-6-O-tert-butyldimethylsilyl- β -D-manno-hex-4-eno-1,5-pyranoside **149**



To a solution of **148** (135 mg, 0.47 mmol, 1.0 equiv.) in MeCN (5 mL) was added DMAP (29 mg, 0.24 mmol, 0.5 equiv.). The solution was cooled to 0 °C then imidazole (35 mg, 0.52 mmol, 1.1 equiv.) and TBDMSCI (107 mg, 0.71 mmol, 1.5 equiv.) were added successively before warming to RT. After stirring for 3 h, the reaction mixture was extracted with EtOAc (40 mL) and washed with H_2O (2 \times 30 mL), brine (30 mL), dried (MgSO_4), filtered and concentrated *in vacuo*. Purification by silica gel column chromatography, eluting in Hex/EtOAc (1/1) afforded **149** as a yellow oil (103 mg, 0.26 mmol, 54%).

R_f 0.58 (Hex/EtOAc, 2/1);

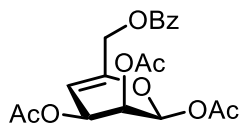
$[\alpha]_D^{26} +5.1$ ($c = 2.35$, CHCl_3);

$^1\text{H NMR}$ (400 MHz, CDCl_3) δ_{H} 6.26 (1H, d, $J = 2.7$ Hz, H_1), 5.49 (1H, td, $J = 5.1$, 1.2 Hz, H_3), 5.25 (1H, dd, $J = 5.1$, 2.7 Hz, H_2), 5.05 (1H, dt, $J = 5.1$, 1.3 Hz, H_4), 3.98 (2H, brs, H_6 , H_6'), 2.07 (3H, s, C(O)CH_3), 2.01 (6H, s, C(O)CH_3), 0.85-0.81 (15H, m, $2 \times -\text{SiCH}_3$, $3 \times -\text{SiC(CH}_3)_3$);

$^{13}\text{C NMR}$ (100 MHz, CDCl_3) δ_{C} 170.5 (C=O), 169.7 (C=O), 169.4 (C=O), 154.6 (C_5), 93.6 (C_4), 87.6 (C_1), 66.0 (C_2), 61.5 (C_3), 61.5 (C_6), 25.9 ($-\text{SiC(CH}_3)_3$), 25.8 ($-\text{SiC(CH}_3)_3$), 25.6 ($-\text{SiC(CH}_3)_3$), 20.9 (2C, C(O)CH_3), 20.6 (C(O)CH_3); 18.3 ($-\text{SiC(CH}_3)_3$), -5.4 (2C, $2 \times -\text{SiCH}_3$);

HRMS m/z (ESI $^+$) [Found: $(\text{M}+\text{Na})^+$ 425.1610 $\text{C}_{18}\text{H}_{30}\text{O}_8\text{Si}$ requires $\text{M}+\text{Na}^+$, 425.1608].

1,2,3-Tri-O-acetyl-4-deoxy-6-O-benzoyl- β -D-manno-hex-4-eno-1,5-pyranoside **150**



To a solution of **148** (0.20 g, 0.7 mmol, 1.0 equiv.) in DCM (6.9 mL) was added DMAP (43 mg, 0.35 mmol, 0.5 equiv.). The solution was cooled to 0 °C then pyridine (62 μL , 0.76 mmol, 1.1 equiv.) and BzCl (0.12 mL, 1.0 mmol, 1.5 equiv.) were added successively before warming to RT. After stirring for 15 h, the reaction mixture was diluted with DCM (50 mL) and washed with 0.5 M HCl (30 mL), saturated aqueous NaHCO_3 solution (2×30 mL), H_2O (30 mL) and brine (30 mL). The organic layer was dried (MgSO_4) filtered and concentrated *in vacuo*. Purification by silica gel

column chromatography, eluting in Hex/EtOAc (1/1) afforded **150** as a colourless oil (0.19 g, 0.49 mmol, 71%).

R_f 0.8 (Hex/EtOAc, 1/2);

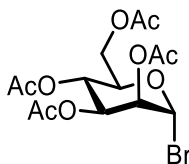
[α]_D²⁶ +5.0 (c = 4.05, CHCl₃);

¹H NMR (400 MHz, CDCl₃) δ_H 8.05 (2H, d, J = 7.5 Hz, Ar-H), 7.59 (1H, t, J = 7.5 Hz, Ar-H), 7.46 (2H, t, J = 7.5 Hz, Ar-H), 6.40 (1H, brs, H₁), 5.59-5.57 (1H, m, H₃), 5.39-5.35 (1H, m, H₂), 5.22 (1H, d, J = 4.6 Hz, H₄), 4.77 (2H, brs, H₆, H_{6'}), 2.14 (3H, s, C(O)CH₃), 2.09 (6H, s, C(O)CH₃);

¹³C NMR (100 MHz, CDCl₃) δ_C 170.4 (C=O), 169.7 (C=O), 169.2 (C=O), 165.7 (C=O), 150.2 (C₅), 133.4 (Ar-C), 129.8 (Ar-C), 129.5 (Ar-C), 128.5 (Ar-C), 97.5 (C₄), 87.8 (C₁), 65.7 (C₂), 62.4 (C₆), 61.4 (C₃), 20.8 (2C, C(O)CH₃), 20.6 (C(O)CH₃);

HRMS m/z (ES⁺) [Found: (M+NH₄)⁺ 410.1472 C₁₉H₂₀O₉ requires M+NH₄⁺, 410.1490].

2,3,4,6-Tetra-O-acetyl-α-D-mannopyranosyl bromide **155**



To a solution of **14** (0.50 g, 1.3 mmol, 1.0 equiv.) in DCM (4 mL) at 0 °C was added successively PBr₃ (0.20 mL, 2.2 mmol, 1.7 equiv.) and H₂O (0.14 mL, 7.7 mmol, 6.0 equiv.). After 15 min, the reaction mixture was warmed to RT and after stirring for 3 h the reaction mixture was quenched with saturated aqueous NaHCO₃ solution (4

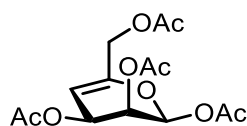
mL) and extracted with DCM (50 mL). The organic layer was washed with H₂O (2 × 40 mL), brine (40 mL), dried (MgSO₄), filtered and concentrated *in vacuo* to afford **155** as a yellow oil (0.44 g, 1.1 mmol, 84%). These data were in good agreement with literature values.¹⁷³

R_f 0.51 (Pet. ether/EtOAc, 2/1);

¹H NMR (400 MHz, CDCl₃) δ_H 6.28 (1H, d, *J* = 1.3 Hz, H₁), 5.70 (1H, dd, *J* = 10.2, 3.4 Hz, H₃) 5.43 (1H, dd, *J* = 3.4, 1.3 Hz, H₂), 5.36 (1H, appt, *J* = 10.2 Hz, H₄), 4.32 (1H, dd, *J* = 12.5, 4.9 Hz, H₆), 4.24-4.18 (1H, m, H₅), 4.12 (1H, dd, *J* = 12.5, 2.2 Hz, H_{6'}), 2.17 (3H, s, C(O)CH₃), 2.10 (3H, s, C(O)CH₃), 2.06 (3H, s, C(O)CH₃), 2.00 (3H, s, C(O)CH₃);

¹³C NMR (100 MHz, CDCl₃) δ_C 170.9 (C=O), 170.1 (C=O), 169.9 (2C, 2 × C=O), 83.4 (C₁), 73.1 (C₅), 72.5 (C₂), 68.3 (C₃), 65.6 (C₄), 61.8 (C₆), 21.1 (C(O)CH₃), 21.0 (2C, C(O)CH₃), 20.9 (C(O)CH₃).

1,2,3,6-Tetra-*O*-acetyl-4-deoxy-β-D-manno-hex-eno-1,5-pyranoside **158**



To a solution of **148** (90 mg, 0.31 mmol, 1.0 equiv.) in DCM (3.1 mL) was added successively DMAP (18 mg, 0.16 mmol, 0.5 equiv.), pyridine (38 μL, 0.47 mmol, 1.5 equiv.) and Ac₂O (60 μL, 0.62 mmol, 2.0 equiv.). After stirring for 3 h, the reaction mixture was diluted with DCM (25 mL), washed with 1M HCl (20 mL), saturated aqueous NaHCO₃ solution (20 mL), H₂O (20 mL), brine (20 mL), dried (MgSO₄), filtered and concentrated *in vacuo*. Purification by silica gel column chromatography,

eluting with Pet. ether/EtOAc (3/1, 1/1) afforded **158** as a colourless oil (62 mg, 0.19 mmol, 61%).

R_f 0.61 (Pet. ether/EtOAc, 1/1);

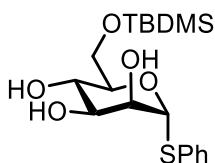
$[\alpha]_D^{26} +19.9$ ($c = 1.80$, CHCl_3);

^1H (400 MHz, CDCl_3) δ_{H} 6.27 (1H, dd, $J = 2.6, 1.0$ Hz, H_1), 5.48-5.44 (1H, dd, $J = 5.0, 1.0$ Hz, H_3), 5.24 (1H, dd, $J = 5.1, 2.6$ Hz, H_2), 5.04 (1H, d, $J = 4.8$ Hz, H_4), 4.42 (2H, brs, H_6, H_6'), 2.06 (3H, s, C(O)CH_3), 2.01 (3H, s, C(O)CH_3), 2.00 (3H, s, C(O)CH_3), 1.99 (3H, s, C(O)CH_3);

^{13}C (100 MHz, CDCl_3) δ_{C} 170.3 (C=O), 170.0 (C=O), 169.6 (C=O), 169.1 (C=O), 149.9 (C_5), 97.5 (C_4), 87.7 (C_1), 65.5 (C_2), 62.0 (C_6), 61.3 (C_3), 20.7 (2C, C(O)CH_3), 20.6 (C(O)CH_3), 20.4 (C(O)CH_3);

HRMS m/z (ESI⁺) [Found: $(\text{M}+\text{NH}_4)^+$ 348.1299 $\text{C}_{14}\text{H}_{18}\text{O}_9$ requires $\text{M}+\text{NH}_4^+$, 348.1334].

Phenyl 6-*O*-*tert*-butyldimethylsilyl-1-thio- α -D-mannopyranose **160**



To a solution of **109** (1.16 g, 4.3 mmol, 1.0 equiv.) in MeCN (21 mL) was added successively DMAP (0.26 g, 2.1 mmol, 0.5 equiv.), imidazole (0.32 g, 4.7 mmol, 1.1 equiv.) and TBDMSCl (0.96 g, 6.4 mmol, 1.5 equiv.). After stirring for 2 h, the solvent was concentrated *in vacuo* and the resultant residue was purified immediately by

silica gel column chromatography, eluting in Pet. ether/EtOAc (1/1, 1/2) to afford **160** as a white solid (1.44 g, 3.7 mmol, 87%). These data were in good agreement with literature values.¹⁷⁴

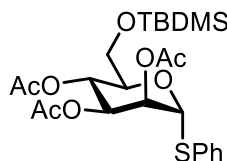
R_f 0.26 (Pet. ether/EtOAc, 1/1);

¹H NMR (400 MHz, CDCl₃) δ_H 7.43-7.39 (2H, m, Ar-H), 7.26-7.17 (3H, m, Ar-H), 5.48 (1H, d, *J* = 1.1 Hz, H₁), 4.16 (1H, brs, H₂), 4.08 (1H, dd, *J* = 5.4, 3.5 Hz, H₄), 3.87-3.79 (3H, m, H₃, H₆, H_{6'}), 3.72 (1H, s, H₅), 3.58 (1H, d, *J* = 3.4 Hz, C₃-OH), 3.28 (1H, d, *J* = 4.2 Hz, C₂-OH), 0.84 (9H, s, 3 × -SiC(CH₃)₃), 0.04 (6H, s, 2 × -SiCH₃);

¹³C NMR (100 MHz, CDCl₃) δ_C 134.2 (Ar-C), 131.6 (Ar-C), 129.2 (Ar-C), 127.5 (Ar-C), 87.9 (C₁), 72.3 (C₅), 72.0 (C₂), 71.7 (C₄), 70.9 (C₃), 64.8 (C₆), 26.0 (3C, 3 × -SiC(CH₃)₃), 18.4 (-SiC(CH₃)₃), -5.3 (2C, 2 × -SiCH₃);

HRMS *m/z* (ES⁺) [Found: (M+NH₄)⁺ 404.1937 C₁₈H₃₀O₅SSi requires M+NH₄⁺, 404.1923].

2,3,4-Tri-O-acetyl-6-O-*tert*-butyldimethylsilyl-1-thio-α-D-mannopyranoside **161**



To a solution of **160** (1.36 g, 3.5 mmol, 1.0 equiv.) in DCM (35 mL) was added successively pyridine (0.85 mL, 10 mmol, 3.0 equiv.), Ac₂O (1.32 mL, 14.0 mmol, 4.0 equiv.) and DMAP (0.21 g, 1.8 mmol, 0.5 equiv.). After stirring for 3 h, the reaction mixture was diluted with DCM (100 mL) then washed with H₂O (2 × 50 mL), brine (2 × 50 mL), dried (MgSO₄), filtered and concentrated *in vacuo*. Purification by

silica gel column chromatography, eluting in Pet. ether/EtOAc (3/1) afforded **161** as a colourless oil (1.54 g, 3.0 mmol, 86%).

R_f 0.79 (Pet. ether/EtOAc, 1/1);

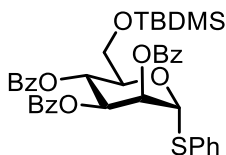
$[\alpha]_D^{26} +91.2$ ($c = 3.50$, CHCl_3);

$^1\text{H NMR}$ (400 MHz, CDCl_3) δ_{H} 7.49-7.45 (2H, m, Ar-H), 7.29-7.22 (2H, m, Ar-H), 5.43 (2H, m, H₂, H₁), 5.31 (1H, appt, $J = 9.8$ Hz, H₄), 5.26 (1H, dd, $J = 9.8, 3.0$ Hz, H₃), 4.31 (1H, ddd, $J = 9.2, 5.2, 2.4$ Hz, H₅), 3.70 (2H, ddd, $J = 14.0, 11.5, 3.9$ Hz, H₆, H_{6'}), 2.08 (3H, s, C(O)CH₃), 2.02 (3H, s, C(O)CH₃), 1.98 (3H, s, C(O)CH₃), 0.87-0.84 (9H, m, 3 × -SiC(CH₃)₃), 0.00 (6H, s, 2 × -SiCH₃);

^{13}C (100 MHz, CDCl_3) δ_{C} 170.2 (2C, C=O), 169.8 (C=O), 133.4 (Ar-C), 132.2 (Ar-C), 129.2 (Ar-C), 128.0 (Ar-C), 85.9 (C₁), 72.6 (C₃), 71.4 (C₂), 69.9 (C₃), 66.8 (C₄), 62.5 (C₆), 26.0 (3C, 3 × -SiC(CH₃)₃), 21.0 (C(O)CH₃), 20.9 (C(O)CH₃), 20.8 (C(O)CH₃), 18.5 (-SiC(CH₃)₃), -5.3 (2C, 2 × -SiCH₃);

HRMS m/z (ES⁺) [Found: (M+NH₄)⁺ 530.2248 C₂₄H₃₆O₈SSi requires M+NH₄⁺, 530.2283].

2,3,4-Tetra-O-benzoyl-6-O-*tert*-butyldimethylsilyl-1-thio- α -D-mannopyranoside **163**



To a solution of **160** (0.74 g, 1.9 mmol, 1.0 equiv.) in DCM (12.5 mL) was added successively DMAP (0.10 g, 1.0 mmol, 0.5 equiv.), pyridine (0.46 mL, 5.7 mmol, 3.0

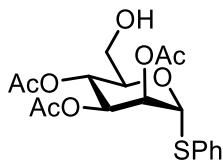
equiv.) and BzCl (1.11 mL, 9.6 mmol, 5.0 equiv.). After stirring for 7 h, the reaction mixture was diluted with DCM (70 mL), washed with H₂O (2 × 30 mL), brine (2 × 30 mL), dried (MgSO₄), filtered and concentrated *in vacuo*. Purification by silica gel column chromatography, eluting with Pet. ether/EtOAc (8/1) afforded **163** as a colourless oil (0.99 g, 1.4 mmol, 74%). These data were in good agreement with literature values.¹⁷⁵

R_f 0.93 (Pet. ether/EtOAc, 2/1);

¹H NMR (400 MHz, CDCl₃) δ_H 8.09 (2H, dd, *J* = 5.2, 3.2 Hz, Ar-*H*), 8.02-7.97 (2H, m, Ar-*H*), 7.91-7.85 (2H, m, Ar-*H*), 6.07 (1H, appt, *J* = 10.1 Hz, H₄), 5.94 (1H, dd, *J* = 3.2, 1.6 Hz, H₂), 5.81 (1H, dd, *J* = 10.1, 3.2 Hz, H₃), 5.76 (1H, d, *J* = 1.6 Hz, H₁), 4.68 (1H, ddd, *J* = 10.0, 4.7, 2.2 Hz, H₅), 3.90 (2H, ddd, *J* = 13.8, 11.5, 3.5 Hz, H₆, H_{6'}), 0.90-0.86 (9H, m, 3 × -SiC(CH₃)₃), 0.02-0.00 (6H, m, 2 × -SiCH₃);

¹³C NMR (100 MHz, CDCl₃) δ_C 165.9 (C=O), 165.8 (C=O), 165.6 (C=O), 133.8 (Ar-C), 133.7 (Ar-C), 133.6 (Ar-C), 133.5 (Ar-C), 130.3 (Ar-C), 130.1 (2C, Ar-C), 129.7 (Ar-C), 129.5 (Ar-C), 129.4 (Ar-C), 128.9 (Ar-C), 128.8 (Ar-C), 128.7 (Ar-C), 128.3 (Ar-C), 86.4 (C₁), 73.1 (C₅), 72.5 (C₂), 71.2 (C₃), 67.2 (C₄), 62.6 (C₆), 26.2 (3C, 3 × -SiC(CH₃)₃), 18.6 (-SiC(CH₃)₃), -5.2 (2C, 2 × -SiCH₃).

Phenyl 2,3,4-tri-O-acetyl-1-thio- α -D-mannopyranoside **162**



To a solution of **161** (0.50 g, 0.98 mmol, 1.0 equiv.) in DCM (9.8 mL) at 0 °C was added $\text{BF}_3 \cdot \text{OEt}_2$ (61 μL , 0.49 mmol, 0.5 equiv.). After stirring for 2.5 h, the reaction mixture was quenched with saturated aqueous NaHCO_3 solution (10 mL) then diluted with DCM (50 mL). The organic layer was washed with H_2O (30 mL), brine (30 mL), dried (MgSO_4), filtered and concentrated *in vacuo*. Purification by silica gel column chromatography, eluting with Tol/acetone (7/1) afforded **162** as a colourless oil (0.29 g, 0.73 mmol, 74%). These data were in good agreement with literature values.^{176,177}

R_f 0.24 (Pet. ether/EtOAc, 2/1);

$[\alpha]_D^{26} +87.5$ ($c = 2.00$, CHCl_3);

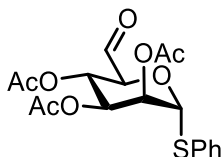
$^1\text{H NMR}$ (400 MHz, CDCl_3) δ_H 7.46 (2H, dt, $J = 4.6, 2.6$ Hz, Ar-*H*), 7.34-7.27 (3H, m, Ar-*H*), 5.50 (1H, dd, $J = 3.2, 1.5$ Hz, H_2), 5.49 (1H, d, $J = 1.4$ Hz, H_1), 5.37 (1H, dd, $J = 10.1, 3.2$ Hz, H_3), 5.30 (1H, appt, $J = 9.9$ Hz, H_4), 4.28 (1H, dd, $J = 9.9, 1.3$ Hz, H_5) 3.71-3.59 (2H, m, H_6, H_6'), 2.13 (3H, s, $\text{C}(\text{O})\text{CH}_3$), 2.09 (3H, s, $\text{C}(\text{O})\text{CH}_3$), 2.02 (3H, s, $\text{C}(\text{O})\text{CH}_3$);

$^{13}\text{C NMR}$ (100 MHz, CDCl_3) δ_C 170.9 (C=O), 170.1 (C=O), 169.9 (C=O), 132.7 (Ar-C), 132.2 (Ar-C), 129.3 (Ar-C), 129.1 (Ar-C), 128.3 (Ar-C), 128.2 (Ar-C), 85.9 (C_1),

71.9 (C₅), 71.1 (C₃), 69.3 (C₂), 66.6 (C₄), 61.3 (C₆), 21.0 (C(O)CH₃), 20.8 (C(O)CH₃), 20.7 (C(O)CH₃);

HRMS *m/z* (ES⁺) [Found: (M+Na)⁺ 421.0936 C₁₈H₂₂O₈S requires *M+Na*⁺, 421.0933].

Phenyl 2,3,4-tri-O-acetyl-1-thio- α -D-manno-hexodialdo-1,5-pyranoside **165**



To a solution of **162** (0.26 g, 0.65 mmol, 1.0 equiv.) in DCM (6.5 mL) was added DMP (0.33 g, 0.78 mmol, 1.2 equiv.). After stirring for 6 h, the reaction mixture was quenched with 10% aqueous Na₂S₂O₃ solution (10 mL) then diluted with DCM (50 mL). The organic layer was washed with 10% aqueous Na₂S₂O₃ solution (25 mL), saturated aqueous NaHCO₃ solution (25 mL), H₂O (25 mL), brine (25 mL), dried (MgSO₄), filtered and concentrated *in vacuo*. Drying under high vacuum afforded **165** as a white solid (0.24 g, 0.60 mmol, 92%) which was used without any further purification.

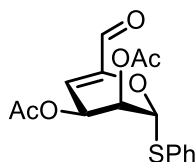
R_f 0.07 (Pet. ether/EtOAc, 2/1);

¹H NMR (400 MHz, CDCl₃) δ _H 9.59 (1H, s, CHO), 7.55-7.44 (3H, m, Ar-H), 7.34-7.28 (2H, m, Ar-H), 5.54 (1H, d, *J* = 2.7 Hz, H₁), 5.47 (1H, appt, *J* = 2.7 Hz, H₂), 5.44 (1H, appt, *J* = 9.3 Hz, H₄), 5.35-5.31 (1H, m, H₃) 4.62 (1H, d, *J* = 9.2 Hz, H₅), 2.13 (3H, s, C(O)CH₃), 2.08 (3H, s, C(O)CH₃), 2.02 (3H, s, C(O)CH₃);

^{13}C NMR (100 MHz, CDCl_3) δ_{C} 196.0 (CHO), 169.9 (2C, C=O), 169.7 (C=O), 133.3 (Ar-C), 132.2 (Ar-C), 132.1 (Ar-C), 129.5 (Ar-C), 128.4 (Ar-C), 85.5 (C_1), 74.9 (C_5), 70.1 (C_2), 68.7 (C_3), 65.6 (C_4), 20.9 (C(O)CH₃), 20.8 (C(O)CH₃), 20.7 (C(O)CH₃).

Phenyl 2,3-di-O-acetyl-4-deoxy-1-thio- α -D-manno-hex-4-enedialdo-1,5-pyranoside

166



To a solution of **165** (0.24 g, 0.60 mmol, 1.0 equiv.) in DCM (6 mL) was added Et₃N (0.10 mL, 0.72 mmol, 1.2 equiv.). After stirring for 3 h, the reaction mixture was diluted with DCM (50 mL), washed with H₂O (2 × 25 mL), brine (25 mL), dried (MgSO₄), filtered and concentrated *in vacuo*. Purification by silica gel column chromatography, eluting with Pet. ether/EtOAc (2/1, 1/1) afforded **166** as a yellow oil (0.11 g, 0.33 mmol, 55%).

R_f 0.80 (Pet. ether/EtOAc, 1/1);

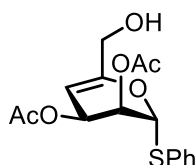
$[\alpha]_{\text{D}}^{26} +221.9$ ($c = 4.70$, CHCl_3);

^1H NMR (400 MHz, CDCl_3) δ_{H} 9.28 (1H, s, CHO), 7.55-7.51 (2H, m, Ar-H), 7.36-7.32 (3H, m, Ar-H), 5.89 (1H, dd, $J = 2.9$ Hz, 1.5 Hz, H₄), 5.81 (1H, dd, $J = 4.4$, 2.9 Hz, H₃), 5.63 (1H, d, $J = 3.8$ Hz, H₁), 5.49 (1H, appt, $J = 4.0$ Hz, H₂), 2.11 (3H, s, C(O)CH₃), 2.09 (3H, s, C(O)CH₃);

^{13}C NMR (100 MHz, CDCl_3) δ_{C} 185.5 (CHO), 169.9 (C=O), 169.8 (C=O), 150.1 (C_5), 133.4 (Ar-C), 131.2 (Ar-C), 129.5 (Ar-C), 129.2 (Ar-C), 129.0 (Ar-C), 128.3 (Ar-C), 116.3 (C_4), 84.9 (C_1), 65.7 (C_2), 63.1 (C_3), 20.8 (2C, $\text{C}(\text{O})\text{CH}_3$);

HRMS m/z (ES^+) [Found: $(\text{M}+\text{NH}_4)^+$ 354.1018 $\text{C}_{16}\text{H}_{16}\text{O}_6\text{S}$ requires $\text{M}+\text{NH}_4^+$, 354.1051].

Phenyl 2,3-di-O-acetyl-4-deoxy-1-thio- α -D-manno-hex-4-eno-1,5-pyranoside **167**



To a solution of **166** (172 mg, 0.51 mmol, 1.0 equiv.) in THF (5.1 mL) was added at 0 °C NaBH_4 (23 mg, 0.61 mmol, 1.2 equiv.). After stirring for 1.5 h, the reaction mixture was quenched with saturated aqueous NH_4Cl solution (5 mL), extracted with EtOAc (30 mL), washed with H_2O (2 \times 25 mL), brine (25 mL), dried (MgSO_4), filtered and concentrated *in vacuo*. Purification by silica gel column chromatography, eluting with Pet. ether/EtOAc (2/1, 1/1, 1/2) afforded **167** as a colourless oil (90 mg, 0.27 mmol, 52%).

R_f 0.30 (Pet. ether/EtOAc, 2/1);

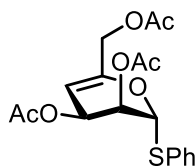
$[\alpha]_D^{26} +180.7$ ($c = 2.40$, CHCl_3);

^1H (400 MHz, CDCl_3) δ_{H} 7.52-7.48 (2H, m, Ar-H), 7.33-7.29 (3H, m, Ar-H), 5.54 (1H, ddd, $J = 4.3, 2.6, 0.9$ Hz, H_3), 5.45 (1H, d, $J = 7.3$ Hz, H_1), 5.17 (1H, dd, $J = 8.0, 4.0$ Hz, H_2), 5.01-4.99 (1H, d, $J = 4.0$ Hz, H_4), 4.04 (2H, d, $J = 4.6$ Hz, H_6, H_6'); 2.08 (3H, s, $\text{C}(\text{O})\text{CH}_3$); 2.04 (3H, s, $\text{C}(\text{O})\text{CH}_3$);

^{13}C (100 MHz, CDCl_3) δ_{C} 170.4 (C=O), 169.7 (C=O), 155.5 (C_5), 133.2 (Ar-C), 131.4 (Ar-C), 129.2 (Ar-C), 128.6 (Ar-C), 94.8 (C_4), 83.0 (C_1), 66.7 (C_2), 63.4 (C_3), 61.9 (C_6), 21.0 ($\text{C}(\text{O})\text{CH}_3$), 20.8 ($\text{C}(\text{O})\text{CH}_3$);

HRMS m/z (ES^+) [Found: ($\text{M}+\text{Na}$) $^+$ 351.0735 $\text{C}_{16}\text{H}_{18}\text{O}_6\text{S}$ requires $\text{M}+\text{Na}^+$, 351.0721].

Phenyl 2,3,6-tri-O-acetyl-4-deoxy-1-thio- α -D-manno-hex-4-eno-1,5-pyranoside **168**



To a solution of **167** (90 mg, 0.27 mmol, 1.0 equiv.) in DCM (2.7 mL) was added successively DMAP (16 mg, 0.14 mmol, 0.5 equiv.), pyridine (33 μL , 0.41 mmol, 1.5 equiv.) and Ac_2O (51 μL , 0.54 mmol, 2.0 equiv.). After stirring for 2 h, the reaction mixture was diluted with DCM (30 mL), washed with 1M HCl (20 mL), saturated aqueous NaHCO_3 solution (20 mL), H_2O (20 mL), brine (20 mL), dried (MgSO_4), filtered and concentrated *in vacuo*. Purification by silica gel column chromatography, eluting with Pet. ether/EtOAc (2/1, 1/1) afforded **168** as a colourless oil (73 mg, 0.19 mmol, 71%).

R_f 0.52 (Pet. ether/EtOAc, 2/1);

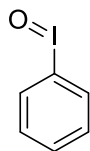
$[\alpha]_D^{26} +247.2$ ($c = 1.40$, CHCl_3);

^1H (400 MHz, CDCl_3) δ_{H} 7.53 (2H, m, Ar-H), 7.33-7.30 (3H, m, Ar-H), 5.55 (1H, appt, $J = 4.3$ Hz, H_3), 5.46 (1H, d, $J = 6.7$ Hz, H_1), 5.21 (1H, dd, $J = 6.7, 4.3$ Hz, H_2), 5.04-5.01 (1H, m, H_4), 4.51 (2H, d, $J = 5.8$ Hz, H_6, H_6'), 2.09 (3H, s, $\text{C}(\text{O})\text{CH}_3$), 2.07 (3H, s, $\text{C}(\text{O})\text{CH}_3$); 2.06 (3H, s, $\text{C}(\text{O})\text{CH}_3$);

^{13}C (100 MHz, CDCl_3) δ_{c} 170.6 (C=O), 170.5 (C=O), 170.0 (C=O), 151.3 (C₅), 133.6 (Ar-C), 131.8 (Ar-C), 129.5 (Ar-C), 129.0 (Ar-C), 98.0 (C₄), 83.6 (C₁), 66.7 (C₂), 63.5 (C₃), 62.9 (C₆), 21.3 (C(O)CH₃), 21.2 (2C, C(O)CH₃);

HRMS m/z (ES⁺) [Found: (M+Na)⁺ 403.0845 C₁₈H₂₀O₇S requires $M+\text{Na}^+$, 403.0828].

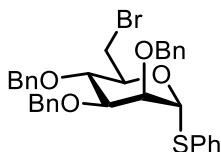
Iodosobenzene **170**



A freshly prepared solution of 3M NaOH (24 mL) was added dropwise to a beaker equipped with stirring bar containing BAIB (5.0 g, 15.5 mmol) at 0 °C. The solution was stirred vigorously and agitated with a spatula to break up solid lumps then after 15 min removed from the ice bath and warmed to RT. After 45 mins, 20 mL of water was added to the vigorously stirring solution and the crude solid was collected in a sinter funnel. This procedure was repeated once again then the solid was dried. The dry yellow solid was triturated with chloroform (20 mL) then collected in a sinter funnel and left to dry under vacuum for 3 h, then dried overnight in a desiccator over P₂O₅ to afford **170** as a yellow solid (3.21 g, 14.6 mmol, 94%).

6.5.8 6-Amino-6-deoxy- α -D-mannopyranose derivatives

6-Bromo-6-deoxy-2,3,4-tri-O-benzyl-1-thio- α -D-mannopyranoside **175**



To a solution of **112** (500 mg, 0.92 mmol, 1.0 equiv.) in DCM (9 mL) at 0 °C was added successively Ph_3P (410 mg, 1.56 mmol, 1.7 equiv.) and CBr_4 (520 mg, 1.56 mmol, 1.7 equiv.) before warming to RT. After stirring for 16 h, the reaction mixture was poured onto H_2O (30 mL) and diluted with DCM (30 mL). The organic layer was washed with H_2O (2 \times 30 mL), brine (30 mL), dried (MgSO_4), filtered and concentrated *in vacuo*. Purification by silica gel column chromatography, eluting with Pet. ether/EtOAc (6/1) afforded **175** as a yellow oil (420 mg, 0.69 mmol, 75%).

R_f 0.90 (Pet. ether/EtOAc, 3/1);

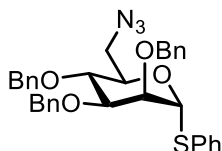
$[\alpha]_D^{26} +51.4$ ($c = 0.70$, CHCl_3);

^1H NMR (400 MHz, CDCl_3) δ_H 7.48-7.45 (2H, m, Ar-H), 7.40-7.27 (18H, m, Ar-H), 5.59 (1H, d, $J = 1.5$ Hz, H_1), 5.01 (1H, d, $J = 10.9$ Hz, CH_2Ph), 4.76-4.60 (5H, m, CH_2Ph), 4.31-4.25 (1H, m, H_5), 4.06-4.00 (2H, m, H_2, H_4), 3.87 (1H, dd, $J = 9.3, 3.0$ Hz, H_3), 3.69-3.66 (2H, m, H_6, H_6');

^{13}C NMR (100 MHz, CDCl_3) δ_C 138.3 (Ar-C), 138.1 (Ar-C), 137.9 (Ar-C), 134.2 (Ar-C), 131.8 (Ar-C), 129.2 (Ar-C), 128.6 (2C, Ar-C), 128.5 (Ar-C), 128.2 (Ar-C), 128.0 (3C, Ar-C), 127.9 (Ar-C), 127.7 (Ar-C), 86.0 (C_1), 80.1 (C_3), 76.9 (C_4), 76.3 (C_2), 75.6 (CH_2Ph), 72.3 (C_5), 72.2 (CH_2Ph), 72.1 (CH_2Ph), 33.4 (C_6);

HRMS m/z (ESI⁺) [Found: (M+Na)⁺ 628.1184 C₃₃H₃₃BrO₄S requires M+Na⁺, 628.1180].

6-Azido-6-deoxy-2,3,4-tri-O-benzyl-1-thio- α -D-mannopyranoside **176**



To a solution of **175** (0.36 g, 0.59 mmol, 1.0 equiv.) in DMF (4 mL) was added NaN₃ (77 mg, 1.2 mmol, 2.0 equiv.). The reaction mixture was heated to 75 °C and stirred for 18 h, before being cooled to RT, poured onto H₂O (15 mL) and extracted with EtOAc (30 mL). The organic layer was washed saturated aqueous Na₂S₂O₃ solution (20 mL), H₂O (20 mL), brine (20 mL), dried (MgSO₄), filtered and concentrated *in vacuo*. Purification by silica gel column chromatography, eluting with Tol/EtOAc (12/1, 9/1, 6/1) afforded **176** as a yellow oil (214 mg, 0.38 mmol, 64%).

R_f 0.74 (Tol/EtOAc, 6/1);

[α]_D²⁶ +35.5 (*c* = 0.45, CHCl₃);

¹H NMR (400 MHz, CDCl₃) δ _H 7.46-7.28 (20H, m, Ar-H), 5.58 (1H, d, *J* = 1.6 Hz, H₁), 5.00 (1H, d, *J* = 11.0 Hz, CH₂Ph), 4.77-4.68 (2H, m, CH₂Ph), 4.69-4.62 (3H, m, CH₂Ph), 4.29-4.23 (1H, m, H₅), 4.03 (1H, dd, *J* = 2.9, 1.6 Hz, H₂), 3.99 (1H, appt, *J* = 9.4 Hz, H₄), 3.88 (1H, dd, *J* = 9.4, 2.9 Hz, H₃), 3.48 (2H, m, H₆, H_{6'});

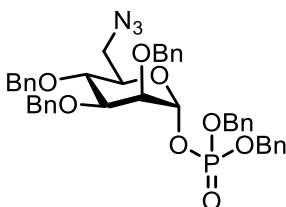
¹³C NMR (100 MHz, CDCl₃) δ _C 138.3 (Ar-C), 138.1 (Ar-C), 137.9 (Ar-C), 134.1 (Ar-C), 131.6 (Ar-C), 129.3 (Ar-C), 128.6 (2C, Ar-C), 128.2 (Ar-C), 128.1 (Ar-C), 128.0

(2C, Ar-C), 127.9 (Ar-C), 127.7 (Ar-C), 85.8 (C₁), 80.1 (C₃), 76.3 (C₂), 75.6 (CH₂Ph), 75.5 (C₄), 72.7 (C₅), 72.2 (2C, CH₂Ph), 51.6 (C₆);

HRMS *m/z* (ESI⁺) [Found: (M+Na)⁺ 590.2113 C₃₃H₃₃N₃O₄S requires M+Na⁺, 590.2090];

$\nu_{\max}/\text{cm}^{-1}$ 2097 (N=N=N stretching).

Dibenzyl 6-azido-6-deoxy-2,3,4-tri-O-benzyl- α -D-mannopyranosyl phosphate **177**



Prepared as per Procedure A using thioglycoside **176** (196 mg, 0.26 mmol, 1.0 equiv.), DBP (108 mg, 0.39 mmol, 1.5 equiv.), NIS (88 mg, 0.39 mmol, 1.5 equiv.) and AgOTf (20 mg, 78 μmol , 0.3 equiv.) in DCM (2.6 mL). Reaction time: 45 min. Purification by silica gel column chromatography, eluting with Pet. ether/EtOAc (5/1, 3/1, 2/1) afforded **177** as a yellow oil (124 mg, 0.16 mmol, 65%).

R_f 0.44 (Tol/EtOAc, 6/1);

$[\alpha]_D^{26} +53.6$ ($c = 0.2$, CHCl₃);

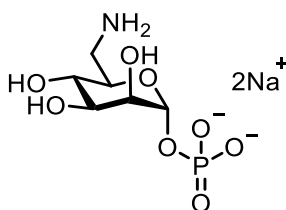
¹H NMR (400 MHz, CDCl₃) δ_H 7.34-7.28 (23H, m, Ar-H), 7.26-7.24 (2H, m, Ar-H), 5.70 (1H, dd, $J_{H1-P} = 6.1$ Hz, $J_{H1-H2} = 1.9$ Hz, H₁), 5.08-4.89 (5H, m, CH₂Ph), 4.63 (2H, s, CH₂Ph), 4.56 (1H, d, $J = 11.0$ Hz, CH₂Ph), 4.48 (2H, s, CH₂Ph), 3.95 (1H, appt, $J = 9.5$ Hz, H₄), 3.83 (1H, ddd, $J = 9.5, 4.5, 2.7$ Hz, H₅), 3.78 (1H, dd, $J = 9.5, 3.0$ Hz, H₃), 3.70-3.68 (1H, m, H₂), 3.35-3.25 (2H, m, H₆, H_{6'});

$^{13}\text{C}\{^{31}\text{P}\}$ NMR (100 MHz, CDCl_3) δ_{C} 138.1 (Ar-C), 138.0 (Ar-C), 137.7 (Ar-C), 135.6 (2C), 135.5 (2C, Ar-C), 128.7 (3C, Ar-C), 128.4 (3C, Ar-C), 128.1 (Ar-C), 128.0 (Ar-C), 127.9 (2C, Ar-C), 127.8 (2C, Ar-C), 127.7 (Ar-C), 96.0 (C_1), 78.6 (C_3), 75.3 (CH_2Ph), 74.3 (C_4), 74.2 (C_2), 73.3 (C_5), 72.8 (CH_2Ph), 72.1 (CH_2Ph), 69.6 (CH_2Ph), 69.5 (CH_2Ph), 51.0 (C_6);

^{31}P NMR (161 MHz, CDCl_3) δ_{P} -2.8 (1P, d, $J_{\text{H1-P}} = 6.1$ Hz);

HRMS m/z (ESI $^+$) [Found: ($\text{M}+\text{Na}$) $^+$ 758.2647 $\text{C}_{41}\text{H}_{42}\text{N}_3\text{O}_8\text{P}$ requires $\text{M}+\text{Na}^+$, 758.2608].

6-Amino-6-deoxy- α -D-mannopyranosyl phosphate (disodium salt) **174**



A suspension of **177** (48 mg, 65 μmol , 1.0 equiv.), Pd/C (10% loading, 11 mg, 11 μmol , 0.03 equiv. per benzyl) and Pd(OH) $_2$ /C (20% loading, 8 mg, 11 μmol , 0.03 equiv. per benzyl) in EtOH/THF (2:1, 0.05 M, 0.9/0.4 mL) and 0.1M HCl (0.76 mL, 76 μmol , 1.18 equiv.) was stirred vigorously under an atmosphere of H_2 for 18 h. The reaction mixture was filtered over CeliteTM and washed with MeOH/water (2:1 then 1:1, 20 mL total) then passed through Dowex[®] 50W-X8 resin (Na^+ form) before being concentrated under reduced pressure. The resultant residue was re-suspended in D_2O and lyophilised to afford **174** as a white solid (15 mg, 58 μmol , 90%).

R_f 0.07 (MeCN/H₂O, 3/1 plus 3 drops AcOH);

[α]_D²⁶ +24.0 (c = 0.46, H₂O);

¹H NMR (400 MHz, D₂O) δ_H 5.42 (1H, d, J_{H1-P} = 5.6 Hz, H₁), 3.99 (2H, brs, H₂, H₃), 3.89 (1H, d, J = 8.3 Hz, H₅), 3.58 (1H, appt, J = 9.5 Hz, H₄), 3.46 (1H, d, J = 12.9 Hz, H₆), 3.19-3.06 (1H, m, H_{6'});

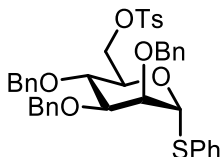
¹³C NMR (100 MHz, D₂O) δ_C 95.8 (C₁), 70.3 (C₂ or C₃), 70.2 (C₂ or C₃), 69.2 (C₄), 68.1 (C₅), 40.5 (C₆);

³¹P NMR (161 MHz, D₂O) δ_P -2.0 (1P, d, J_{H1-P} = 5.6 Hz);

HRMS *m/z* (ESI⁻) [Found: (M-H)⁻ 258.0388 C₆H₁₃NO₈P requires M-H⁻, 258.0378].

6.5.9 6-Deoxy-6-methoxyamino-α-D-mannopyranose derivatives

2,3,4-Tri-O-benzyl-6-tosyl-1-thio-α-D-mannopyranoside **180**



To a solution of **112** (0.25 g, 0.46 mmol, 1.0 equiv.) in pyridine (3 mL) was added *p*TsCl (0.26 g, 1.4 mmol, 3.0 equiv.). After stirring for 7 h, the reaction mixture was poured onto H₂O (30 mL) and extracted with CHCl₃ (30 mL). The organic layer was washed with 1M HCl (20 mL), saturated aqueous NaHCO₃ solution (20 mL), H₂O (20 mL), brine (20 mL), dried (MgSO₄), filtered and concentrated *in vacuo*. Drying under high vacuum afforded **180** as a yellow syrup (0.25 g, 0.36 mmol, 78%).

R_f 0.87 (Pet. Ether/EtOAc, 2/1);

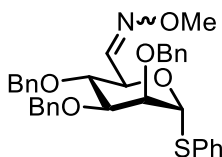
$[\alpha]_D^{26} +54.4$ ($c = 2.1$, CHCl_3);

$^1\text{H NMR}$ (400 MHz, CDCl_3) δ_{H} 7.72 (2H, d, $J = 7.9$ Hz, Ar-*H*), 7.36-7.30 (13H, m, Ar-*H*), 7.27-7.24 (4H, m, Ar-*H*), 7.23-7.16 (5H, m, Ar-*H*), 5.39 (1H, d, $J = 1.6$ Hz, H_1), 4.86 (1H, d, $J = 10.7$, CH_2Ph), 4.65-4.52 (4H, m, CH_2Ph), 4.44 (1H, d, $J = 10.7$ Hz, CH_2Ph), 4.25 (3H, m, H_3 , H_6 , H_6'), 3.91 (1H, dd, $J = 2.7$, 1.6 Hz, H_2), 3.87 (1H, appt, $J = 9.3$ Hz, H_4), 3.76 (1H, dd, $J = 9.3$, 3.0 Hz, H_5), 2.33 (3H, s, -Oph CH_3);

$^{13}\text{C NMR}$ (100 MHz, CDCl_3) δ_{C} 144.7 (Ar-C), 138.1 (Ar-C), 137.9 (Ar-C), 137.8 (Ar-C), 134.0 (Ar-C), 133.0 (Ar-C), 131.7 (Ar-C), 129.8 (Ar-C), 129.2 (Ar-C), 128.6 (Ar-C), 128.5 (Ar-C), 128.1 (Ar-C), 127.9 (Ar-C), 127.7 (Ar-C), 85.7 (C_1), 80.1 (C_5), 76.1 (C_2), 75.2 (CH_2Ph), 74.1 (C_4), 72.1 (CH_2Ph), 72.0 (CH_2Ph), 70.9 (C_3), 68.8 (C_6), 21.7 (-Oph CH_3);

HRMS m/z (ESI $^+$) [Found: ($\text{M}+\text{Na}$) $^+$ 719.2152 $\text{C}_{40}\text{H}_{40}\text{O}_7\text{S}_2$ requires $\text{M}+\text{Na}^+$, 719.2113].

Methyl 2,3,4-tri-*O*-benzyl-6-deoxy-1-thio- α -D-mannopyranosyl oxime **181**



To a solution of **113** (0.98 g, 1.8 mmol, 1.0 equiv.) in THF (18 mL) was added dropwise at RT a solution of $\text{MeONH}_2\cdot\text{HCl}$ (0.15 g, 1.8 mmol, 1.0 equiv.) in H_2O (3.6 mL). The reaction mixture was stirred for 10 min, cooled to 0 $^\circ\text{C}$ then a solution of Na_2CO_3 (0.23 g, 2.2 mmol, 1.0 equiv.) in H_2O (2.2 mL) was added dropwise before being warmed to RT. After 18 h, the reaction mixture was poured onto H_2O (50 mL)

and extracted with EtOAc (50 mL). The organic layer was washed with H₂O (2 × 50 mL), brine (50 mL), dried (MgSO₄), filtered and concentrated *in vacuo*. Purification by silica gel column chromatography, eluting with Pet. Ether/EtOAc, (5/1, 4/1) afforded **181** as a colourless oil (0.50 g, 0.88 mmol, 48%).

R_f 0.87 (Pet. Ether/EtOAc, 3/1);

[α]_D²⁶ +290.6 (c = 0.35, CHCl₃);

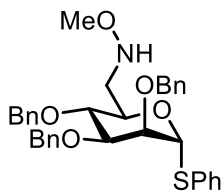
¹H NMR (400 MHz, CDCl₃) δ_H 7.41-7.37 (1H, m, HC=N), 7.35-7.31 (4H, m, Ar-H), 7.30-7.27 (12H, m, Ar-H), 7.23-7.20 (4H, m, Ar-H), 5.44 (1H, d, J = 1.5 Hz, H₁), 4.80 (1H, d, J = 10.9 Hz, CH₂Ph), 4.67 (1H, m, H₃), 4.63 (2H, m, CH₂Ph), 4.61 (2H, m, CH₂Ph), 4.59 (1H, m, CH₂Ph), 3.99-3.90 (2H, m, H₂, C₄), 3.83-3.81 (1H, m, H₅);

¹³C NMR (100 MHz, CDCl₃) δ_C 146.9 (C=N), 138.3 (Ar-C), 138.2 (Ar-C), 137.9 (Ar-C), 134.1 (Ar-C), 131.9 (Ar-C), 129.2 (Ar-C), 128.6 (2C, Ar-C), 128.4 (Ar-C), 128.3 (Ar-C), 128.1 (Ar-C), 128.0 (2C, Ar-C), 127.9 (Ar-C), 86.2 (C₁), 79.6 (C₅), 76.6 (C₄), 76.5 (C₂) 75.1 (CH₂Ph), 72.6 (CH₂Ph), 72.4 (CH₂Ph), 71.0 (C₃), 62.0 (OCH₃);

HRMS *m/z* (ESI⁺) [Found: (M+H)⁺ 570.2321 C₃₄H₃₅NO₅ requires *M+H*⁺, 570.2315].

Methyl 2,3,4-tri-O-benzyl-6-deoxy-6-methoxyamine-1-thio- α -D-mannopyranoside

182



To a solution of oxime **181** (0.20 g, 0.35 mmol, 1.0 equiv.) in glacial AcOH (17.5 mL) was added NaCNBH₃ (56 mg, 0.88 mmol, 5.0 equiv.). After stirring for 15 h, the reaction mixture was concentrated *in vacuo* and co-evaporated with Tol to aid removal of AcOH. Purification by silica gel column chromatography, eluting with Pet. Ether/EtOAc (5/1) affording **182** as a colourless oil (0.12 g, 0.20 mmol, 57%).

R_f 0.73 (Pet. Ether/EtOAc, 2/1);

[α]_D²⁶ +86.6 (*c* = 1.05, CHCl₃);

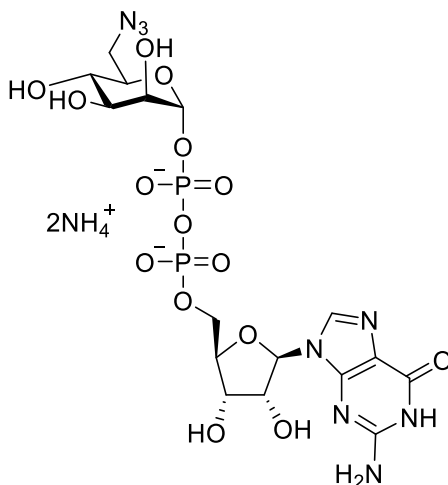
¹H NMR (400 MHz, CDCl₃) δ _H 7.44-7.42 (2H, m, Ar-*H*), 7.34-7.31 (11H, m, Ar-*H*), 7.30-7.26 (3H, m, Ar-*H*), 5.45 (1H, d, *J* = 1.3 Hz, H₁), 4.97-4.92 (1H, m, CH₂Ph), 4.68-4.60 (5H, m, CH₂Ph), 4.34-4.30 (1H, m, H₅), 3.98 (1H, brs, H₂), 3.86-3.84 (2H, m, H₃, H₄), 3.46 (3H, s, -NHOCCH₃), 3.38 (1H, d, *J* = 13.3, 2.5 Hz, H₆'), 3.02 (1H, dd, *J* = 13.3, 7.8 Hz, H₆);

¹³C NMR (100 MHz, CDCl₃) δ _C 138.5 (Ar-C), 138.2 (Ar-C), 137.9 (Ar-C), 134.0 (Ar-C), 132.6 (Ar-C), 132.0 (Ar-C), 129.2 (Ar-C), 129.1 (Ar-C), 128.5 (3C, Ar-C), 128.1 (2C, Ar-C), 128.0 (2C, Ar-C), 127.9 (3C, Ar-C), 127.8 (Ar-C), 86.1 (C₁), 80.3 (C₃ or C₄), 77.0 (C₃ or C₄), 76.5 (C₂), 75.3 (CH₂Ph), 72.4 (CH₂Ph), 72.3 (CH₂Ph), 69.5 (C₅), 61.3 (-NHOCCH₃), 52.5 (C₆);

HRMS m/z (ESI⁺) [Found: (M+H)⁺ 572.2478 C₃₄H₃₇NO₅ requires $M+H^+$, 572.2471].

6.5.10 Modified GDP-Man analogues

Guanosine diphosphate-6-azido-6-deoxy-mannose (*bis*-ammonium salt) **91**



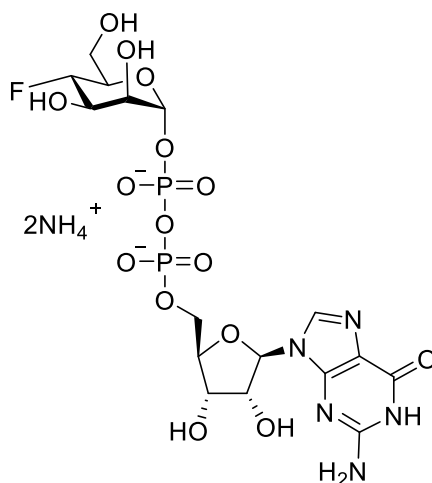
Prepared as per Procedure G using **119** (4.25 mg, 15.0 μmol , 1.0 equiv.) and GTP (7.32 mg, 14.0 μmol , 0.93 equiv.). Reaction time: 16 h. **91** was afforded as a white solid (1.48 mg, 2.36 μmol , 16%).

^1H NMR (600 MHz, D_2O) δ_{H} 8.12 (1H, s, H_8'), 5.94 (1H, d, $J = 6.1$ Hz, $\text{H}_{1'}$), 5.51 (1H, d, $J_{\text{H}_1-\text{P}} = 8.9$ Hz, H_1), 4.79 (1H, hidden, H_2'), 4.52 (1H, dt, $J = 7.3, 3.7$ Hz, $\text{H}_{3'}$), 4.35 (1H, d, $J = 10.8$ Hz, $\text{H}_{4'}$), 4.24-4.20 (2H, m, $\text{H}_{5'a}, \text{H}_{5'b}$), 4.05 (1H, brs, H_2), 3.97-3.93 (1H, m, H_5), 3.92 (1H, dd, $J = 9.8, 3.4$ Hz, H_3), 3.68 (1H, appt, $J = 8.1$ Hz, H_4), 3.65 (1H, d, $J = 2.4$ Hz, H_6'), 3.58 (1H, dd, $J = 12.0, 4.0$ Hz, H_6);

$^{31}\text{P}\{^1\text{H}\}$ NMR (161 MHz, D_2O) δ_{P} -11.5 (1P, s), -14.0 (1P, s);

HRMS m/z (ES^-) [Found: $(\text{M}-\text{H})^-$ 629.0778 $\text{C}_{16}\text{H}_{22}\text{N}_8\text{O}_{15}\text{P}_2$ requires $\text{M}-\text{H}^-$, 617.0651].

Guanosine diphosphate-4-deoxy-4-fluoro-mannose (bis-ammonium salt) **128**



Prepared as per Procedure G using **130** (1.38 mg, 5.30 μmol , 1.0 equiv.) and GTP (2.57 mg, 4.92 μmol , 0.93 equiv.). Reaction time: 27 h. **128** was afforded as a white solid (1.70 mg, 2.80 μmol , 53%).

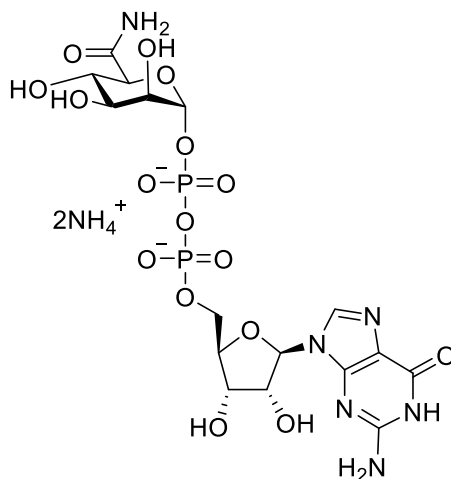
^1H NMR (400 MHz, D_2O) δ_{H} 8.12 (1H, s, H_8), 5.94 (1H, d, $J = 6.2$ Hz, $\text{H}_{1'}$), 5.51 (1H, d, $J_{\text{H}_{1'-\text{P}}} = 7.5$ Hz, H_1), 4.98 (1H, hidden, H_2') 4.66 (1H, appt, $J = 10.0$ Hz, H_4), 4.56 (1H, dd, $J = 5.0, 3.3$ Hz, $\text{H}_{3'}$), 4.36 (1H, brs, $\text{H}_{4'}$), 4.24-4.19 (2H, m, $\text{H}_{5'a}, \text{H}_{5'b}$), 4.19-4.14 (1H, m, H_3), 4.11 (1H, brs, H_2), 4.05-3.96 (1H, m, H_5), 3.86 (1H, d, $J = 12.6$ Hz, H_6), 3.76 (1H, dd, $J = 12.6, 3.3$ Hz, $\text{H}_{6'}$),

$^{19}\text{F}\{^1\text{H}\}$ NMR (376 MHz, D_2O) δ_{F} -205.6 (1F, s);

$^{31}\text{P}\{^1\text{H}\}$ NMR (161 MHz, D_2O) δ_{P} -12.0 (1P, s), -14.0 (1P, s);

HRMS m/z (ES^-) [Found: $(\text{M}-\text{H})^-$ 606.0649 $\text{C}_{16}\text{H}_{23}\text{FN}_5\text{O}_{15}\text{P}_2$ requires $\text{M}-\text{H}^-$, 606.0655].

Guanosine diphosphate-6-amido-6-deoxy-mannose (*bis*-ammonium salt) **173**



Prepared as per Procedure G using **183** (1.70 mg, 6.3 μmol , 1.0 equiv.) and GTP (3.02 mg, 5.8 μmol , 0.93 equiv.). Reaction time: 27 h. **173** was afforded as a white solid (1.60 mg, 2.6 μmol , 41%).

^1H NMR (400 MHz, D_2O) δ_{H} 8.11 (1H, s, H_8), 5.94 (1H, d, $J = 6.2$ Hz, $\text{H}_{1'}$), 5.57 (1H, d, $J_{\text{H}_1-\text{P}} = 7.0$ Hz, H_1), 4.89 (1H, hidden, $\text{H}_{2'}$), 4.53-4.48 (1H, m, $\text{H}_{3'}$), 4.35 (1H, brs, $\text{H}_{4'}$), 4.27 (1H, d, $J = 9.8$ Hz, H_5), 4.21 (2H, d, $J = 4.5$ Hz, $\text{H}_{5'a}$, $\text{H}_{5'b}$), 4.06 (1H, brs, H_2), 3.97 (1H, dd, $J = 9.7$, 3.2 Hz, H_3), 3.85 (1H, appt, $J = 9.8$ Hz, H_4);

$^{31}\text{P}\{^1\text{H}\}$ NMR (161 MHz, D_2O) δ_{P} -11.5 (1P, s), -14.0 (1P, s);

HRMS m/z (ES^-) [Found: $(\text{M}-\text{H})^-$ 617.0655 $\text{C}_{16}\text{H}_{23}\text{N}_6\text{O}_{16}\text{P}_2$ requires $\text{M}-\text{H}^-$, 617.0651].

7. References

- 1 S. Charman, R. Connon, R. Cosgriff, A. Lee and S. Carr, *UK Cystic Fibrosis Registry Annual Data Report*, 2018.
- 2 J. C. Davies, E. W. F. W. Alton and A. Bush, *BMJ*, 2007, **335**, 1255–1259.
- 3 J. R. Riordan, *Annu. Rev. Physiol.*, 1993, **55**, 609–630.
- 4 J. H. Widdicombe, M. J. Welsh and W. E. Finkbeiner, *Proc. Natl. Acad. Sci. U. S. A.*, 1985, **82**, 6167–71.
- 5 B. P. O'Sullivan and S. D. Freedman, *Lancet*, 2009, **373**, 1891–1904.
- 6 T. Bjarnsholt, *APMIS. Suppl.*, 2013, **121**, 1–51.
- 7 P. M. Quinton, *Physiol. Rev.*, 1999, **79**, S3–S22.
- 8 Condition Overview Part 2| KALYDECO® (ivacaftor), <https://www.kalydeco.com/condition-overview-2>, (accessed 8 July 2019).
- 9 J. R. Riordan, J. M. Rommens, B.-S. Kerem, N. Alon, R. Rozmahel, Z. Grzelczak, J. Zielenski, S. Lok, N. Plavsic, J.-L. Chou, M. L. Drumm, M. C. Iannuzzi, F. S. Collins and L.-C. Tsui, *Science*, 1989, **245**, 1066–1073.
- 10 M. T. Clunes and R. C. Boucher, *Drug Discov. Today Dis. Mech.*, 2007, **4**, 63–72.
- 11 Z. Zhang and J. Chen, *Cell*, 2016, **167**, 1586–1597.
- 12 W. B. Guggino, *Cell*, 1999, **96**, 607–610.
- 13 J. B. Lyczak, C. L. Cannon and G. B. Pier, *Am. Soc. Microbiol.*, 2002, **15**, 194–222.
- 14 R. . Boucher, *Adv. Drug Deliv. Rev.*, 2002, **54**, 1359–1371.
- 15 H. Matsui, B. R. Grubb, R. Tarran, Randell. S. H., J. T. Gatzky, C. W. Davis and R. C. Boucher, *Cell*, 1998, **95**, 1005–1015.
- 16 J. J. Smith, S. M. Travis and E. P. Greenberg, *Cell*, 1996, **85**, 229–236.

- 17 J. A. Dodge, P. A. Lewis, M. Stanton and J. Wilsher, *Eur. Respir. J.*, 2007, **29**, 522–526.
- 18 K. Hurt and D. Bilton, *Expert Rev. Respir. Med.*, 2012, **6**, 19–26.
- 19 M. E. Condren and M. D. Bradshaw, *J. Pediatr. Pharmacol. Ther.*, 2013, **18**, 8–13.
- 20 BBC, 'Deadlock must end' over cystic fibrosis drug Orkambi - BBC News, <https://www.bbc.co.uk/news/health-47115039>, (accessed 28 May 2019).
- 21 M. J. Franklin, D. E. Nivens, J. T. Weadge and P. L. Howell, *Front. Microbiol.*, 2011, **2**, 1–16.
- 22 W. Wu, Y. Jin, F. Bai and S. Jin, *Mol. Med. Microbiol.*, 2015, **2**, 753–767.
- 23 N. Dasgupta, M. C. Wolfgang, A. L. Goodman, S. K. Arora, J. Jyot, S. Lory and R. Ramphal, *Mol. Microbiol.*, 2003, **50**, 809–824.
- 24 C. Alexander and E. T. Rietschel, *J. Endotoxin Res.*, 2001, **7**, 167–202.
- 25 S. Galdiero, A. Falanga, M. Cantisani, R. Tarallo, M. Elena Della Pepa, V. D'Orlando and M. Galdiero, *Curr. Protein Pept. Sci.*, 2012, **13**, 843–854.
- 26 S. Bleves, V. Viarre, R. Salacha, G. P. F. Michel, A. Filloux and R. Voulhoux, *Int. J. Med. Microbiol.*, 2010, **300**, 534–543.
- 27 M. Hentzer, G. M. Teitzel, G. J. Balzer, A. Heydorn, S. Molin, M. Givskov and M. R. Parsek, *J. Bacteriol.*, 2001, **183**, 5395–5401.
- 28 I. D. Hay, Z. U. Rehman, A. Ghafoor and B. H. A. Rehm, *J. Chem. Technol. Biotechnol.*, 2010, **85**, 752–759.
- 29 U. Remminghorst and B. H. A. Rehm, *Biotechnol. Lett.*, 2006, **28**, 1701–1712.
- 30 C. E. Chitnis and D. E. Ohman, *Mol. Microbiol.*, 1993, **8**, 583–93.
- 31 E. Zhou, A. B. Seminara, S. K. Kim, C. L. Hall, Y. Wang and V. T. Lee, *ACS Chem. Biol.*, 2017, **12**, 3076–3085.

- 32 D. W. Rowen and V. Deretic, *Mol. Microbiol.*, 2000, **36**, 314–327.
- 33 U. Remminghorst and B. H. A. Rehm, *Appl. Environ. Microbiol.*, 2006, **72**, 298–305.
- 34 L. L. Oglesby, S. Jain and D. E. Ohman, *Microbiology*, 2008, **154**, 1605–1615.
- 35 I. D. Hay, Z. U. Rehman, M. F. Moradali, Y. Wang and B. H. A. Rehm, *Microb. Biotechnol.*, 2013, **6**, 637–650.
- 36 S. A. Douthit, M. Dlakic, D. E. Ohman and M. J. Franklin, *J. Bacteriol.*, 2005, **187**, 4573–4583.
- 37 J. C. Whitney, I. D. Hay, C. Li, P. D. W. Eckford, H. Robinson, M. F. Amaya, L. F. Wood, D. E. Ohman, C. E. Bear, B. H. Rehm and P. L. Howell, *Proc. Natl. Acad. Sci. U. S. A.*, 2011, **108**, 13083–13088.
- 38 R. M. Donlan, *Emerg. Infect. Dis.*, 2002, **8**, 881–890.
- 39 T.-F. Mah, B. Pitts, B. Pellock, G. C. Walker, P. S. Stewart and G. A. O’Toole, *Nature*, 2003, **426**, 306–310.
- 40 T. Bjarnsholt, P. Ø. Jensen, M. J. Fiandaca, J. Pedersen, C. R. Hansen, C. B. Andersen, T. Pressler, M. Givskov and N. Høiby, *Pediatr. Pulmonol.*, 2009, **44**, 547–558.
- 41 T. Bjarnsholt, O. Ciofu, S. Molin, M. Givskov and N. Hoiby, *Nat. Rev. Drug Discov.*, 2013, **12**, 791–808.
- 42 N. Høiby, T. Bjarnsholt, M. Givskov, S. Molin and O. Ciofu, *Int. J. Antimicrob. Agents*, 2010, **35**, 322–332.
- 43 J. W. Costerton, P. S. Stewart and E. P. Greenberg, *Science*, 1999, **284**, 1318–22.
- 44 H. Li, K. F. Mo, Q. Wang, C. K. Stover, A. Digiandomenico and G. J. Boons, *Chem. - A Eur. J.*, 2013, **19**, 17425–17431.
- 45 L. Ma, H. Lu, A. Sprinkle, M. R. Parsek and D. J. Wozniak, *J. Bacteriol.*, 2007,

- 189**, 8353–8356.
- 46 A. Ghafoor, I. D. Hay and B. H. A. Rehm, *Appl. Environ. Microbiol.*, 2011, **77**, 5238–5246.
- 47 M. F. Moradali, S. Ghods and B. H. A. Rehm, *Front. Cell. Infect. Microbiol.*, 2017, **7**, 1–29.
- 48 L. K. Jennings, K. M. Storek, H. E. Ledvina, C. Coulon, L. S. Marmont, I. Sadovskaya, P. R. Secor, B. S. Tseng, M. Scian, A. Filloux, D. J. Wozniak, P. L. Howell and M. R. Parsek, *Proc. Natl. Acad. Sci. U. S. A.*, 2015, **112**, 11353–8.
- 49 D. Passos da Silva, M. L. Matwichuk, D. O. Townsend, C. Reichhardt, D. Lamba, D. J. Wozniak and M. R. Parsek, *Nat. Commun.*, 2019, **10**, 2183.
- 50 L. Friedman and R. Kolter, *Mol. Microbiol.*, 2004, **51**, 675–690.
- 51 M. S. Byrd, I. Sadovskaya, E. Vinogradov, H. Lu, A. B. Sprinkle, S. H. Richardson, L. Ma, B. Ralston, M. R. Parsek, E. M. Anderson, J. S. Lam and D. J. Wozniak, *Mol. Microbiol.*, 2009, **73**, 622–638.
- 52 E. B. M. Breidenstein, C. de la Fuente-Núñez and R. E. W. Hancock, *Trends Microbiol.*, 2011, **19**, 419–426.
- 53 A. H. A. M. Van Hoek, D. Mevius, B. Guerra, P. Mullany, A. P. Roberts and H. J. M. Aarts, *Front. Microbiol.*, 2011, **2**, 1–27.
- 54 C. C. Sanders, W. E. Sanders, C. C. Sanders and W. E. Sanders, *J. Infect. Dis.*, 1986, **154**, 792–800.
- 55 K. M. Papp-Wallace, A. Endimiani, M. A. Taracila and R. A. Bonomo, *Antimicrob. Agents Chemother.*, 2011, **55**, 4943–4960.
- 56 K. Poole, *Antimicrob. Agents Chemother.*, 2005, **49**, 479–487.
- 57 H. Li, Y.-F. Luo, B. J. Williams, T. S. Blackwell and C.-M. Xie, *Int. J. Med. Microbiol.*, 2012, **302**, 63–68.

- 58 R. E. W. Hancock and D. P. Speert, *Drug Resist. Updat.*, 2000, **3**, 247–255.
- 59 Y.-P. Pan, · Yuan-Hong Xu, · Zhong-Xin Wang, Y.-P. Fang and J.-L. Shen, *Arch. Microbiol.*, 2016, **198**, 565–571.
- 60 P. J. Tatnell, N. J. Russell and P. Gacesa, *J. Gen. Microbiol.*, 1993, **139**, 119–127.
- 61 X. Ge, L. C. Penney, I. Van De Rijn and M. E. Tanner, *Eur. J. Biochem.*, 2004, **271**, 14–22.
- 62 X. Ge, R. E. Campbell, I. Van de Rijn and M. E. Tanner, *J. Am. Chem. Soc.*, 1998, **120**, 6613–6614.
- 63 J. Gruszczyk, A. Fleurie, V. Olivares-Illana, E. Béchet, I. Zanella-Cleon, S. Moréra, P. Meyer, G. Pompidor, R. Kahn, C. Grangeasse and S. Nessler, *J. Biol. Chem.*, 2011, **286**, 17112–17121.
- 64 C. M. Lawrence, V. W. Rodwell and C. V. Stauffacher, *Science (80-.)*, 1995, **268**, 1758–1762.
- 65 J. A. R. G. Barbosa, J. Sivaraman, Y. Li, R. Larocque, A. Matte, J. D. Schrag and M. Cygler, *Proc. Natl. Acad. Sci.*, 2002, **99**, 1859–1864.
- 66 C. F. Snook, P. A. Tipton and L. J. Beamer, *Biochemistry*, 2003, **42**, 4658–4668.
- 67 S. Egger, A. Chaikuad, K. L. Kavanagh, U. Oppermann and B. Nidetzky, *Biochem. Soc. Trans.*, 2010, **38**, 1378–85.
- 68 A. Nakagawa, T. Hosoyama, K. Chubachi, S. Takahashi, T. Ohkubo and S. Iyobe, *J. Antibiot. (Tokyo)*, 1994, **50**, 286–288.
- 69 S. H. Ashoor and F. S. Chu, *Food Cosmet. Toxicol.*, 1973, **11**, 617–624.
- 70 J. L. Kimmel and P. A. Tipton, *Arch. Biochem. Biophys.*, 2005, **441**, 132–140.
- 71 N. Elloumi, B. Moreau, L. Aguiar, N. Jaziri, M. Sauvage, C. Hulen and M. Capmau, *Eur. J. Med. Chem.*, 1992, **27**, 149–154.

- 72 G. K. Wagner, T. Pesnot and R. Field, *Nat. Prod. Rep.*, 2009, **26**, 1172–1194.
- 73 K. C. Nicolaou and H. J. Mitchell, *Angew. Chem., Int. Ed.*, 2001, **40**, 1576–1624.
- 74 S. Karamat and W. M. F. Fabian, *J. Phys. Chem. A*, 2006, **110**, 7477–7484.
- 75 D. MacDonald, *J. Org. Chem.*, 1962, **27**, 1107–1109.
- 76 L. Zou, R. B. Zheng and T. L. Lowary, *Beilstein J. Org. Chem.*, 2012, **8**, 1219–1226.
- 77 V. L. Schultz, X. Zhang, K. Linkens, J. Rimel, D. E. Green, P. L. DeAngelis and R. J. Linhardt, *J. Org. Chem.*, 2017, **82**, 2243–2248.
- 78 C. I. Lin, E. Sasaki, A. Zhong and H. W. Liu, *J. Am. Chem. Soc.*, 2014, **136**, 906–909.
- 79 S. Wolf, R. M. Berrio and C. Meier, *European J. Org. Chem.*, 2011, **31**, 6304–6313.
- 80 M. Chen, L. L. Chen, Y. Zou, M. Xue, M. Liang, L. Jin, W. Y. Guan, J. Shen, W. Wang, L. Wang, J. Liu and P. G. Wang, *Carbohydr. Res.*, 2011, **346**, 2421–2425.
- 81 K. Huang, F. Parmeggiani, E. Pallister, C. J. Huang, F. F. Liu, Q. Li, W. R. Birmingham, P. Both, B. Thomas, L. Liu, J. Voglmeir and S. L. Flitsch, *ChemBioChem*, 2018, **19**, 388–394.
- 82 M. M. Muthana, J. Qu, M. Xue, T. Klyuchnik, A. Siu, Y. Li, L. Zhang, H. Yu, L. Li, P. G. Wang and X. Chen, *Chem. Commun.*, 2015, **51**, 4595–4598.
- 83 G. K. Wagner, T. Pesnot and R. A. Field, *Nat. Prod. Rep.*, 2009, **26**, 1172–1194.
- 84 S. Ahmadipour and G. J. Miller, *Carbohydr. Res.*, 2017, **451**, 95–109.
- 85 S. Roseman, J. J. Distler, J. G. Moffatt and H. G. Khorana, *J. Am. Chem. Soc.*, 1961, **83**, 659–663.

- 86 V. Wittmann and C. H. Wong, *J. Org. Chem.*, 1997, **62**, 2144–2147.
- 87 H. Tsukamoto and D. Kahne, *Bioorg. Med. Chem. Lett.*, 2011, **21**, 5050–5053.
- 88 L. M. Tedaldi, M. Pierce and G. K. Wagner, *Carbohydr. Res.*, 2012, **364**, 22–27.
- 89 Q. Sun, X. Li, J. Sun, S. Gong, G. Liu and G. Liu, *Tetrahedron*, 2014, **70**, 294–300.
- 90 S. Wolf, T. Zismann, N. Lunau and C. Meier, *Chem. Eur. J.*, 2009, **15**, 7656–7664.
- 91 H. Tanaka, Y. Yoshimura, M. R. Jürgensen, J. A. Cuesta-Seijo and O. Hindsgaul, *Angew. Chem., Int. Ed.*, 2012, **51**, 11531–11534.
- 92 A. Depaix, S. Peyrottes and B. Roy, *European J. Org. Chem.*, 2017, **2017**, 241–245.
- 93 P. Dabrowski-Tumanski, J. Kowalska and J. Jemielity, *European J. Org. Chem.*, 2013, **2013**, 2147–2154.
- 94 S. Ahmadipour, L. Beswick and G. J. Miller, *Carbohydr. Res.*, 2018, **469**, 38–47.
- 95 G. M. Watt, S. L. Flitsch, S. Fey, L. Elling and U. Kragl, *Tetrahedron Asymmetry*, 2000, **11**, 621–628.
- 96 S. Marchesan and D. Macmillan, *Chem. Commun.*, 2008, **36**, 4321–4323.
- 97 R. M. Mizanur, C. J. Zea and N. L. Pohl, *J. Am. Chem. Soc.*, 2004, **126**, 15993–15998.
- 98 R. M. Mizanur and N. L. B. Pohl, *Org. Biomol. Chem.*, 2009, **7**, 2135–2139.
- 99 A. Miller and J. Tanner, *Essentials of Chemical Biology: Structure and Dynamics of Biological Macromolecules*, John Wiley & Sons, Ltd, 2008.
- 100 R. E. Campbell and M. E. Tanner, *Angew. Chem., Int. Ed.*, 1997, **36**, 1520–1522.

- 101 M. Weïwer, T. Sherwood, D. E. Green, M. Chen, P. L. DeAngelis, J. Liu and R. J. Linhardt, *J. Org. Chem.*, 2008, **73**, 7631–7637.
- 102 M. Rejzek, V. S. Kannathasan, C. Wing, A. Preston, E. L. Westman, J. S. Lam, J. H. Naismith, D. J. Maskell and R. A. Field, *Org. Biomol. Chem.*, 2009, **7**, 1203–1210.
- 103 G. M. Lin, H. G. Sun and H. W. Liu, *Org. Lett.*, 2016, **18**, 3438–3441.
- 104 M. Rejzek, B. Mukhopadhyay, C. Q. Wenzel, J. S. Lam and R. A. Field, *Carbohydr. Res.*, 2007, **342**, 460–466.
- 105 Q. Zhang, P. L. Howell, H. S. Overkleeft, D. V. Filippov, G. A. Van Der Marel and J. D. C. Codée, *Carbohydr. Res.*, 2017, **450**, 12–18.
- 106 L. Beswick and G. J. Miller, *Molbank*, 2017, **3**, M947.
- 107 A. Wadouachi and J. Kovensky, *Molecules*, 2011, **16**, 3933–3968.
- 108 J. Zhang and P. Kováč, *J. Carbohydr. Chem.*, 1999, **18**, 461–469.
- 109 S. M. Andersen, M. Heuckendorff and H. H. Jensen, *Org. Lett.*, 2015, **17**, 944–947.
- 110 Z. Dinev, A. Z. Wardak, R. T. C. Brownlee and S. J. Williams, *Carbohydr. Res.*, 2006, **341**, 1743–1747.
- 111 R. Roy, S. Vidal and P. Kováč, *Carbohydrate Chemistry: Proven Synthetic Methods*, CRC Press Taylor and Francis Group, Volume 3., 2015.
- 112 D. Sail and P. Kováč, *Carbohydr. Res.*, 2012, **357**, 47–52.
- 113 J. G. Moffatt and H. G. Khorana, *J. Am. Chem. Soc.*, 1961, **83**, 649–658.
- 114 T. Mukaiyama and M. Hashimoto, *Tetrahedron Lett.*, 1971, **44**, 2284.
- 115 A. Collier and G. K. Wagner, *Chem. Commun.*, 2008, **2**, 178–180.
- 116 L. Beswick, S. Ahmadipour, J. P. Dolan, M. Rejzek, R. A. Field and G. J. Miller, *Carbohydr. Res.*, 2019, **485**, 107819.

- 117 A. Heeres, H. A. van Doren, K. F. Gotlieb and I. P. Bleeker, *Carbohydr. Res.*, 1997, **299**, 221–227.
- 118 S. Ahmadipour, G. Pergolizzi, M. Rejzek, R. A. Field and G. J. Miller, *Org. Lett.*, 2019, **21**, 4415–4419.
- 119 *C&EN Glob. Enterp.*, 2019, **97**, 4.
- 120 J. M. Ostrem, U. Peters, M. L. Sos, J. A. Wells and K. M. Shokat, *Nature*, 2013, **503**, 548–551.
- 121 V. L. Schultz, X. Zhang, K. Linkens, J. Rimel, D. E. Green, P. L. Deangelis and R. J. Linhardt, *J. Org. Chem.*, 2017, **82**, 2243–2248.
- 122 L. Beswick, S. Ahmadipour, G. J. Hofman, H. Wootton, E. Dimitriou, J. Reynisson, R. A. Field, B. Linclau and G. J. Miller, *Carbohydr. Res.*, 2020, **488**, 107896.
- 123 C. Mathieu and E. Degrande, *Vasc. Health Risk Manag.*, 2008, **4**, 1349–1360.
- 124 B. Ahrén, A. Schweizer, S. Dejager, E. B. Villhauer, B. E. Dunning and J. E. Foley, *Diabetes, Obes. Metab.*, 2011, **13**, 775–783.
- 125 C. S. Li, D. Deschenes, S. Desmarais, J. P. Falguyret, J. Y. Gauthier, D. B. Kimmel, S. Léger, F. Massé, M. E. McGrath, D. J. McKay, M. D. Percival, D. Riendeau, S. B. Rodan, M. Thérien, V. L. Truong, G. Wesolowski, R. Zamboni and W. C. Black, *Bioorg. Med. Chem. Lett.*, 2006, **16**, 1985–1989.
- 126 M. Mende, M. Nieger and S. Bräse, *Chem. - A Eur. J.*, 2017, **23**, 12283–12296.
- 127 H. Sajiki, K. Hattori and K. Hirota, *J. Org. Chem.*, 1998, **63**, 7990–7992.
- 128 T. Maegawa, Y. Fujita, A. Sakurai, A. Akashi, M. Sato, K. Oono and H. Sajiki, *Chem. Pharm. Bull. (Tokyo)*, 2007, **55**, 837–839.
- 129 M. Adinolfi, L. Guariniello, A. Iadonisi and L. Mangoni, *Synlett*, 2000, **9**, 1277–1278.
- 130 S. Hartlieb, A. Günzel, R. Gerardy-Schahn, A. K. Münster-Kühnel, A.

- Kirschning and G. Dräger, *Carbohydr. Res.*, 2008, **343**, 2075–2082.
- 131 J. Elhalabi and K. G. Rice, *Nucleosides, Nucleotides and Nucleic Acids*, 2004, **23**, 195–205.
- 132 T. Murakami, R. Hirono, Y. Sato and K. Furusawa, *Carbohydr. Res.*, 2007, **342**, 1009–1020.
- 133 A. Fadlan, H. Tanimoto, T. Ito, Y. Aritomi, M. Ueno, M. Tokuda, S. Hirohara, M. Obata, T. Morimoto and K. Kakiuchi, *Bioorg. Med. Chem.*, 2018, **26**, 1848–1858.
- 134 I. Ojima, *ChemBioChem*, 2004, **5**, 628–635.
- 135 G. M. Lin, H. G. Sun and H. W. Liu, *Org. Lett.*, 2016, **18**, 3438–3441.
- 136 S. Hartlieb, A. Gunzel, R. Gerardy-Schahn, A. K. Munster-Kuhnel, A. Kirschning and G. Dräger, *Carbohydr. Res.*, 2008, **343**, 2075–2082.
- 137 M. Ohlin, R. Johnsson and U. Ellervik, *Carbohydr. Res.*, 2011, **346**, 1358–1370.
- 138 K. V. Rao, P. R. Patil, S. Atmakuri and K. P. R. Kartha, *Carbohydr. Res.*, 2010, **345**, 2709–2713.
- 139 J. Luche, *J. Am. Chem. Soc.*, 1979, **78**, 2226–2227.
- 140 N. Wu, A. Messinis, A. S. Batsanov, Z. Yang, A. Whiting and T. B. Marder, *Chem. Commun.*, 2012, **48**, 9986.
- 141 K. R. Broberg, E. Avizienyte, M. Helliwell, J. Raftery, G. C. Jayson and J. M. Gardiner, *J. Org. Chem.*, 2012, **77**, 7823–7843.
- 142 A. T. Tran, S. Deydier, D. Bonnaffé and C. Le Narvor, *Tetrahedron Lett.*, 2008, **49**, 2163–2165.
- 143 S. C. Timmons and D. L. Jakeman, *Org. Lett.*, 2007, **9**, 1227–1230.
- 144 E. J. Corey and A. Venkateswarlu, *J. Am. Chem. Soc.*, 1972, **94**, 6190–6191.

- 145 B. Karimi, A. Zamani and D. Zareyee, *Tetrahedron Lett.*, 2004, **45**, 9139–9141.
- 146 A. DattaGupta, R. Singh and V. K. Singh, *Synlett*, 1996, 69–71.
- 147 M. Wakao, K. Fukase and S. Kusumoto, *J. Org. Chem.*, 2002, **67**, 8182–8190.
- 148 D. Crich and W. Li, *Org. Lett.*, 2006, **8**, 959–962.
- 149 D. E. Levy and P. Fugedi, *The Organic Chemistry of Sugars*, CRC Taylor and Francis Group, 2006.
- 150 N. J. Turner, *Chem. Rev.*, 2011, **111**, 4073–4087.
- 151 E. E. Snell and S. J. Di Mari, *Enzymes*, 1970, **2**, 335–370.
- 152 J. Jung and B. Nidetzky, *J. Biol. Chem.*, 2018, **293**, 3720–3733.
- 153 M. C. Lawrence, J. A. R. G. Barbosa, B. J. Smith, N. E. Hall, P. A. Pilling, H. C. Ooi and S. M. Marcuccio, *J. Mol. Biol.*, 1997, **266**, 381–399.
- 154 F. Peri, C. Marinzi, M. Barath, F. Granucci, M. Urbano and F. Nicotra, *Bioorg. Med. Chem.*, 2006, **14**, 190–199.
- 155 M. J. Frisch, *Gaussian 16*, Wallingford CT, 2019.
- 156 A. D. Becke, *J. Chem. Phys.*, 1993, **98**, 1372–1377.
- 157 M. J. Frisch, J. A. Pople and J. S. Binkley, *J. Chem. Phys.*, 1984, **80**, 3265–3269.
- 158 P. C. Hariharan and J. A. Pople, *Theor. Chim. Acta*, 1973, **28**, 213–222.
- 159 *Scigress ultra*, Fijitsu Limited, 2008.
- 160 N. L. Allinger, *J. Am. Chem. Soc.*, 1977, **99**, 8127–8134.
- 161 L. Elling, J. E. Ritter and S. Verseck, *Glycobiology*, 1996, **6**, 591–597.
- 162 L. E. Naught, S. Gilbert, R. Imhoff, C. Snook, L. Beamer and P. Tipton, *Biochemistry*, 2002, **41**, 9637–9645.

- 163 K. Lin and A. M. Kasko, *Biomacromolecules*, 2013, **14**, 350–357.
- 164 D. Reynolds and W. M. Lloyd, *J. Am. Chem. Soc.*, 1940, **62**, 66–69.
- 165 S. Knapp and S. R. Nandan, *J. Org. Chem.*, 1994, **59**, 281–283.
- 166 T. Yang and M. Bar-Peled, *Biochem. J.*, 2010, **429**, 533–543.
- 167 J. A. Watt and S. J. Williams, *Org. Biomol. Chem.*, 2005, **3**, 1982–1992.
- 168 G. van der Marel and J. Codée, *Carbohydrate Chemistry: Proven Synthetic Methods*, CRC Press Taylor and Francis Group, Volume 2., 2014.
- 169 D. C. M. Kong and M. Von Itzstein, *Carbohydr. Res.*, 1997, **305**, 323–329.
- 170 T. Oshitari, M. Shibasaki, T. Yoshizawa, M. Tomita, K.-I. Takao and S. Kobayashi, *Tetrahedron*, 1997, **53**, 10993–11006.
- 171 D. Crich and M. Smith, *J. Am. Chem. Soc.*, 2002, **124**, 8867–8869.
- 172 K. Suzuki, I. Ohtsuka, T. Kanemitsu, T. Ako and O. Kanie, *J. Carbohydr. Chem.*, 2005, **24**, 219–236.
- 173 S. C. Timmons and D. L. Jakeman, *Carbohydr. Res.*, 2008, **343**, 865–874.
- 174 V. Dimakos, G. E. Garrett and M. S. Taylor, *J. Am. Chem. Soc.*, 2017, **139**, 15515–15521.
- 175 M. K. Christensen, M. Meldal and K. Bock, *J. Chem. Soc. Perkin Trans. 1*, 1993, **1**, 1453–1460.
- 176 R. K. Jain and K. L. Matta, *Carbohydr. Res.*, 1996, **282**, 101–111.
- 177 D. Waschke, Y. Leshch, J. Thimm, U. Himmelreich and J. Thiem, *European J. Org. Chem.*, 2012, 948–959.